Utilising embryonic and extra-embryonic stem cells to model early mammalian embryogenesis *in vitro*

Sarah Ellys Harrison

Faculty of Biology

University of Cambridge

This dissertation is submitted for the degree of

Doctor of Philosophy

Corpus Christi College

September 2017

Thesis Summary for the Degree of Doctor of Philosophy

Utilising embryonic and extra-embryonic stem cells to model early mammalian embryogenesis *in vitro*

Sarah E. Harrison

Successful mammalian development to term requires that embryonic and extra-embryonic tissues communicate and grow in coordination, to form the body. After implanting into the uterus, the mouse embryo is comprised of three cell lineages: first, the embryonic epiblast (EPI) that forms the embryo proper, second, the extra-embryonic ectoderm (ExE) which contributes to the foetal portion of the placenta, and third, the visceral endoderm (VE) that contributes to the yolk sac. These three tissues form a characteristic 'egg-cylinder' structure, which allows signals to be exchanged between them and sets the stage for body axis establishment and subsequent tissue patterning.

The mechanisms underlying this process are difficult to study *in vivo* because a different genetically manipulated mouse line must be generated to investigate each factor involved. This difficulty has prompted efforts to model mammalian embryogenesis *in vitro*, using cell lines, which are more amenable to genetic manipulation. The pluripotent state of the EPI can be captured *in vitro* as mammalian embryonic stem cells (ESCs). Although mouse ESCs have been shown to contribute to all adult tissues in chimeric embryos, they cannot undertake embryogenesis when allowed to differentiate in culture. Previous studies have shown that ESCs formed into three-dimensional (3D) aggregates, called embryoid bodies, can become patterned and express genes associated with early tissue differentiation. However, embryoid bodies cannot recapitulate embryonic architecture and therefore may not accurately reflect what happens in the embryo.

In this study, a new technique was developed to model early mouse development which is more faithful to the embryo. ESCs were co-cultured with stem cells derived from the ExE, termed trophoblast stem cells (TSCs), embedded within extracellular matrix (ECM). These culture conditions lead to the self-assembly of embryo-like structures with similar architecture to the mouse egg cylinder. They were comprised of an embryonic compartment derived from ESCs abutting an extra-embryonic compartment derived from TSCs, and hence were named 'ETS-embryos'. These structures developed a continuous cavity at their centre, which formed via a similar sequence of events to those that lead to pro-amniotic cavity formation in the mouse embryo, and required active Nodal/Activin signalling.

After cavitation, 'ETS-embryos' developed regionalised mesodermal tissue and primordial germ cell-like cells originating at the boundary between embryonic and extra-embryonic compartments. Inhibitor studies revealed that this occurred in response to endogenous Wnt and BMP signalling, pathways which also govern these tissue specification events in the early mouse embryo.

To demonstrate that 'ETS-embryos' were comparable to mouse embryos at the global transcriptional level, RNA-sequencing was then performed on different tissue regions of 'ETS-embryos' and the resulting transcriptomes were compared to datasets from mouse embryos. These data showed that 'ETS-embryos' were highly similar to mouse embryos at post-implantation stages in their overall gene expression patterns. Taken together, these results indicate that 'ETS-embryos' are an accurate *in vitro* model of mammalian embryogenesis, which can be used to complement studies undertaken *in vivo* to investigate early development.

Declaration

This dissertation is the result of my own work and includes nothing which is the outcome of work done in collaboration, except where this is specified in the text. It is not substantially the same as any work that I have submitted, or, is being concurrently submitted for a degree or diploma or other qualification at the University of Cambridge or any other University or similar institution. I further state that no substantial part of my dissertation has already been submitted, or, is being concurrently submitted for any such degree, diploma or other qualification at the University of Cambridge or any other University or similar institution. This thesis does not exceed the word limit prescribed by the degree committee.

Sarah Ellys Harrison

Acknowledgements

Firstly, I would like to thank my supervisor, Professor Magdalena Zernicka-Goetz, for giving me the opportunity to work in her lab and for her guidance throughout my PhD.

I am also extremely grateful to all the scientists who have contributed to this work, whether it be by providing assistance with experiments or data analysis, or simply through helpful and stimulating discussion. In particular, I am indebted to Neophytos Christodoulou, Christos Kyprianou, Berna Sozen, Ran Wang, and Naihe Jing, whose work has helped to make this study possible. Thank you also to all the past and present members of the Zernicka-Goetz lab for being a wonderfully supportive set of colleagues, and for teaching me the secrets of early mouse embryogenesis with such passion and enthusiasm.

I would also like to acknowledge all the staff at the University of Cambridge, who maintain our buildings and keep our animal facilities running smoothly, and without whom our science wouldn't be possible.

I thank the BBSRC for providing the financial support necessary to make my dream a reality and for the administrative support and training opportunities the DTP has provided throughout. I also thank my friends and fellow PhD students, who have made my years at Cambridge all the more enjoyable.

Thank you to Daniel, for lending an ear to listen to my outlandish ideas and for being by my side to keep me going when times got tough.

Finally, I thank my parents, Ana and Jonathan, for imbuing in me a passion for science, and for your endless love and support. I dedicate this work to you both.

Table of Contents

List of Figures

List of Tables

List of Abbreviations

2D	Two-dimensional
2i	Two-inhibitor
3D	Three-dimensional
A-P	Anterior-posterior
aPKC	atypical protein kinase C
AVE	Anterior visceral endoderm
BMP	Bone Morphogenetic Protein
CARM1	Coactivator Associated Arginine Methyltransferase 1
Cc-3	Cleaved-caspase-3
cDNA	Complementary DNA
d.p.c	Days post coitum
DAPI	4',6-diamidon-2-phenylindole
DEGs	Differentially expressed genes
DNA	Deoxyribonucleic Acid
DVE	Distal visceral endoderm
E-cad	E-cadherin
ECM	Extracellular Matrix
EGF-CFC	Epidermal growth factor-Cripto-FRL1-Cryptic
EMT	Epithelial-to-mesenchymal transition
EPI	Epiblast
EPISCs	Epiblast stem cells
ERK	Extracellular signal–regulated kinase
ESCs	Embryonic stem cells
ExE	Extra-embryonic ectoderm
F-actin	Fibrillar actin
FBS	Foetal Bovine Serum
FGF	Fibroblast Growth Factor
FPKM	Fragments per kilobase million
GFP	Green-Fluorescent protein
GO	Gene ontology

GSK3β	Glycogen synthase kinase 3-β
H3R26	Histone 3 methylation on arginine 26
hESCs	Human embryonic stem cells
ICM	Inner cell mass
iPSCs	Induced pluripotent stem cells
LIF	Leukaemia inhibitory factor
MAPK	Mitogen-activated protein kinase
MDCK	Madin-Darby Canine Kidney Epithelial
MEF	Mouse embryonic fibriblast
mRNA	messenger Ribonucleic acid
PaE	Pareital endoderm
PBS	Phosphate buffered saline
PBS-T	PBS with 0.1% Tween
PCA	Principal component analysis
PCC	Pearson's correlation coefficient
PCR	Polymerase chain reaction
PE	Primitive endoderm
PGCs	Primordial germ cells
Podxl	Podocalyxin
qRT-PCR	Quantitative real-time PCR
TE	Trophectoderm
TGCs	Trophoblast giant cells
TGFβ	Transforming growth factor β
TSCs	Trophoblast stem cells
VE	Visceral endoderm
Wnt	Wingless-Type MMTV Integration Site Family
XEN	Extra-embryonic endoderm stem cells

Italics	Refers to gene or RNA
Standard	Refers to protein

List of Genes

Activin A	Activin A
Amot	Angiomotin
AP2-γ (Tfap2C)	Activating Enhancer-binding Protein 2 Gamma
aPKC	Atypical Protein kinase C
Axin1	Axis Inhibition Protein 1
Blimp1/ Prdm1	Beta-Interferon Gene Positive-Regulatory Domain I Binding Factor /Positive Regulatory Domain I-Binding Factor 1
BMP4	Bone morphogenetic protein 4
Cbx7	Chromobox 7
Cdx2	Caudal Type Homeobox 2
Cer-I	Cerberus-like
Cripto/ Tdgf1	Epidermal Growth Factor-Like Cripto Protein CR1 /Teratocarcinoma-Derived Growth Factor 1
Dab2	Disabled 2, mitogen-responsive phosphoprotein
Ddx4	DEAD (Asp-Glu-Ala-Asp) box polypeptide 4
Dkk1	Dickkopf WNT signaling pathway inhibitor 1
E-cadherin	Cadherin 1, type 1
Elf5	E74-like factor 5
Eomes	Eomesodermin
Fgf2	Fibroblast growth factor 2
Fgf4	Fibroblast growth factor 4
Fgf5	Fibroblast growth factor 5

Fgfr2	Fibroblast growth factor receptor 2
Furin	Furin (paired basic amino acid cleaving enzyme)
Gapdh	Glyceraldehyde-3-phosphate dehydrogenase
Gata3	GATA binding protein 3
Gata4	GATA binding protein 4
Gata6	GATA binding protein 6
Hand1	Heart and neural crest derivatives expressed 1
Hnf4α	Hepatic nuclear factor 4, alpha
Klf4	Kruppel-like factor 4
LATS1/2	Large tumour suppressor kinase 1/2
Lefty1	Left right determination factor 1
Mesp1/2	Mesoderm posterior 1/2
Mixl1	Mix1 homeobox-like 1
Myc	Myelocytomatosis oncogene
Nanog	Nanog homeobox
Nanos3	Nanos homolog 3
Nodal	Nodal
Otx2	Orthodenticle homeobox 2
Pcsk6 (Pace4)	Proprotein convertase subtilisin/kexin type 6
Pgdfrα	Platelet derived growth factor receptor, alpha polypeptide
Podxl	Podocalyxin-like
Pou3f1/ Oct6	POU domain, class 3, transcription factor 1 /Octamer-binding transcription factor 6
Pou5f1 /Oct4	POU domain, class 5, transcription factor 1 /Octamer-binding transcription factor 4

Prdm14	Positive Regulatory Domain I-Binding Factor 14
Sall2	Sal-like 2 (Drosophila)
Sall3	Sal-like 3 (Drosophila)
Slc7a3	Solute carrier family 7 (cationic amino acid transporter, y+ system), member 3
Snai1	Snail family zinc finger 1
Sox17	SRY (sex determining region Y)-box 17
Sox2	SRY (sex determining region Y)-box 2
Sox21	SRY (sex determining region Y)-box 21
Sox7	SRY (sex determining region Y)-box 7
Sp5	Trans-acting transcription factor 5
Stella/ Dppa3	Developmental pluripotency-associated 3
T/Bra	T-box transcription factor/ Brachyury
Tcf3	Transcription factor 3
Tead4	TEA domain family member 4
Utf1	Undifferentiated embryonic cell transcription factor 1
Wnt3	Wingless-type MMTV integration site family, member 3
YAP	Yes associated protein
Zfp462	Zinc finger protein 462
αFP	Alpha-fetoprotein

Abstract

Successful mammalian development to term requires that embryonic and extra-embryonic tissues communicate and grow in coordination, to form the body. After implanting into the uterus, the mouse embryo is comprised of three cell lineages: first, the embryonic epiblast (EPI) that forms the embryo proper, second, the extra-embryonic ectoderm (ExE) which contributes to the foetal portion of the placenta, and third, the visceral endoderm (VE) that contributes to the yolk sac. These three tissues form a characteristic 'egg-cylinder' structure, which allows signals to be exchanged between them and sets the stage for body axis establishment and subsequent tissue patterning.

The mechanisms underlying this process are difficult to study *in vivo* because a different genetically manipulated mouse line must be generated to investigate each factor involved. This difficulty has prompted efforts to model mammalian embryogenesis *in vitro*, using cell lines, which are more amenable to genetic manipulation. The pluripotent state of the EPI can be captured *in vitro* as mammalian embryonic stem cells (ESCs). Although mouse ESCs have been shown to contribute to all adult tissues in chimeric embryos, they cannot undertake embryogenesis when allowed to differentiate in culture. Previous studies have shown that ESCs formed into three-dimensional (3D) aggregates, called 'embryoid bodies' can become patterned and express genes associated with early tissue differentiation. However, embryoid bodies cannot recapitulate embryonic architecture and therefore may not accurately reflect what happens in the embryo.

In this study, a new technique was developed to model early mouse development which is more faithful to the embryo. ESCs were co-cultured with stem cells derived from the ExE, termed trophoblast stem cells (TSCs), embedded within extracellular matrix (ECM). These culture conditions lead to the self-assembly of embryo-like structures with similar architecture to the mouse egg cylinder. They were comprised of an embryonic compartment derived from ESCs abutting an extra-embryonic compartment derived from TSCs, and hence were named 'ETS-embryos'. These structures developed a continuous cavity at their centre, which formed via a similar sequence of events to those that lead to pro-amniotic cavity formation in the mouse embryo, and required active Nodal/Activin signalling.

After cavitation, 'ETS-embryos' developed regionalised mesodermal tissue and primordial germ cell-like cells originating at the boundary between embryonic and extra-embryonic compartments. Inhibitor studies revealed that this occurred in response to endogenous Wnt and BMP signalling, pathways which also govern these tissue specification events in the early mouse embryo.

To demonstrate that 'ETS-embryos' were comparable to mouse embryos at the global transcriptional level, mRNA-sequencing was then performed on different tissue regions of 'ETS-embryos' and the

resulting transcriptomes were compared to datasets from mouse embryos. These data showed that 'ETS-embryos' were highly similar to mouse embryos at post-implantation stages in their overall gene expression patterns. Taken together, these results indicate that 'ETS-embryos' are an accurate *in vitro* model of mammalian embryogenesis, which can be used to complement studies undertaken *in vivo* to investigate early development.

1. Introduction

1.1 Early mouse embryonic development: from zygote to blastocyst

The great majority of our knowledge about early mammalian embryonic development comes from studies on the mouse embryo. For decades, this has been used as a model system to elucidate how development progresses from a single cell, the fertilised egg, to form all the different tissues and organs of the body at birth. The first step in this complex process is the segregation of the embryonic tissues which will form the foetus from the extra-embryonic lineages of the conceptus. In the mouse, this process occurs over the first four days post-coitum (d.p.c), via two cell fate decisions which first define the trophectoderm (TE), a precursor of the foetal portion of the placenta, from the inner cell mass (ICM) of the embryo. Subsequently the cells of the ICM segregate to form the embryonic epiblast (EPI) and the yolk-sac precursor tissue, the primitive endoderm (PE). This lineage segregation is coupled to the physical separation of the three lineages to form a hollow blastocyst, ready to implant into the uterus (Fig. 1.1. A, B).

1.1.1 Cleavage divisions and zygotic genome activation, and early heterogeneity

After the moment of conception, the fertilised egg is a totipotent cell with the potential to give rise to all the embryonic and extra-embryonic lineages required to form a completely new individual (Ishiuchi and Torres-Padilla, 2013; Wu, Lei and Schöler, 2017). This totipotent zygote then undertakes several rounds of cleavage divisions, without increasing the overall volume of the embryo, resulting in the formation of smaller and smaller cells, called 'blastomeres' (Aiken *et al.*, 2004). At the two-cell stage, corresponding to embryonic day 1.5 (E1.5), the embryo has cleaved into two morphologically identical blastomeres, which remain totipotent. However, experiments by Andrezj Tarkowski and others showed that even at this early stage, the blastomeres might be different from one another, as in the majority of cases, only one of these blastomeres has the potential to give rise to a separate individual when isolated (Tarkowski, 1959; Tsunoda and McLaren, 1983). These experiments are supported by more recent molecular data showing that the progeny of these two blastomeres contribute unequally to the developing embryonic lineage (Casser *et al.*, 2017) and suggest that that both cells may not retain the same fate potential even at these early stages. The embryo is initially reliant on the expression of maternal mRNAs laid down in the oocyte before fertilisation (Bachvarova, 1985) but at the two-cell stage, the zygotic genome becomes activated with two waves of gene expression. The first, minor wave of genome activation occurs as early as the zygote stage, and this is followed by a subsequent major wave of genome activation in the two-cell stage embryo (Hamatani *et al.*, 2004; Wang *et al.*, 2004).

It is at the four cell-stage, subsequent to this second wave of zygotic genome activation, that there is evidence for the four cells of the embryo first becoming distinctly different from one another (Piotrowska *et al.*, 2001; Piotrowska-Nitsche *et al.*, 2005). Differences in cleavage patterns can give rise to four cells within the embryo with different developmental potential (Piotrowska-Nitsche and Zernicka-Goetz, 2005) and this has been linked to differences in epigenetic marks such as methylation of histone H3R26 (mediated by the histone arginine methyltransferase CARM1) in the four blastomeres (Torres-Padilla, Parfitt, *et al.*, 2007). More recently, single-cell RNA sequencing performed on the individual blastomeres of the four cell stage mouse embryo directly revealed heterogeneity in the expression of genes including the transcription factor *Sox21*, which could bias cell fate towards extra-embryonic lineages in blastomeres where its expression was knocked down (Goolam *et al.*, 2016). Furthermore, it has been also shown that blastomeres at the four-cell stage differ in the binding kinetics of key transcription factors essential for early development, such as Sox2 (White, Angiolini, *et al.*, 2016). Despite this heterogeneity, it has been shown on a number of occasions that compromised embryos at this stage still have the ability to give rise to viable pups (Hillman, Sherman and Graham, 1972; Zernicka-Goetz, 1998), suggesting that whilst the cells may be biased towards a certain fate at these early stages, they are not yet fully committed, and hence can adapt to developmental perturbation.

1.1.2 The first cell fate decision and the formation of the blastocyst

At E2.5, a further cleavage division forms a morula comprised of eight blastomeres, which remain morphologically identical. At this time, the embryo undergoes its first major morphogenetic event, known as 'compaction'. This involves the flattening of the blastomeres as E-cadherin mediated cell adhesion increases (Hyafil *et al.*, 1980), tension at the cell-medium interface increases (Maitre *et al.*, 2015) and they become more tightly associated (Calarco and Brown, 1969; Ducibella and Anderson, 1975; White, Bissiere, *et al.*, 2016). Compaction occurs concomitantly with polarisation of the blastomeres, which acquire an apical domain which is free of cell-cell contact, in contrast to the basolateral domain which is closely associated with neighbouring cells (Ziomek and Johnson, 1981; Cockburn and Rossant, 2010). The apical domain established at this time is enriched for filamentous-actin (F-actin), a highly-conserved apical protein complex which includes PAR-polarity proteins, and atypical protein kinase C (aPKC) (Yamanaka *et al.*, 2006). Both aPKC and the PAR-polarity complex are important for the formation of this apical domain, and later inheritance of this domain by daughter cells after division governs cell fate (Korotkevich *et al.*, 2017), thus linking morphogenesis with tissue specification at this time.

Compaction and polarisation sets the stage for the next two rounds of cell division (from eight to sixteen cells, and then from sixteen to thirty-two cells respectively) (Fig. 1.1. A, B). If the cell divides along the apico-basal axis, then this division is asymmetric, and generates one 'outside' daughter cell, which inherits the apical domain and is exposed to the external environment on one side, and one 'inside' daughter which is confined to the centre of the embryo and maintains cell-cell contact on all sides. The inheritance of the apical or basolateral domain from the mother cell results in the differential inheritance of molecular components in the daughters, making these cells different from one another. The picture is complicated by the fact that 'inside' cells can also be generated as a result of active cell internalisation, and engulfment (McDole *et al.*, 2011; Anani *et al.*, 2014). In contrast, if a cell divides perpendicular to its apico-basal axis, it forms two identical 'outside' cells which are molecularly indistinct. These outside cells go on to form the first extra-embryonic lineage of the embryo, the TE, whilst the inside cells form the ICM (Johnson and Ziomek, 1981; Johnson and McConnell, 2004; Rossant and Tam, 2009).

The molecular mechanisms that underpin this first cell fate decision and specification of the TE have been well studied. The transcription factor, Cdx2, is expressed exclusively in the TE and is required for its formation in the mouse embryo (Niwa *et al.*, 2005; Strumpf *et al.*, 2005). Cdx2 mRNA is localised to the apical domain of polarised cells in the compacted embryo, and thus it can be unequally inherited between two daughters when a cell divides asymmetrically. As a result, the inheritance of higher levels of Cdx2 mRNA by outside cells has been proposed to lead to an upregulation of the TE fate program in these blastomeres (Jedrusik *et al.*, 2008; Skamagki *et al.*, 2013).

The Hippo/YAP signalling pathway has also been linked to the first cell fate decision, through the transcription factor Tead4. In embryos which lack Tead4, the TE does not become specified and Cdx2 is downregulated (Yagi *et al.*, 2007; Nishioka *et al.*, 2008). YAP1 can bind to Tead 4 when it is in turn bound to DNA, and is an essential co-factor required for Tead4 to initiate downstream transcription (Nishioka *et al.*, 2009). In an un-phosphorylated state, YAP can translocate to the nucleus and initiate the transcription of TE-specific genes such as Cdx2 and Gata3 by associating with Tead4. However, when it is phosphorylated by LATS1/2, a Hippo pathway kinase, it cannot enter the nucleus and thus the TE-specification program is not initiated (Nishioka *et al.*, 2009; Ralston *et al.*, 2010). This is the case for inside cells, which do not become TE.

But what links differential Hippo/YAP pathway activity in inside versus outside cells of the morula? The key to this is thought to be the differential localisation of the membrane-associated Hippo pathway component Angiomotin (Amot). In outside cells, polarity determinants anchor Amot to the apical domain of the cell, whereas in inner cells, which lack these polarity determinants, Amot is

phosphorylated and evenly distributed throughout the cell membrane at adherens junctions (Hirate *et al.*, 2013; Leung and Zernicka-Goetz, 2013). In inside cells, Amot is free to bind YAP and thus prevents its translocation to the nucleus and it can also phosphorylate YAP at Lats1/2 phosphorylation sites. In contrast, in outside cells, Amot is sequestered at the apical domain and thus it cannot bind YAP. Here, YAP is free to enter the nucleus and initiate the TE-specific transcription, so outside cells acquire this fate (Leung and Zernicka-Goetz, 2013; Bedzhov, Graham, *et al.*, 2014).

At the 32-cell stage, the TE precursors have become specified and are positioned on the outside of the embryo. As the embryo undergoes its next cleavage, the blastocoel cavity opens via the passive diffusion of water across an osmotic gradient from the outside to the inside of the embryo, which acts in combination with the active transport of water by aquaporins present on the apical and basolateral sides of the nascent TE cells (Barcroft *et al.*, 2003; Bedzhov, Graham, *et al.*, 2014). The tight junctions present between these cells result in the formation of a polarised epithelium, which seals fluid inside the expanding cavity (Ducibella *et al.*, 1975). The formation of the blastocoel cavity separates the TE into two subpopulations; the polar TE which surrounds the ICM, and the mural TE which surrounds the emerging cavity. The expansion of this cavity also pushes the ICM to one side of the embryo, establishing the embryonic-abembryonic axis of the blastocyst (Bischoff, Parfitt and Zernicka-Goetz, 2008). By the 64-cell stage, a hollow, spherical blastocyst has formed, which continues to expand as the number of cells increases.

1.1.3 The second cell fate decision and blastocyst maturation

After segregation from the TE, the ICM becomes separated into two distinct cell types; a second extra-embryonic lineage known as the PE, and the cells of the embryo proper, the EPI cells. A lot less is known about the mechanisms underpinning the second cell fate decision compared with the first, and conflicting hypotheses exist in the literature about how much a cell's position within the ICM can influence its fate as opposed to the activity of specific genes (Hermitte and Chazaud, 2014).

Like the first cell fate decision, lineage specification in the ICM is coupled to spatial segregation of the cells, which occupy characteristic domains within the blastocyst. Whilst the EPI cells form an apolar mass which is in contact with the mural TE, the PE cells form an epithelial layer surrounding them, and in contact with the blastocoel cavity (Fig.1.1. B). The EPI cells can be distinguished from the PE at the blastocyst stage by the expression of transcription factors associated with pluripotency, such as Pou5f1/Oct4, Sox2, and Nanog (Nichols *et al.*, 1998; Avilion *et al.*, 2003; Chambers *et al.*, 2003; Mitsui *et al.*, 2003). In contrast, PE cells upregulate endodermal genes including *Sox17, Pdgfrα*, *Gata4* and *Gata6* (Molkentin *et al.*, 1997; Koutsourakis *et al.*, 1999; Niakan *et al.*, 2010). Nanog and Gata6 are

the earliest markers of EPI and PE respectively, and they mutually repress each other, to reinforce either the EPI or PE cell fate program downstream (Chazaud *et al.*, 2006). In the undifferentiated blastomeres of the morula, both markers are expressed, but by the 32-cell stage their expression becomes mutually exclusive and Nanog and Gata6 are restricted to EPI and PE precursors respectively (Plusa *et al.*, 2008; Guo *et al.*, 2010).

The specification of EPI and PE lineages is heavily dependent on the interaction of these genes with the Fibroblast Growth Factor (FGF) signalling pathway. Nanog-positive EPI precursor cells in the ICM secrete FGF4 ligand, whilst Gata6-positive PE precursors express FGF-receptor2 (Fgfr2) at high levels (Frankenberg *et al.*, 2011; Ohnishi *et al.*, 2014). The transduction of the FGF signal in Gata6-positive cells initiates the downstream Mitogen-activated protein kinase/Extracellular signal- regulated kinase (MAPK/ERK) pathway, which promotes a program of PE differentiation. Thus, when FGF/ERK signalling is inhibited, no PE is specified. Conversely, the addition of exogenous FGF4 ligand or overexpression of the gene results in the opposite phenotype, with each cell becoming PE and no EPI being formed (Feldman *et al.*, 1995; Arman *et al.*, 1998).

Although this has traditionally considered to be a separate specification event from the segregation of the TE and ICM, the first and second cell fate decisions are not independent. At morula stage, inside and outside cells are generated by two waves of asymmetric cell division, which not only segregates ICM and TE, but also influences how EPI and PE are segregated in the ICM (Fig. 1.1. A, B). Cells internalised in the first wave switch on Fgf4 expression and are thus predisposed towards EPI fate, whilst cells internalised later instead inherit higher levels of Fgfr2 and are thus biased towards the PE (Morris *et al.*, 2013; Krupa *et al.*, 2014).

Although this mechanism biases cell fate choice in the ICM, it does not predetermine it. It has been shown that unequal numbers of inside cells can be generated between the first and second waves of asymmetric division, and thus the number of cells predisposed to one fate over the other can be unequal. The fate of ICM cells must therefore be plastic, which ensures that a critical minimum number of EPI cells has been generated by E4.5 in order for development to progress normally (Morris, Guo and Zernicka-Goetz, 2012). There is evidence that EPI precursors are more restricted in their fate potential than PE precursors, which have been shown to contribute to embryonic lineages after implantation, as well as extra-embryonic tissue (Kwon, Viotti and Hadjantonakis, 2008; Grabarek *et al.*, 2012). This is thought to be the result of cells in the second wave of internalisation having increased exposure to the TE cell fate programme in outside cells, and thus inherit a greater flexibility in fate choice (Morris *et al.*, 2013).

Initially, the Nanog-positive EPI precursors and the GATA6-positive PE precursors are distributed in a 'salt and pepper' fashion through the ICM, before sorting into the correct position to form two separate tissues within the blastocyst (Chazaud *et al.*, 2006; Rossant and Tam, 2009). The cells of each lineage sort into the correct spatial positions by a combination of active cell migration, apoptosis of incorrectly positioned cells, and positional induction (Plusa *et al.*, 2008; Meilhac *et al.*, 2009).

Once the three cell lineages have successfully become segregated, the blastocyst continues to expand and hatches from the glycoprotein shell that surrounds it, which is known as the 'zona pellucida'. Successful hatching acts as a checkpoint to permit further development, and the mature blastocyst goes on to elongate in preparation for implantation into the uterus (Bedzhov, Graham, *et al.*, 2014).

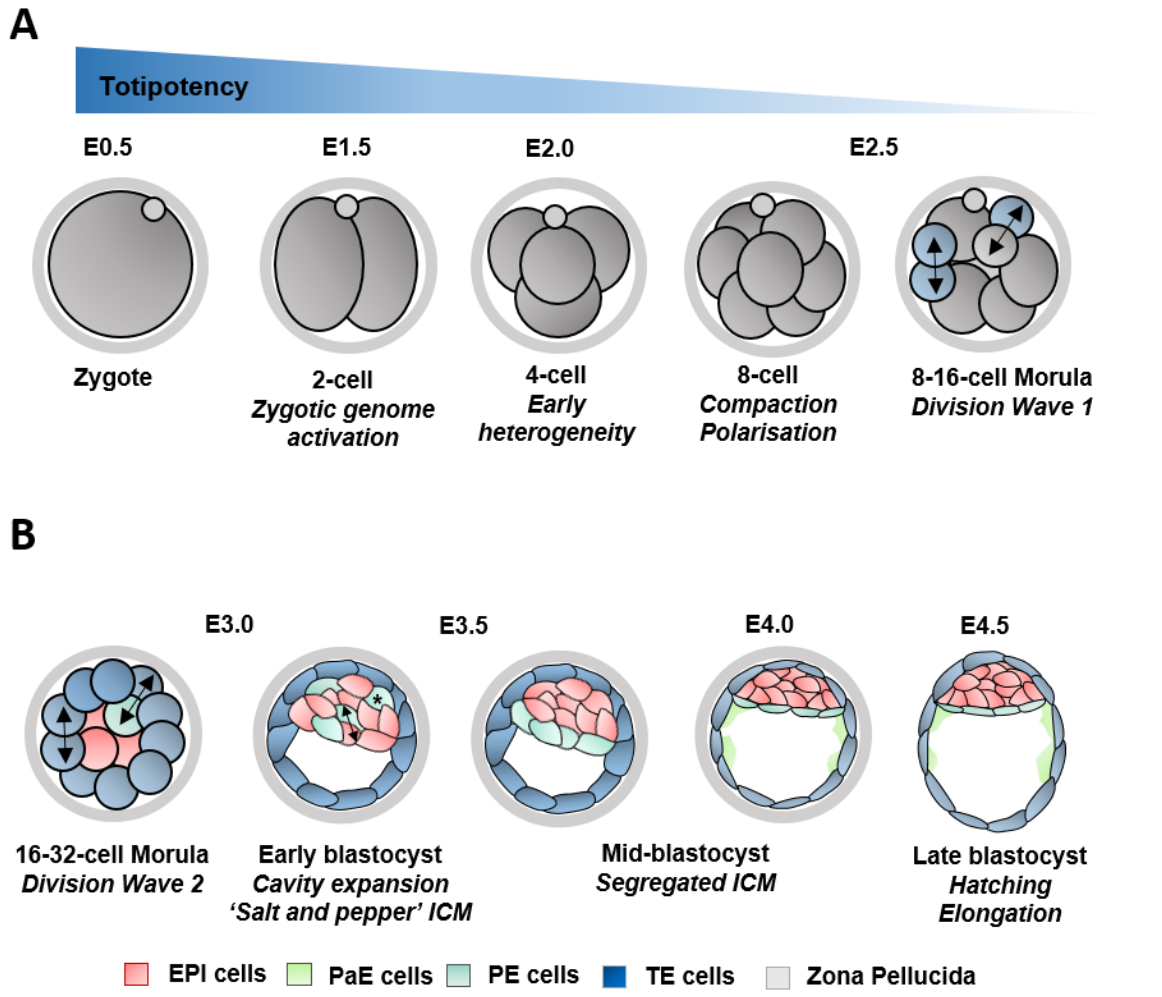

Fig. 1.1. Pre-implantation mouse embryo development (A) Schematic representation outlining the first 2.5 days of mouse embryo development, from fertilisation to E2.5, and the first wave of asymmetric cell division. Grey cells, totipotent; blue cells, biased towards TE fate. Grey ring = zona pellucida. Arrows indicate the angle of cell division. **(B)** Schematic representation outlining the transition from morula to blastocyst, and the second wave of asymmetric cell division, plus

EPI/PE specification in the ICM. Blue cells, TE cells; red cells, biased towards EPI fate; green cells, biased towards PE fate. Grey ring = zona pellucida. Arrows show the direction of cell division. Asterisk indicates a cell which will undergo apoptosis.

1.2 Implantation of the embryo

When the blastocyst has hatched, expanded, and enters the uterine cavity, it is ready to implant into the maternal tissues. Oestrogen and progesterone released from the ovaries prepares the uterus for implantation, and makes the tissue receptive to invasion by the embryo (Ma *et al.*, 2003). The uterine lumen narrows to bring the embryo close to the luminal epithelium, which interacts with the TE via microvilli. This initially loose attachment becomes stabilised by interaction between cadherins and integrins at the interface between the TE and the luminal epithelium (Basak, Dhar and Das, 2002; Xiao *et al.*, 2002). This first contact between the blastocyst and the maternal tissues initiates the terminal differentiation of the mural TE into trophoblast giant cells (TGCs) and induces regulated apoptosis in the luminal epithelium at the site-of-contact (Parr, Tung and Parr, 1987). These TGCs invade the uterine stroma and secret factors to promote the formation of decidual tissue (Bany and Cross, 2006). TGC subtypes then induce angiogenesis at the site of implantation to mediate the exchange of nutrients, gas, and waste between the embryo and the mother (Simmons, Fortier and Cross, 2007). At the same time, the polar TE initiates proliferation to form the extra-embryonic ectoderm tissue (ExE) and the ectoplacental cone. The ExE contains a self-renewing population of progenitor cells, known as trophoblast stem cells (TSCs) and will later give rise to the placental tissue.

1.3 Post implantation mouse embryo development

1.3.1 Egg cylinder morphogenesis

Implantation initiates a burst of cell proliferation, which results in the growth of both embryonic and extra-embryonic tissues of the embryo, as well as a dramatic change in shape. At E5.0, the embryo has implanted into the uterine tissue and the blastocyst transforms into a structure known as the egg cylinder within 24 hours (Bedzhov, Graham, *et al.*, 2014). The polar TE of the blastocyst proliferates to give rise to the ExE tissue, which occupies the proximal side of the embryo, close to the site of implantation. Immediately adjacent to the ExE is the EPI, which becomes a cup-shaped, polarised epithelium with a lumen at its centre. At the same time, the PE also expands to form the parietal endoderm (PaE), which lines the surface of the mural TE, and the visceral endoderm (VE), (Fig. 1.2) (Bedzhov, Graham, *et al.*, 2014). The VE, which will later form the yolk-sac, not only secretes basement membrane components and maintains the embryo's shape (Miner *et al.*, 2004), but it also plays a critical role in early body axis patterning. This tissue forms a monolayer of epithelial cells which

envelops the nascent ExE and the now cup-shaped EPI, resulting in the formation of a cylinder-shaped structure with a cavity running through its centre, known as the pro-amniotic cavity. The apical surface of the cells of the EPI and ExE face into this cavity, whilst the basal sides face the basement membrane that separates the EPI and ExE from the VE (Fig.1.2).

This cylinder shape is unique to the post-implantation development of rodents. The embryos of other mammals (including humans) instead form a planar structure with a flat, circular epiblast sandwiched between the hypoblast (equivalent to the VE) underneath, and the trophoblast on top, closest to the site of implantation (Moore, Persaud and Torchia, 2013; Rossant, 2015). However, the topology of the tissues within this so-called 'blastodisc' and the egg cylinder are the same, as is the formation of a cavity at the centre of the embryo (Deglincerti *et al.*, 2016; Shahbazi *et al.*, 2016), making the mouse embryo a relevant model for the study of mammalian post-implantation development.

In order to form the characteristic cup-shaped epithelium associated with the EPI of the egg cylinder, the apolar, EPI cells of the pre-implantation blastocyst must first become polarised, and form a lumen at their centre. EPI cell polarisation is induced by β1-integrin signalling, mediated by laminin present in the basement membrane, which is secreted by the PE and TE and envelopes the EPI as the blastocyst implants. As the cells polarise, the Golgi apparatus, centrosome and F-actin become apically localised, whilst the nucleus moves basally. The accumulation of F-actin at the apex of each cell results in apical constriction, forcing the cells into a triangular shape, so that they meet at a common central point and form a 'rosette-like' structure in the tissue (Fig. 1.2.). The cells of this 'rosette-like' structure also express the negatively charged silomucin protein, podocalyxin (Podxl) at their apical surfaces. The charge repulsion force generated by the accumulation of this protein at apical cell membranes in the centre of the rosette forces these membranes apart to give rise to a small lumen (Bedzhov and Zernicka-Goetz, 2014; Bedzhov, Graham, *et al.*, 2014). This process can be mimicked *in vitro* when stem cells derived from the EPI, known as embryonic stem cells (ESCs), or intact epiblasts are embedded in extracellular matrix (ECM).

The importance of the polarisation cues provided by the ECM in guiding this process is highlighted by the fact that when the laminin-γ1 subunit is knocked out in the early embryo, the basement membrane between the EPI and the developing VE fails to assemble, and the embryo dies during implantation (Smyth *et al.*, 1999). Furthermore, the absence of the β1-integrin receptor also leads to a defect in the EPI (Stephens *et al.*, 1995) and β1-integrin knockout ESCs are incapable of forming a lumen when embedded in ECM (Bedzhov and Zernicka-Goetz, 2014). In the embryo, the lumen at the centre of the EPI expands as the egg cylinder elongates, and subsequently fuses with an independent cavity which forms at the centre of the ExE. This cavity is also lined by Podxl which is localised to the

apical surfaces of ExE cells, and so may also form by a similar process of cell polarisation and membrane repulsion (Bedzhov and Zernicka-Goetz, 2014). However, this process in the ExE remains largely unexplored (Bedzhov, Graham, *et al.*, 2014).

In synchrony with this morphogenetic event at implantation, the cells of the EPI tissue also undergo transcriptional and epigenetic change to restrict their fate potential. The EPI cells transition from a 'naïve' pluripotent state, capable of giving rise to all tissues of the foetus to a 'primed' state of pluripotency (Nichols and Smith, 2009). During this process, the EPI cells begin to express early differentiation markers for the first time, including FGF5 (Pelton et al, 2002). The cells also acquire methylation marks on their DNA, and in females, one X-chromosome becomes silenced (Heard, 2004). Exit from the 'naïve' state of pluripotency primes the cells towards differentiation, and sets the stage for body axis patterning of the EPI to begin.

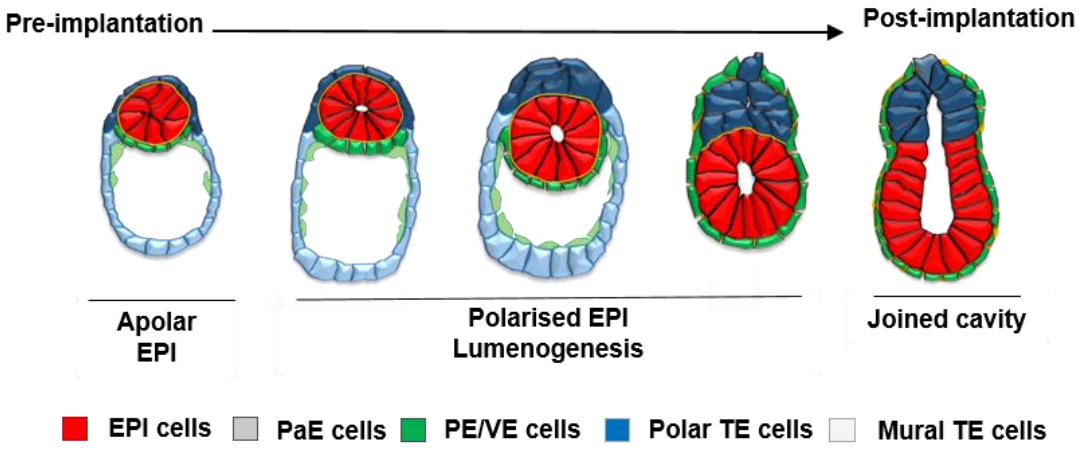

Fig. 1.2. Schematic representation of the morphogenetic events involved in the blastocyst-to-egg cylinder transition, which occurs as the embryo implants into the uterus. Red cells, epiblast; dark blue cells, polar trophectoderm/ extra-embryonic ectoderm; light blue cells, mural trophectoderm; green cells, primitive endoderm/visceral endoderm cells; light green cells, parietal endoderm.

1.3.2 Symmetry breaking and DVE migration

Before overt axial patterning, the egg cylinder first becomes patterned along the proximal-distal axis, which is established at implantation. From E5.0 to E5.5, the egg cylinder elongates along this axis as a result of growth and proliferation of all three of its constituent tissues and the pro-amniotic cavity expands through the contiguous EPI and ExE. The configuration of the EPI, ExE and VE in the egg cylinder facilitate signalling interactions between these tissues which are critical for the tissue patterning events which lay the foundations for the body plan.

The VE is first of the three tissues to become clearly subdivided into several distinct populations, which are characterised by the expression of different molecular markers (Perea-Gomez *et al.*, 2007; Pfister, Steiner and Tam, 2007; Trichas *et al.*, 2012). This subdivision results from the interaction between signals produced by the EPI, and signals from the ExE which induce differences in gene expression to distinguish the VE overlying the ExE from the VE overlying the EPI. At the centre of this is the TGFβ ligand Nodal, which is first expressed in the EPI and PE of the blastocyst at E3.5, and persists through the peri-implantation stages (Papanayotou and Collignon, 2014). Nodal is secreted from the EPI cells in a precursor form which must be processed before the signal can be transduced. The secretion of the pro-Nodal protein induces the expression of pro-Nodal processing factors Furin and Pace4/Pcsk6 in the ExE, which cleave the Nodal precursor protein secreted by the EPI to form mature Nodal. Mature Nodal can then signal to the VE covering the EPI and results in repression of genes associated with the extra-embryonic VE (including *Gata4*, and *Hnf4)* (Beck *et al.*, 2002; Tam and Loebel, 2007).

Signals from the EPI and ExE are also important for the induction of a specialised population of VE cells at the distal tip of the embryo, named the distal visceral endoderm (DVE). These cells are morphologically distinct from neighbouring VE cells, as they convert from squamous to a columnar epithelium, and increase in apicobasal height when compared with the cells in the rest of the tissue. This results in tissue thickening at the distal tip of the embryo (Rivera-Pérez, Mager and Magnuson, 2003; Srinivas *et al.*, 2004). Nodal produced by the EPI once again signals to the overlying VE tissue, to induce the phosphorylation of the intracellular effector, SMAD-2. In turn, this initiates the expression of DVE marker genes including expression of the transcription factors Hex, FOXA2 and LIM1 (Waldrip *et al.*, 1998; Perea-Gomez *et al.*, 1999; Yamamoto *et al.*, 2009). Together, these factors induce the production of Nodal antagonists, Cerberus-like protein 1 (Cer-l) and Left-right determining factor 1 (Lefty1), plus the canonical Wnt antagonist, Dikkopf1 (Dkk1), which are also characteristic markers of the DVE population (Fig. 1.3. A) (Yamamoto *et al.*, 2004; Pfister, Steiner and Tam, 2007). Secretion of these factors from the DVE at the distal tip of the embryo inhibits Nodal in the distal part of the EPI, leading to a gradient of signalling activity which is high in the proximal EPI and low in the

distal EPI (Brennan *et al.*, 2001; Arnold and Robertson, 2009). At the same time, the ExE secretes its own signal, BMP4, which is high in concentration at the proximal side of the embryo (Winnier *et al.*, 1995; Lawson *et al.*, 1999). This signal is thought to restrict the specification of the DVE cells to the distal tip of the embryo only. If the ExE is removed from the egg cylinder, the domain of expression of DVE markers is expanded to a larger population of VE cells, as opposed to being restricted to those only at the distal tip (Rodriguez *et al.*, 2005; Richardson, Torres-Padilla and Zernicka-Goetz, 2006).

Whilst Nodal is essential for DVE formation (Mesnard, Guzman-Ayala and Constam, 2006), canonical Wnt signalling is also thought to be involved in the specification of this tissue. B-catenin mutant embryos have impaired DVE formation, but loss of Wnt3 does not affect this tissue (Liu *et al.*, 1999; Huelsken *et al.*, 2000). The discovery that Nodal signalling in this context requires a specific co-factor, the epidermal growth factor-Cripto-FRL1-Cryptic (EGF-CFC) protein Tdgf1/ Cripto, and later that this gene is a downstream target of β-catenin might link the two signalling pathways in this context, but knocking out Tdgf1/Cripto affects DVE migration only, as opposed to its formation (Ding *et al.*, 1998).

Subsequent to their specification at E5.5, the DVE cells proliferate, to give rise to a population which become motile, and collectively migrate as a group from the distal tip to the future anterior of the embryo (Morris *et al.*, 2012; Stower and Srinivas, 2014). They cease their migration when they are parallel with the boundary between the EPI and the ExE (Rivera-Pérez, Mager and Magnuson, 2003), and in their new anterior location, they are called the 'anterior visceral endoderm' (AVE). The movement of this source of inhibitors effectively converts the proximal-distal asymmetry across the EPI into the future head-tail axis of the embryo (Perea-Gomez *et al.*, 2004) (Fig 1.3. B).

What drives the migration of the AVE cells to the future anterior? Although it has been proposed that a localised increase in the rate of cell proliferation in the VE might lead to passive displacement of AVE cells towards the anterior (Yamamoto *et al.*, 2004), given that the AVE translocates within 5-7 hours (Rivera-Perez, Mager and Magnuson, 2003; Srinivas *et al.*, 2004), it is thought that active cell movement might be involved. DVE/AVE cells extend oriented filipodia suggesting they migrate actively towards the anterior (Srinivas *et al.*, 2004), and there is evidence that AVE tissue contains 'leader cells' which, when ablated, results in a failure in migration (Morris *et al.*, 2012). Interestingly, it has recently been shown that specifically deleting Nodal expression in the VE feeds back to reduce Nodal expression in the EPI, and also results in failed AVE migration, suggesting that it is Nodal signalling in the VE that drives the migration event (Kumar *et al.*, 2015).

What determines the direction of AVE migration is ultimately unknown, though it can be directed to one side of the embryo by experimental manipulation of Wnt and Nodal signalling (Kimura-Yoshida *et*

al., 2005; Tam and Loebel, 2007). There is some evidence to suggest that the earliest signs of anterior-posterior polarity might be as early as blastocyst stage, where asymmetry in gene expression has been detected in cells of the PE (Takaoka *et al.*, 2006; Torres-Padilla, Richardson, *et al.*, 2007). This evidence, combined with the fact that the contribution of different cell clones from the ICM to the VE is asymmetric (Weber *et al.*, 1999), may indicate that in fact, symmetry breaks earlier than at egg cylinder stages, and AVE migration is simply the first morphogenetic event in line with this (Tam and Loebel, 2007). However, if this is the case, the factor that lies upstream of DVE migration and links this to asymmetries observed at pre-implantation stages remains unclear.

1.3.3 Primitive streak formation and gastrulation

Once symmetry has become broken in the egg cylinder, the body plan can be established. Gastrulation is the process by which the three germ layers; the ectoderm, the endoderm and the mesoderm are formed, and this process transforms the embryo from a two-layered structure to a trilaminar one (Stern, 2004). The three germ layers are the precursors from which all tissues of the future body are formed and thus, their segregation is an important step in the establishment of the body plan. In amniotes, the onset of gastrulation is marked by the formation of a specialised structure, known as the primitive streak, which is formed at the posterior side of the epiblast (Stower and Bertocchini, 2017). The formation of the primitive streak occurs after a period of rapid cell proliferation in the EPI (Snow, 1977), at E6.5.

It is important that the primitive streak forms in the correct part of the EPI in order that the germ layers are positioned correctly, and so gastrulation is tightly coupled to anterior-posterior (A-P) axis establishment in the embryo. In the mouse, the primitive streak forms at the proximo-posterior side of the EPI, at the junction with the ExE, and extends distally as gastrulation progresses (Williams *et al.*, 2013). It is marked by the expression of the T-box transcription factor T/Brachyury (T/Bra), which is expressed in the cells of the nascent mesoderm, in a characteristic triangular-shaped pattern at the posterior side of the embryo (Wilkinson, Bhat and Herrmann, 1990; Herrmann, 1991; Wilson *et al.*, 1995). T/Bra expression can be first detected at the mRNA level at E6.0 in a concentric ring around the embryo, before it becomes confined to the proximo-posterior at E6.5 (Rivera-Pérez and Magnuson, 2005; Rivera-Pérez and Hadjantonakis, 2015).

Many of the same signals responsible for DVE induction are also implicated in the formation of the primitive streak. At this stage in mouse embryogenesis, the DVE/AVE is fully translocated to the anterior, and anterior-posterior polarity has therefore become established. At the anterior side of the embryo, the AVE acts as a signalling centre which continues to secrete inhibitors of Nodal and Wnt,

restricting the activity of these pathways to the proximo-posterior region of the EPI (Tam and Loebel, 2007; Arnold and Robertson, 2009; Rivera-Pérez and Hadjantonakis, 2015). Both Nodal and Wnt signalling are required for primitive streak specification, with Nodal and Wnt mutant embryos failing to gastrulate or specify germ layers correctly (Liu *et al.*, 1999; Brennan *et al.*, 2001; Camus *et al.*, 2006). Wnt3, which is directly upstream of T/Bra first becomes expressed in the posterior VE at E5.5 and is subsequently expressed in the posterior EPI. It has been shown that such localised expression of Wnt3 precedes T/Bra induction at the primitive streak, and both embryonic and extra-embryonic sources of Wnt3 are required for primitive streak induction and maintenance (Rivera-Pérez and Magnuson, 2005; Tortelote *et al.*, 2013; Yoon *et al.*, 2015).

At the same time, BMP4 secreted from the ExE is also required at the posterior to initiate mesoderm specification and induce primitive streak markers (Winnier *et al.*, 1995; Donnison *et al.*, 2005). BMP4 production in the ExE is in fact induced and maintained by Nodal production from the EPI, which induces Wnt3 and also feeds back on itself to promote Nodal expression in the EPI (Ben-Haim *et al.*, 2006). These discoveries led to the proposal of a model where a positive feedback loop of signalling interactions between the EPI and the ExE robustly specifies the molecular identity of the proximo-posterior EPI (Tam and Loebel, 2007; Arnold and Robertson, 2009; Rivera-Pérez and Hadjantonakis, 2015), whilst the secretion of signalling inhibitors by the AVE prevents the formation of multiple primitive streaks throughout the EPI (Perea-Gomez *et al.*, 2002) (Fig. 1.3.2 B).

1.3.4 Epithelial to mesenchymal transition

Upon establishment of the primitive streak at the posterior, gastrulation progresses with the segregation of the ectoderm, endoderm and mesoderm. This occurs as the cells of the EPI delaminate from the columnar epithelium and ingress through the streak to form a new tissue layer within the embryo (Rivera-Pérez and Hadjantonakis, 2015). In order to delaminate from the EPI, cells of the future mesoderm must undergo a process of epithelial-to-mesenchymal transition (EMT) and then migrate away from the streak as a sheet of mesenchymal cells which are directed by a gradient of FGF from posterior to anterior (Ciruna *et al.*, 1997; Ciruna and Rossant, 2001). In order for the cells of the EPI to ingress and undergo EMT, the basement membrane separating the EPI and the VE in the egg cylinder must be degraded locally at the posterior side, so the cells can escape and migrate between the two tissues. Subsequent to this, the cells alter their behaviour and shape to become motile (Williams *et al.*, 2013). Wnt, Nodal, and FGF signals initiate the EMT-program in the cells, which express marker genes such as the transcription factors Snai1 and Eomes, and the intermediate filament protein Vimentin. Snai1 represses tight-junctional and adhesion proteins such as E-cadherin, allowing the cells to break away from the tightly ordered columnar epithelium (Cano *et al.*, 2000;

Carver *et al.*, 2001; Thiery *et al.*, 2009). Snai1 is induced by FGF signalling (Ciruna and Rossant, 2001) and its expression results in loss of apico-basal polarity, changes in cell shape, and cell motility at the streak.

The timing and position at which cells ingress through the streak determines their subsequent fate, with cells from the very posterior primitive streak being first to ingress, giving rise to extra-embryonic mesoderm, whilst cells from the mid primitive streak ingress later and contribute to cardiac, lateral plate, and paraxial mesoderm. The latest cells to ingress do so through the anterior primitive streak and contribute to axial mesoderm (including the notochord) and definitive endoderm (Tam and Beddington, 1987; Tam, Kanai-Azuma and Kanai, 2003).

1.3.5 Primordial germ cell specification

Whilst the majority of cells in the proximo-posterior EPI ingress through the primitive streak to contribute to the germ layers, a small population of cells do not ingress, and instead are fated to become the primordial germ cells (PGCs)- the precursor cells to the gametes. These cells are totipotent, and can give rise to an entirely new individual at fertilisation. PGCs first become specified in the mouse embryo at E6.25, then subsequently migrate to the genital ridges by E10.5.

The cells which are assigned PGC fate as opposed to contributing to the somatic lineages are positioned at the very proximal end of the primitive streak, adjacent to the interface between the EPI and the ExE (Lawson and Hage, 1994). In this location, the cells sense BMP4 secreted from the ExE, which acts through a SMAD-dependent mechanism to activate the expression of three key transcription factors, Blimp1 (Prdm1), Prdm14 and AP2-γ which act in synergy to drive PGC fate (Lawson *et al.*, 1999; Ying, Qi and Zhao, 2001; Ohinata *et al.*, 2005; Yamaji *et al.*, 2008; Weber *et al.*, 2009; Günesdogan, Magnúsdóttir and Surani, 2014). BMP4 directly induces Blimp1 and Prdm14, whilst AP2-γ is induced by Blimp1 (Magnusdottir *et al.*, 2013). This transcriptional programme is then followed by the re-expression of pluripotency factors associated with the pre-implantation EPI, such as Nanog and Sox2 (Günesdogan, Magnúsdóttir and Surani, 2014; Murakami *et al.*, 2016). In addition to BMP, the Wnt signalling pathway has also been shown to confer competence on EPI cells to acquire PGC fate. Wnt3 mutant embryos cannot specify PGCs (Ohinata *et al.*, 2009), and these individuals also fail to gastrulate and specify the mesoderm, since T/Bra is a direct target of the Wnt pathway. T/Bra is also required for the specification of PGCs (Aramaki *et al.*, 2013), and hence early PGCs in the epiblast are T/Bra positive. However, the question remains as to how the Wnt and BMP pathways are able to delineate between the specification of PGCs and the specification of mesoderm, given both pathways are required for each of these events (Günesdogan, Magnúsdóttir and Surani, 2014).

Interestingly, the position of the cells in the EPI seems to play a role in whether they will become PGCs. Although in normal circumstances only cells in the proximal EPI, at the posterior side will give rise to PGCs, it has been shown that if distal EPI cells are transplanted into this location, they can initiate the germ-cell specification program (Tam and Zhou, 1996).

In addition to the expression of PGC-specific transcription factors, PGCs also undergo substantial epigenetic changes to reprogram them back to a totipotent state and to make them different from the soma. By egg cylinder stage, the somatic cells of the EPI have undergone random X-chromosome inactivation as their fate becomes more restricted (Rastan, 1982; Takagi, Sugawara and Sasaki, 1982). PGCs re-activate the silenced X-chromosome, and also undergo global DNA demethylation, erasure of imprints, and alter their histone modifications (Hajkova *et al.*, 2002; Seki *et al.*, 2005). These epigenetic changes, which take place in the cells between E8.5 and E12.5, are not only important to induce totipotency in the cells but they also allow imprints to be re-established in the cells in a gender-specific manner, so that when they are passed onto the next generation, their expression depends on the parental origin of an allele (Surani, 2001).

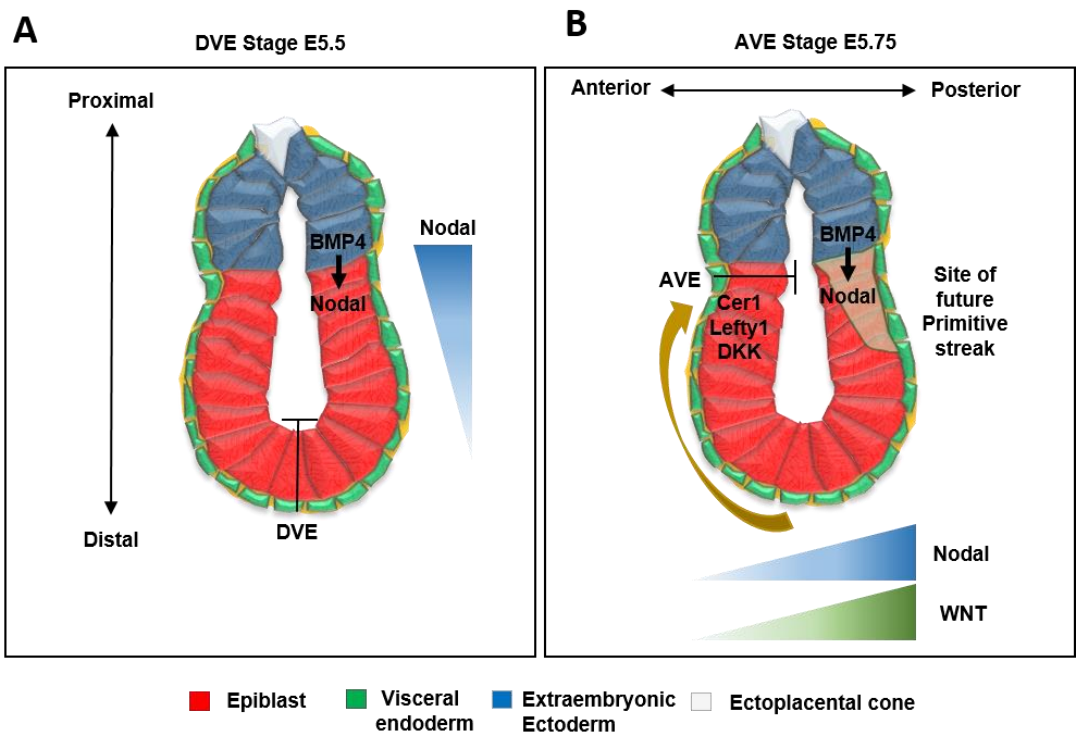

Fig. 1.3. Schematic representation of signalling interactions occurring between embryonic and extra-embryonic tissues leading to symmetry breaking in the mouse egg cylinder. Red cells, epiblast; dark blue cells, extra-embryonic ectoderm; grey cells, ectoplacental cone; green cells, visceral endoderm cells. **(A)** The DVE stage egg cylinder at E5.5 days of development. The proximal-distal axis of the embryo runs from ExE to EPI to DVE. BMP4 and Nodal signalling activity is high in the proximal EPI but is inhibited at the distal side by antagonists secreted from the DVE cells. **(B)** The AVE stage egg cylinder

at E5.75 days of development. The proximal-distal asymmetry in signalling activity is converted to the future anterior-posterior axis by active migration of the DVE to the anterior of the embryo (indicated by the yellow arrow). Nodal, Wnt, and BMP signalling activity in the EPI is restricted to the proximo-posterior region, which is the future site of the primitive streak.

1.3.5 Anterior-posterior axis specification in non-mammalian vertebrates

The general mechanism of axis patterning is broadly conserved across vertebrates, and in all cases, three major signalling pathways are involved: Nodal, Wnt and BMP. An initial event breaks symmetry, resulting in asymmetric Wnt and Nodal signalling activity. In turn, this signalling leads to induction of an anterior organiser, equivalent to the AVE in the mouse embryo. This organiser secretes BMP antagonists, and thus a gradient of BMP signalling activity is set up across the embryo. These morphogen signalling gradients direct initial cell differentiation towards anterior and posterior fates, drive morphogenesis, and thus initiate body patterning.

In addition to the mouse embryo, several other vertebrate species are routinely used as models to understand the development of the animal body plan, including Zebrafish (*Danio rerio)* the tropical frog (*Xenopus laevis)* and the chicken (*Gallus gallus)*. The events underpinning body axis specification in these species are described briefly below.

Amphbians (*Xenopus laevis*):

In *Xenopus*, similar to the mouse oocyte, the egg has an animal-vegetal axis which is laid down before fertilisation. The animal pole is defined as the side of the egg closest to the site of polar-body extrusion. At the ventral-most region, Dishevelled protein (Dsh), a component of the Wnt signalling pathway is sequestered during oogenesis (Larabell *et al.*, 1997). When the egg is fertilised, the sperm can enter anywhere on the animal side of the oocyte, but the point of sperm entry determines the future dorsal-ventral axis of the embryo, as the dorsal-most point lies directly opposite the point of sperm entry. After the egg has been fertilised but before cleavage has begun, a cytoplasmic rearrangement occurs within the egg. The outer cortex of the egg rotates with respect to the more denser yolk on the inside. This is referred to as 'cortical rotation'. The result of this is that the vegetal cortex (and the maternal mRNAs and proteins associated with it) moves towards the animal pole by approximately 30 degrees (Vincent and Gerhart, 1987). This re-localises Dsh to the dorsal side of the embryo, resulting in β-catenin stabilisation in this half of the embryo, and subsequent Wnt signalling activity (Miller *et al.*, 1999). In this way, cortical rotation establishes the dorsal-ventral axis of the *Xenopus* embryo perpendicular to the animal-vegetal axis of the egg, by establishing molecular asymmetries across this axis. Along the animal-vegetal axis, activity of TGF-β signalling components VegT and Veg1 establishes a gradient of TGF-β along this axis. Where activity of Wnt and TGF-β

signalling intersect, at the dorsal and vegetal-most region, cells are induced to form the 'Nieuwkoop centre'(Gerhart *et al.*, 1989). In turn, the Nieuwkoop centre induces the anterior 'organiser', which secretes inhibitors of BMP and Wnt. The side of the embryo where the organiser is located becomes the future anterior, whilst the opposite side develops into mesoderm and becomes the posterior. The amphibian 'organiser' was named as such because of its ability to organise a secondary axis. Famously, it was discovered by Hans Spemann and Hilde Mangold, who demonstrated that transplantation of this tissue, which is located at the blastopore lip, to a host embryo, leads to the formation of 'twins' (Spemann and Mangold, 1924).

Zebrafish (*Danio rerio*):

After the initial cleavages, the zebrafish embryo is made up of three distinct cell layers similar to the mammalian embryo. These are the 'yolk syncytial layer' (at the vegetal side), the 'enveloping layer' (at the animal pole of the embryo), with cells in between the two called the 'deep cells', which give rise to the embryo-proper. These three cell layers make up the blastoderm, which is initially located at the animal cap of the fertilised zebrafish egg (Gilbert, 2010).

Before gastrulation, the cells of the blastoderm expand to eventually envelop the entire yolk cell, in a process known as epiboly (Warga and Kimmel, 1990). Once the blastoderm has covered approximately 50% of the yolk, it begins to thicken at its margin. The thickened area is known as the 'germ ring' and is composed of the superficial epiblast tissue, and the hypoblast, equivalent to the VE, which forms underneath. At the future dorsal side of the embryo, these tissues intercalate, leading to further local thickening in this area, and the formation of the 'embryonic shield'. The formation of the embryonic shield is key to axial patterning in zebrafish, as, when transplanted, it can induce a secondary axis in a host embryo (Oppenheimer, 1936). The cells in the yolk syncytial layer which lie beneath those which form the embryonic shield accumulate β-catenin, and thus Wnt signalling is active in this part of the embryo (Schneider *et al.*, 1996). In this way, they are the equivalent of the Nieuwkoop centre in amphibians, with the cells of the embryonic shield therefore becoming equivalent to the amphibian organiser, which patterns the anterior-posterior axis (Gilbert, 2010).

Chick (*Gallus gallus*):

Similar to the zebrafish, the early chick embryo is a flat disc of cells, termed the 'blastodisc', which lie on top of the yolk of the egg. The blastodisc can be subdivided into three regions. The one-cell thick embryonic epiblast makes up the central part of the disc, and is known as the 'area pellucida'. This is surrounded by a peripheral ring of blastoderm cells, called the 'area opaca', and between the two lies the third area, known as the 'marginal zone'. The cells from these tissues form a continuous layer on

top of the yolk, whilst the cells of a second embryonic tissue, known as the hypoblast, form as a separate layer underneath the blastodisc (Gilbert, 2010). The 'primary hypoblast' tissue in the chick embryo and is formed by the delamination of cells from the epiblast, which first form isolated clusters underneath the EPI layer. Shortly after these clusters have formed, a sheet of cells originating from the posterior marginal zone (marked by a local thickening of the tissue known as the 'Koller's sickle') migrate anteriorly, and join the clusters of cells together to form a continuous tissue layer, known as the secondary hypoblast (Eyal-Giladi, Debby and Harel, 1992). The posterior marginal zone is thought to act as the avian equivalent of the Nieuwkoop centre, and is the region in the early embryo where active TGF-β signalling coincides with nuclear localisation of β-catenin. The secondary hypoblast can be thought of as the equivalent of the mammalian AVE, and like its equivalent tissue in the mouse, this tissue secretes inhibitors or Wnt and Nodal signalling such as DKK1 and Cerberus (Bertocchini and Stern, 2002). Thus, the anterior-posterior axis becomes patterned by the migration of the hypoblast to the future anterior of the embryo, where it continues to secrete antagonists of Wnt and TGF-β signalling, generating a gradient of signalling activity from anterior to posterior.

1.4 *In vitro* models in mammalian developmental biology

1.4.1 Stem cell derivation from the early embryo

As discussed above, the potency of constituent cells in an embryo is gradually restricted as development progresses; from a totipotent zygote, consisting of one cell which can give rise to a whole new individual, to the terminally differentiated cells of an adult which make up each lineage in the body. During pre-and post-implantation mouse development, the EPI cells represent two different stages of pluripotency. In the pre-implantation EPI, the cells are considered to be 'naïve' pluripotent, in that they can contribute to all embryonic tissues of the foetus, and do not express differentiation genes. These cells are not yet polarised, nor are have they silenced one of the X-chromosomes (if female). In contrast, cells of the post-implantation EPI are considered to be in a 'primed' state of pluripotency, where they can still contribute to any embryonic lineages of the foetus, but they have begun to express some differentiation genes (Nichols and Smith, 2009). These cells have undergone X-chromosome inactivation and have methylated DNA, and thus are primed for differentiation.

Each of these states, and the multipotent states of the extra-embryonic tissues present at this time in development can be captured *in vitro* in the form of embryonic and extra-embryonic 'stem cells'. Each of these stem cells, have the ability to self-renew indefinitely, and act as a tool in the study of developmental biology, as well as a source of cells for use in therapeutics (Morgani, Nichols and Hadjantonakis, 2017).

Embryonic stem cells

Embryonic stem cells (ESCs) can be derived from the pre-implantation blastocyst, and were the first stem cell line to be derived from the mouse embryo (Evans and Kaufman, 1981; Martin, 1981). They can contribute to all embryonic lineages when injected into the blastocyst and do not express any differentiation markers, and hence represent the 'naïve' pluripotent state of the early embryonic tissue *in vitro*. ESCs are transcriptionally equivalent to the EPI of the E4.5 mouse embryo (Boroviak *et al.*, 2014), although they can be derived as early as E0.5 (Delhaise *et al.*, 1996; Tesar, 2005). ESCs were first derived from blastocysts and grown in the presence of mouse embryonic fibroblasts (MEFs), in medium containing serum (Evans and Kaufman, 1981; Martin, 1981) and it was later discovered that the factors maintaining pluripotency in these conditions were the leukaemia inhibitory factor (LIF) and BMP signalling pathways (Williams *et al.*, 1988; Q. L. Ying *et al.*, 2003). These factors stimulate the expression of pluripotency related transcription factors in ESCs, including Oct4, Sox2, KLf4, and Nanog (Morikawa *et al.*, 2016; Morgani, Nichols and Hadjantonakis, 2017), which are characteristic of the pluripotent EPI. Additionally, BMP can inhibit signalling via the MAPK/ERK pathway, and thus prevent differentiation of the cells (Li *et al.*, 2012).

Knowledge of how the MAPK/ERK pathway can affect pluripotency has since led to the development of completely defined conditions for ESC culture, which do not rely on MEF feeders or serum-containing medium. Instead, these conditions contain LIF, plus two small molecule inhibitors, and are thus known as '2i' (2- inhibitors) conditions. One of these inhibitors blocks MAPK/ERK signalling and thus prevents differentiation, whilst the other, known as 'Chiron' inhibits GSK3β, a repressor of Wnt signalling (Q.-L. Ying *et al.*, 2003; Ying and Smith, 2003). Chiron is added to the medium cocktail in these conditions in order to promote active Wnt signalling, which in turn relieves repression of pluripotency factors by TCF3 (ten Berge *et al.*, 2011; Wray *et al.*, 2011). These defined conditions maintain ESCs in a homogeneous, 'ground state' of naïve pluripotency, which is in contrast to conditions based on serum and LIF alone, which promote heterogeneity and spontaneous differentiation (Ying *et al.*, 2008). However, it has been discovered that even in these 'ground state' cultures, some heterogeneity in cell potency can exist, with some rare populations of cells acquiring a state which is more similar to the totipotent cells of the 2-cell stage embryo (Morgani *et al.*, 2013).

ESCs also have an epigenetic state that reflects the EPI of the early embryo. They have hypomethylated DNA and an open chromatin structure, and female ESC lines have both X-chromosomes in an active state (Meissner *et al.*, 2008; Williams *et al.*, 2011; Chen *et al.*, 2016). However, when ESCs are maintained in culture for a sustained amount of time, they are prone to chromosome aberrations and aneuploidy. In addition, it has recently been shown that sustained self-renewal of ESC cultures leads

to acquisition of DNA methylation, suggesting that whilst ESCs are a useful tool to study the pluripotent state, they drift away from the state of the early EPI when maintained for too long in culture (Choi *et al.*, 2017; Yagi *et al.*, 2017).

The naïve pluripotent state can be induced in somatic mouse cells via 'reprogramming' which involves the forced expression of four key pluripotency genes: Oct4, Sox2, Klf4 and cMyc. These are referred to as the 'Yamanaka factors' and their forced expression results in the production of cells which share the characteristics and expression patterns of mouse ESCs but are derived from terminally differentiated cells, such as fibroblasts. Such cells have been termed 'induced pluripotent stem cells' (iPSCs) (Takahashi and Yamanaka, 2006).

Epiblast stem cells

In contrast to ESCs, epiblast stem cells (EPISCs) are more similar to the post-implantation mouse EPI (Brons *et al.*, 2007). They represent a 'primed' state of pluripotency *in vitro* (Nichols and Smith, 2009). They can be derived from the post-implantation egg cylinder from E5.0 to E8.0, but efficiency is decreased at later stages of development (Kojima *et al.*, 2014; Morgani, Nichols and Hadjantonakis, 2017). EPISCs are morphologically different from ESCs, forming flattened, epithelial colonies as opposed to compact, rounded colonies in culture, and they express some pluripotency markers, such as Oct4 and Sox2 in combination of early differentiation markers, such as FGF5, T/Bra, Lefty, Nodal, and Otx2 (Tesar *et al.*, 2007; Chenoweth, McKay and Tesar, 2010). In addition, they are cultured in the presence of FGF2 and Activin A, which prevents their differentiation into neural lineages (Camus *et al.*, 2006; Mesnard, Guzman-Ayala and Constam, 2006). Like the post-implantation EPI, they also have a distinct epigenetic status, and female lines have one inactive X-chromosome. Typically, they make little or no contribution to embryonic lineages when introduced into pre-implantation embryos, but will contribute to embryonic lineages when grafted into the post-implantation embryo, suggesting that they match this pluripotent state (Huang *et al.*, 2012).

Human pluripotent stem cells

As well as the mouse, pluripotent stem cells have been derived from several other mammalian embryos, including humans (Thomson *et al.*, 1996, 1998; Mitalipov *et al.*, 2006; Wang *et al.*, 2007). Unlike ESCs from the mouse, conventional human embryonic stem cells (hESCs) rely on Activin A and FGF2 in order to self-renew, and like EPISCs, have a flattened colony morphology. Although teratoma assays have shown that these cells can give rise to all three germ layers, they are prone to expression of early differentiation markers such as T/Bra and GATA 4, alongside the expression of pluripotency markers, and thus are considered to represent the 'primed' state of pluripotency in the human embryo

(Hough *et al.*, 2017). Somewhat surprisingly, attempts to derive hESCs using culture conditions known to support naïve mouse ESCs have been unsuccessful (Brons *et al.*, 2007), perhaps reflecting early interspecific differences between human and mouse pluripotent cells. However, more recently it has been shown that hESCs can be 'reprogrammed' back to a more naïve state by culturing the cells in a cocktail of inhibitors (Gafni *et al.*, 2013; Theunissen *et al.*, 2014), and can even be derived from the blastocyst using similar conditions (Lian *et al.*, 2016).

Human iPSCs can also be acquired from reprogrammed human somatic cells, via forced expression of transcription factors (Yu *et al.*, 2007). They carry the advantage that they can be derived from soma and thus do not require the destruction of human embryos. The potential of these cells has been harnessed by using them as a tool to study human organogenesis *in vitro*, which is discussed in the next section, below.

Trophoblast stem cells

Trophoblast stem cells (TSCs) represent the self-renewing population present in the ExE tissue of the mouse embryo at early post-implantation stages. They were first derived in from blastocyst-stage embryos, and can be maintained on a bed of MEF feeder cells and in medium containing serum and FGF4/2, pus the FGF co-factor, heparin (Tanaka *et al.*, 1998). If these factors are removed from the culture media, TSCs differentiate into TGCs, and a small population also give rise to other differentiated trophoblast lineages such as spongiotrophoblast or labyrinthine trophoblast (Yan *et al.*, 2001; Hughes *et al.*, 2004). Since their original derivation, two methods have been established for the culture of TSCs in defined conditions. These conditions are similar to those used for the culture of EPISCs and conventional hESCs (Kubaczka *et al.*, 2014; Ohinata and Tsukiyama, 2014).

Like mouse ESCs, TSCs will contribute to chimeric foetuses when injected into blastocyst stage embryos, but they are only capable of contributing to extra-embryonic, trophoblast-derived lineages such as those of the placenta (Tanaka *et al.*, 1998). There is evidence that ESCs which are forced to express the trophoblast marker Cdx2, or are knockout for Oct4 (Lu *et al.*, 2008) can be reprogrammed into TSC-like cells, but the extent to which these are similar to bone fide TSCs is still under debate, as these cells appear to retain epigenetic marks associated with ESCs, suggesting that the first-cell fate decision cannot be fully reversed *in vitro* (Cambuli *et al.*, 2014).

TSCs can also be derived from the embryos of other mammals, including the rabbit and the rhesus monkey (Vandevoort, Thirkill and Douglas, 2007; Tan *et al.*, 2011), but to date, no human TSC equivalent exists.

Extra-embryonic endoderm (XEN) cells

Like trophoblast stem cells, XEN cells are self-renewing cells which represent the extra-embryonic tissue of the mouse embryo. XEN cells can be derived either from the PE tissue present in the pre-implantation mouse blastocyst (Kunath *et al.*, 2005) or from the VE present in egg cylinder stage embryos (E5.5, E6.5 and E7.5)(Lin *et al.*, 2016). Additionally, XEN-like cells can be generated by overexpression of the transcription factors GATA4 and GATA6 in ESCs (Niakan *et al.*, 2013). Despite these different modes of derivation, pre-implantation XEN cells are very similar to post-implantation XEN cells, and very few differences have been demonstrated between them. Both pre-implantation XEN cells and post-implantation XEN cells frequently contribute to PaE rather than VE when introduced into chimeras, and this is reflected by the molecular markers that the cells express. Markers for PE such as GATA4, GATA6, Sox17, Sox7, and DAB2 are expressed, as are all the markers present in PaE. However, XEN cells only express a few VE markers such as Hnf4, whilst others, such as α-fetoprotein (αFP) are not present (Kunath *et al.*, 2005).

Although all XEN cell lines express these markers consistently, there is evidence that XEN cells actually represent a mixed population of different extra-embryonic endoderm lineages. In XEN cell cultures there are often two types of cell morphology- rounded, refractile cells and also cells with a more epithelial-like morphology, suggesting that two-different sub-populations exist. To date, there has been little investigation into the identities of these two sub-populations, but it has been shown that an individual cell can switch between different morphologies when in culture (Kunath *et al.*, 2005). It could be that the more refractile population is more pre-disposed to contribute to the PaE rather than the VE when introduced into chimeras and indeed, in the original paper where they were first derived, of all the clones that were stabilised, only one of these contributed purely to the VE, and this clone had an overwhelmingly epithelial morphology (Kunath *et al.*, 2005).

Several studies have shown that treating XEN cells with BMP4 can generate XEN cells with more VE-like characteristics (Artus *et al.*, 2012; Paca, C. A. Séguin, *et al.*, 2012), and that treatment with Nodal/ Cripto can upregulate the expression of AVE markers in XEN cells (Liu *et al.*, 2012). However, these XEN cells 'primed' for contribution towards the VE have never been introduced into chimeras, so their true developmental potential is unknown.

1.4.2 Use of ESCs to model development and organogenesis

Given their ability to differentiate into any tissue type, mouse ESCs, hESCs and iPSCs have been used extensively to model mammalian development and organogenesis. The mechanisms by which ESCs can be directed to differentiate into specific tissue types has been well studied, and the differentiation protocols that have been developed represent a useful system for the study of how tissue specification

events occur during embryonic development. Furthermore, the ability to derive almost any tissue from ESCs *in vitro* creates a source of cells for regenerative medicine and an opportunity for the development of drug screens and therapeutics (Murry and Keller, 2008).

Whilst previous efforts have resulted in the specification of pure tissue populations in 2D, more recent studies have focussed on the use of 3D culture techniques to generate complex organ-like structures, termed 'organoids' (Lancaster and Knoblich, 2014). Like real organs, organoids originate from a homogeneous starting population of cells, which differentiate into multiple tissue types and self-organise into structured tissue layers in culture. Such structures have been generated from pluripotent stem cells which model retinal tissue, brain tissue, intestine and kidney (Eiraku *et al.*, 2011; Spence *et al.*, 2011; Lancaster *et al.*, 2013; Takasato *et al.*, 2014), whilst others can be generated from adult tissue precursor cells such as those for liver (Huch *et al.*, 2013) and pancreas (Greggio *et al.*, 2013). Critically, these organoids not only resemble real organs in terms of their structure and constituent cells, they are also able to recapitulate some of the *in vivo* function of the organ they resemble (Lancaster and Knoblich, 2014). Thus, they are not only useful for the study of how the organ develops, but can also model disease, with cerebral organoids having been used to model congenital brain disorders such as microcephaly and Timothy syndrome when made using iPSCs derived from patients who suffer with these conditions (Lancaster *et al.*, 2013; Birey *et al.*, 2017).

Despite their huge utility, organoids are only capable of modelling the development of a single organ in isolation, as opposed to embryonic development as a whole. Developmental biologists have also attempted develop ESC culture techniques to model embryogenesis at early stages, before organs become specified. The great majority of these approaches rely on the aggregation of mouse ESCs into tissue masses known as 'embryoid bodies', which can recapitulate aspects of mouse embryogenesis and gastrulation.

After several days in serum-based culture, these structures are capable of inducing mesoderm and primitive streak-like populations in response to asymmetric Wnt signalling, and can break symmetry in a manner similar to that which underpins axial patterning in the mouse EPI (ten Berge *et al.*, 2008; Fuchs *et al.*, 2012; Tsakiridis *et al.*, 2014). Symmetry breaking and germ layer specification in these structures can occur with reproducible timing, which are sometimes termed 'gastruloids', by inducing active Wnt signalling 24 hours after their formation, then culturing the embryoid bodies in suspension for five further days (van den Brink *et al.*, 2014). In addition, germ layers can become specified in a radially organised pattern in 2D micropatterned cultures of hESCs stimulated with BMP. Mesodermal cells specified in these colonies undergo EMT and form a primitive-streak-like structure, and thus resemble the gastrulating human embryo (Warmflash *et al.*, 2014). These systems have been

particularly useful in elucidating how signalling ligands can induce feedback mechanisms in cell populations, which lead to the production of their own inhibitors, and thus induce boundaries between cells resulting in spontaneous pattern formation. Additionally, it has also been shown that edge-effects and the position of signalling receptors can influence this process (Etoc *et al.*, 2016). However, these structures fail to recapitulate embryonic architecture accurately and do not represent extra-embryonic cell populations known to be the sources of signals *in vivo*, and thus the extent to which the mechanisms involved in pattern formation in 'gastruloids' compared with embryogenesis are similar is subject to discussion (Denker, 2016).

Embryoid bodies have also been used to model aspects of mouse embryogenesis that precede gastrulation. In particular, they have been used to investigate the mechanisms governing PE specification, egg cylinder morphogenesis and pro-amniotic cavity formation (Coucouvanis and Martin, 1999), because the embryo itself was inaccessible to study once implanted into the maternal tissues. However, the recent development of a system allowing the *in vitro* culture of mouse embryos through the blastocyst-to-egg-cylinder transition has somewhat alleviated the need for embryoid-body based models of embryogenesis at these stages (Morris *et al.*, 2012; Bedzhov, Leung, *et al.*, 2014). Additionally, the study of embryos developing in this system has called into question some findings from embryoid body studies about how the embryo develops (Bedzhov and Zernicka-Goetz, 2014).

Despite this, the major advantage to using ESC-based culture systems in the study of mammalian developmental biology is their amenability to genetic manipulation. Whilst genes can be over-expressed or downregulated easily and robustly in cell culture, this is extremely difficult in the post-implantation mouse embryo, even when the embryos are cultured *in vitro*. Such limitations highlight the need for an *in vitro* model of embryogenesis which recapitulates both the morphogenesis and tissue specification events that occur in the egg cylinder, and can thus be used to investigate the molecular mechanisms underpinning this process, which have proved to be inaccessible *in vivo*.

1.5 Project aims

Although considerable progress has been made in utilising pluripotent stem cells to model aspects of mammalian organogenesis, a system which captures the architecture of the whole embryo remains elusive. The aim of the present study was to build upon previous work to generate an *in vitro* model of early post-implantation embryogenesis, which recapitulates both the morphogenesis and cell-fate decisions associated with these stages of development. The approach taken was to combine embryonic and extra-embryonic stem cells in a scaffold of ECM to model the EPI and ExE of the embryo

respectively. This three-dimensional co-culture system resulted in the self-assembly of embryo-like structures *in vitro*. The morphogenesis of these structures was then characterised in comparison to the mouse embryo, as were the germ-layer specification events which occurred in the structures. Finally, mRNA-sequencing was used to compare the transcriptome of these embryo-like structures to published datasets from both embryos and stem cells in culture, allowing an assessment of the overall similarity between the stem-cell model and the mouse embryo, and facilitating further investigation of axial patterning.

2. Materials and Methods

2.1 Cell lines used in this study

The cell lines used to perform experiments were the following:

Embryonic stem cells

- E14 ESCs (Hooper *et al.*, 1987).
- CAG:GFP ESCs (derived in-house) (Rhee *et al.*, 2006).
- T/Bra:GFP ESCs (Fehling *et al.*, 2003).
- Inducible Nodal-/- ESCs (Wu *et al.*, 2013).
- H2B-GFP::Tcf/LEF ESCs (derived in-house) (Ferrer-Vaquer *et al.*, 2010).
- Stella:GFP ESCs (Payer *et al.*, 2006).

Trophoblast stem cells

- R26 Wildtype TSCs (Tanaka *et al.*, 1998; Soriano, 1999).
- Confetti x Rt2Cre TSCs (phenotypically wildtype) (Livet *et al.*, 2007; Snippert *et al.*, 2010)

2.2 Cell culture

2.2.1 Embryonic stem cell culture

Embryonic stem cells (ESCs) were cultured in 'FC medium' or N2B27 (see table 2.1) supplemented with PD0325901 (1μM), CHIR99021 (3μM) (2i) and leukaemia inhibitory factor (0.1mM, LIF). Cells were grown on gelatinized, tissue-culture grade plastic at 5% CO2 and 37°C, and were passaged once they reached confluency. The medium was changed the day after passage, and every other day subsequently.

For passage, the medium was removed from culture wells and cells were washed in sterile phosphate-buffered saline (PBS). After washing, cell colonies were dissociated to single cells by incubation in 0.05% Trypsin-EDTA (Gibco) at 37°C. After 5 minutes, serum-containing medium was added to trypsinized cells and the cell suspension was pelleted by centrifugation at *1000g* for 5 minutes. The cell pellet was dissociated in fresh culture medium, and cells were re-plated on gelatin-coated plates at a density of 1:10.

2.2.2 Trophoblast stem cell culture

Trophoblast stem cells (TSCs) were cultured in 'TS medium' (see table 2.1) supplemented with 25ng/ml of recombinant mouse FGF4 (Peprotech) and 500ng/ml of heparin (Sigma). Cells were

grown on a layer of mitotically-inactive mouse embryonic fibroblast (MEF 'feeder' cells) and were passaged when they reached 80% confluency.

For passage, the medium was removed from culture wells and cells were washed in sterile PBS. After washing, cell colonies were dissociated by incubation in 0.05% Trypsin-EDTA or Accutase solution (Gibco) at 37°C. After 3 minutes, serum-containing medium was added to the dissociated cells, which were gently agitated by pipetting to preserve small clumps. The cell suspension was pelleted by centrifugation at *1000g* for 3 minutes. The cell pellet was dissociated in fresh culture medium, and cells were re-plated on MEF-coated plates at a density of 1:20.

2.3 Media for cell and embryo culture

Table 2.1: Culture Medium compositions

Medium	Composition
Feeder cell (FC) medium	DMEM (Gibco) supplemented with 15% FBS (HyClone), 2mM L-glutamine (Gibco), 0.1mM 2-ME (Gibco), 0.1mM NEAA (Gibco), 1mM sodium pyruvate (Gibco), and 1% penicillin-streptomycin (Gibco).
TS medium	'MegaCell' RPMI (Sigma) with 20% FBS (HyClone), 2mM L-glutamine (Gibco), 0.1mM 2-ME (Gibco), 1mM sodium pyruvate (Gibco), and 1% penicillin-streptomycin (Gibco).
N2B27 medium	50% DMEM F-12 and 50% Neurobasal A supplemented with 2mM L-glutamine (Gibco), 0.1mM 2ME (Gibco), 0.5x N2 supplement (made in house), 1x B27 supplement (Gibco), or SOS supplement (Cell Guidance Systems Ltd, Cambridge).
'In house' N2 supplement	DMEM F-12 supplemented with 10% apo-transferrin (Sigma), 10% BSA fraction V (Gibco), 25% human insulin solution (Sigma), putrescine dihydrochloride (1611 µg/ml), sodium selenite (0.6 µg/ml) and progesterone (0.6 µg/ml).
ETS embryo medium	50% RPMI, 25% DMEM F-12 and 25% Neurobasal A supplemented with 10% FBS (HyClone), 2mM L-glutamine (Gibco), 0.1mM 2ME (Gibco), 0.5mM sodium pyruvate (Gibco), 0.25x N2 supplement (made in house), 0.5x B27 supplement (Gibco), or SOS supplement (Cell Guidance Systems Ltd, Cambridge), plus 12.5 ng/ml FGF4 (Peprotech) and 500ng/ml heparin (Sigma). 1% penicillin-streptomycin (Gibco) was also added.
IVC 1 medium	Advanced DMEM F-12 (Gibco) supplemented with 20% FBS (HyClone), with 2mML-glutamine (Gibco), 1mM sodium pyruvate (Gibco), 1x ITS-X (Invitrogen), 8nM ß-estradiol (Sigma), 200 ng/ml progesterone (Sigma), and 25 mM N-acetyl-L-cysteine (Sigma).
IVC 2 medium	Advanced DMEM F-12 (Gibco) supplemented with 30% Knockout Serum Replacement (Gibco), with 2mML-glutamine (Gibco), 1mM sodium pyruvate (Gibco), 1x ITS-X (Invitrogen), 8nM ß-estradiol (Sigma), 200 ng/ml progesterone (Sigma), and 25 mM N-acetyl-L-cysteine (Sigma).

2.4 Derivation of Embryonic Stem Cells

2.4.1 Generation of embryonic stem cell colonies

To derive H2B-GFP::Tcf/LEF ESCs and CAG-GFP ESCs from the corresponding mouse strains, six-week old mice were naturally mated and females were sacrificed 2.5 days post-coitum (E2.5). Pre-compaction 8-cell stage embryos were recovered from the oviducts in M2 medium and were cultured overnight in KSOM medium (Millipore) supplemented with PD0325901 (1μM), CHIR99021 (3μM) (2i) and leukaemia inhibitory factor (0.1mM, LIF). The following day, embryos were washed in N2B27 medium and cultured for a further 48 hours in N2B27 supplemented with 2i plus LIF until they formed hatched blastocysts.

Single blastocysts were plated in each well of a tissue-culture grade 96-well, flat-bottomed plate on top of a layer of mitotically inactivated MEF feeder cells. They were cultured in FC medium supplemented with 2i plus LIF at 5% CO2 and 37°C until they formed small outgrowths. These outgrowths were dissociated by washing with PBS and incubating at 37°C in 0.05% Trypsin-EDTA for 10 minutes, and by gentle agitation by pipetting. Dissociated cells were then re-plated on MEFs and cultured until they formed ESC colonies. Colonies were passaged once they reached confluency and were propagated in N2B27 supplemented with 2i plus LIF on gelatin-coated tissue culture plates.

2.4.2 Genotyping of embryonic stem cell lines

For both newly derived ESC lines, the presence of the reporter allele was confirmed by checking live ESC colonies for GFP by fluorescence microscopy and verified by Polymerase Chain Reaction (PCR).

When confluent, DNA was extracted from newly-derived ESC colonies for genotyping by PCR. Cells were washed in sterile PBS then treated with 0.5 mg/ml proteinase K in TNES buffer (50 mM Tris-HCl pH 8.0, 100 mM EDTA pH 8.0, 100 mM NaCl, 1% SDS) then incubated overnight at 55°C. After incubation, samples were treated with 100% Ethanol and then centrifuged. The supernatant was discarded and DNA pellets were washed in 70% ethanol several times before being left to air dry and re-dissolved in Tris-EDTA buffer or in DNAse-free H2O. 2μl of this solution was then used for genotyping by PCR. The PCR reaction was performed using a Qiagen Fast Cycling PCR Kit, which was used according to the manufacturer's instructions. The PCR reaction mixture had a total volume of 20μl, and contained a maximum of 300ng of template DNA in a volume of 2μl, 10μl of Qiagen Fast Cycling PCR Master Mix (containing Contains HotStarTaq Plus PCR Master Mix DNA Polymerase, 1x Fast Cycling Buffer, 200 μM of deoxynucleoside triphosphate (dNTP) solution, and Mg2+ at an

optimized concentration), 1µl of each of the forward and reverse primers (at a final concentration of 0.5µM) and 6µl of RNase-free water (Qiagen).

Primer sequences were as follows:

Forward (5' to 3'): AAGTTCATCTGCACCACCG

Reverse (3' to 5'): TCCTTGAAGAAGATGGTGCG

The PCR amplification products were analysed by gel electrophoresis using 1.8% agarose gel dissolved in Tris-Acetate EDTA (TAE) buffer (containing 40mM Tris base, 20mM Acetic acid and 2mM EDTA diluted with Milli-Q water) with SYBR safe DNA gel stain (Thermofisher Scientific). The gel was visualised under an ultraviolet light, and a positive template yielded a PCR product of approximately 600 base pairs (bp).

2.5 Three-dimensional culture in Extracellular Matrix

2.5.1 '3D embedded' protocol

When cells were confluent, ESCs were dissociated to single cells and TSCs dissociated into small clumps by first washing in PBS then incubation with 0.05% Trypsin-EDTA at 37°C. After 4 minutes, dissociated cells were suspended in FC medium or TS medium respectively, then pelleted by centrifugation at *1000g* for 4 minutes. ESCs and TSCs were then re-suspended in PBS and re-pelleted twice, before final re-suspension in PBS. Care was taken with TSCs to gently pipette and thus preserve small clumps of cells, whilst ESCs were dissociated singly. 5,000 ESCs and 5,000 TSC-clumps were then counted using a haemocytometer and a stereomicroscope, and were then mixed in 20µl volume to achieve a 1:1 mixed suspension of ESCs and TSC-clumps with an approximate density of $1x10^5$ cells/ml. After mixing, the cells were pelleted again by centrifugation at 1000g for 3 min, then re-suspended in 100µl Matrigel (BD, Corning). The cell-ECM mixture was then plated in 20µl drops on 8-well optical grade tissue culture µ-plates (Ibidi), and incubated at 37°C to allow the Matrigel to solidify. Once cultures had gelled, each well of the plate was flooded with culture medium and cells were incubated at 5% CO2 and 37°C for up to six days.

2.5.2 3D 'on top' protocol

For imaging, it was convenient to grow cells in 3D in a single layer, as described by Lee et al (Lee *et al.*, 2007). 8-well optical grade tissue culture µ-plates (Ibidi) were covered with a 35µl of liquid Matrigel (BD, Corning) which was allowed to solidify at 37°C before cells were seeded on top at an approximate density of $1x10^5$ cells/ml. The mixture of cells were left to attach to the substrate for 15 minutes,

before the excess PBS from the cell suspension was removed from wells, which were then filled with culture medium supplemented with 10-30% Matrigel (BD, Corning).

2.6 Embryo recovery and culture

Six-week old f1 (CBAxC57BL/6) mice were naturally mated and females were checked for coital plugs the day after pairing. The day a plug was found was denoted as 0.5 days post-coitum (d.p.c).

For peri-implantation culture, females were sacrificed at 4.5 dpc and the uterus was dissected out. Blastocysts at embryonic day 4.5 (E 4.5) were recovered by flushing from the uterus in M2 medium. Upon recovery, the mural trophectoderm was dissected away using a flame-polished glass needle, and embryos were cultured in IVC1 and IVC2 medium for 48 hours as described in Bedzhov et al (Bedzhov, Leung, *et al.*, 2014).

To obtain post-implantation egg cylinders, females were sacrificed at 5.5-6.5 d.p.c and embryos were dissected from the uterine tissue and the decidua in M2 medium using fine forceps. A fine metal needle was used to remove the Reichert's membrane from embryos, which were then fixed or cultured in IVC2.

2.7 Immunofluorescence staining

2.7.1 Cells

Cells were fixed in ice cold 4% paraformaldehyde (PFA) either on glass coverslips or in 8-well optical grade tissue culture μ-plates for 15 minutes at room temperature (RT), and were then rinsed twice in PBS. Cells were then permeabilised at RT for 10 minutes in 0.3% Triton-X-100, 0.1% glycin in PBS. Primary antibody incubation was performed overnight at 4°C in blocking buffer (PBS with 3% BSA or PBS plus 10% FBS, 1% Tween-20). The following day, cells were washed in PBS for 5 minutes and then incubated in secondary antibody in blocking buffer (as above) overnight at 4°C or for 2 hours at RT. Subsequently, cells were washed again in PBS for 5 minutes and then incubated in DAPI plus PBS for 1 hour at room temperature, prior to confocal imaging. 'ETS-embryos' in figures 5.4.1 C, and 5.5.1 A & B were immunostained and imaged together with Berna Sozen (researcher in Magdalena Zernicka-Goetz's laboratory).

2.7.2 Post-implantation / *in vitro* cultured embryos

Embryos were fixed in 4% PFA for 20 minutes at RT, then washed twice for 5 minutes in PBS plus 0.05% Tween-20 (PBT). After washing, embryos were permeabilised at RT for 15 minutes in 0.3% Triton-X-100, 0.1% glycin in PBS. Primary antibody incubation was performed overnight at 4°C in blocking buffer (as above), and then washed twice in PBT for 5 minutes each. Secondary antibody incubation was performed overnight at 4°C in blocking buffer (as above). After a further two washes in PBT, embryos

were incubated for 1 hour at RT in DAPI plus PBT (5mg/ml). Prior to confocal imaging, embryos were mounted in DAPI plus PBT on glass slides under coverslips or in drops on glass-bottomed dishes (MatTek). Embryos in figures 4.2.5, C and 4.2.6, B were immunostained and imaged by Neophytos Christodoulou (post-doctoral researcher in Magdalena Zernicka-Goetz's laboratory).
For antibodies used, see table 2.2.

Table 2.2: Antibodies used in this study

Antibody (species)	Vendor	Number	Dilution
Oct3/4 (mouse)	Santa cruz	sc-5279	1:200
Tbr2/Eomes(rabbit)	Abcam	ab23345	1:400
aPKC(rabbit)	Santa cruz	sc-17781	1:200
Podocalyxin(rat)	R&D systems	MAB1556	1:400
Brachyury/T (goat)	Santa cruz	sc-17745	1:50
GFP(rat)	Nacalai biochemicals	04404-84	1:2000
AP2γ/ Tfap2c (rabbit)	Santa cruz	sc-8977	1:200
Laminin (rabbit)	Sigma	L9393	1:400
Cdx2 (mouse)	Launch diagnostics	MU392-UC	1:200
E-cadherin (rat)	Life Technologies (Thermofisher scientific)	13-1900	1:400
Phospho-SMAD2/3	Cell signalling technologies	8828P	1:200
Phospho-SMAD 1/5/9	Cell signalling technologies	13820P	1:200
Gata4 (Goat)	Santa cruz	sc-1237	1:200
CC-3 (rabbit)	Cell signalling technologies	#9664	1:200
F-actin (Phalloidin488)	Life Technologies (Thermofisher scientific)	A12379	1:1000
Alexa 488 (Donkey anti-rat)	Life Technologies (Thermofisher scientific)	A21208	1:500
Alexa 568 (Donkey anti-mouse)	Life Technologies (Thermofisher scientific)	A10037	1:500
Alexa 647 (Donkey anti-rabbit)	Life Technologies (Thermofisher scientific)	A31573	1:500
Alexa 647 (Donkey anti-goat)	Life Technologies (Thermofisher scientific)	A21447	1:500

2.8 Sample collection and RNA isolation from 'ETS-embryos'

To collect RNA, whole ESC and TSC compartments were manually dissected from 'ETS-embryos' and collected in extraction buffer (from the Arcturus Pico Pure RNA Isolation Kit). Alternatively, for some analyses GFP-positive and GFP-negative cells from 'ETS-embryos' were collected. In this case, 'ETS-embryos' were first treated with an Enzyme Free Hanks'-Based Cell Dissociation Buffer (Thermofisher Scientific) for 2 minutes then had their TSC-compartment dissected away. Then, the ESC compartment was incubated with 0.05% trypsin-EDTA at 37˚C and then gently pipetted to dissociate it into single cells. Subsequently, 15-20 GFP positive and negative cells were collected separately under a fluorescent microscope and transferred into extraction buffer. Total RNA was extracted from samples using the Arcturus Pico Pure RNA Isolation Kit (Applied Biosciences) which was used according to the manufacturer's instructions.

2.9 Quantitative Real-Time –PCR (qRT-PCR)

For all samples, qRT–PCR was performed on a minimum of three biological replicates using the Power SYBR Green RNA-to-CT 1-Step Kit (Life Technologies) and a Step One Plus Real-time PCR machine (Applied Biosystems). The amounts of mRNA were measured using SYBR Green PCR Master Mix (Ambion). Relative levels of transcript expression were assessed by the ΔΔCt method, and *Gapdh* was used as an endogenous control. See table 2.3 for primer sequences of target genes. Sample collection and qPCR was done together with Berna Sozen (researcher in Magdalena Zernicka-Goetz's laboratory).

Table 2.3: Sequences of qRT-PCR primers used in this study

Gene	Forward (5' to 3')	Reverse (5' to 3')
Prdm14	ACAGCCAAGCAATTTGCACTAC	TTACCTGGCATTTTCATTGCTC
Stella	AGGCTCGAAGGAAATGAGTTTG	TCCTAATTCTTCCCGATTTTCG
Nanos3	CACTACGGCCTAGGAGCTTGG	TGATCGCTGACAAGACTGTGGC
Ddx4	GCAGTGTTGTAACGTCAGCATTTC	TTCTTCTGTTCTTCCTCCCAACC
Mixl1	GACAGACCATGTACCCAGAC	GCTTCAAACACCTAGCTTCAG
Hand1	ACGTGCTGGCCAAGGATGCA	TGGTTTAGCTCCAGCGCCCA
GAPDH	CGTATTGGGCGCCTGGTCAC	ATGATGACCCTTTTGGCTCC
Dnmt3b	CTCGCAAGGTGTGGGCTTTTGTAAC	CTGGGCATCTGTCATCTTTGCACC
AP2γ	TGCCCACGTCACTCTCCTCA	TCCGTCCCCCAAGATGTGGT
T	GCTGGATTACATGGTCCCAAG	GGCACTTCAGAAATCGGAGGG
Blimp1	CGGAAAGCAACCCAAAGCAATAC	CCTCGGAACCATAGGAAACATTC
Wnt3	CAAGCACAACAATGAAGCAGGC	TCGGGACTCACGGTGTTTCTC
Axin1	ACGGTACAACGAAGCAGAGAGCT	CGGATCTCCTTTGGCATTCGGTAA

Pou3f1	TTCAAGCAACGACGCATCAA	TGCGAGAACACGTTACCGTAGA
Oct4	GATGCTGTGAGCCAAGGCAAG	GGCTCCTGATCAACAGCATCAC
Slc7a3	TTCTGGCCGAGTTGTCTATGTTTG	AGTGCGGTTCTGTGGCTGTCTC
Utf1	GGATGTCCCGGTGACTACGTCTG	GGCGGATCTGGTTATCGAAGGGT
Cdx2	AGTGAGCTGGCTGCCACACT	GCTGCTGCTGCTTCTTCTTGA
Eomes	TCGCTGTGACGGCCTACCAA	AGGGGAATCCGTGGGAGATGGA
Elf5	ATTCGCTCGCAAGGTTACTCC	GGATGCCACAGTTCTCTTCAGG
Gata3	GGGTTCGGATGTAAGTCGAG	CCACAGTGGGGTAGAGGTTG
Otx2	TATCTAAAGCAACCGCCTTACG	GCCCTAGTAAATGTCGTCCTCTC
Acsl4	CCTGAGGGGCTTGAAATTC	GTTGGTCTACTTGGAGGAACG
Fgf5	AACTCCATGCAAGTGCCAAAT	CGGACGCATAGGTATTATAGCTG

2.10 mRNA-sequencing

2.10.1 Sample collection

All samples were collected as described for qRT-PCR experiments, and placed in lysis buffer (2.3 µl of 0.2 % Triton X-100 (Sigma) supplemented with 1 U/µl RNAsIN (Ambion)). Sample collection was done together with Berna Sozen (researcher in Magdalena Zernicka-Goetz's laboratory).

2.10.2 RNA-sequencing and mapping of reads:

Amplification of mRNA was performed using the SMART-Seq2 protocol (Picelli *et al.*, 2013, 2014). Nextera XT (Illumina) was used to generate multiplex sequencing libraries from amplified cDNA. These libraries were then sequenced on a HiSeq 2500 running in rapid mode. Reads were mapped to the *M. musculus* genome (Ensembl version 38.77). Counting of mapped reads was done using the HTSeq-count (Anders, Pyl and Huber, 2015). RNA sequencing and mapping was completed by Lia Chappell (post-doctoral researcher in the laboratory of Thierry Voet).

2.10.3 Quality assessment and analysis of differential gene expression

All quality assessment and clustering analysis, and identification of differentially expressed genes of published datasets and sequencing datasets generated in this study was carried out by Ran Wang (researcher in the laboratory of Naihe Jing). This is described briefly below, and in Peng et al (Peng *et al.*, 2016).

Pre-processing of RNA-Sequencing data

Raw reads were mapped to the *Mus musculus* genome (assembly mm10, ENSEMBL) using the Tophat2 v2.0.4 program (Trapnell, Pachter and Salzberg, 2009). Reads for all samples were subjected to quality

assessment using the FASTQC tool (Andrews, 2010). In addition, the distribution of gene expression for all samples was also plotted to mine for outliers and check for consistency between samples. Gene expression level was calculated as 'fragment per kilobase per million' (FPKM) using the Cufflinks program (v2.0.2) with default parameters set (Kim et al., 2013). Genes with the FPKM > 1.0 in at least one sample across all samples were retained for further analysis. Finally, the measure of gene expression was transformed to logarithmic space by using the function $\log_2$(FPKM+1).

Functional enrichment analysis

Functional enrichment of gene sets identified as differentially expressed between samples was performed using the Database for Annotation, Visualization and Integrated Discovery v6.7 (DAVID v6.7) (Huang da et al., 2009).

'Corn-plot' analysis to compare T:GFP-positive and T:GFP-negative cells in 'ETS-embryos' to regions of the mouse epiblast

The transcriptome data from 'ETS-embryos' were compared to pre-existing data from reference embryos at three different stages; E6.5, E7.0 and E7.5. The reference embryos were subdivided into different epiblast regions as in Peng et al (2016) (E6.5: 13 samples, E7.0: 42 samples, E7.5: 46 samples- each reference sample corresponds to a different domain of the embryo at each stage). To assess the similarity between gene expression in cells isolated from different parts of 'ETS-embryos' and different regions of the epiblast a Pearson Correlation Coefficient (PCC) was calculated as a measure of correlation between gene expression in each reference sample (E6.5: 13 samples, E7.0: 42 samples, E7.5: 46 samples) and transcriptome data from cells isolated from 'ETS-embryos'. This PCC was calculated based on the expression of 158 'zip code mapping' genes identified by Peng *et al.* which are robust markers of different regions of the EPI of the post-implantation egg cylinder (Peng *et al.*, 2016).

PCCs (r) was calculated using the following formula:

$$r = r_{xy} = \frac{1}{n-1}\sum_{i=1}^{n}\left(\frac{x_i - \bar{x}}{s_x}\right)\left(\frac{y_i - \bar{y}}{s_y}\right)$$

Where n is defined as the sample size, x and y are the values for experimental and reference (epiblast domain) samples respectively, s is defined as the standard deviation in each case.

A PCC of 1 would mean the expression of a gene in the sample taken from the 'ETS-embryo' and a region of the EPI was identical, and therefore the two were perfectly correlated. A PCC of 0 would indicate no correlation in the expression of a gene between the 'ETS-embryo' sample and a region in the EPI. Therefore, a high PCC value indicates that gene expression patterns are closely matching between 'ETS-embryo' samples and egg cylinder reference samples.

The PCC values for each 'ETS-embryo' sample compared to each reference region of the epiblast for each of the three mouse embryos was depicted in the form of a 'corn plot' (see Results IV and (Peng *et al.*, 2016)). Each circle represents a different reference sample, representing a different domain of the EPI, color-coded to indicate the PCC value. Each 'ETS-embryo' sample was compared to each set of reference samples at each embryonic stage respectively, and as opposed to normalising on a single standard, each dataset is shown as a separate corn-plot (see Fig. 6.10).

2.11 Image acquisition, processing and analyses

All multichannel images were acquired using a Leica SP5 inverted confocal microscope, using a 40x oil-immersion objective, or a Leica SP8 inverted confocal microscope using a water-immersion 25x objective, operating with Leica LAS-AF software. Confocal Z-stacks were exported to the open-source image analysis software 'Fiji' and 'de-noised' where appropriate using built-in functions. All analyses were performed using built-in functions in 'Fiji' or using 'Bioemergences' software (Faure *et al.*, 2016).

2.11.1 Estimation of tissue volume

Tissue volume was estimated assuming that both 'ETS-embryos' and natural embryos were approximately cylinder shaped. The length and radius of each compartment was measured using the built-in 'measure' function in 'Fiji', then the volume of the cylinder was calculated from these measurements as $V= \pi r^2 l$.

2.11.2 2D Nuclear vector analysis

The middle z-section in a stack of confocal sections was identified and imported into 'Fiji', and the DNA/DAPI channel was used to assign a scalar line along the long axis of each nucleus in the structure. The scalar lines were then given a directional arrowhead according to their apico-basal axis (with the arrowhead pointing towards the apical side). Apical-basal axis for each cell was determined by using the distribution of aPKC staining and the location of the central cavity. Once each cell was assigned an arrow with both direction and length, these arrows, which overlaid the confocal image were exported as a .tiff image to build the figure.

2.11.3 Assessment of asymmetric gene expression

Confocal Z-stacks were imported into 'Fiji' and a line corresponding to the long axis, equivalent to the 'midline' of an ETS-embryo or real embryo (perpendicular to the embryonic-extra-embryonic

boundary) was drawn. At each Z-step, the number of cells positioned either side of this line which expressed the marker-of-interest was counted. If >70% of cells were found to lie on one side of this line, then expression was judged to be asymmetric.

In some cases, this was verified by importing data into 'Bioemergences' image analysis software ('MovIT'), and using the DAPI channel of an acquired image series to mark all cells in a structure and record their position by x, y, and z coordinates. The coordinates of cells expressing the marker-of-interest were also recorded. The long axis, corresponding to the 'midline' was determined from the median coordinates in each dimension. A custom R script (http://www.R-project.org/) used coordinates data to group cells according to their position relative to the midline of the whole structure and whether they expressed the marker of interest. A Fisher's exact test was performed to determine if position relative to the midline was related to expression of the gene by comparing the distribution of the data to the binomial.

2.12 Statistical analysis

Statistical tests were performed on GraphPad Prism 7.0 software for Windows (www.graphpad.com). Data were checked for normal distribution and equal variances before each parametric statistical test was performed. Data were normalised using an appropriate transformation where stated. Welch's correction was applied to student's t-tests if variance between groups was not equal. ANOVA tests were performed with a Geisser-Greenhouse correction if variance between groups was not equal. Error bars represent standard error of the mean in all cases, unless otherwise specified. Figure legends indicate the number of independent experiments performed in each analysis.

2.12.1 Analysis of statistical power

The power analyses on the data presented in Fig. 3.4A and 3.4B were performed on a post-hoc basis, using the statistical calculator G*Power (Version 3.1.9.2 (Faul *et al.*, 2007)).

Statistical power was calculated for a two-tailed t-test with input parameters defined as follows: α=0.05, n per group=20, and effect size, d.

Effect size was calculated as Cohen's *d* using the following formula:

$$d = \frac{\mu_1 - \mu_2}{s}$$

Where μ is equal to the mean of each group, and s is equal to the standard deviation (equal for both groups).

3. Results I- Developing a co-culture technique to generate embryo-like structures *in vitro*

3.1 Introduction:

ESCs in culture have been used to model the development of the pluripotent tissue *in vitro* for many years (Irion *et al.*, 2008; Murry and Keller, 2008). ESCs derived from the pre-implantation ICM (Evans and Kaufman, 1981; Martin, 1981; Ying *et al.*, 2008) and EPISCs derived from the post-implantation EPI (Brons *et al.*, 2007) represent different developmental stages of the embryonic epiblast in culture (Tesar *et al.*, 2007; Nichols and Smith, 2009; Chenoweth, McKay and Tesar, 2010; Boroviak *et al.*, 2014). The process of ESC differentiation has been well studied and can elucidate the mechanisms of cell fate decisions occurring during embryogenesis that lead to the formation of different tissues- ectoderm, endoderm, and mesoderm (Wu *et al.*, 2015; Turner *et al.*, 2016). However, these studies are limited because they cannot recapitulate the three-dimensional nature of embryogenesis in adherent culture conditions.

Previous approaches to generate three-dimensional *in vitro* models of embryogenesis have focussed on using ESCs in aggregates of hundreds or even thousands of cells to form structures called embryoid bodies (Chen and Kosco, 1993; Desbaillets *et al.*, 2000; Weitzer, 2006). These have been used to elucidate mechanisms governing early morphogenetic events in the mouse embryo but what can be extrapolated to the real embryo from such studies is still under debate. Whilst some investigations using embryoid bodies have been informative about how embryonic tissues, particularly epithelia, can take shape (Li et al, 2003), some conclusions drawn from such studies have later proved incorrect (Coucouvanis and Martin, 1999). Despite this, embryoid bodies are routinely used in ESC differentiation protocols (Murry and Keller, 2008; Eiraku *et al.*, 2011; Takasato *et al.*, 2016) and culture in three-dimensions can give rise to germ layer specification more efficiently than in 2D (Pineda, Nerem and Ahsan, 2013). Embryoid bodies will spontaneously induce polarised domains of early germ layer markers, and this can be promoted through activation of Wnt signalling (Ten Berge et al, 2008; Van den Brink et al, 2014). Some such structures have been called 'gastruloids' because cells in the mesodermal layer appear to undertake cell movements similar to those associated with cell ingression at the primitive streak during gastrulation (van den Brink *et al.*, 2014). Similar structures can be obtained using hESCs (Itskovitz-Eldor *et al.*, 2000) but perhaps the most convincing 'gastruloid' made from human cells was in fact grown on 2D micropatterned substrates to create colonies with precisely defined boundaries (Warmflash *et al.*, 2014). Despite the fact that these structures are able to induce

polarised domains of gene expression associated with germ layer specification at gastrulation, they do not faithfully recapitulate embryonic architecture.

Bedzhov *et al* showed that ESCs are able to recapitulate the morphogenesis of the embryonic epiblast by transduction of laminin mediated β1-integrin signalling when embedded in extracellular matrix (ECM) to form a 'rosette' –like structure (Bedzhov and Zernicka-Goetz, 2014). In forming these rosette-like structures, ESCs more faithfully mimic embryonic architecture than embryoid bodies. However, without the provision of extra-embryonic tissues, or representations of these, the ESC 'rosette' represents the epiblast only.

In this chapter, ESCs were combined with TSCs embedded in three-dimensional ECM to generate embryo-like structures which mimic embryonic architecture. These self-organised structures are similar to the embryo in size, morphology and composition. Like the natural post-implantation egg cylinder, they consist of an embryonic and an abutting extra-embryonic compartment surrounding a shared cavity at their centre, but they do not comprise any tissue equivalent to the extra-embryonic visceral endoderm (VE). The results presented here demonstrate how embryonic and extra-embryonic stem cells can self-organise to recapitulate the post-implantation mouse embryo, and hence the resulting embryo-like structures may be a useful model system to study the early stages of mammalian embryogenesis *in vitro*.

3.2 ESCs and TSCs in extra-cellular matrix self-assemble into embryo-like architecture

3.2.1 Method of co-culture and medium

It was hypothesised that to recapitulate the architecture of the egg cylinder *in vitro*, the method developed to culture ESC 'rosettes' described in Bedzhov et al, (2014) would have to be modified to also accommodate TSCs, which would provide a mimic of the ExE tissue in the embryo (Tanaka et al, 1998).

To achieve this, ESCs in conventional adherent culture in medium containing 2i/LIF (Materials & Methods) were first dissociated to single cells by trypsinisation and washed with PBS to remove residual medium. TSCs in 2D adherent culture were also treated with trypsin to generate a second cell suspension. TSC viability is reduced when plated as single cells, so TSCs were re-suspended in medium without washing and gently agitated by pipetting to preserve small clumps of cells. TSC clumps and single ESCs were mixed in a one-to-one ratio in suspension, and cultured together in a mixture (Figure 3.1. A).

To support both ESCs and TSCs simultaneously in culture, a medium was developed containing a 25% (vol/vol) Neurobasal A medium, 25% (vol/vol) DMEM/F-12 and 40% RPMI medium, and thus was a mixture of the basal components of medium that supports ESCs alone (Ying and Smith, 2003) and TSCs alone (Tanaka et al., 1998). The medium was also supplemented with L-glutamine and sodium pyruvate to promote cell growth and survival in culture. Additionally, the medium included FGF4 and heparin, to promote TSC self-renewal *in vitro*, but the inhibitors PD0325901, CHIR99021, and LIF were excluded to promote the differentiation of ESCs in co-culture. Finally, 10% (vol/vol) FBS was added. Given that FBS is known to contain undefined factors which promote cell proliferation and differentiation in culture, it was hypothesised that serum may provide essential signalling components to ESCs and TSCs. FBS is also required for mouse blastocysts to develop into egg cylinders *in vitro* (Morris *et al.*, 2010; Bedzhov, Leung, *et al.*, 2014) and so it was hoped that it may promote self-assembly of embryo-like structures. However, the overall percentage of FBS in the medium was kept low to minimise the possibility of precocious differentiation.

In vivo, the EPI and ExE compartments of the egg cylinder are surrounded by a basement membrane which lies between these tissues and the VE. To mimic the presence of this basement membrane *in vitro*, the ESCs and TSCs were co-cultured in the presence of an ECM derived from mouse Engelbreth-Holm Swarm (EHS) carcinoma, known commercially as 'Matrigel'. This reagent is liquid between 2-8°C, but forms a solid gel above this temperature. Two methods were developed to culture the cells in the Matrigel (see Materials and Methods). One method involved fully immersing a mixture of ESCs and TSCs in liquid Matrigel, then allowing the Matrigel to solidify in drops, plated in wells of tissue culture dishes. Each 20µl drop contained approximately 10,000 cells (5000 ESCs and 5000 TSC clumps), mixed in a 1:1 ratio. Once the drops had solidified, the wells containing the Matrigel droplets were flooded with medium (Fig.3.1 A).

Since this method of fully embedding cells in ECM resulted in cells being positioned at different depths within the Matrigel, a second method was also developed to ensure that all cells remained in one optical plane and were thus more amenable to high-thoughput confocal imaging. In this method, optical grade tissue culture plates were covered with a thin layer of liquid Matrigel, which was allowed to solidify at 37°C before the missed suspension of ESCs and TSC clumps was seeded on top at an approximate density of 10,000 cells per cm^2, equivalent to $1x10^5$ cells/ml. The mixture of cells were left to attach to the substrate for 15 minutes, before the wells were filled with culture medium supplemented with 10-30% Matrigel.

Importantly, the initial cell-density plated to generate ETS embryos ($1x10^5$ cells/ml) is approximately half that which is used in other protocols to embed cells in ECM. This density was chosen for two

reasons. Firstly, the TSC-clumps used in the culture, which averaged between 2-8 cells, were counted as single entities during cell suspension and mixing, making 10,00 cells an underestimate of the actual cell number plated. Furthermore, for experiments where structures in culture were left to grow for up to six days, an even lower number of cells were initially plated (6000 per droplet in suspension, made up of 3,000 single ESCs and 3,000 TSC clumps). This is because the structures were anticipated to grow to a size of several hundred microns, and were therefore plated at low density to begin with to allow structures which develop to have sufficient room to reach this size in culture over this time period. Although this low-plating density has the advantage that structures have space to grow unrestricted in the culture system, it also carries the disadvantage that the probability of ESCs and TSCs meeting initially in culture is lower than if plated at a higher density.

Once the cells were embedded in ECM, the ESC-TSC mixture was cultured in the custom-designed medium described above for up to six days.

3.2.2 Co-culture of ESCs and TSCs leads to self-assembly of an egg-cylinder-like structure

Within 4 days of culture in these conditions, a compound structure comprising both cell types had self-assembled in the system. These structures were comprised of both embryonic cells (derived from ESCs) and extra-embryonic cells (derived from TSCs) which formed two separate compartments and did not mix. A CAG:GFP reporter ESC line (Rhee et al, 2006) was used in combination with unlabelled TSCs to demonstrate that both cell types were present in a single structure, and allowed the monitoring of structure development over time. The number of GFP-labelled ESCs was quantified at each timepoint, and revealed that single ESCs divided within the first 12h of co-culture and eventually contributed to an ESC compartment containing a mean of ~114 cells within 96h of culture (n=16 structures counted) (Fig 3.1. B, C).

The distribution of two key EPI and ExE markers in these structures was examined by immunofluorescence. To mark the embryonic compartment, these structures were stained with Oct3/4 antibody, and with TBR2/Eomes antibody to mark the extra-embryonic domain. These stainings were compared to stainings performed in parallel on E5.5 embryos recovered from the mother and cultured *in vitro* and revealed a striking similarity (Figure 3.2. A, B). Thus, these embryo-like structures were named ‘embryonic and trophoblast stem cell-derived embryos’, or ‘ETS embryos’, in the shorthand.

Despite their morphological resemblance to the mouse egg cylinder, it was noticed that ‘ETS embryos’ lacked a monolayer epithelium surrounding the ESC and TSC compartments equivalent to the VE tissue. Since ESCs are known to generate endoderm lineages in culture (Hamazaki *et al.*, 2004; Murry

and Keller, 2008), the absence of this lineage was confirmed by immunofluorescence. In contrast to the post-implantation egg cylinder (cultured *in vitro*) no GATA4-potive VE-like cells could be detected, hence a third cells layer was not present (Figure 3.3. A).

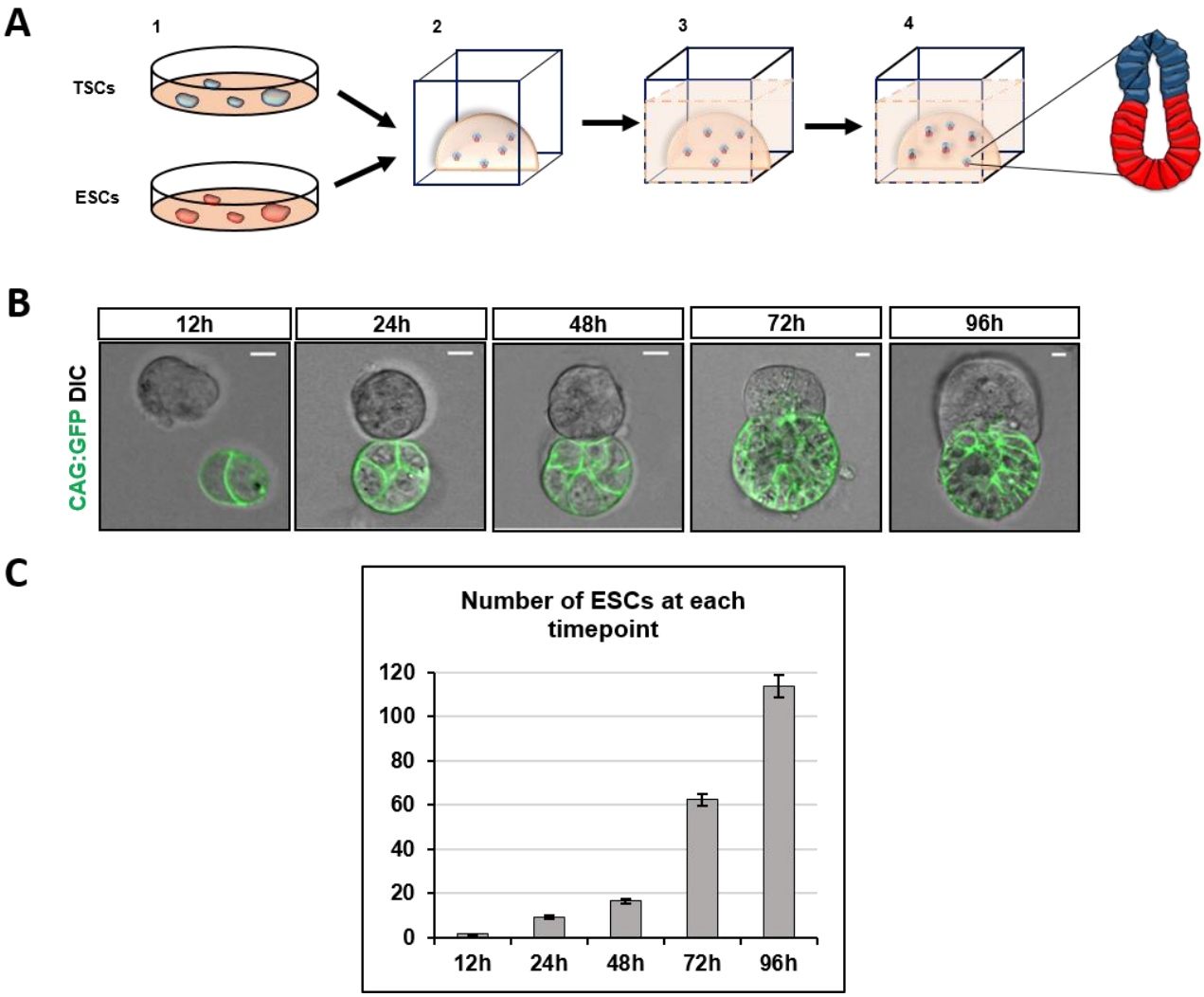

Fig. 3.1. (A) Scheme of protocol to generate ETS-embryos. ESCs and TSCs cultured in standard conditions (1). Single ESCs and small clumps of TSCs suspended in 3D ECM of Matrigel, plated in drops and allowed to solidify (2), before culturing in ETS-embryo medium established for this purpose (3; Materials & Methods). Embryo-like structures emerge within 96 hours (4). **(B)** Confocal snapshots of an ETS embryo developing over 96h from clumps of cells. Within 12h, the single ESC divides to give rise to a doublet and later a spheroid of polarised cells, which later merges with the TSCs to generate an embryo-like structure. The ESC compartment is labelled with a CAG-GFP membrane marker to demarcate it from the TSC compartment. Scale bar= 10µm. **(C)** Quantification of the mean number of cells contributing to the ESC compartment at each timepoint from 12-96 hours in culture. N= 16 structures counted per timepoint.

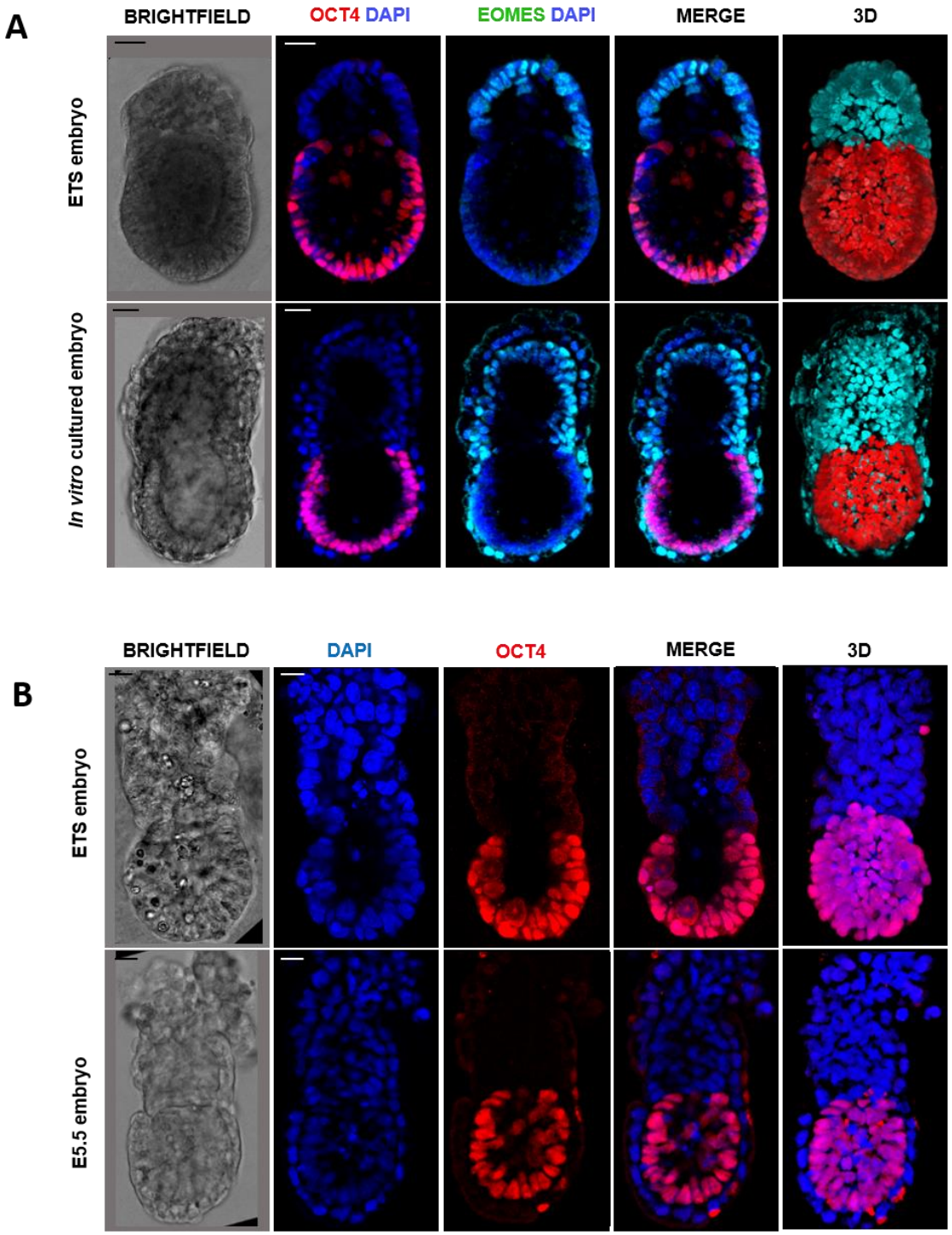

Fig. 3.2. (A) Upper row: ETS-embryo of size approximately 100µmx200µm after 96 hours of culture stained to reveal: Oct4, red; Eomes, green, embryonic and extra-embryonic markers respectively; DNA, blue; white line highlights cavity. Scale Bar=20µm; n=20. Rightmost panel: 3D rendering of same ETS-embryo: Red, Oct4; Cyan, Eomes. **Lower row:** Embryo cultured *in vitro* for 48 hours from the blastocyst stage: Oct4, red; Eomes, green; DNA, blue; white line highlights cavity; Scale Bar= 20µm; n=20. Rightmost panel: 3D rendering of same *in vitro* cultured embryo: Oct4, red; Eomes, cyan. **(B) Upper row:** ETS-embryo: Oct4, red; DNA, blue. Scale Bar =20µm; n=20. Rightmost panel: 3D rendering of same ETS-embryo: Red, Oct4; Blue, DAPI. **Lower row:** Post-implantation embryo recovered at E5.5: Oct4, red; DNA, blue. Scale Bar =20µm; n=20. 3D rendering of same E5.5 embryo: Red, Oct4; Blue, DAPI.

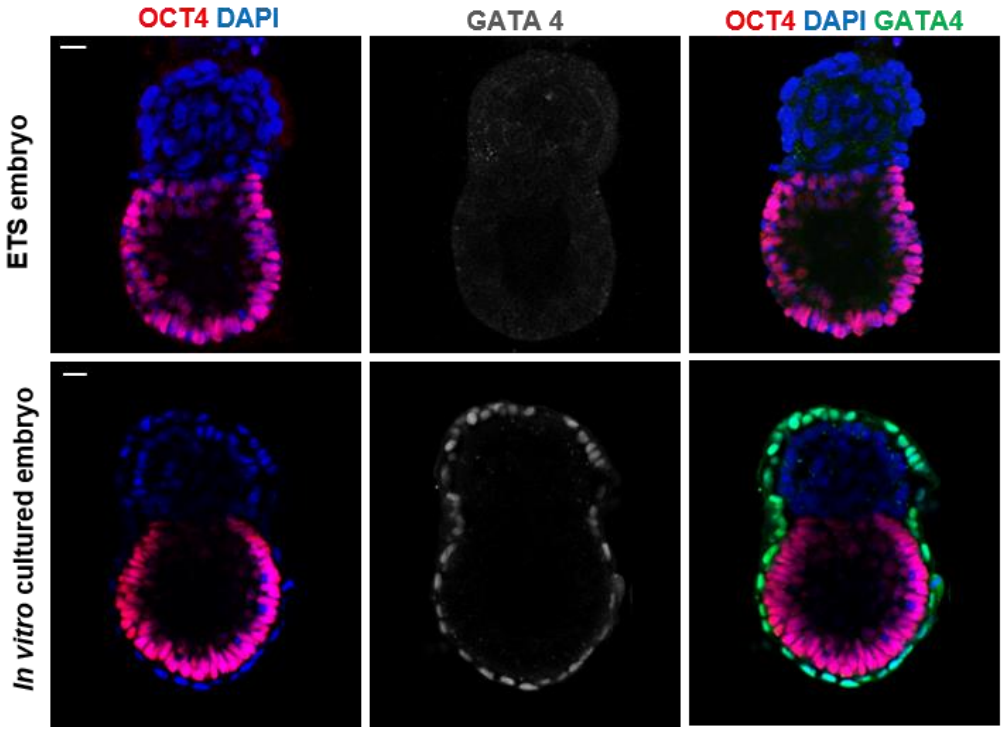

Fig. 3.3. Upper row: ETS-embryo stained to reveal: Oct4, red; DNA, Blue; Gata4, grey/green. Scale Bar = 20µm. n=10. **Lower panels:** Embryo cultured *in vitro* for 48 hours from the late blastocyst stage: Oct4, red; DNA, Blue; Gata4, grey/green. n=30. Scale Bar = 20µm.

3.3 'ETS-embryos' resemble the post-implantation egg cylinder at E5.5

3.3.1 'ETS-embryos' have a similar tissue composition to the post-implantation egg cylinder at E5.5

Having established a protocol to support the culture of both ESCs and TSCs in ECM (Fig. 3.1 A), the resulting embryo-like structures which emerged were compared to the post-implantation mouse embryo. The number of cells in the ESC and TSC compartment of the 'ETS-embryos' were compared to the number of cells in the EPI and ExE of an early post-implantation mouse egg cylinder cultured *in vitro*. When the contribution of the VE was excluded in the real embryo, cell number in each compartment was similar between 'ETS-embryos' and egg cylinders (Fig. 3.4. A).

Tissue volume of both 'ETS-embryos' and egg cylinders was also estimated, based on the assumption that both structures were approximately cylinder-shaped (Materials & Methods). Again, 'ETS-embryos' had comparable tissue volume to mouse embryos when the volume occupied by the VE was excluded from the latter (Fig. 3.4. B), supporting the idea that 'ETS-embryos' were able to faithfully recapitulate embryonic tissue morphology and architecture.

The statistical power of the analyses performed in Fig 3.4A and 3.4B was calculated on a post-hoc basis, after the experiments had been performed and the data analysed. Since the variation in both cell number and tissue volume between groups was small, the statistical power of the analyses performed was modest (especially when comparing embryonic cells and tissue volume), given a sample size of n=20 per group. The sample size of n=20 was chosen as this was in line with original studies to estimate the number of cells in the early post-implantation embryo (Snow, 1976, 1977), and to reduce the number of mice that needed to be sacrificed to obtain embryos. This was especially important at early stages of the project when only broad comparisons were made between *the in vitro* model and the real embryo. However, if the analyses were to be performed again, it might benefit from larger sample sizes and thus have greater statistical power to lower the chances of obtaining a false-negative result.

3.3.2 Expression of EPI and ExE markers in 'ETS-embryos'

To verify the embryonic and extra-embryonic identities of ESC and TSC compartments within 'ETS-embryos', q-RT PCR analysis was performed on ESC and TSC compartments dissected from 'ETS-embryos' for markers of EPI and ExE tissues in the egg cylinder. In agreement with results at the protein-level, ESC compartments expressed higher levels of EPI markers *Ascl4, Fgf5,* and *Otx2*, which were not detected in TSC compartments (Fig 3.4. C, top row). In contrast, TSC compartments expressed the ExE/ trophoblast markers *Cdx2,* and *Gata3*, which were not detected in ESC compartments (Fig 3.3.1 C, bottom row). Importantly, TSC markers *Elf5* and *Eomes* were also detected

in the extra-embryonic compartments of ‘ETS-embryos’ and *Oct4* was expressed in ESC compartments, suggesting that both compartments had not only begun to differentiate in culture, but simultaneously maintained a self-renewing state, much like the tissues of the post-implantation embryo (Fig. 3.4. C, top and bottom rows). These results confirm that ‘ETS-embryos’ consist of embryonic both embryonic and extra-embryonic compartments, and that the stem-cell character of cells in each compartment was not compromised in these culture conditions, thus mimicking the EPI and ExE compartments of the egg cylinder.

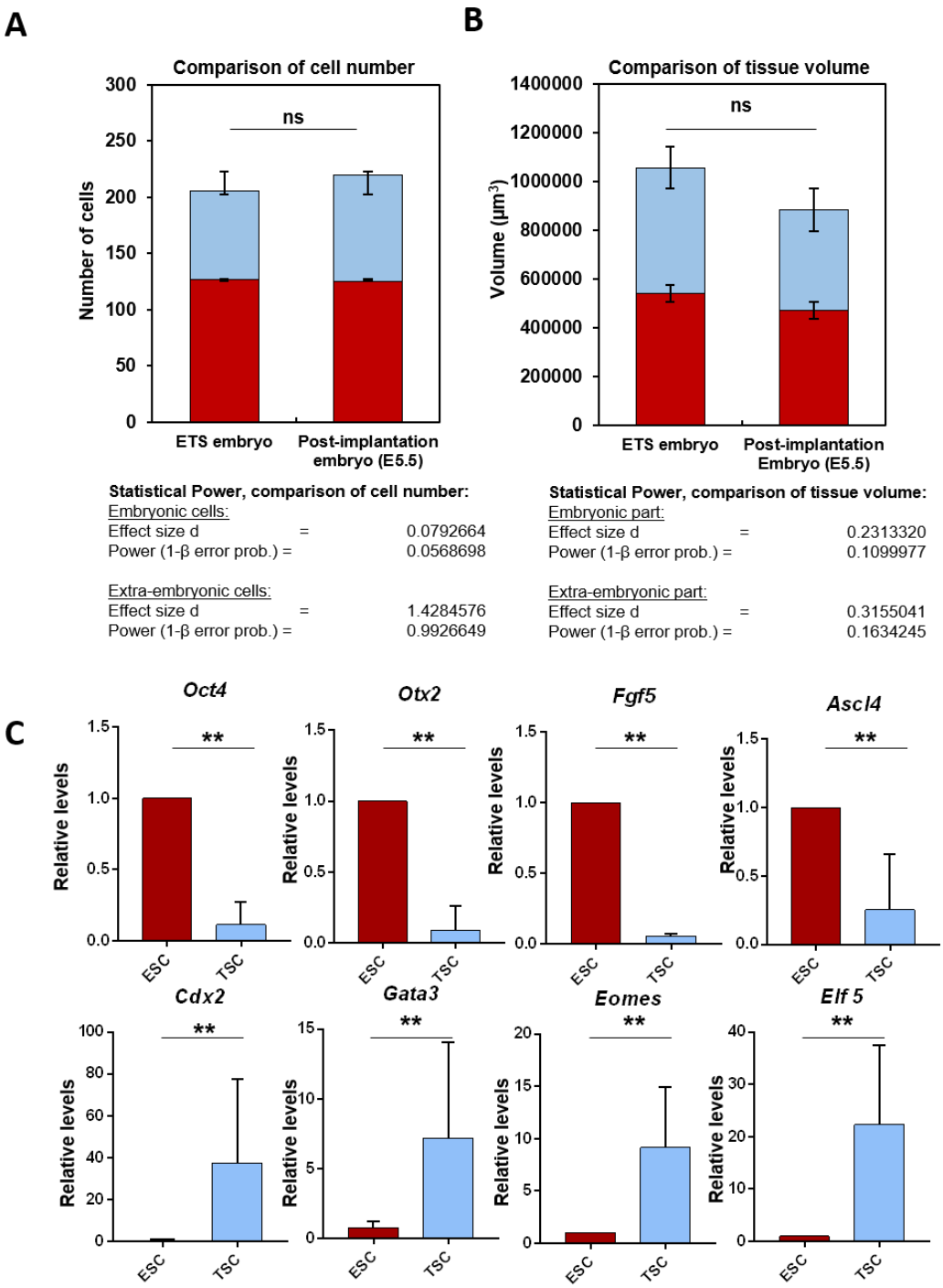

Fig. 3.4. (A) ETS-embryos have similar number of cells after 96 hours to natural embryos (cultured for 48 hours from the late blastocyst stage; equivalent to E5.5 embryos) in embryonic and extra-embryonic compartments (Student's t-test, n=20 per group, (2 separate experiments; not significant). Error bars = SEM. **(B)** Mean tissue volumes of embryonic and extra-embryonic parts are similar for ETS-embryos after 96 hours and natural embryos cultured for 48 hours *in vitro* from the late blastocyst stage (equivalent to E5.5 embryos). Student's t-test, n=20 per group, 2 separate experiments; not significant. Error bars=SEM. NB: Volume occupied by the visceral endoderm was excluded from quantification in natural embryos. Effect size and statistical power was calculated on a post-hoc basis and are shown for the data in (A) and (B). See Materials & Methods for how volume and statistical power was calculated. B is equal to the probability of a type II error. **(C)** q-RT-PCR analysis of and epiblast markers (*Oct4*, *Acsl4*, *Otx2*, *Fgf5*) – upper row- and ExE markers (*Cdx2*, *Eomes*, *Elf5*, *Gata3*)- lower row-in ESC and TSC derived compartments of ETS-embryos cultured for 96 hours. Student's t-test, $P<0.05$. n=4 biological replicates. Error bars= SEM.

3.4 Efficiency of the co-culture system to produce 'ETS-embryos'

Having established that 'ETS-embryos' were similar to the mouse embryo in terms of both morphology and marker expression, the efficiency of the generation of 'ETS-embryos' in the system was quantified. Four different types of structure were present in the culture system, detectable at varying frequencies (Fig 3.5. A). In a single experiment, 61% of all structures embedded in the ECM were cyst-like, with a central lumen and consisted of ESCs only which were positive for the pluripotent epiblast marker Oct4. 17% of all structures consisted of TSCs only, and were positive for the ExE marker Eomes. The remaining 22% of structures were compound, consisting of both ESCs and TSCs which always formed separate compartments (n=400) (Fig. 3.5 A, B). In the vast majority of cases (92.68% of structures, n=88) the compound structures were made up of a single ESC compartment abutted by a single TSC compartment, to form a characteristic egg-cylinder-like architecture. A small number of structures (7.32%, n=88) instead consisted of two ESC compartments joined by a shared TSC compartment (Fig. 3.5. A-C). These results show that the co-culture system developed in this study can reproducibly generate embryo-like structures in culture, but that ESCs and TSCs do not always form 'ETS-embryos', as ESCs and TSCs must lie in close proximity to each other in order to form embryo-like structures consisting of both embryonic and extra-embryonic compartments.

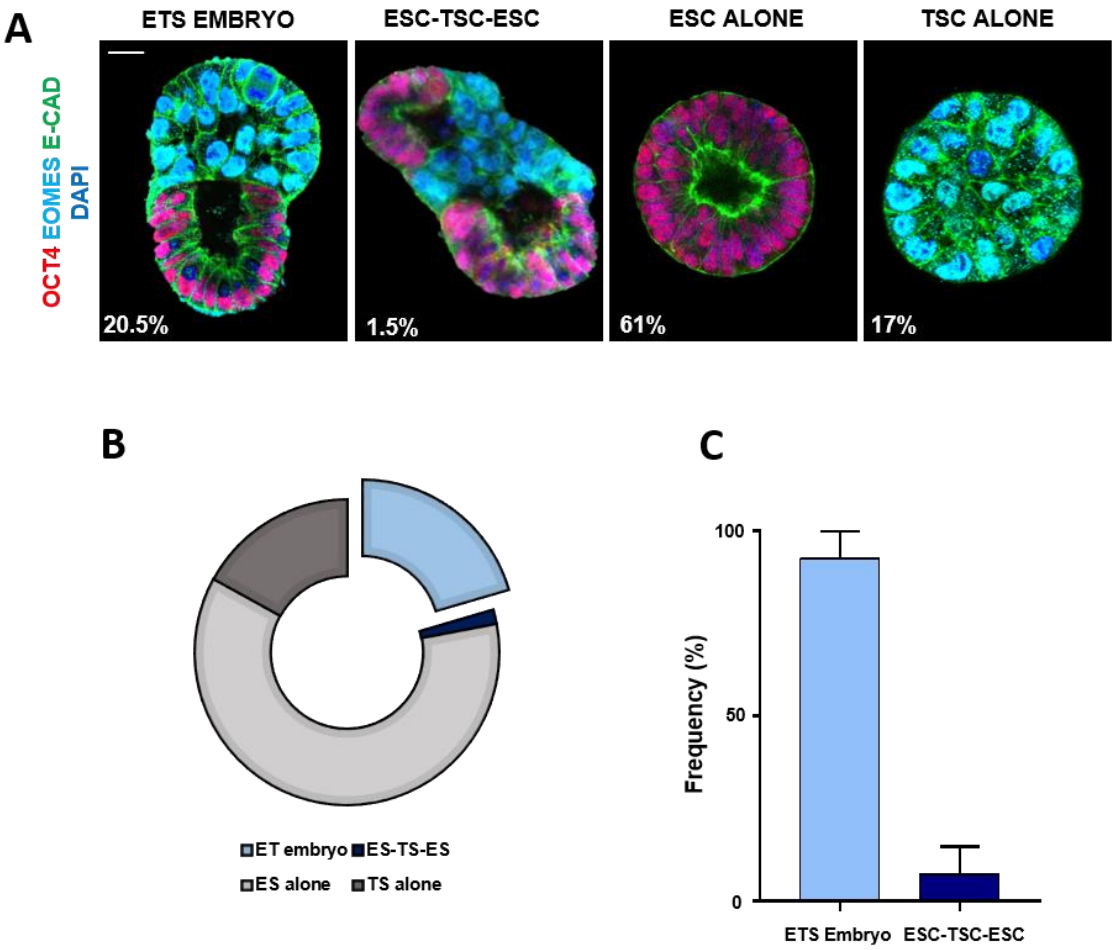

Fig. 3.5. **(A)** Frequency of ETS-embryos, "twin" (ESC-TSC-ESC) structures, and individual TSC or ESC structures in a representative experiment. Red, Oct4; green, E-cadherin, cyan, Eomes; blue, DNA. Scale Bar=20µm. 100 structures counted per experiment; 4 separate experiments. **(B)** Pie chart showing the relative frequency of different structures in co-culture. **(C)** Proportion of ESC- and TSC-structures that form ETS-embryos versus "twin structures". n=88; 4 separate experiments. Error bars= SEM.

3.5 Discussion

Taken together, the results presented in this chapter suggest that ESCs and TSCS can self-assemble in ECM to form an embryo-like structure *in vitro* when combined in culture. This self-organisation event is reproducible, and can be exploited to generate 'ETS-embryos' from ESCs and TSCs after just 96 hours of development in the system.

Owing to the fact that cells are initially mixed in suspension and then seeded into culture to generate 'ETS-embryos' (see Materials & Methods), ESC and TSC co-cultures generated using this method are heterogeneous. Whilst 22% of all structures generated are 'ETS-embryos', the great majority of 3D cell-aggregates consist of either ESCs or TSCs alone. This may be explained by the initially low plating density of cells ($1x10^5$ cells/ml) used to generate 'ETS-embryo's, which makes the probability of ESCs and TSCs meeting in culture somewhat low. However, since greater than $1/5^{th}$ of all structures in culture were 'ETS-embryos', there may be some mechanism that increases the initially low-chance of cells meeting. For example, it is possible that cells of different types can actively move towards each other in the Matrigel, perhaps directed by sensing attractive signals. Whilst this is an intriguing idea, further experiments using live-imaging techniques to observe how ESCs and TSC-clumps meet in the culture system would be required in order to test this hypothesis, which are not explored in the present study.

Interestingly, although the cells in this system were prone to generate 3D spheroids and compound structures consisting of both ESC and TSC compartments, the cells never mixed to form spheroids with a mosaic ESC and TSC structure. Given that the cells are initially mixed in suspension, this suggests that they were sorting in the culture to remain as two distinct populations in space.

Classical experiments on Sponge (Wilson, 1907) chick embryonic cells (Moscona and Moscona, 1952; Weiss and Taylor, 1960; Layer and Willbold, 1993) and more recently using zebrafish retinal cells (Eldred *et al.*, 2017) have demonstrated that cells in an organ can sort out after disaggregation to re-form their original structure. Such cell-sorting is a critical feature of organogenesis (Lancaster and Knoblich, 2014), and this principle has been used with great success to generate *in vitro* 'organoid' models of many tissues using either mouse and human pluripotent stem cells (Eiraku *et al.*, 2011; Spence *et al.*, 2011; Lancaster *et al.*, 2013; Takasato *et al.*, 2014; Takebe *et al.*, 2014; Xia *et al.*, 2014) or adult precursors (Sato *et al.*, 2009; Barkauskas *et al.*, 2013; Greggio *et al.*, 2013; Huch *et al.*, 2013).

It has been hypothesised that the expression of different cell-adhesion molecules between different cell types can enable cells to sort into two sub-populations within an initially mixed population of cells to generate tissue boundaries (Steinberg, 1963; Amack and Manning, 2012). This was later

demonstrated experimentally (Foty *et al.*, 1996), and the expression of a particular class of adhesion proteins, the cadherins, have been shown to be important for cell sorting during embryonic development (Fujimori, Miyatani and Takeichi, 1990). Cadherin-mediated cell sorting can be achieved via differences in adhesive strength between cadherins on the cell surface, or differences in the intracellular signalling cascades they induce.

Worthy of note in this context is the adhesion molecule E-cadherin, which is the only classical cadherin expressed in EPI cells before gastrulation starts (Stemmler, 2008). It is known that TSCs express higher levels of E-cadherin than ESCs (Ohinata and Tsukiyama, 2014). This makes E-cadherin a good candidate for the adhesion molecule that is differentially expressed between these two cell types, that may play a role in the cell sorting observed in this system. It follows that this could account for why spheroids made up of both populations of cells mixed together are never observed.

Studies on ESCs cultured *in vitro* have shown that modulating levels of E-cadherin expression can result in cell sorting both in 2D (Blancas *et al.*, 2011) and in 3D using embryoid bodies (Moore *et al.*, 2014), so a similar mechanism for cell sorting could be acting here. This, combined with differential morphogen signalling between the two tissue types (Guzman-Ayala *et al.*, 2004; Tam and Loebel, 2007) may provide an explanation for the profound spatial separation of the two populations observed in this system.

However, studies in other systems *in vivo*, such as zebrafish, have proposed that the sorting of cells into specific tissues with defined boundaries is also dependent on the extent of acto-myosin contractility in a particular cell type (Krieg *et al.*, 2008). The extent to which these factors play a role in the cell sorting observed in the 'ETS-embryo' culture system, and whether these mechanisms are physiologically relevant to mouse embryogenesis *in vivo* remain to be investigated.

Another feature common to both organoids and the method to generate 'ETS-embryos' is the use of ECM to support the development of organised tissue. It was the work of Mina Bissell and colleagues which first showed that the morphology of breast epithelial cells in culture could be dramatically altered when grown in the presence of ECM and that this could also lead to the functional differentiation of the cells *in vitro* (Hagios, Lochter and Bissell, 1998). Similar results were also obtained using kidney epithelial cells (Montesano, Schaller and Orci, 1991). This inspired attempts to embed cell cultures in a gel-derivative of Engelbreth-Holm Swarm Carcinoma ECM (Li *et al.*, 1987), which is rich in laminin, and has become known commercially as 'Matrigel'. This technique allowed the recapitulation of tissue ultrastructure in 3D using cells in culture, and its success means that the majority of organoid studies cited above, involve a step which utilises Matrigel to generate complex

organ-like tissues. In the present study, whilst the requirement to recapitulate a 3D structure was essential, the rationale for the embedding of ESCs and TSCs in Matrigel to generate 'ETS-embryos' goes beyond that for organoids.

As well as simply providing mechanical support to the growing 3D structure, and acting as a barrier to separate tissue layers in the early embryo, Bedzhov et al. showed that the basement membrane is essential for epiblast morphogenesis, which is induced by β1-integrin signalling mediated by laminin (Bedzhov and Zernicka-Goetz, 2014). The epithelialisation of the EPI which occurs upon implantation can be mimicked *in vitro* using ESCs embedded in Matrigel, which is very rich in laminin proteins. The ESCs form a spheroid which can open a lumen akin to that in the mouse EPI within 48 hours of culture, demonstrating that β-1 integrin signalling is sufficient to induce epithelialisation even *in vitro* (Bedzhov and Zernicka-Goetz, 2014). This was therefore the obvious starting point to generate embryo-like structures in culture.

It is unsurprising that by providing ECM, the ESCs are induced to form an epithelium, as this has been shown in other systems and a basement membrane is known to be required to maintain the integrity of tissue epithelia *in vivo* (Miner *et al.*, 2004). However, the role of β1-integrin signalling in TSC morphogenesis and by extension, ExE morphogenesis, remains to be studied. 'ETS-embryos' provide an interesting opportunity to address this gap in knowledge, but this is beyond the scope of this current work.

Additionally, the fact that 'ETS-embryos' resemble the egg cylinder so closely, and yet the two stem cell populations maintain distinct identities despite being in common culture means that this represents an accurate yet simplified model system to investigate interactions between EPI and ExE tissues during embryogenesis. Whilst several *in vivo* studies have reported that the development of the EPI is compromised when there is no ExE (Donnison *et al.*, 2005; Rodriguez *et al.*, 2005) specific interactions might be easier to elucidate than in the real embryo because the third tissue of the embryo, the VE, is not present, which would otherwise confound results.

Undoubtedly, ESCs and TSCs are able to sort-out to give rise to embryonic architecture in a similar manner to how organ precursors can sort themselves to build organ architecture. A second feature of organogenesis is regulated cell differentiation in a spatially restricted area. This gives rise to specialised cell types in the areas of the tissue where they are required to perform their function (Lancaster and Knoblich, 2014). In subsequent chapters, the possibility that similar spatially restricted cell fate decisions associated with post-implantation embryogenesis might occur in 'ETS-embryos' is explored.

One major limitation of the culture system is the lack of incorporation of extra-embryonic endoderm-like cells in a VE-like layer enveloping the ESC- and TSC-derived compartments. At no time did 'ETS-embryos' spontaneously develop a layer of extra-embryonic endoderm-like cells, as shown in Fig. 3.3., although this has been shown to occur in embryoid bodies (Soudais *et al.*, 1995; Morrisey *et al.*, 1998; Coucouvanis and Martin, 1999; Hamazaki *et al.*, 2004). Even though ESCs have some potential to generate endoderm, perhaps endoderm specification does not occur in this system simply because the ESCs do not have enough time in culture to do this. In embryoid body cultures, it takes up to 12 days (Soudais *et al.*, 1995; Morrisey *et al.*, 1998) for endoderm cells to appear in the culture. In the 'ETS-embryos', egg-cylinder-like structures assemble within 96 hours. Hence, if the ESCs are expected to behave in the 'ETS-embryo' system as they do in embryoid bodies, it may be that they would need to be left longer in culture before endoderm-like cells would appear. Secondly, the presence of the ECM surrounding the cells may inhibit differentiation to VE-like cells, because endoderm specification in embryoid bodies is usually outside of the lamina, with the epiblast-like cells on the inside (Li *et al.*, 2001, 2002).

By embedding the ESCs and TSCs in ECM, the VE layer is partially compensated for, because the VE is known to secrete the basement membrane which is critical for EPI morphogenesis, as discussed above. However, the ECM cannot substitute for the role of the VE in providing all the developmental signals required for subsequent development and patterning. As well as the specialised DVE/AVE population acting as an organising centre, with a localised source of morphogen antagonists, other regions of the VE have also been shown to secrete key molecules which feedback to the EPI and instruct development (Kumar *et al.*, 2015) including at the posterior (Yoon *et al.*, 2015). One obvious way to include this tissue would be to add stem-cell representatives of the VE into the *in vitro* model to complete the mimic of the embryo. Stem cells from the extra-embryonic endoderm ('XEN') cells have been derived from both the pre-implantation and more-recently, the post-implantation mouse embryo (Kunath *et al.*, 2005; Lin *et al.*, 2016). These cells would be good candidates to introduce into the co-culture system to mimic the VE, and since these cells secrete basement membrane proteins including laminin (Hogan, Cooper and Kurkinen, 1980; Artus *et al.*, 2012), a culture system including this tissue may not require Matrigel.

However, in conventional culture, XEN cells more closely resemble primitive endoderm or parietal endoderm (PaE) lineages, and in fact when introduced into chimeras, these cells rarely contribute to the VE and instead are more prone to contributing to the PaE (Kunath *et al.*, 2005; Brown *et al.*, 2010). Therefore, XEN cells may require some manipulation prior to co-culture in order to become more 'VE-like'. Several studies have demonstrated how XEN cells can be converted into VE-like lineages either

by culturing cells on different ECM substrates to induce different morphology or by modulating different signalling factors such as BMP (Artus *et al.*, 2012; Paca *et al.*, 2012) and Nodal (Liu *et al.*, 2012). It would make sense to 'prime' XEN cells by exposing them to these treatments before their use in co-culture to attempt to generate a more embryo-like outcome. However, the possibility that signals secreted by cells in co-culture and the interactions between them may also drive a more VE-like state also warrants consideration.

In summary, this chapter has shown that the combination of mouse ESCs and TSCs in 3D culture surrounded by ECM is sufficient to generate embryo-like structures which closely resemble the mouse egg cylinder at early post-implantation stages. The self-assembly of these structures suggests that embryonic and extra-embryonic stem cells have an intrinsic ability to interact, and their similarity to the embryo makes 'ETS-embryos' a potential tool to complement *in vivo* studies of early mammalian development. In the subsequent chapters, 'ETS-embryos' have been characterised in further detail and compared to the mouse embryo in terms of their morphogenesis, and cell fate specification events.

4. Results II: 'ETS embryos' model pro-amniotic cavity formation in the post-implantation mouse embryo

4.1 Introduction:

The formation of a luminal space within a polarised, epithelial tissue is a process critical to the proper development of organs in many systems. In the main, a lumen can form between unpolarised precursor cells during organogenesis as a result of two main processes: cavitation, when regulated programmed cell death at the centre of a solid mass of tissue generates the luminal space, or hollowing, which does not involve apoptosis (Andrew and Ewald, 2011). Instead, during hollowing, the cavity appears as a result of uniform cell polarisation, followed by actomyosin-contractility at the apical side of cells in the tissue, which constrict, before apical cell membranes are forced apart from one another creating a space between them (Martín-Belmonte *et al.*, 2008). Lumens are critical for the exchange of fluid and ions between epithelia and their formation has been characterised in a variety of systems. These include *C.elegans* gut formation and mammalian kidney podocytes cultured *in vitro* which use hollowing as the mechanism (Leung, Hermann and Priess, 1999; Martín-Belmonte *et al.*, 2008), and during mammalian mammary and salivary gland morphogenesis, which use directed apoptosis as the mechanism (Humphreys *et al.*, 1996; Teshima *et al.*, 2016).

Given the intensive study of lumenogenesis in other contexts, and the fact that cavitation of the early embryo is a morphogenetic event that is conserved across mammals, it is somewhat surprising that, until recently, relatively little was known about how the pro-amniotic cavity forms in the mammalian embryo. Furthermore, the function of this cavity during development remains completely mysterious. The pro-amniotic cavity in the mouse embryo initiates as the embryo implants into the uterus, between embryonic day 4 and 5. This is coupled to a global reorganisation of the embryonic tissues, which transform from free-floating ball of cells which make up the blastocyst, into the egg cylinder.

The development of an *in vitro* culture system by the Zernicka-Goetz laboratory (Morris *et al.*, 2012; Bedzhov, Leung, *et al.*, 2014) has enabled the study of morphogenesis through these stages, which is otherwise impossible without the use of an *in vitro* model. Bedzhov et al. demonstrated that cavitation in the embryonic epiblast occurred by a process of apical constriction of the cells, which formed a 'rosette-like' structure (Bedzhov and Zernicka-Goetz, 2014). Laminin secreted as part of the basement membrane that forms between EPI and VE acts as a polarisation cue, which is transduced by the cells in the EPI via β1-integrin signalling, resulting in apical constriction and rosette formation. The rosette-like structure subsequently resolves to give rise to a lumen at the centre of the tissue. Prior to this discovery, which challenged the 'textbook model' of pro-amniotic cavity formation, models of

embryogenesis using embryoid bodies cultured *in vitro* suggested that cavity formation in the EPI was instead due to directed apoptosis of cells in the centre of the embryo, mediated by BMP signalling from the VE (Coucouvanis & Martin, 1995).

Although the formation of the 'rosette'-like structure at the centre of the EPI and its resolution leading to lumenogenesis has now been accurately described, cavitation in the ExE is still relatively poorly understood, and no faithful 3D *in vitro* model for this tissue exists. Indeed, the changes in cell shape and behaviour which result in the fusion of lumens in the EPI and ExE to give rise to the continuous pro-amniotic cavity also remain uncharacterised.

With this in mind, cavity formation in 'ETS-embryos' was characterised and compared to cavitation in the mouse embryo. The results presented in this chapter demonstrate that 'ETS-embryos' faithfully mimic the sequence of events leading to pro-amniotic cavity formation in the mouse embryo, and these events occur with similar timing in both systems. Just as in the embryo, 'ETS-embryos' initiate cavitation in the embryonic compartment, and the extra-embryonic compartment cavitates subsequently. Later, these two cavities fuse together to form a continuous lumen at the centre of the structure. Cavity fusion is concomitant with both cell rearrangements in 'ETS-embryos' and a remodelling of the ECM. Upon inhibition of Nodal/Activin signalling, cavitation is profoundly disrupted in 'ETS embryos'. This phenocopies the situation in cavitating mouse embryos, supporting the idea that 'ETS embryos' are a good model for the study of morphogenetic events which occur during egg cylinder formation.

4.2 Characterisation of cavity morphogenesis in 'ETS-embryos'

4.2.1 'ETS-embryos' undertake cavitation via a reproducible sequence of events

To better characterise cavity morphogenesis in 'ETS-embryos', structures in culture were fixed at consecutive 12 hour intervals, and stained for EPI marker Oct4, to demarcate the ESC compartment from the TSC compartment, and also for the cell adhesion protein E-cadherin (E-cad) to assess cell shape. Immunofluorescence revealed that 'ETS-embryos' underwent a reproducible sequence of events to give rise to the shared cavity present at 96 hours. First, when 'ETS-embryos' were fixed after 72 hours of culture, a single lumen could only be detected in the ESC compartment. Cells in this compartment were columnar in shape and vector analysis of the long axis of each nucleus (see Materials & Methods) indicated that the cells were aligned to surround a central cavity. In contrast, no cavity could be detected in the TSC compartment, where cells were not columnar and the nuclei did not consistently align in any direction (Fig. 4.1. A, D). Strikingly, when 'ETS-embryos' were allowed to develop for a further 12 hours before fixation at 84 hours, cavities were detected in the TSC

compartment. Cells acquired a more columnar shape and the analysis of the nuclear long axis suggested that they were also now aligned to surround a central point. In some cases, up to three separate cavities were observed in the TSC compartment after 84 hours, in contrast to in the ESC compartment where only one cavity was present (Fig. 4.1. B, E & Fig. 4.2.). However, cavities in ESC and TSC compartments were never joined at this stage. It was only after 96 hours in cultured that these separate cavities merged together, with all cells acquiring a columnar morphology, and becoming aligned to form a continuous epithelium (Fig. 4.1. C).

To confirm this sequence of events, 'ETS-embryos' were fixed and stained over the same time-course but this time to show the distribution of the negatively-charged transmembrane silomucin, podocalyxin (Podxl). This protein is known to line the emerging cavities present within the mouse embryo during egg cylinder formation (Bedzhov and Zernicka-Goetz, 2014), and it may function to help keep cell membranes apart in kidney podocytes and Madin-Darby canine kidney (MDCK) cells by repulsion (Orlando *et al.*, 2001; Meder *et al.*, 2005). As in the egg cylinder, Podxl lined the cavities present in 'ETS embryos' and co-staining to reveal cell polarity using atypical protein-kinase C (aPKC) showed that it was accumulated along the apical sides of cells which faced into the cavity (Fig. 4.3. A, B). Analysis of Podxl distribution by both co-staining with aPKC and by measuring staining intensity and identifying peaks at the apical surfaces of cells across each tissue compartment confirmed the sequence of events by which cavity formation and fusion occurred (Fig 4.4.). At 72 hours there was an accumulation of Podxl and aPKC at the apical side of cells arranged around a clear cavity in the ESC compartment, and when Podxl staining intensity was quantified, two clear peaks in intensity could be identified corresponding to the apical sides of the cells lining the lumen. However, in the TSC compartment, no such accumulation was observed, nor were there identifiable peaks in the staining intensity profile, indicating that no cavity was present at this time (Fig 4.3. A, B, Fig. 4.4. A). After 84 hours, cavities were detected in the TSC compartment and these were lined with Podxl, and after 96 hours these cavities had fused and become continuous (Fig. 4.3. A, B 4.4. B, C).

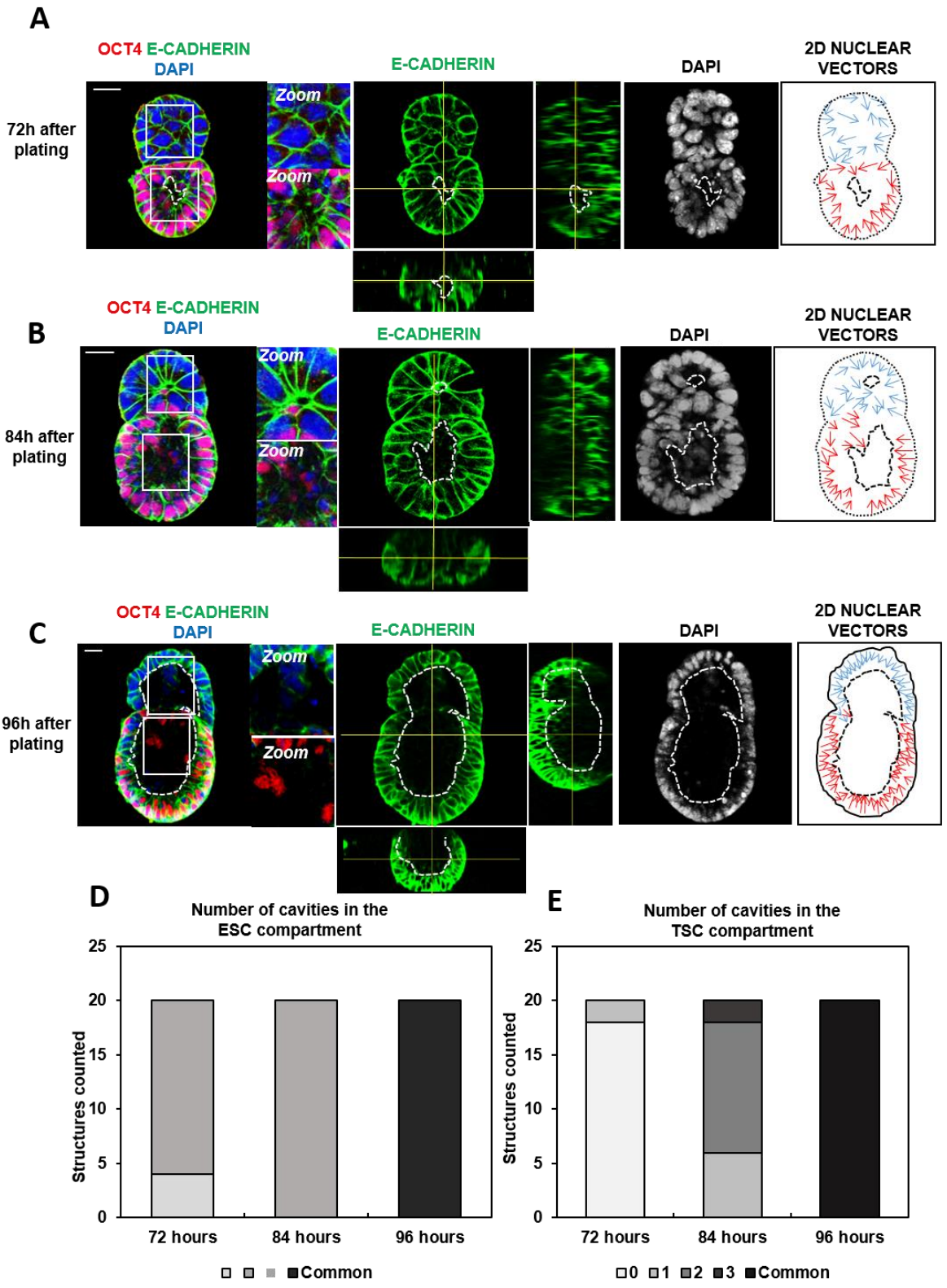

Fig. 4.1. (A-C): ETS-embryos after 72, 84 and 96 hours showing progression of cavitation. Oct4, red; E-cadherin, green; DNA, blue/grey. Orthogonal views are shown for E-cadherin staining at each time-point. Zoomed fields highlight cavitated areas at each time-point; white or black dotted lines highlight cavities. Lower right panel for each time-point show orientation of nuclei in ESC compartments (red) and TSC compartments (blue) – nuclei become aligned to cavities; n=20 ETS-embryos per time-point, at least 2 separate experiments per time-point. Scale Bar=20µm. **(D-E)** Quantification of number of cavities in respective ESC- and TSC-compartments of ETS-embryos at 72, 84, and 96 hours. n=20 ETS-embryos analysed per time-point.

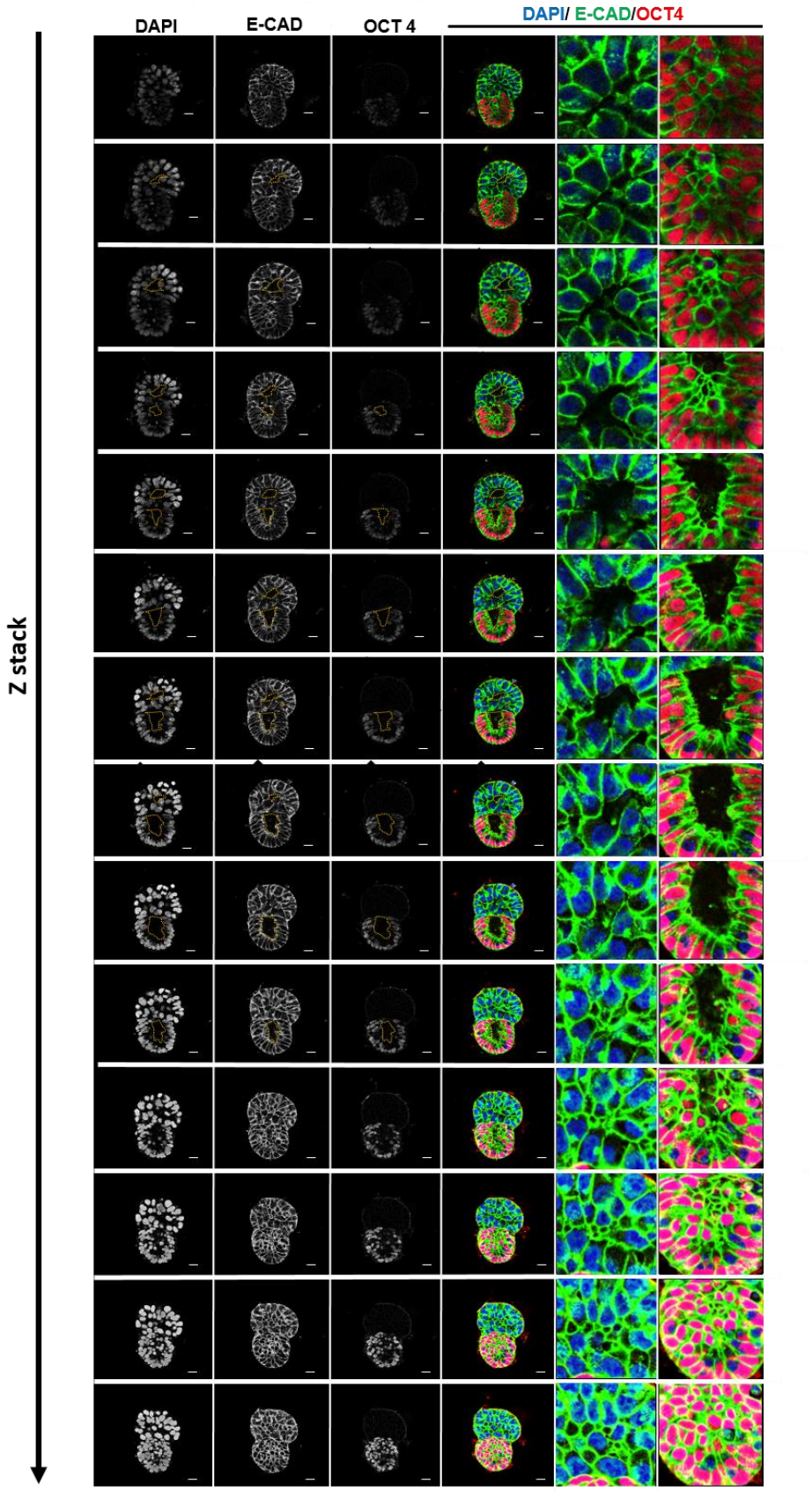

Fig. 4.2. A montage of a complete Z-stack through a representative ETS-embryo to illustrate scoring of cavities (outlined with yellow dotted lines and shown in zoomed images in right-most two columns). Red, Oct4; Green, E-cadherin; Blue, DNA. Scale Bar=20µm.

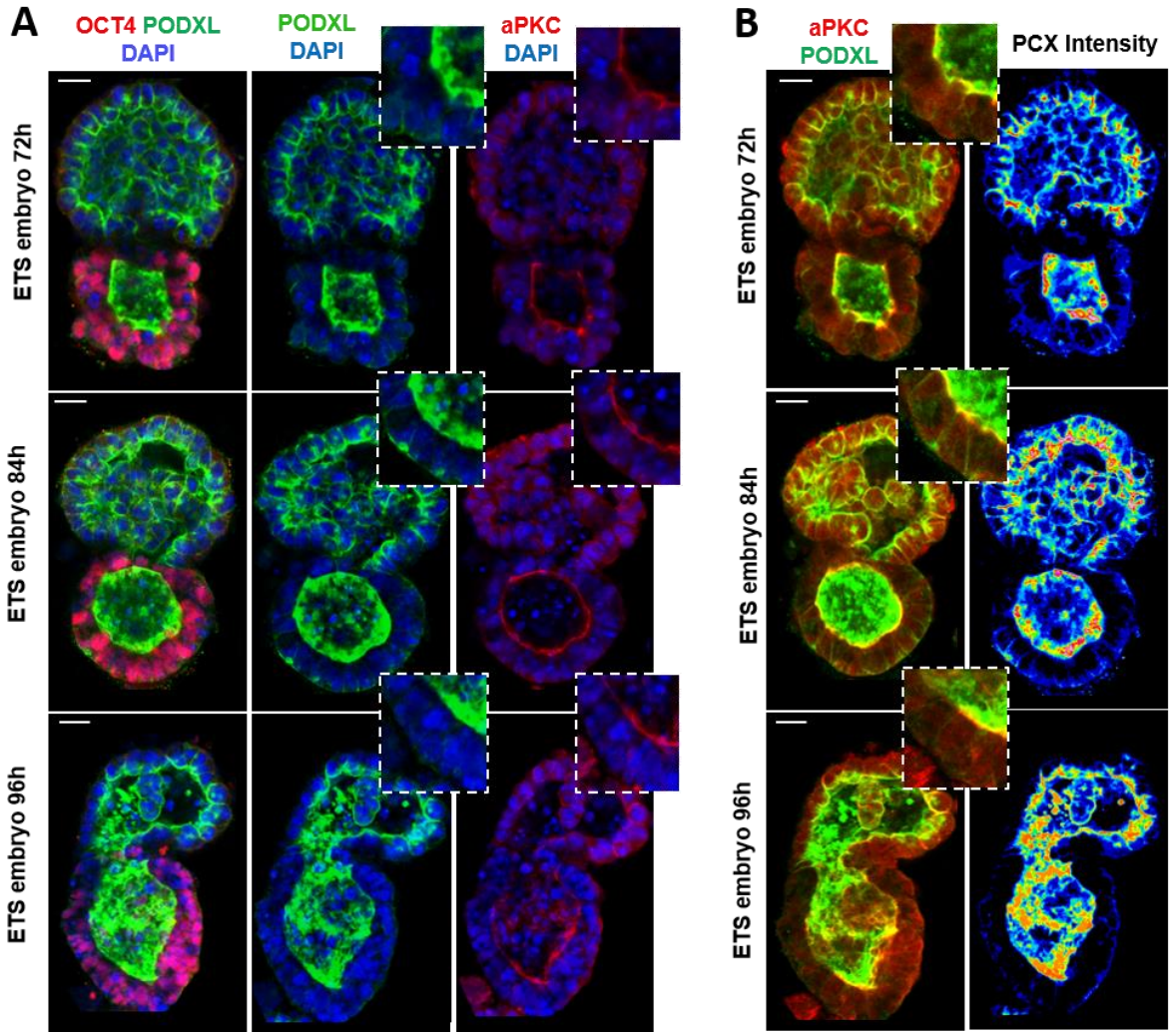

Fig. 4.3. **(A)** ETS-embryos at three successive time-points during cavitation (72 hours, top row; 84 hours, middle row; 96 hours, bottom row) stained to reveal Oct4/aPKC, red; Podxl, green; DNA, blue. Zoomed insets highlight regions where the apical sides of the cells face into the cavity. Scale Bar=20µm. n=30, 3 separate experiments. **(B) Left panels:** The same ETS-embryos at successive time-points with aPKC (red) and Podxl (green channels) overlaid to show co-staining at the apical sides of the cells. Zoomed insets highlight regions of co-localisation. **Right panels:** False-coloured images of the Podxl channel to highlight variation in staining intensity. Scale Bar= 20 µm.

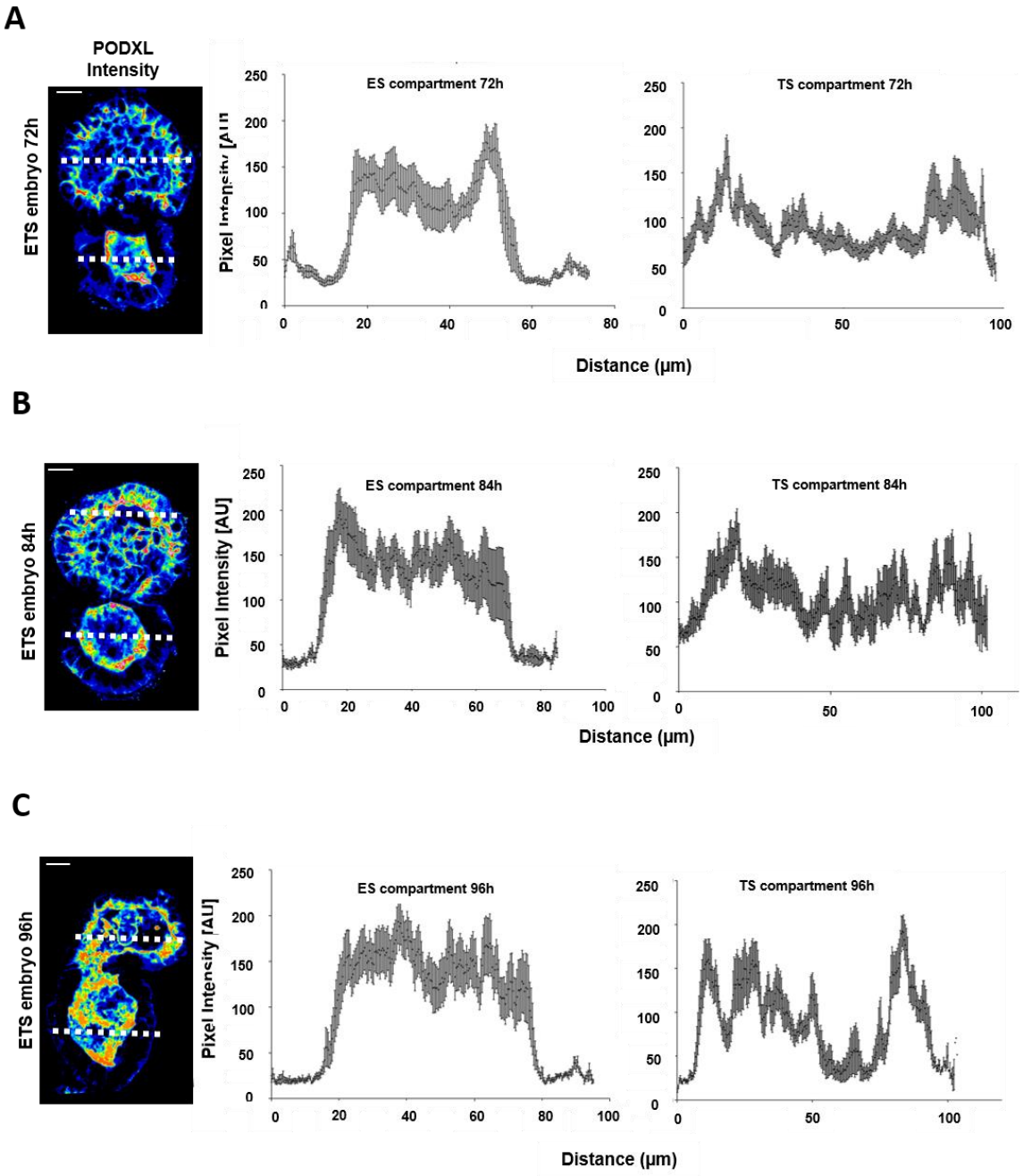

Fig. 4.4. (A-C) False-coloured images of the Podxl staining of ETS-embryos at three successive time-points during cavitation and accompanying graphical quantification of Podxl staining intensity plotted as mean +/- SEM for eight different cross-sections of the ETS-embryo shown taken at the middle z plane. PCX accumulates on the apical sides of cells (marked by aPKC) facing a lumen, so the presence of a cavity is indicated by two strong peaks in the intensity profile. Y-axis: PCX fluorescence intensity. N=30 structures analysed per timepoint.

4.2.3 'ETS-embryos' cavitate similarly to the mouse embryo

This sequence of events is very similar to the sequence of events shown to lead to pro-amniotic cavity formation in the mouse embryo (Bedzhov and Zernicka-Goetz, 2014) and this suggests that 'ETS-embryos' undergo a similar morphogenetic event *in vitro*. This is supported by the fact that immunofluorescence staining of Podxl distribution in a mouse embryo during pro-amniotic cavity formation is very similar to that in 'ETS-embryos' at mid-cavitation stages. When 'ETS-embryos' and mouse embryos were fixed and stained in parallel, Podxl was found to line the expanding cavity at the centre of the tissue, accumulating at the apical sides of the columnar shaped cells facing into the cavity in both mouse embryos and 'ETS-embryos' undergoing cavitation (Fig. 4.5. A).

To exclude the possibility that cavities in 'ETS-embryos' appeared as a result of apoptosis, a process shown to play little role in mouse embryo cavitation (Bedzhov and Zernicka-Goetz, 2014), dying cells in cavitating 'ETS-embryos' were stained with a cleaved-caspase-3 (cc3) antibody, and counted. A mean of 2 apoptotic cells were detected in each tissue compartment, which was similar to the number detected in each compartment of the cavitating mouse embryo. Furthermore, where dying cells were present, they were not consistently located close to the site of lumen opening in either 'ETS-embryos' or mouse embryos (Fig. 4.5 B, C, D, E). This result suggests that programmed cell death does not drive cavitation in 'ETS-embryos', and thus reflects pro-amniotic cavity formation during mouse embryogenesis.

Next, to understand how the ECM becomes remodelled at the embryonic-extra-embryonic interface during cavitation, 'ETS-embryos' were fixed at consecutive time-points during cavitation and stained for laminin. This revealed that a boundary of laminin was present between ESC and TSC compartments at 72 hours, before a cavity was detectable in the TSC compartment (Fig. 4.6. A, leftmost panel). This ECM deposition was reminiscent of the basement membrane that is present between the embryonic and extra-embryonic compartments of the peri-implantation E4.75 mouse embryo (Fig. 4.6. B, leftmost panel). As 'ETS-embryos' underwent cavitation, the ECM between tissue compartments became broken and displaced, reflecting the process of basement membrane breakdown that occurs during egg cylinder morphogenesis *in vivo*. In 'ETS-embryos', laminin was consistently displaced towards the TSC compartment. This was in contrast to what happened at the interface when two structures comprised of only ESCs merged together. Here, laminin was not preferentially displaced in one direction, and quantification of the angle of laminin displacement in 'ETS-embryos' and structures made of fusing ESCs confirmed this (Fig. 4.6. A & C). These results indicated that laminin displacement

was therefore a characteristic of the ESC-TSC junction. In both the mouse embryo and in 'ETS-embryos', when the cavity was fully expanded, no laminin between the embryonic and extra-embryonic compartments could be detected (Fig. 4.6 A & B). These results support the idea that the remodelling of the ECM lying between embryonic and extra-embryonic tissues that takes place *in vivo* can be recapitulated *in vitro* using the 'ETS-embryo' model.

Taken together, these results demonstrate that 'ETS-embryos' are an accurate model of pro-amniotic cavity morphogenesis in the mouse embryo, and can therefore be used to study this process *in vitro*.

4.2.4 Characterisation of the ESC-TSC boundary during cavitation

Given that the above results support the idea that 'ETS-embryos' can be used as an accurate model of pro-amniotic cavity morphogenesis, the model was then used to gain insight into the cellular mechanisms underlying this process, which are still unknown in the mouse embryo (Bedzhov and Zernicka-Goetz, 2014).

To further characterise this morphogenetic event and understand the cell shape changes that occur at the embryonic-extra-embryonic boundary during 'ETS-embryo' cavitation, the cell aspect ratio (cell width divided by cell length) was measured for cells within different tissue compartments. Immunofluorescence staining to reveal Oct4 and E-cad showed that in 'ETS-embryos' fixed after 84 hours of culture (when cavities have emerged in both compartments but are not yet fused), ESCs had a smaller aspect ratio than TSCs, indicating that these cells were more columnar in shape (Student's t-test, $p<0.05$) (Fig. 4.7. A, B). Furthermore, when the location of TSCs within the tissue compartment was taken into account, it was clear that the shapes of the TSCs at the embryonic-extra-embryonic interface differed from those not at this boundary. TSCs at the boundary were more rounded and their aspect ratio differed significantly from the more columnar TSCs located further away from this interface (ANOVA test, $p<0.05$) (Fig. 4.7. A, zoomed insets, C).

Concomitant with changes in TSC shape during cavitation, it was also noted that cells in the ESC compartment would re-orient during cavity fusion in 'ETS-embryos'. These cells invaded into the TSC compartment and formed chimeric cell arrangements at the ESC-TSC boundary as laminin was displaced from the junction Fig. 4.8. A, B, white arrows). Such cell rearrangements may account for the changes in TSC shape observed at the ESC-TSC boundary, and warrant further study to determine their role in cavitation. Similar cell arrangements have recently been discovered at the EPI-ExE boundary of the cavitating mouse embryo, suggesting that they do indeed play a role in cavity morphogenesis (Christodoulou, Kyprianou and Zernicka-Goetz, 2017; Harrison *et al.*, 2017).

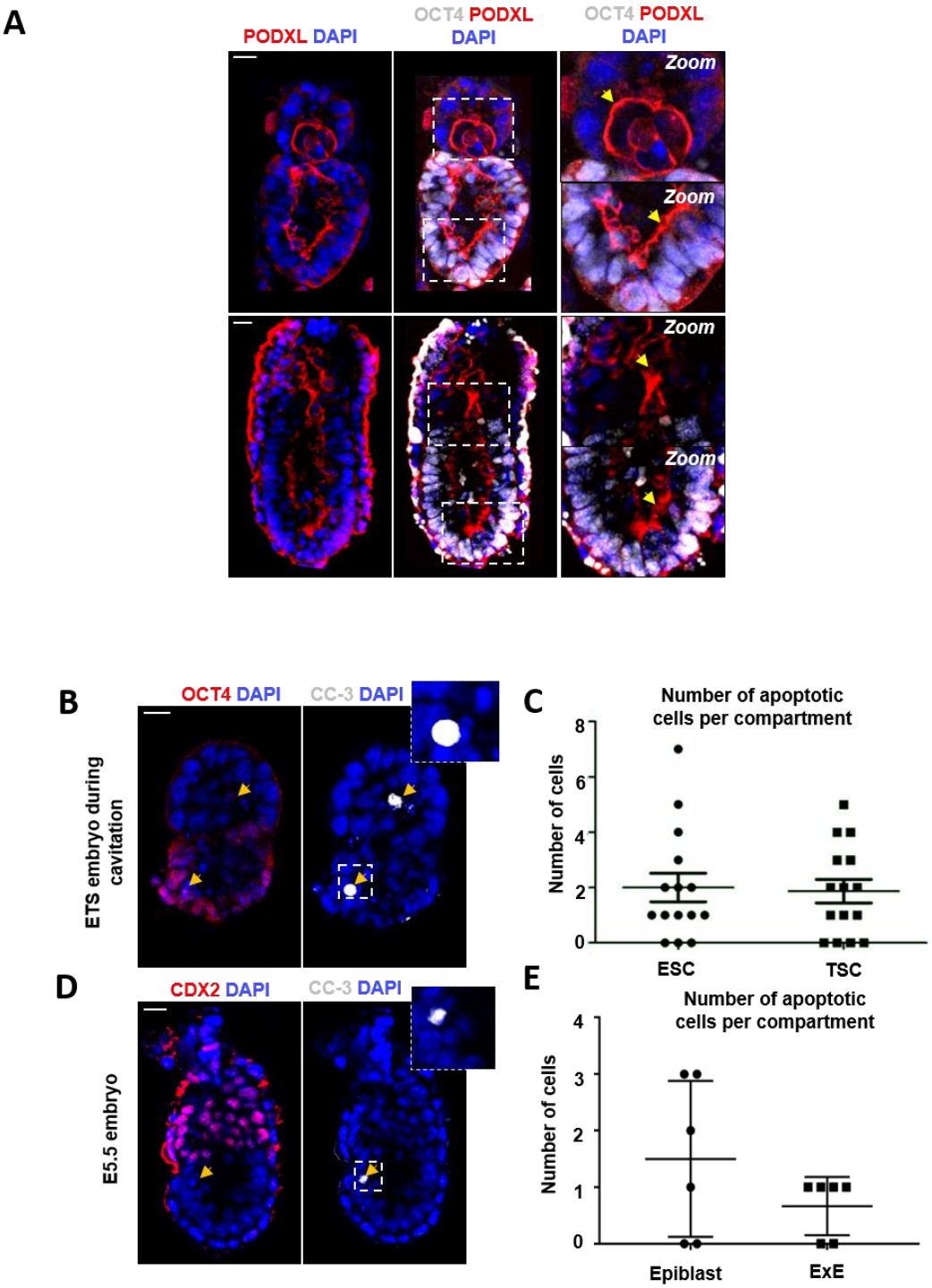

Fig. 4.5. **(A)** ETS Embryo mid-cavitation (upper panels) and an embryo recovered from the mother at E5.5 at (lower panels) stained to reveal Oct4, white; Podxl, red; DNA, blue. Zoomed insets and yellow arrowheads highlight cavities and build-up of Podxl at the apical sides of cells in embryonic and extra-embryonic compartments respectively. Scale Bar= 20µm. n=20 embryos or ETS-embryos each analysed in at least 2 separate experiments. **(B)** ETS-embryo stained to reveal: Oct4, red; DNA, blue; Cleaved-caspase-3, white. Scale Bar=20µm. Yellow arrowhead and inset indicates a dying cell. **(C)** Quantification of dying cells in ESC and TSC compartments. n=15. **(D)** E5.5 embryo recovered from mother and stained to reveal: Cdx2, red; DNA, blue; Cleaved-caspase-3, white. Scale Bar=20µm. Yellow arrowhead and inset indicates a dying cell. **(E)** Quantification of dying cells in the embryonic (EPI) and extra-embryonic (ExE) compartments of the embryo. n=6.

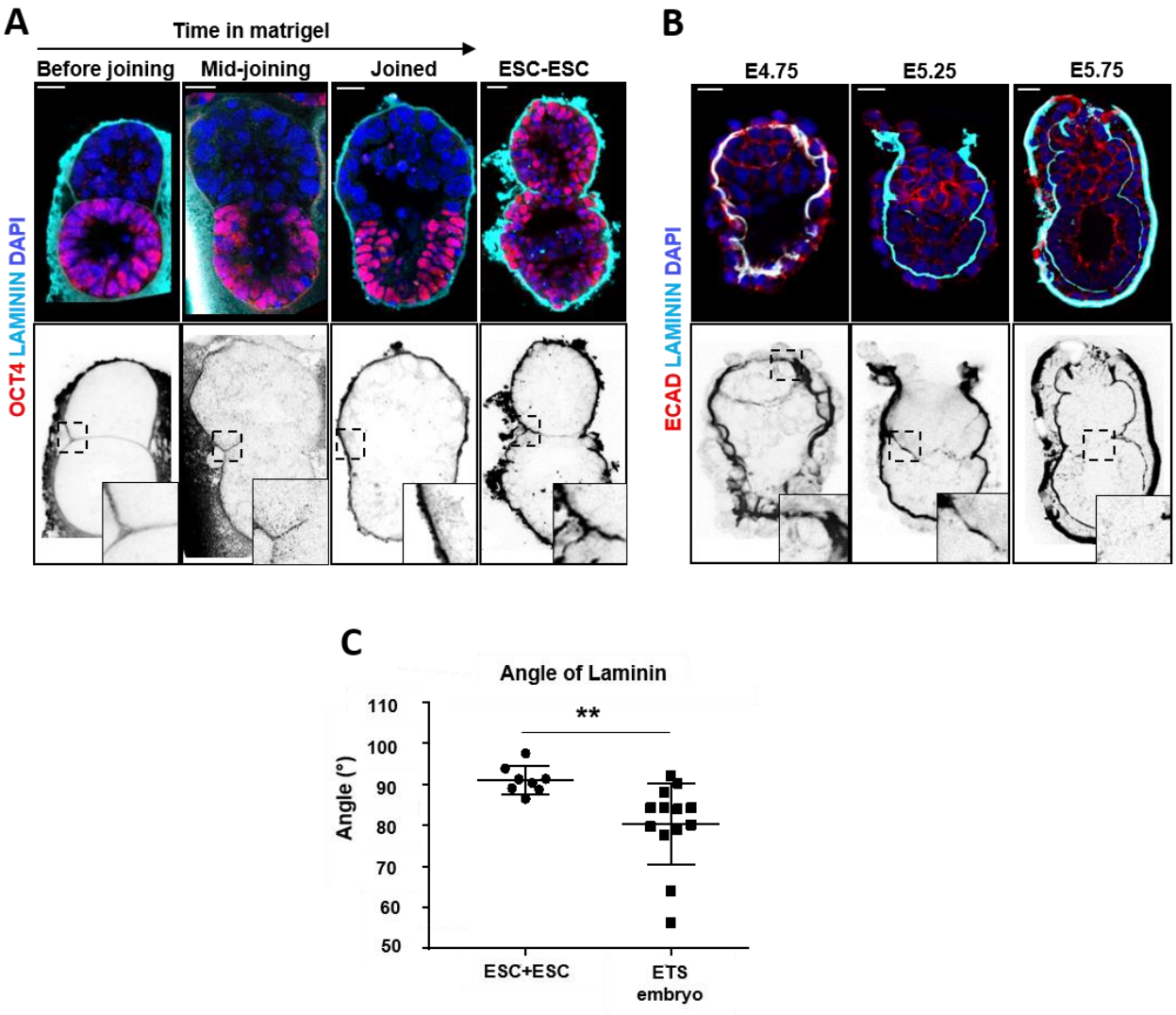

Fig. 4.6. **(A)** ETS-embryos during cavitation showing: Upper: Oct4, red; DNA, blue; laminin, cyan. Lower panel shows the laminin staining inverted for better contrast. Black boxes indicate the region of the zoomed inset. Scale Bar =20µm; n=20, 2 separate experiments. Rightmost panel shows two fused ESC-structures after 84 hours. Inset shows residual laminin that is not broken down between the fusing compartments. n=8, 2 separate experiments. **(B)** Peri-implantation embryos showing breakdown of basement membrane between embryonic and extra-embryonic compartments; Upper: E-cadherin, red; DNA, blue; laminin, cyan. Lower panel shows the laminin staining inverted for better contrast. Black boxes indicate the region of the zoomed inset. Scale Bar=20µm. n=10 per stage, 2 separate experiments. **(C)** Laminin is not displaced from the horizontal in ESC-ESC structures (n=8, mean angular displacement Θ= 91.05˚; pooled from 2 separate experiments) compared with ETS-embryos (n=13, mean angular displacement Θ= 80.3˚; pooled from 2 separate experiments). Student's t-test, $P<0.01$, Error bars= SEM. For description of measurement of angular displacement, see Materials & Methods.

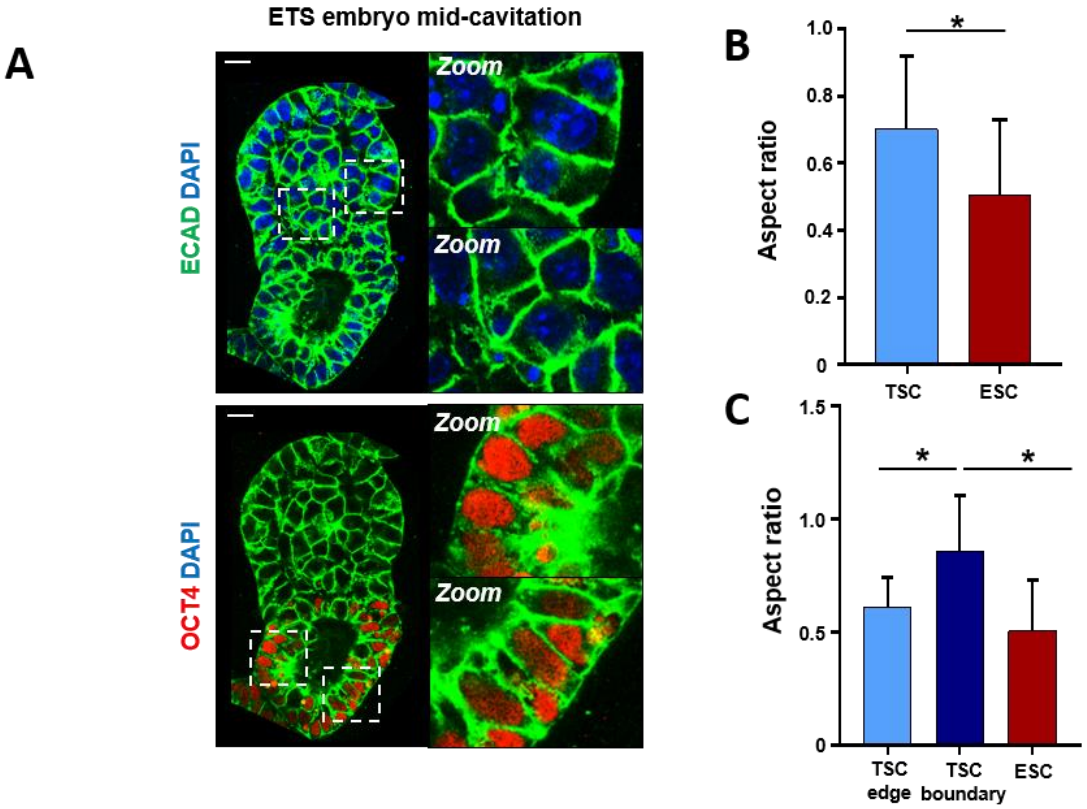

Fig. 4.7. **(A)** ETS-embryo at 84 hours stained to reveal Oct4, red; E-cadherin, green; DNA, blue. Zoomed insets highlight individual cells with different shapes. Scale Bar= 20µm. n=30, 3 separate experiments. **(B)** Graphical quantification of the mean cell aspect ratio (width of cell divided by length) is significantly different between ESC and TSC compartments of ETS-embryos at 84 hours of development. ANOVA test, $P<0.05$, n=30 per group, 3 separate experiments. Error bars= SEM. **(C)** Graphical quantification of the mean cell aspect ratio (width of cell divided by length) is significantly different between cells in the ESC compartment, cells in the TSC compartment, and cells in the TSC compartment at the boundary with ESCs at 84 hours of development. ANOVA test, $P<0.05$, n=30 per group, 3 separate experiments. Error bars= SEM.

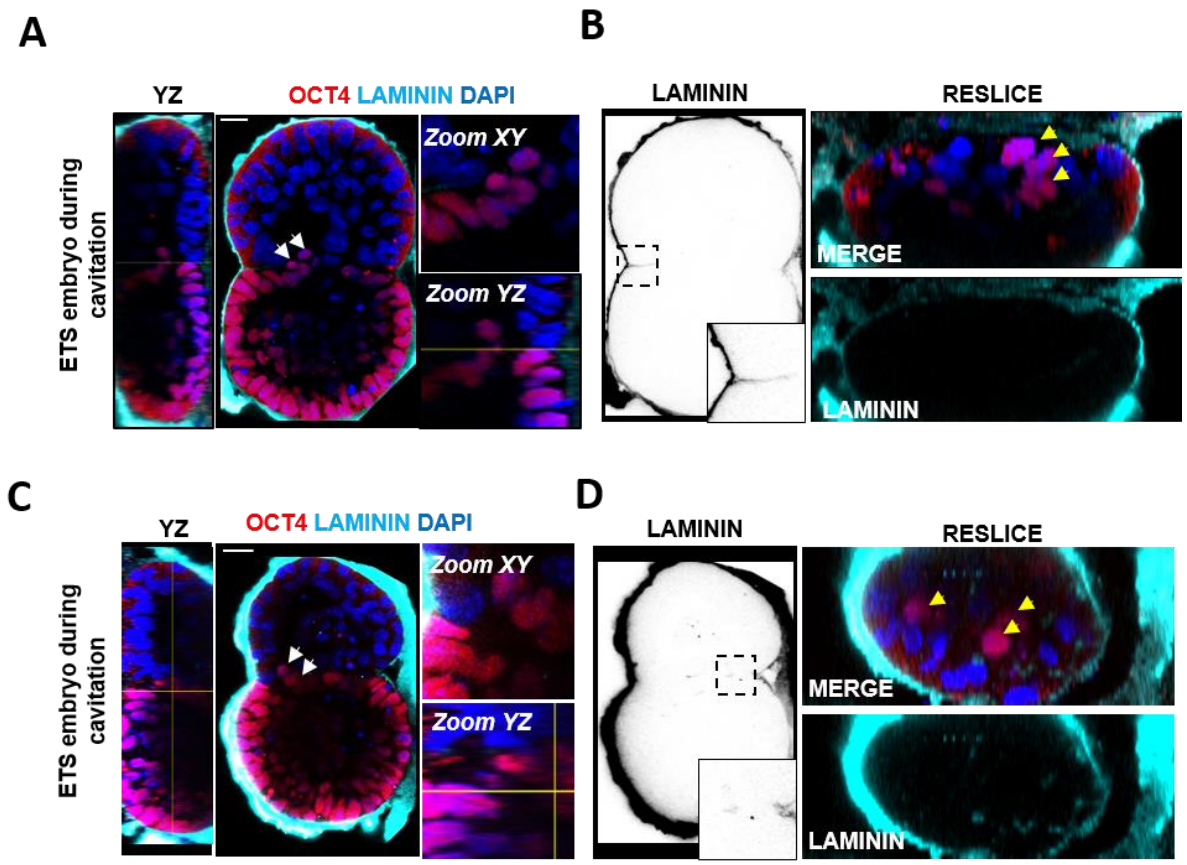

Fig. 4.8. (A) ETS-embryo during cavitation after 84 hours of culture stained to reveal: Oct4, red; laminin, cyan; DNA, blue. YZ orthogonal view is also shown. White arrows indicate ESCs at the boundary invading into the TSC compartment. Scale Bar= 20µm. n=15, 2 separate experiments. **(B)** The same ETS-embryo with laminin staining inverted (black) to make this more visible. Black boxes and insets highlight residual laminin in the cavity. A re-slice of the merged image in (A) at the ESC-TSC boundary is also shown and yellow arrows indicate ESCs invading into the TSC compartment. **(C)** Another example of a ETS-embryo during cavitation at 84 hours. Oct4, red; laminin, cyan; DNA, blue. YZ orthogonal view is also shown. White arrows indicate ESCs at the boundary invading into the TSC compartment. Scale Bar= 20µm. **(D)** The same ETS-embryo with laminin staining inverted (black) to make this more visible. Black boxes and insets highlight residual laminin in the cavity. A re-slice of the merged image in (C) at the ESC-TSC boundary is also shown and yellow arrows indicate ESCs invading into the TSC compartment.

4.3 The role of Nodal/ activin signalling in 'ETS-embryo' morphogenesis

4.3.1 Nodal/ activin signalling is required for 3D morphogenesis of TSCs in ECM

To further investigate cavity morphogenesis in 'ETS-embryos' the signalling mechanisms underpinning this event were also examined. During co-culture it was noted that although TSC-aggregates developing in the presence of ESCs are able to undertake cavitation, the great majority of TSCs embedded in ECM but not in the presence of ESCs failed to do this when cultured over the same amount of time. When cavities emerged in TSC aggregates in co-culture, foci of F-actin co-localised with aPKC could be detected, but these were not detected in TSCs cultured alone (Fig. 4.9. A, B, zoomed insets).

Given that TSCs had to be in the presence of ESCs but not necessarily in physical contact in order to cavitate, it was hypothesised that ESCs were secreting a signal in co-culture with TSCs which promoted extra-embryonic tissue morphogenesis. The identity of this signal was unknown, but one good candidate was Nodal/ Activin, because Nodal is known to be secreted by ESCs in culture (Watabe and Miyazono, 2009) and is critical for early post-implantation embryogenesis in the mouse (Brennan *et al.*, 2001; Camus *et al.*, 2006; Mesnard, 2006). Furthermore, Nodal/Activin signalling is required for the self-renewal of TSCs (Guzman-Ayala *et al.*, 2004) and is provided to cultured TSCs either by mouse embryonic fibroblast (MEF) feeder cells or exogenously in the medium (Kubaczka *et al.*, 2014; Ohinata and Tsukiyama, 2014).

It was confirmed that Nodal/Activin signalling played a role in TSC morphogenesis *in vitro* first by adding exogenous recombinant Activin A to TSCs embedded in Matrigel alone. This experiment rescued cavitation in treated structures, mimicking the effect of the ESCs with a significant majority becoming cavitated within 84 hours of culture (70%, Fisher's exact test, $P<0.001$) (Fig. 4.9. D). This result suggested that Nodal/Activin is required for the formation of the extra-embryonic compartment.

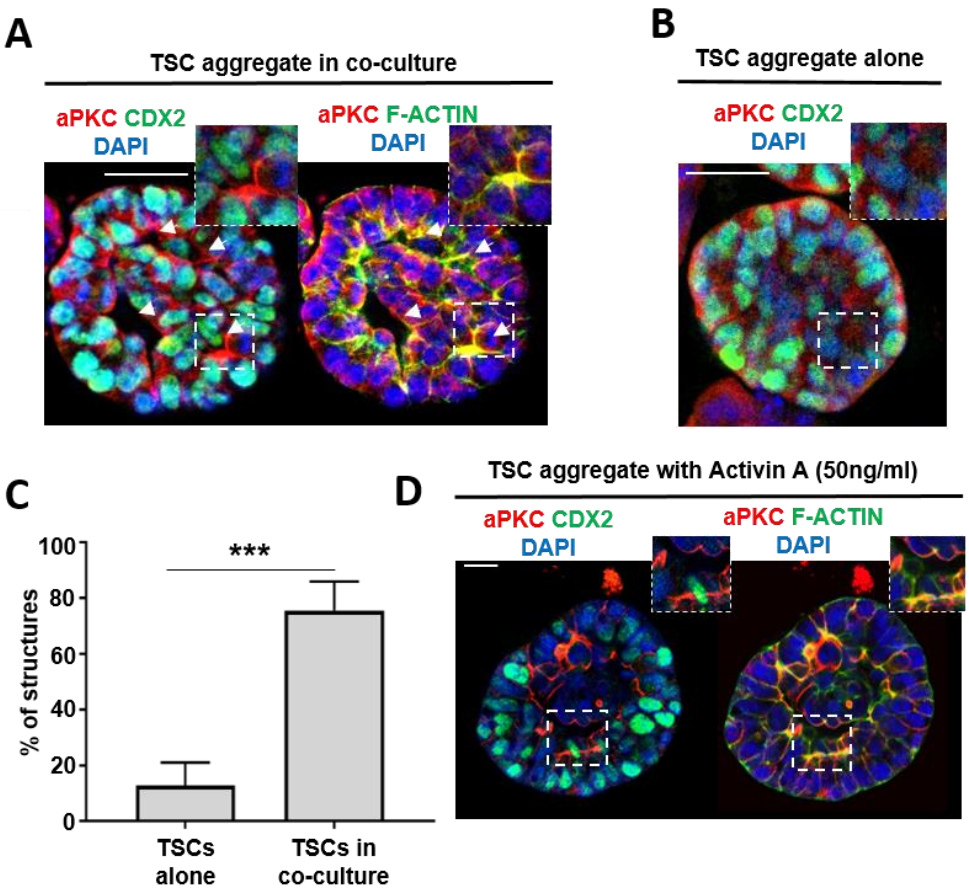

Fig. 4.9. **(A)** TSC aggregate at 84 hours in co-culture but not in contact with ESCs, stained to reveal Cdx2, green; DNA, blue; aPKC, red (left-hand panel) and F-actin, green; DNA, blue; aPKC, red (right-hand panel). White arrowheads indicate cavities. Zoomed inset displays a small cavity opening at a point of aPKC and F-actin enrichment. Scale Bar= 30µm. n=20, 2 separate experiments. **(B)** Sole TSC aggregate in 3D Matrigel at 84 hours. Cdx2, green; DNA, blue; aPKC, red. No cavities could be detected and aPKC is not polarised. n=20 structures analysed that all displayed this morphology, 2 separate experiments. Scale Bar=30µm. **(C)** Quantification of cavitation in TSC- aggregates cultured either alone or in the presence of ESCs for 84 hours. n=10 structures counted per condition per experiment; 2 separate experiments. Student's t-test, $P<0.001$. **(D)** TSC aggregate cultured in 50ng/ml Activin A for 72 hours (left-hand panel) Cdx2, green; DNA, blue; aPKC, red. (right-hand panel): F-actin, green; DNA, blue; aPKC, red. Zoomed inset displays small cavity opening where aPKC and F-actin are enriched. Bar=50µm. n=20, 3 separate experiments.

4.3.2 Nodal/Activin signalling is required for cavity morphogenesis in 'ETS-embryos'

The role of this pathway during early development is very difficult to investigate *in vivo* because any early phenotype of Nodal knockout embryos might be masked by the presence of Nodal ligand that is known to be secreted in the reproductive tract (Park and Dufort, 2011). Therefore, 'ETS-embryos' were used to assess whether Nodal/Activin signalling might be required for cavity morphogenesis in the extra-embryonic compartment. 'ETS-embryos' were generated in control conditions, or in the presence of the Nodal/Activin inhibitor SB431542 (Inman *et al.*, 2002), which was added after 48 hours. The structures were fixed after 96 hours of culture and their morphology was assessed by immunofluorescence staining.

In comparison to controls, 'ETS-embryos' cultured in the presence of 10µm SB431542 failed to produce any cavity in the TSC compartment, and no fused, continuous cavity was present in the structures despite growing for 96 hours. Although cavitation in the ESC compartment was not affected, Oct4 staining intensity was greatly reduced in these conditions, as was staining for Phospho-Smad2/3 (PSMAD2/3), confirming that Nodal/Activin signalling had been inhibited (Fig. 4.3.2 A, top and middle panels & B). This result was confirmed by the analysis of Podxl in the TSC compartment of SB-treated 'ETS-embryos', which accumulated but was not distributed in a recognisable pattern, indicating that no cavity was present (Fig. 4.10. A & B, Fig. 4.11. A, B).

To further dissect the possible role of Nodal/Activin in 'ETS-embryo' morphogenesis, tamoxifen inducible Nodal knockout ESCs (Wu *et al.*, 2013) were used to generate 'ETS-embryos'. Compared with wildtype structures, Nodal -/- 'ETS-embryos' once again failed to induce a cavity in the TSC compartment and did not have a fused cavity by 96 hours of culture. PSMAD2/3 staining was abrogated, confirming that Nodal/Activin signalling was inactive, and, similarly to the phenotype observed with SB431542 treatment, although cavitation in the ESC compartment was not affected, Oct4 was downregulated (Fig. 4.10. A, bottom panel, Fig. 4.11. C).

4.3.3 Nodal/ Activin signalling is required for pro-amniotic cavity morphogenesis in developing embryos

Since these results strongly indicated that Nodal/Activin signalling was involved in cavity morphogenesis in 'ETS-embryos', the effect of Nodal/Activin signalling on the morphogenesis of mouse embryos was also tested. Embryos were recovered from the mother at E5.0, just before cavitation, and cultured *in vitro* in control conditions or in the presence of 10µm SB431542 for 36 hours, to allow the pro-amniotic cavity to develop. In comparison to controls, the pro-amniotic cavity

failed to develop in the significant-majority of SB-treated embryos (90% of structures, $P<0.05$, Fisher's exact-test, Fig.4.12, A,B). Analysis of Podxl distribution again revealed that no cavity was present in the extra-embryonic compartment, and although a cavity still formed in the embryonic compartment, this was coupled to a down-regulation in Oct4 (Fig. 4.12. A, B). This phenotype was strikingly similar to the phenotype observed in 'ETS-embryos' upon inhibition of Nodal/activin signalling.

Taken together, these results strongly suggest that Nodal/ Activin signalling plays an important role in the morphogenesis of both 'ETS-embryos' and in mouse embryos, and is required for formation of a continuous cavity which is shared between tissue compartments.

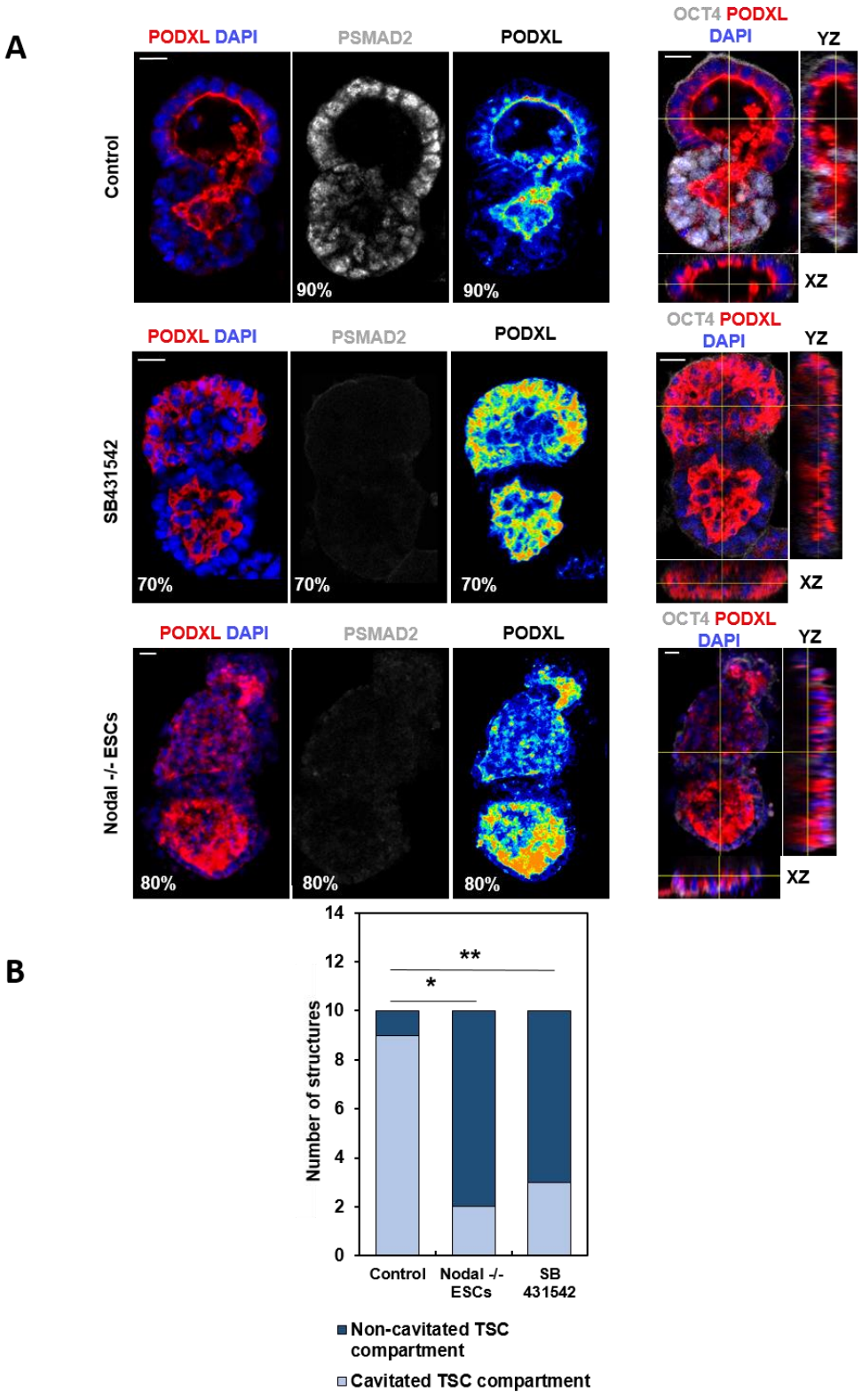

Fig. 4.10. **(A)** ETS-embryos built from either control (upper panels) or *Nodal* -/- ESCs (lower panels) or cultured in 10µM SB431542 (middle panels) for 96 hours: Oct4, white; Podxl/ false-colour, red; DNA, blue; P-SMAD2, grey. YZ orthogonal views highlight cavity where present. n=20 structures analysed per group. Scale Bar=20µm. **(B)** Quantification showing the number of ETS-embryos with cavitated TSC compartments after 96 hours in culture in control, SB431542 and Nodal-/- ESC conditions. n=10 per group, 2 separate experiments. Count data are presented as a bar chart, and a contingency table was used to perform the statistical test. Fisher's exact test, $P<0.05$.

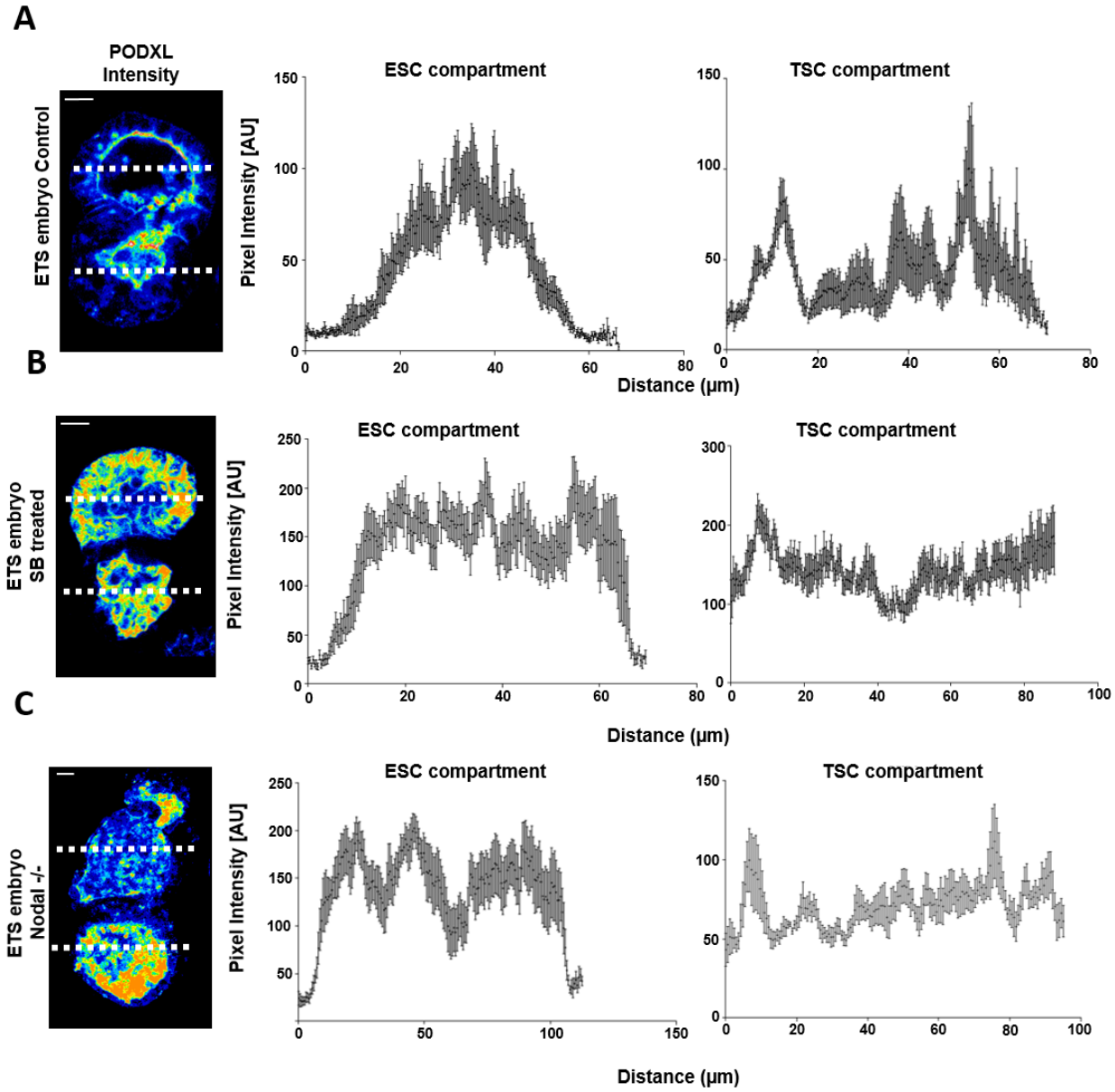

Fig. 4.11. (A-C) False-coloured images of the Podxl staining of control, Nodal -/- and SB431542-treated ETS-embryos accompanying graphical quantification of Podxl staining intensity plotted as mean +/- SEM for eight different cross-sections of the ETS-embryo shown taken at the middle z plane. Y-axis: PCX fluorescence intensity. n=20 structures analysed per group.

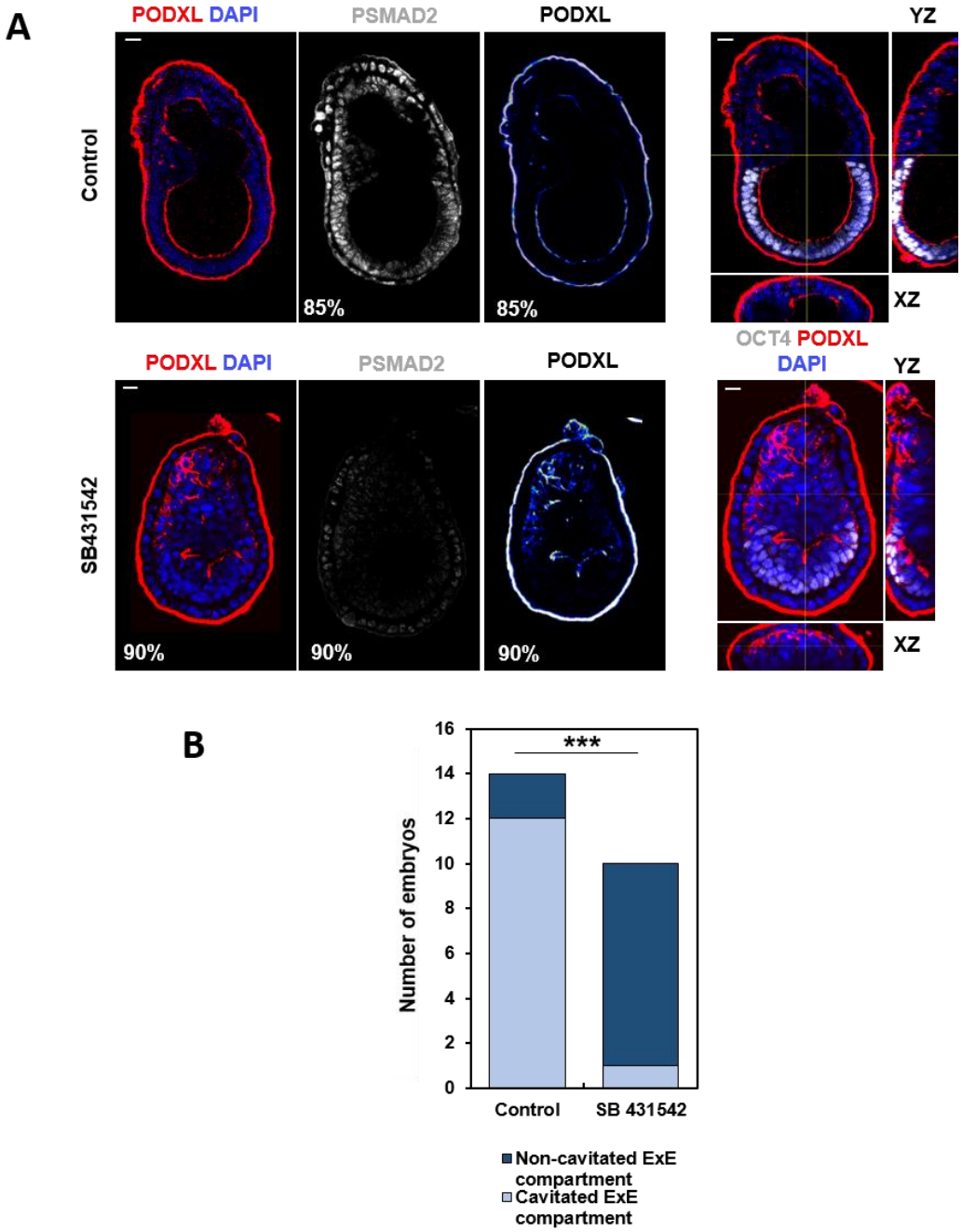

Fig. 4.12. (A) Embryos recovered at E5.0 and cultured *in vitro* for 36 hours in control (DMSO; n=14, 3 separate experiments) or in the presence of SB431542 (10μM; n=10, 3 separate experiments). Oct4, white; Podxl/ false-colour, red; DNA, blue; P-SMAD2, grey. YZ orthogonal views highlight cavity where present. Scale Bar=20μm. **(B)** Quantification showing the number of embryos with cavitated extra-embryonic compartments when recovered at E5.0 and cultured for 36 hours in control (n=14) or SB431542 (n=10) conditions, 2 separate experiments. Count data are presented as a bar chart, and a contingency table was used to perform the statistical test. Fisher's exact test, P<0.001.

4.4 Discussion

The formation of a cavity during embryogenesis is an event common to all mammalian embryos, including humans, even though the shapes of these embryos differ profoundly (Bedzhov and Zernicka-Goetz, 2014; Rossant, 2015; Deglincerti *et al.*, 2016; Shahbazi *et al.*, 2016). However, the function of the pro-amniotic cavity during early mammalian development is unknown. In other systems, such as the zebrafish lateral-line system, Darren Gilmour and colleagues showed that lumens, which develop between the constituent cells of the developing lateral line organs, can act as shared reservoirs of signalling molecules including FGF (Durdu *et al.*, 2014). They suggest that in this way, the lumen can serve to enhance and coordinate cell communication as the organ develops.

It is possible that the pro-amniotic cavity may function in a similar manner, to coordinate tissue growth in early development and allow signalling ligands to be shared between EPI and ExE cells via the continuous cavity which expands through the tissues. Unfortunately, owing to a lack of genetic and molecular tools which can be used to study the post-implantation mouse embryo (Soares *et al.*, 2005) the function of the pro-amniotic cavity and its effect on signalling is difficult to investigate directly. The results presented here demonstrate that 'ETS-embryos' can faithfully recapitulate egg cylinder and cavity morphogenesis *in vitro*. The ease with which constituent ESCs and TSCs can be genetically manipulated (Himeno, Tanaka and Kunath, 2008; Southon and Tessarollo, 2009) presents a new opportunity to study these processes in greater depth, using 'ETS-embryos' as a tool to complement experiments performed on the mouse embryo.

In a similar manner to the egg cylinder, cavitation in 'ETS-embryos' initiates with the formation of a single lumen in the embryonic (ESC) compartment. Lumenogenesis is concomitant with the cells acquiring a columnar shape, and becoming polarised to form a continuous epithelial tissue. 'ETS-embryos' differ from embryoid body models of embryogenesis in that they are able to recapitulate cavitation without using regulated cell death as a mechanism. In this way, a single cavity forms in the ESC compartment, whereas in embryoid bodies, apoptosis can lead to the formation of multiple cavities which later fuse together (Coucouvanis and Martin, 1999). The results presented here also show that within 24 hours of cavity initiation in the ESC compartment, cavities appear independently in the TSC compartment and then fuse to form a continuous lumen shared between both tissue compartments of 'ETS-embryos'. This event also occurs independently of site-directed apoptosis, as is the case in the mouse embryo, making cavitation of 'ETS-embryos' analogous to pro-amniotic cavity formation in the egg cylinder. This is something that cannot be claimed for traditional embryoid body models of mouse embryo development.

It may not be so surprising that the mechanism of lumenogenesis differs between embryoid bodies and in the mouse embryo, given that they also differ from the embryo in the timing of cavitation and the number of cells present in the embryonic tissue at this time. Embryoid bodies can take between 4-7 days to cavitate (Li *et al.*, 2003), comprise several hundred cells at early stages, prior to cavitation (Wang and Yang, 2008), and cell numbers can vary greatly between aggregates. It has been shown using MDCK cells cultured *in vitro* that when the cells are grown at high density, with a large number of cells in each MDCK cyst, the mechanism of lumen formation switches from hollowing to apoptosis-mediated cavitation, owing to the slow growth of the cells. This also occurs as a result of the absence of a strong polarisation cue (Martín-Belmonte *et al.*, 2008), which would normally be provided by culturing the cells in the presence of ECM. Whilst embryoid bodies can secrete laminin in culture (Li *et al.*, 2001, 2002), they are often not routinely cultured on ECM (Wang and Yang, 2008) and thus they do not have a strong integrin-mediated signal to promote rapid cell polarisation and lumenogenesis. Instead, the lumen takes time to form, after the cells have divided several times and generated a dense tissue mass. In these conditions, the cells cannot polarise to form an epithelium without the removal of some cells at the centre through apoptosis (Martín-Belmonte *et al.*, 2008). In contrast, the 'ETS-embryo' system uses ECM as part of the culture method to induce rapid cell polarisation as occurs in the EPI of the mouse embryo at implantation. These structures are more similar to the embryo in the number of cells present at the time of cavitation, and thus the cavity can form without the need for clearance of hundreds of cells from the centre.

The fact that 'ETS-embryos' are able to closely phenocopy the mouse embryo under conditions of signalling inhibition again supports the idea that 'ETS-embryos' are a faithful model of mouse embryogenesis. Furthermore, this system has uncovered a possible novel role for Nodal/Activin signalling in early embryonic morphogenesis, which should be studied in greater detail both *in vivo* and using this new system. Upon inhibition of Nodal/Activin signalling, both 'ETS-embryos' and cavitating mouse embryos failed to initiate cavitation in the extra-embryonic compartment, and no continuous cavity can form running through the centre of the cylinder in either case. These results suggested that Nodal/Activin signalling plays a role in ExE formation during early post-implantation mouse embryo development. However, these results are in contrast with studies using knockout mouse embryos, which instead suggest that Nodal/Activin signalling activity is not essential until gastrulation.

In all studies to date, the developmental phenotypes present in animals mutant for components of the Nodal/Activin signalling pathway fall into one of three categories, which differ in severity. Whilst Activin A, Activin B, the receptor Alk7 and the intracellular effector Smad7 mutants are born, but

possess craniofacial defects, mutants for other components of the pathway such as Nodal, Alk4, and Smad2 result in primitive streak and axial patterning defects which are often lethal (Papanayotou and Collignon, 2014). A common feature of all these phenotypes however is that they manifest themselves in later post-implantation mouse development, after formation of the egg cylinder and the pro-amniotic cavity. Results presented here using the 'ETS-embryo' system suggest that Nodal/Activin signalling may have a previously undiscovered role in mouse development at earlier stages in embryogenesis, namely to promote cavitation in the ExE of the developing egg cylinder. Supporting experiments performed on mouse embryos cultured *in vitro* during cavitation stages also support this hypothesis.

In support of these data, there is some evidence from the mouse embryo that Nodal/Activin signalling may play a role in mouse embryogenesis at earlier stages, possibly even during pre-implantation development (Papanayotou and Collignon, 2014). Both Nodal and Activin are expressed in the pre-implantation ICM at E3.5, and Nodal expression persists in the EPI and PE once these tissues have segregated, whilst Activin expression instead becomes confined to the TE (Lu *et al.*, 1993; Jones *et al.*, 2006; Granier *et al.*, 2011). It is possible that if Nodal/Activin signalling is important in earlier development, early phenotypes in zygotic knockouts have been masked by the expression of both ligands in the maternal tissues. Activin is expressed in the oocyte, the oviduct, and in the uterus (Jones *et al.*, 2006). Nodal is also expressed in maternal tissues (Park and Dufort, 2011). These maternal ligands may function in early embryonic development, because embryos cultured *in vitro* develop better when the medium is supplemented with recombinant Activin (Orimo *et al.*, 1996; Yoshioka, Suzuki and Iwamura, 1998).

Evidence from stem cells also indicates that Nodal/Activin may play a role in development earlier than the mutant phenotypes might suggest, and support the results observed here using the 'ETS-embryo' system. Although cavitation of the embryonic compartment was not affected by abrogation of Nodal/ Activin signalling, in both 'ETS-embryos' and cavitating mouse embryos, a down-regulation in the pluripotency marker Oct4 was observed in this tissue. These results are consistent with studies performed using EPISCs, which, unlike ESCs, critically require exogenous Activin to be supplemented in the medium in order to maintain their self-renewal capacity (Brons *et al.*, 2007; Tesar *et al.*, 2007).

With regard to the phenotype in the extra-embryonic tissue, there are several lines of evidence to suggest that Nodal/Activin signalling is important during egg cylinder formation. *In vivo*, FGF and Nodal interact to maintain the self-renewing TSC population in the ExE compartment. FGF4 expression and TSC markers are induced downstream of Nodal and its processing factors Furin and Pace4/ Pcsk6, and these are abrogated when Nodal/Activin signalling is absent (Guzman-Ayala *et al.*, 2004). If Activin A

is removed from TSCs maintained in defined culture conditions, the cells reduce their proliferation rate, downregulate TSC markers and differentiate into flattened, TGC-like cells (Ohinata and Tsukiyama, 2014). These results indicate that Nodal/Activin is critical for the correct development and tissue specification of the ExE compartment, and the results presented here now also suggest that Nodal/Activin signalling is required for proper ExE morphogenesis. Intriguingly, in the 'ETS-embryo' system, exogenous FGF4 ligand is provided in the culture medium, so the effect of inhibiting Nodal/Activin in this system must be independent of FGF. Perhaps then, when Nodal/Activin acts to induce FGF signalling, TSC identity is maintained in the ExE, but Nodal/Activin also acts independently of FGF to play a role in ExE morphogenesis. Further experiments both *in vitro* and *in vivo* would be required to verify that this is the case, and the 'ETS-embryo' system, when used in combination with experiments on the mouse embryo, provides a unique platform to investigate this.

If it is indeed the case that Nodal/Activin is essential to cavitation of the ExE, the role of the EGF-CFC protein, 'Cripto' would warrant further investigation. Activin can signal independently of Cripto, whereas in many contexts, Nodal is considered to require this EGF-CFC co-receptor in order to activate the receptor complex for signal transduction (Yeo and Whitman, 2001; Yan *et al.*, 2002). Since Cripto is not expressed in TSCs nor in the ExE until these cells begin to differentiate (Natale *et al.*, 2009), it is likely that the effect of Nodal/Activin signalling on promoting cavitation of the extra-embryonic compartment is independent of this EGF-CFC co-receptor. Whilst there is some evidence of Cripto-independent Nodal signalling during egg cylinder development in the mouse (Yeo and Whitman, 2001; Liguori *et al.*, 2008), it may instead be that the Activin branch of this pathway is more relevant to this phenotype than Nodal per se. However, when Nodal-/- ESCs were used to generate 'ETS-embryos', a defect in cavitation was observed, indicating that Nodal, produced by the embryonic tissue specifically, is the ligand that induces cavitation. Further experiments will be required to elucidate the precise mechanism by which Nodal induces cavitation in this system, and indeed in the mouse embryo.

Taken together, the evidence from 'ETS-embryos' and mouse embryos suggests that Nodal/Activin may be important in peri- and early post-implantation mouse development, before gastrulation. This is particularly important in the context of ExE morphogenesis. Further work should focus on elucidating the full extent of the phenotype uncovered here especially given that previous studies on Nodal signalling during early post-implantation development have tended to focus on the EPI (Brennan *et al.*, 2001; Lu and Robertson, 2004).

Finally, it is important to note that the active Nodal/Activin signalling observed in 'ETS-embryos' results from endogenous production of ligand from the cells in the culture system, as no exogenous Nodal/Activin is added to the culture medium. Given that TSCs do not produce Nodal/Activin in culture

(Erlebacher, Price and Glimcher, 2004; Oda, Shiota and Tanaka, 2006; Roberts and Fisher, 2011) the ESCs present in co-culture must be the source of this signal, just as it is provided by the EPI *in vivo*. This is interesting, given that the most striking effect of blocking this signalling in developing 'ETS-embryos' was on the TSC compartment. This highlights how signalling interactions between tissues in these structures are essential for their development, and is a feature shared with the mammalian embryo. Undoubtedly, other signalling pathways also function between tissue-types in this system, and may reveal how the ESCs and TSCs can coordinate their growth and development with respect to one another, to generate a compound structure in a reproducible manner. In the next chapter, the effect of such signals on germ layer specification, as opposed to morphogenesis in 'ETS-embryos' is investigated.

5. Results III: Cell fate specification and pattern formation in ‘‘ETS-embryos’’

5.1 Introduction:

Subsequent to implantation, the next major morphogenetic event the mammalian embryo undertakes is gastrulation, which is tightly coupled to A-P axis establishment. The first morphological sign of A-P axis specification in the mouse embryo is the migration of the AVE cells to the future anterior of the embryo, breaking symmetry. At the anterior side, the AVE acts as a signalling centre which secretes inhibitors of Wnt and Nodal, restricting the activity of these signalling pathways to the opposite side of the EPI to where the AVE is positioned (Thomas and Beddington, 1996; Yamamoto *et al.*, 2004). This leads to a gradient of Wnt and Nodal signalling from posterior to anterior. The restriction of Wnt and Nodal activity to the proximo-posterior epiblast only, confers a particular molecular identity on this region (Arnold and Robertson, 2009).

As a result of signalling from the ExE, this region becomes competent to undertake mesoderm specification (Winnier *et al.*, 1995), which is marked by the expression of the T-Box transcription factor T/Brachyury (T/Bra) in a triangular-shaped region at the boundary between EPI and ExE which appears at E6.5 (Wilkinson, Bhat and Herrmann, 1990; Herrmann, 1991). This T/Bra-positive region of cells is known as the primitive streak, and it is a characteristic feature of the posterior side of the post-implantation EPI. In this specialised structure, cells will ingress and undergo EMT to form the nascent germ layers during gastrulation.

During primitive streak formation at E6.25, a small group of EPI cells fail to ingress through the streak, and instead become re-programmed to form the primordial germ cells (PGCs), precursors to the gametes. Like the mesoderm, specification of these cells occurs via BMP signalling from the ExE (Lawson *et al.*, 1999), leading to the expression of a network of transcription factors *Blimp1*, *Prdm14*, and *Ap2-γ*, which act in synergy to drive PGC fate (Günesdogan, Magnúsdóttir and Surani, 2014).

In this chapter, ‘ETS-embryos’ are shown to develop mesodermal and PGC-like lineages in a similar manner to the post-implantation mouse embryo. Lineage specification occurs on the ESC-TSC boundary and a gradient of cell fates is present across the ESC compartment, which resembles the EPI at E6.5. Mesoderm and PGC-like cells are induced in response to local BMP signalling from the TSC compartment, equivalent to BMP signalling from the ExE of the mouse embryo, which interacts with localised Wnt signalling. In this way, cell fate specification in ‘‘ETS-embryos’’ faithfully mimics cell fate specification associated with post-implantation embryonic development.

5.2 Mesodermal cell fate specification in 'ETS-embryos'

5.2.1 'ETS-embryos' specify regionalised mesoderm

Previous studies have demonstrated that the ExE compartment of the mouse embryo is required for mesoderm specification in the EPI (Donnison *et al.*, 2005; Rodriguez *et al.*, 2005). The ExE secretes BMP4, which induces Wnt signalling in the adjacent proximal EPI, leading to the expression of mesodermal transcription factors, including T/Bra (Winnier G, *et al.* 1995). With this in mind, it was hypothesised that the TSC compartment of 'ETS-embryos', if indeed equivalent to the ExE of the egg cylinder, might promote mesoderm specification in adjoining ESC compartments via a similar mechanism.

To test this, 'ETS-embryos' were generated using T:GFP ESCs (Fehling *et al.*, 2003) to make up the ESC compartment, whilst wild-type TSCs were used to make up the TSC compartment. 'ETS-embryos' were monitored through each day of culture to determine whether the ESCs would express GFP and hence report mesoderm specification. Between 96h and 120h in culture, 'ETS-embryos' began to express T:GFP. To address whether, as in the embryo, the presence of the extra-embryonic cells facilitates mesoderm specification, 'ETS-embryos' were grown in parallel to ESC cysts in ECM (as described by (Bedzhov and Zernicka-Goetz, 2014; Meinhardt *et al.*, 2014)) which were made from T:GFP reporter ESCs Fig. (5.1. A). In comparison with structures made of T:GFP ESCs alone (lacking the TSC compartment) but cultured in the same medium, a significantly increased proportion of 'ETS-embryos' were GFP-positive after 96 hours (66%, 42/64 'ETS-embryos' versus 21%, 12/44 ESC cysts), (Fig. 5.1. B).

The spatial distribution of GFP-positive cells was assessed in structures of each type (see Materials & Methods). It was noted that 43% of 'ETS-embryos' (n=100) not only expressed T:GFP, but that this expression was 'asymmetric' across the ESC compartment, in that the number of GFP-positive cells lying either side of the long axis of the structure was not equal. Although some structures comprised of ESCs alone also exhibited asymmetric T:GFP expression (as judged by the same criteria), the proportion was significantly lower (14%, n=100) (Fig. 5.1. A,C). These results suggest that the presence of the TSC compartment indeed promotes mesodermal specification in the culture system.

The asymmetric mesodermal region present in 'ETS-embryos' originated at the boundary between ESC and TSC compartments and extended into the embryonic region, resembling the pattern of T/Bra expression associated with the primitive streak at the initiation of gastrulation in the mouse embryo. To further assess the similarity between the spatial distribution of mesoderm in 'ETS-embryos' and

real embryos, the proportion of area occupied by mesoderm in each case was measured (See Materials and Methods), and found to be similar (Student's t-test, not significant) (Fig. 5.1. D).

To complement the experiments performed on live 'ETS-embryos', structures were fixed after 100h in culture and stained to reveal T:GFP expression or endogenous T/Brachyury protein, then analysed using confocal imaging (Fig. 5.2, A-D). This confirmed that the spatial distribution of T:GFP in 'ETS-embryos' reflected that of endogenous T/Bra protein in the cells of the structures. Notably, analysis of the T/Bra-expressing cells in whole-mount 'ETS-embryos' indicated that these cells remained within the tissue epithelium of the embryonic compartment, as opposed to migrating out. This indicated that despite the cells expressing T/Bra, they had not undergone EMT and become motile. In addition to qualitative assessment of the T/Bra expression pattern, an 'asymmetry analysis' pipeline was designed to quantitatively assess this, by relating the spatial distribution of T/Bra to the long axis of the whole 'ETS-embryos' (see Materials and Methods). Using nuclear staining from confocal imaging as a template, each T:GFP positive cell was plotted in 2D upon a projection of each cell in a single 'ETS-embryo', and positive and negative cells were then counted. Subsequent to this, a contingency analysis and Fisher's exact-test were used to determine whether GFP-expression in a cell was related to its position within the structure (Fig. 5.2. A). As a proof-of-principle, the same analysis was also performed on transgenic T:GFP reporter embryos at E6.5 (Fig. 5.2. B), and on wild-type 'ETS-embryos' and E6.5 embryos stained to reveal endogenous T/Bra protein (Fig. 5.2. C, D). In each case, this method identified a cluster of cells expressing T/Bra which were concentrated on one side of the long-axis. Thus, T/Bra expression in these structures was deemed asymmetric.

5.2.2 Formation of mesoderm in 'ETS-embryos' is not accompanied by changes in cell shape and motility and basement membrane breakdown associated with cell ingression at the embryonic primitive streak

To further investigate whether T/Bra-expressing cells in 'ETS-embryos' might undergo cell ingression and EMT associated with the primitive streak, structures were fixed during mesodermal specification and stained to reveal endogenous T/Bra protein and the cell-adhesion marker E-cadherin, which is known to be lost when cells undergo EMT. Interestingly, the T/Bra-positive cells remained within the single-layered epithelium of the embryonic compartment as opposed to forming a new cell layer. In addition, they continued to express E-cadherin protein (Fig. 5.3 A). The shapes of these cells remained columnar, and measurement of the cell-aspect ratio of T/Bra-positive cells in the embryonic compartment compared with T/Bra-negative cells indicated that there was no difference in cell shape between those which expressed T/Brachyury and those which did not (Fig. 5.3 B). Taken together, this

suggested that the T/Bra cells in 'ETS-embryos' did not undertake the changes in cell shape and behaviour associated with EMT at the embryonic primitive streak.

To explain this result, it was hypothesised that the T/Bra-positive cells remained within the epithelium of the embryonic compartment because the extracellular matrix surrounding them was not broken down, allowing them to move out of the structure. To test this. 'ETS-embryos' were generated using T:GFP ESCs and fixed at different time-points during the specification of the presumptive mesoderm. Staining for laminin and analysis by confocal imaging revealed that before T:GFP-postive cells were present in the 'ETS-embryo', a continuous, unbroken layer of ECM surrounded the 'ETS-embryo', and when T:GFP positive cells were specified, this was not breached. An average projection of laminin indicated that the thickness of the extracellular matrix did not visibly differ close to the region of tissue containing the T:GFP-positive cells compared with the rest of the structure, even after an asymmetric region of mesoderm had become specified.

Taken together, these results suggest that whilst 'ETS-embryos' can develop a region of T/Bra positive cells comparable in shape and location to those at the primitive streak of the mouse embryo, these cells do not break down the basement membrane and undergo cell ingression to form a new tissue layer, as occurs during gastrulation.

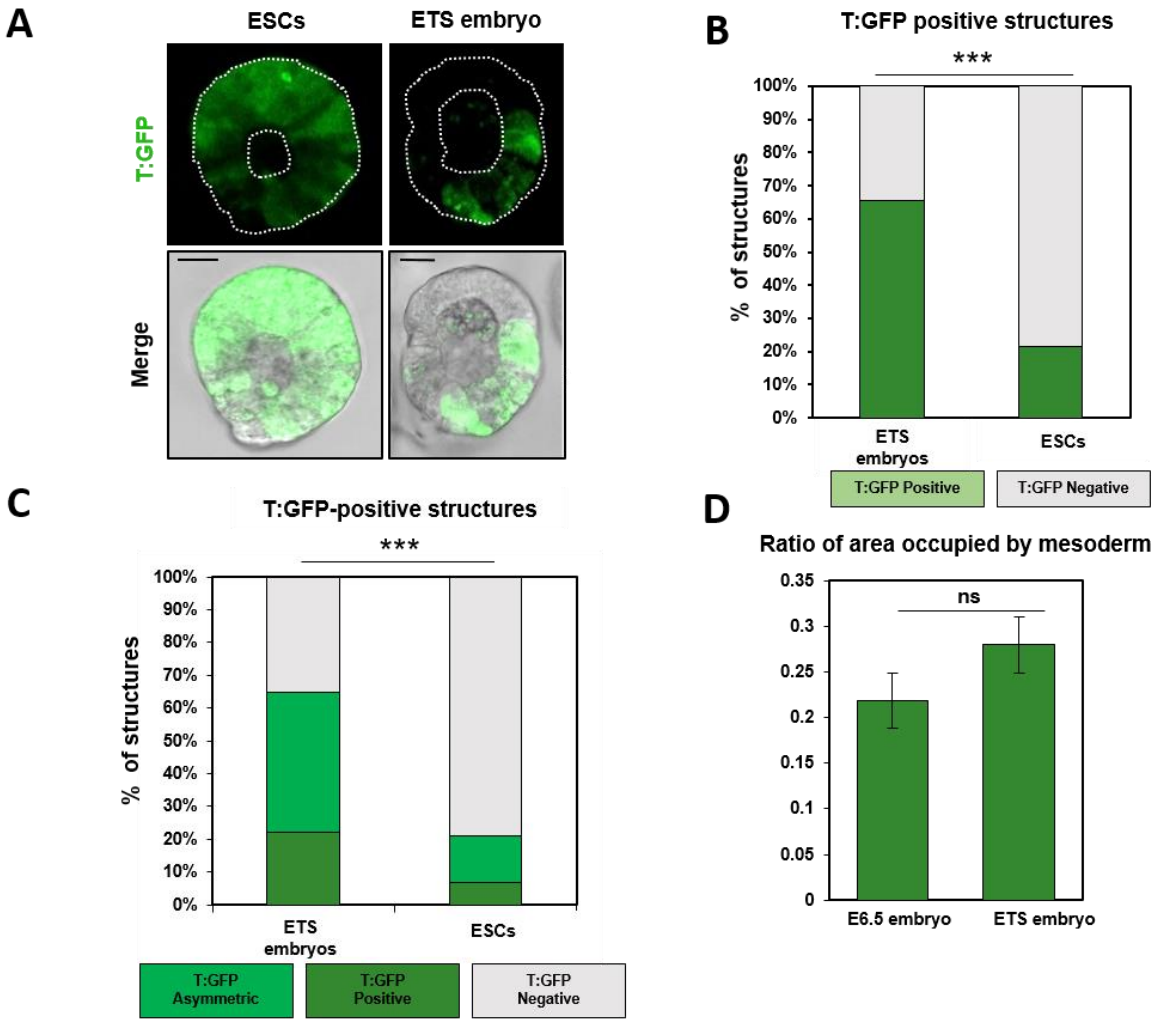

Fig. 5.1. **(A)** T/Bra:GFP-expressing ESCs (green) growing alone (right) or as part of a ETS-embryo (left) in Matrigel. Scale Bar=20µm; white dotted lines outline each structure and its cavity. n=100 "ETS-embryos", 4 experiments; n=65 ESC-alone structures, 4 experiments. **(B)** Proportion of ETS-embryos expressing T:GFP at 96 hours is significantly higher in comparison to ESCs-alone structures. Fisher's exact test, P<0.001, n=108: 64 ETS-embryos and 44 ESC-alone structures counted in 2 separate experiments. Error bars=SEM. **(C)** Proportion of T/Bra expressing ETS-embryos or - structures comprising only ESCs with asymmetric domain of T/Bra expression with respect to the long axis (equivalent to the midline) of the structure (Methods). Student's t-test, P<0.001, n=100 ETS-embryos and n=100 structures comprising only ESCs per experiment. Mean of 4 separate experiments, Error bars= SEM. **(D)** Comparable size of the region of T/Bra expression in ETS-embryos and E6.5 embryos. n=10 per group, Mean ratio of areas of mesodermal domain/total epiblast in E6.5 embryo. Student's t test, not significant, error bars= SEM. For a description of how the ratio was measured and calculated, see Materials & Methods.

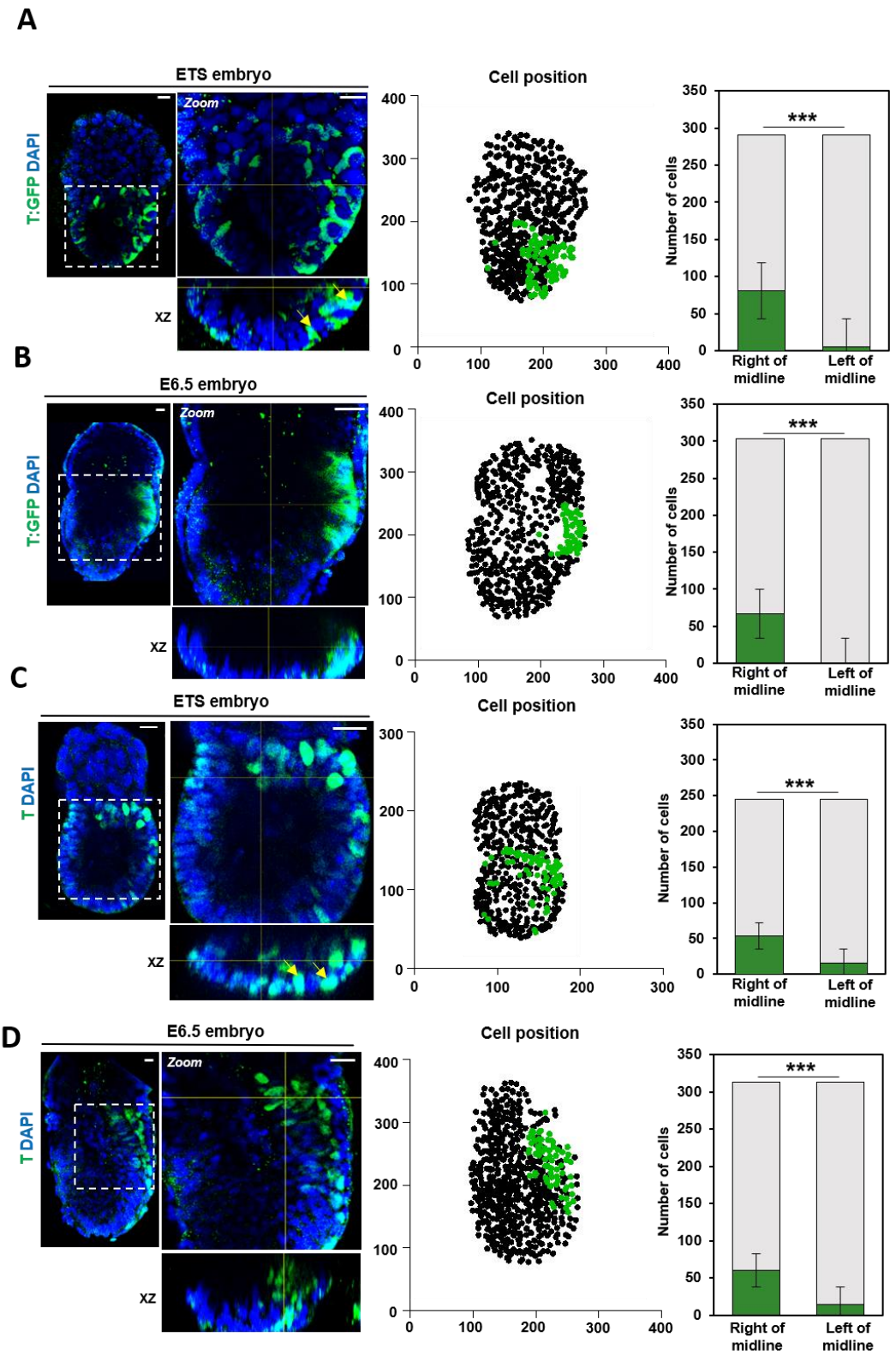

Fig. 5.2. (A-D) Quantitative assessment of T:GFP (A &B) and endogenous T/Bra asymmetry in ETS-embryos at 100 hours (A, C) and in the E6.5 embryo (B, D). **Left panel:** Each structure was stained to reveal T/Bra/ T:GFP, green; DNA, blue. Zoomed insets highlight T/Brachyury-expressing region; yellow arrows in A and C indicate T/Bra-positive cells which remain part of the tissue epithelium, as opposed to migrating out. XZ panels highlight asymmetry in T/Brachyury to one side of structure. Scale Bar=20µm. **Middle panel:** Projection of all cell coordinates in 2D: black points, T/Bra negative cells; green points, T/Bra positive cells. **Right panel:** Proportion of T-positive versus T-negative cells around mid-line, equivalent to the long axis of each structure (See Materials &Methods). Fisher's exact-test, P<0.001. Error bars=SEM.

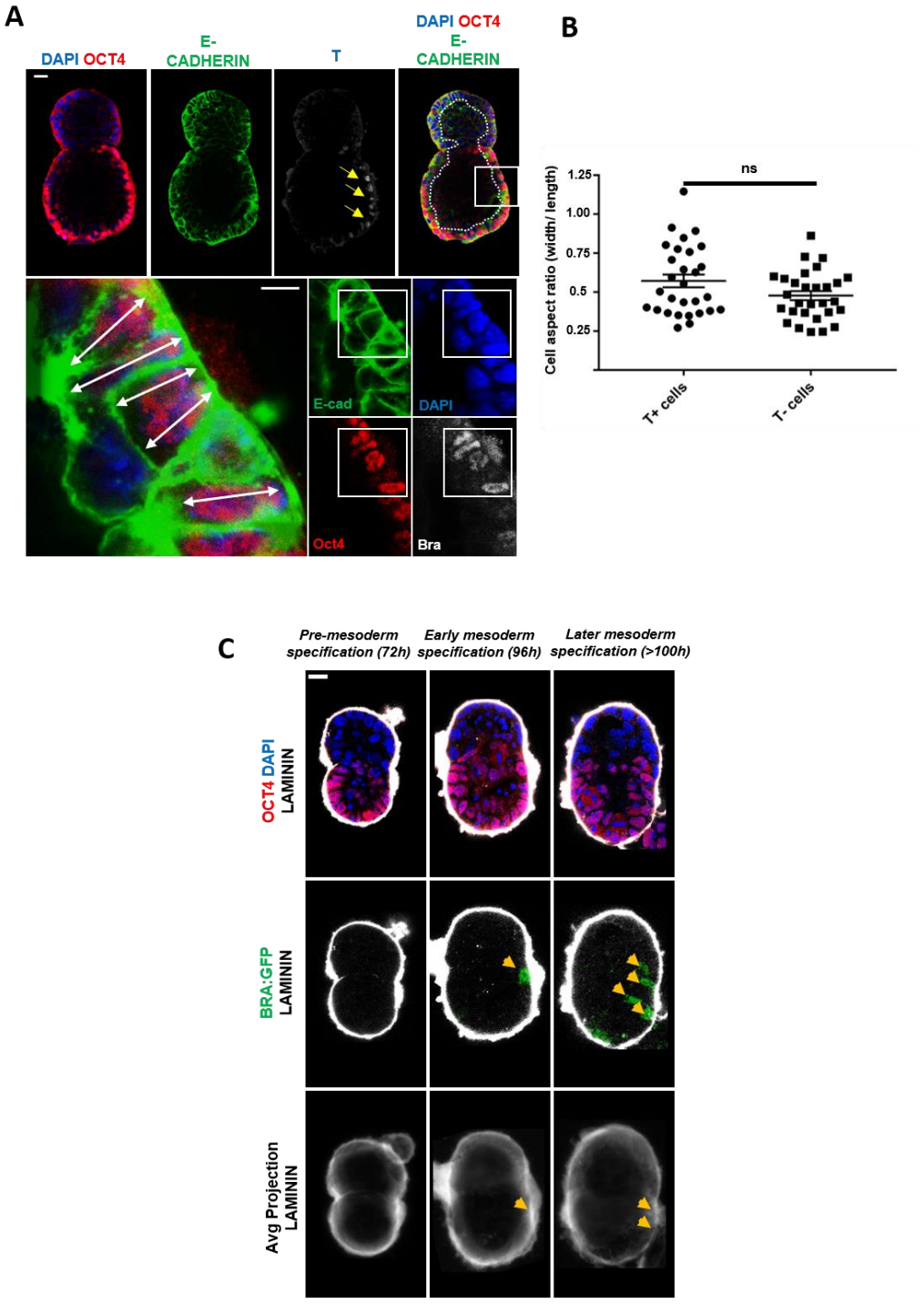

Fig. 5.3 (A) An ETS-embryo after 120h in culture stained to reveal: Oct4, red; E-cadherin, green; T/Brachyury, grey; DNA, blue. Yellow arrows indicate the T/Bra-postive cells on one side of the embryonic compartment. Scale Bar=20µm. Zoomed Inset (Scale Bar=5µm) inset highlights a region of T/Bra-positive cells in the embryonic compartment. White arrows indicate the long axis of each cell. n=15. **(B)** Quantification of the cell aspect ratio (width of cell divided by length) of T/Bra-positive cells compared with T/Bra negative cells. Student's t-test, not significant, n=29 cells per group, 3 separate experiments. Error bars= SEM. An *a-priori* power analysis indicated that a minimum sample size of 27 per group would be required to detect a significant difference given an α=0.05 and *d*=1.0. (C) ETS-embryos before and during asymmetric mesoderm specification (indicated by the expression of T:GFP) stained to reveal: Oct4, red; T:GFP, green; Laminin, white; DNA, blue. Yellow arrows highlight Brachyury-positive mesodermal cells and the intact layer of extracellular matrix adjacent to them. Scale Bar=20µm, n=15 per time point.

5.2.3 Cell fates differ across the ESC compartment in 'ETS-embryos'

Having determined that T/Brachyury-expressing cells occupy an asymmetric region but that the lamina surrounding these cells was not broken down in a manner similar to that which is required for cell ingression at the primitive streak, gene expression analysis was used to confirm that T/Bra-expressing cells in 'ETS-embryos' were indeed of mesodermal lineage. This method was also used to determine the identity of non-mesodermal cells in the ESC compartment. First, 'ETS-embryos' expressing T:GFP in an asymmetric manner were dissected to isolate T:GFP-positive cells from T:GFP-negative cells which lay on the opposite side of the ESC compartment (Fig 5.4. A, B). Each group of cells was then subject to qRT-PCR analysis. T:GFP-positive cells expressed upregulated levels of mesodermal marker genes *T/Bra*, *Mixl1* and *Hand1*, and also expressed elevated levels of EMT-marker genes, the transcription factor *Snai1* and the intermediate filament protein *Vimentin* which are associated with the primitive streak of the mouse embryo (Fig. 5.4. C, top and middle rows, $P<0.01$). By contrast, the T:GFP-negative cells isolated from opposite the presumptive mesoderm expressed increased levels of marker genes associated with the anterior epiblast in gastrula-stage embryos (Fig. 5.4. C, middle and bottom rows) *Pou3f1* (Zhu *et al.*, 2014), *Oct4*, *Slc7a3* and *Utf1 (*$P<0.05$) (Peng *et al.*, 2016; Scialdone *et al.*, 2016).

Next, the expression of one of these markers, Oct4, was verified on the protein-level in 'ETS-embryos'. A gradient of Oct4 expression opposing the gradient of T:GFP expression across the ESC compartment was observed by antibody staining and quantified by analysing the staining intensity across confocal image acquisitions (Fig. 5.5. A, B). Staining intensity was decreased from one side of the ESC compartment to the other. This pattern was similar to the expression pattern of Oct4 in the gastrula stage embryo, which is known to be expressed in a gradient from anterior to posterior (Scholer *et al.*, 1990).

Taken together, these results suggest that 'ETS-embryos' are capable of mesodermal specification. In a subset of cases, this mesoderm becomes specified in an asymmetric region at the embryonic-extra-embryonic boundary akin to that which is specified at the primitive streak in the posterior region of the mouse embryo. This is coupled to a gradient of cell fates which are acquired across the ESC compartment, some equivalent to more anterior regions opposite the mesoderm, suggesting early axial patterning occurs in these structures.

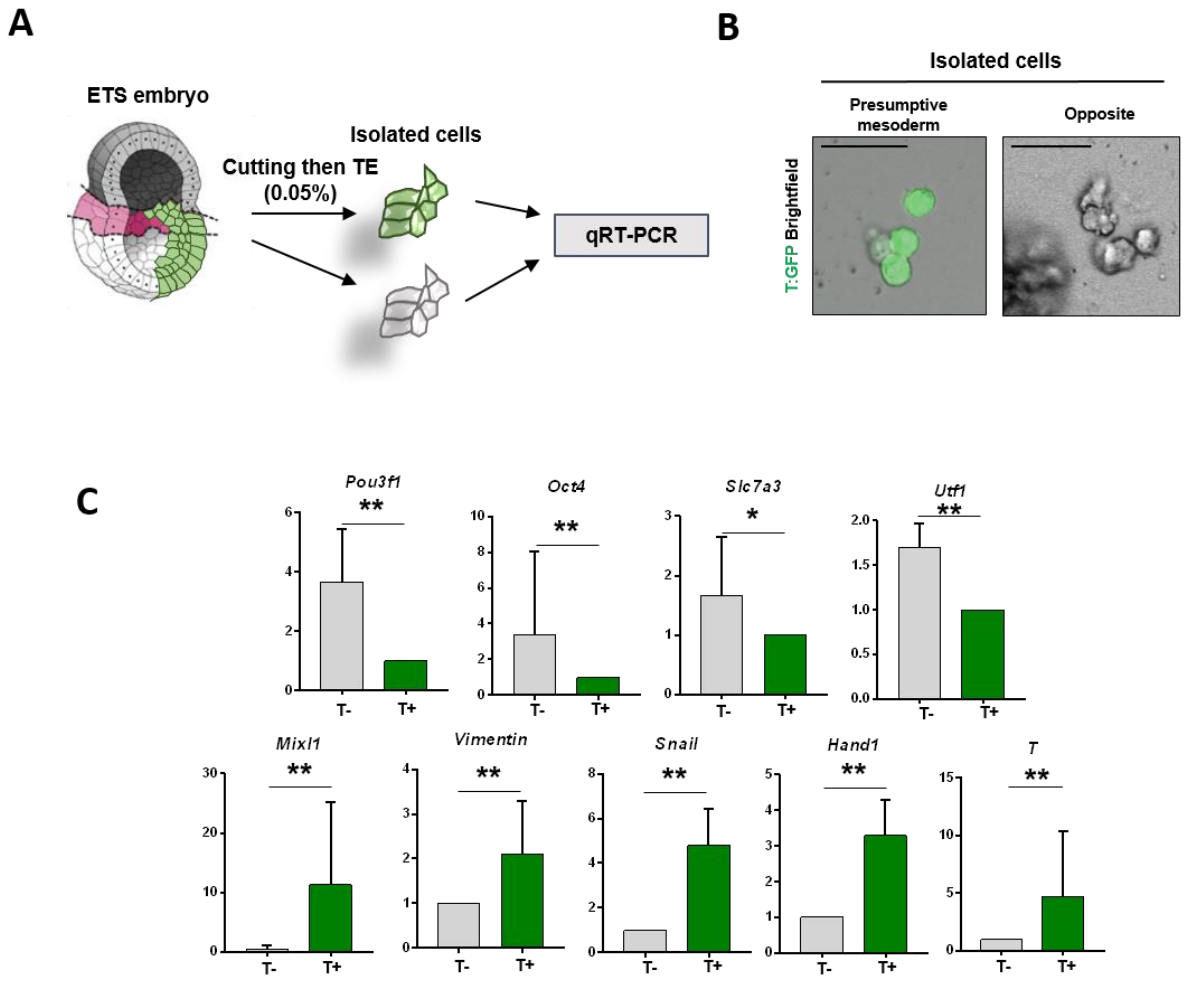

Fig. 5.4. **(A)** Schematic representation of the procedure used to isolate T:GFP positive and negative cells from ETS-embryos for qRT-PCR analysis. 'ETS-embryo' drawn by Dr. Ania Hupalowska (Zernicka-Goetz laboratory) **(B)** Confocal snapshots showing T:GFP positive (green) and negative cells (not green) from one ETS-embryo. Scale Bar= 25µm. **(C)** RT-qPCR analysis of the expression of mesodermal markers (*T, Mixl1* and *Hand1),* epithelial-to-mesenchymal transition (EMT) markers (*Snai1* and *Vimentin)* (bottom row) and markers known to be elevated in the region opposite to the mesoderm region of the E6.5 embryo *(Pou3f1, Oct4, Slc7a3,* and *Utf1,* top row*)* in T:GFP positive cells of a ETS-embryo (collected after 100 hours in culture) compared with T:GFP negative cells from the ESC compartment of the same structure. Mesodermal and EMT marker expression was significantly increased in T:GFP positive cells, whilst cell markers known to be elevated in the region opposite the mesoderm region were significantly decreased. Student's t test, $P<0.05$. N=4 biological replicates. Error bars= SEM. Note that for *Mixl1,* gene expression in some samples of T:GFP-negative cells were undetermined, and so were accepted as zero.

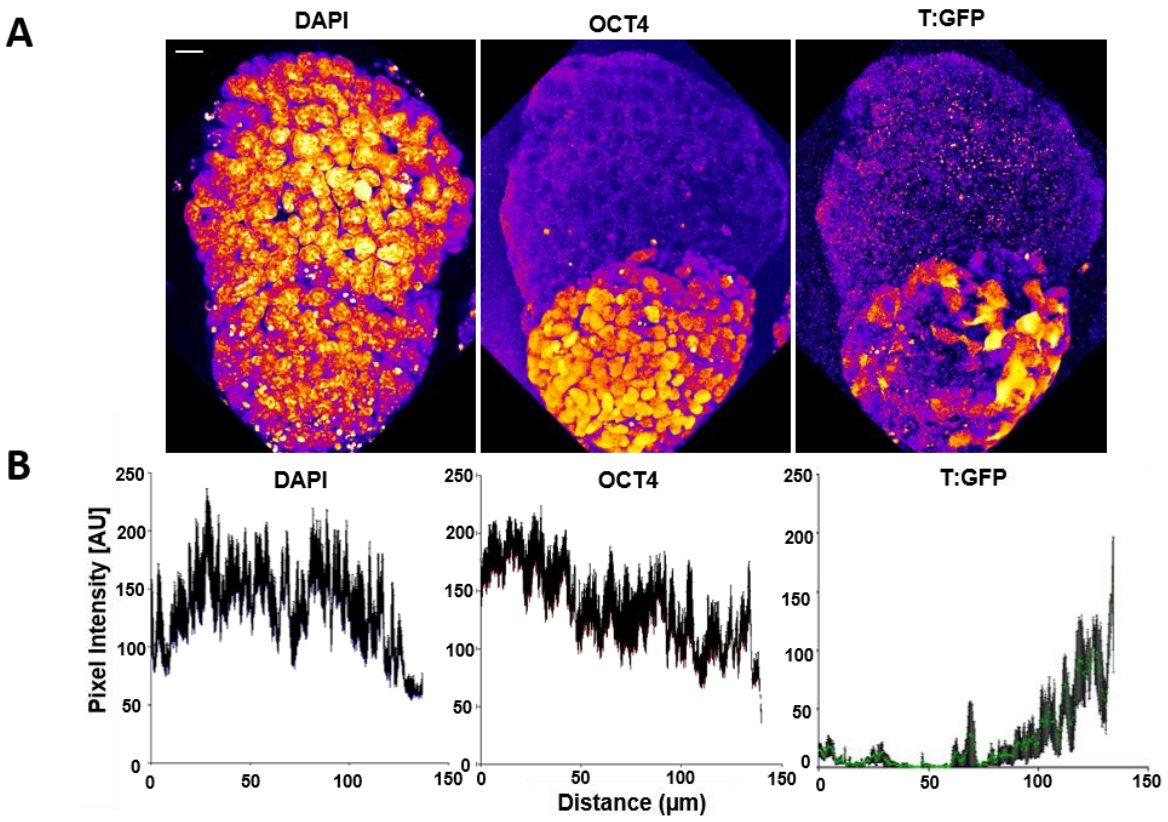

Fig. 5.5. (A) An 'ETS-embryo' after 100 hours immunostained to reveal: DNA, left; Oct4, middle; and T:GFP, right. Images are maximum projections and are false-coloured with the 'fire' "Look-up table" function in Fiji software to highlight intensity gradients. Scale Bar=20µm. **(B)** Intensity profiles for immunofluorescence stainings plotted as the mean +/- SEM for eight different cross-sections of the embryonic compartment of the ETS-embryo shown, taken at the middle z plane.

5.3. Wnt signalling underpins mesoderm specification in 'ETS-embryos'

5.3.1 Regionalised mesoderm in 'ETS-embryos' is preceded by localised Wnt signalling in the ESC compartment

To investigate the mechanisms underpinning mesoderm specification in 'ETS-embryos', the activites of signalling pathways known to promote mesoderm specification *in vivo* were assessed. In the embryo, the formation of the primitive streak is preceded by localised activation of the Wnt pathway at the posterior (Rivera-Pérez and Magnuson, 2005). To test whether a similar mechanism of Wnt activation led to mesoderm specification in 'ETS-embryos', structures were generated using a H2B-GFP::Tcf/LEF ESCs, which would act as a live reporter of active Wnt signalling in the ESC compartment (Ferrer-Vaquer *et al.*, 2010). 'ETS-embryos' were fixed at successive time-points during their development and then were subsequently immune-stained for co-localisation of GFP (reporting active canonical Wnt signalling) and T/Bra protein. After 90 hours in culture, Wnt signalling was active in a small population of cells in the ESC compartment close to the ESC-TSC boundary, but T/Bra was not yet detectable (Fig. 5.5. A, top panel). By 96 hours, GFP-expression was co-localised with T/Bra in cells in the nascent mesodermal region. This domain of double-positive cells expanded over the next six hours, but remained asymmetric with respect to the midline (long-axis) of 'ETS-embryos' (Fig. 5.5., A). This increase in cell number between time-points was statistically significant (ANOVA test with Geisser-Greenhouse correction, $P<0.05$, n=15 per timepoint) reflecting the expansion of the mesodermal compartment as 'ETS-embryos' developed in culture (Fig. 5.5., B). The observation that activity of the H2B-GFP::Tcf/LEF reporter co-localised with T/Bra expression suggested that, as in the mouse embryo, mesoderm specification in 'ETS-embryos' involves active Wnt signalling.

5.3.2 Inhibition of canonical Wnt signalling abrogates mesoderm specification in 'ETS-embryos'

To directly test whether Wnt signalling activity is required for the induction of mesoderm, 'ETS-embryos' were cultured either in control conditions, or in the presence of recombinant Dickkopf1 (DKK1) a canonical Wnt-antagonist (Niida *et al.*, 2004), which was added 48 hours after initial plating of ESCs and TSCs in ECM. 'ETS-embryos' were fixed after 96 hours in experimental and control conditions. In comparison to control conditions, DKK1-treated 'ETS-embryos' failed to specify regionalised mesoderm after 96 hours, with the proportion of structures with asymmetric T/Bra expressing cells in the ESC compartment being significantly reduced (38% of control structures expressed asymmetric T/Bra compared to 4% of DKK1-treated structures. $P<0.05$, n=100 (Fig. 5.6., A, B)). This indicates that Wnt signalling activity is required for robust mesoderm specification in 'ETS-embryos', as is the case in the mouse embryo.

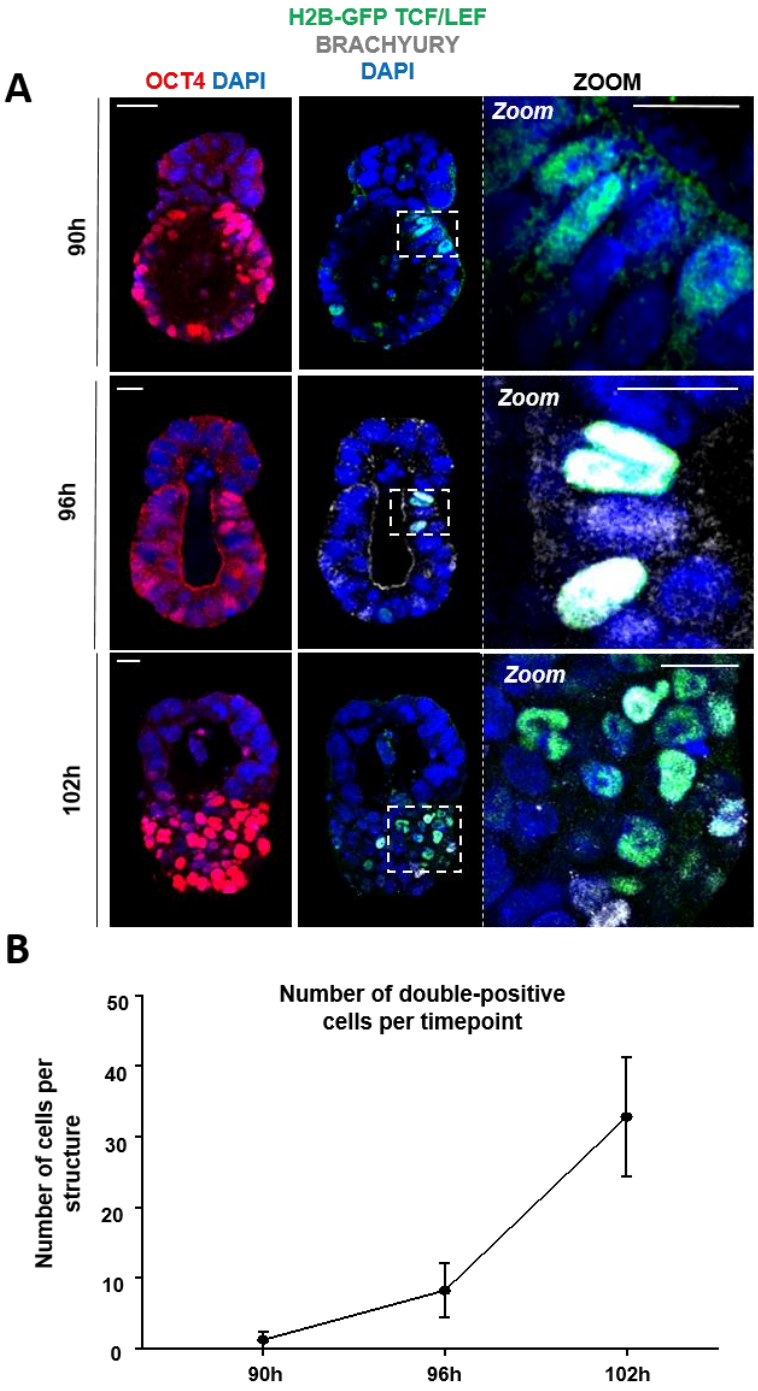

Fig. 5.5. (A) ETS-embryos expressing the Wnt reporter H2B-GFP:Tcf/LEF and T/Brachyury at 90, 96, and 102 hours of culture. Oct4, red; DNA, blue; H2B-GFP:Tcf/LEF, green; T/Brachyury, white. Scale Bar=20µm. Inset (Scale Bar=10µm) highlights cells co-expressing Wnt reporter and T/Brachyury. n=15 per each time-point. **(B)** Quantification of mean number of Wnt/Brachyury co-expressing cells detected in the ESC compartment of ETS-embryos with time. The number of cells is significantly different in each group (ANOVA test, $P<0.01$). n=15 per time-point, 3 separate experiments. Error bars=SEM.

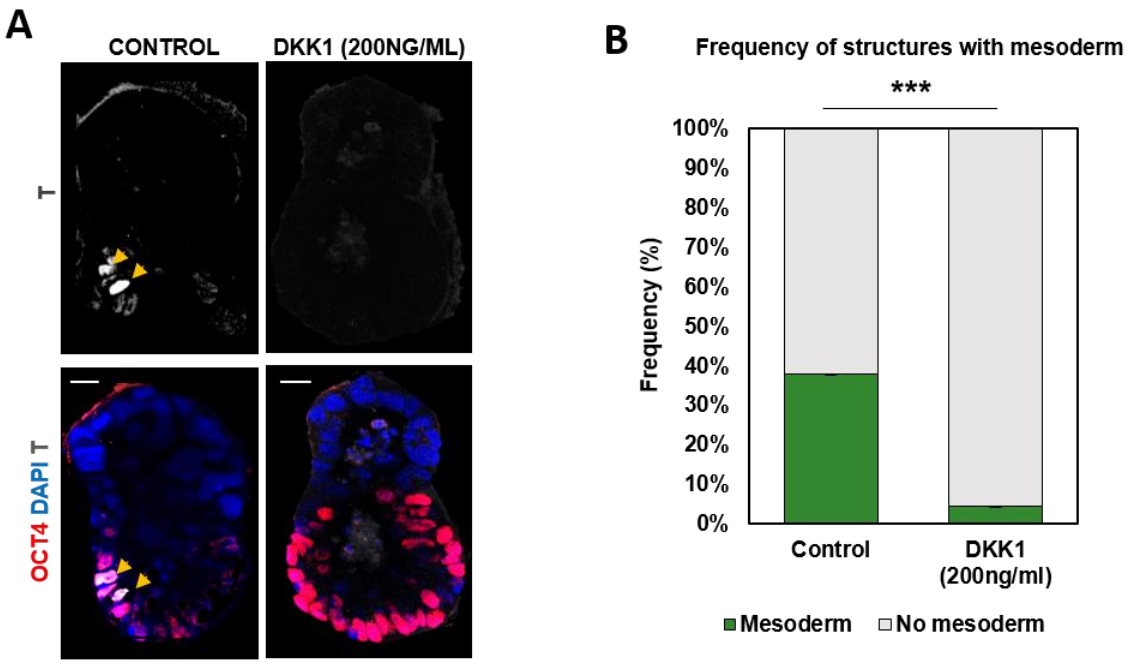

Fig. 5.6. **(A)** Representative ETS-embryos cultured in 200ng/ml DKK1 and control conditions for 96 hours. Oct4, red; DNA, blue; T/Brachyury, white. Yellow arrows indicate T/Brachyury-positive cells in control conditions, undetectable in DKK1 conditions. Scale Bar= 20µm. **(B)** Quantification showing that the proportion of ETS-embryos expressing T/Brachyury is reduced in presence of DKK1 (200ng/ml) compared to controls. Student's t-test, $P<0.001$, n=400, 4 separate experiments.

5.4 PGC-like cell specification in 'ETS-embryos'

5.4.1 'ETS-embryos' specify a population of PGC-like cells at the embryonic-extra-embryonic interface

In addition to mesoderm, the PGCs also become specified in the early post-implantation mouse embryo, in the most proximal part of the posterior EPI. These cells do not ingress through the primitive streak, but at E6.25, PGCs are T/Bra positive (Günesdogan, Magnúsdóttir and Surani, 2014). Given that this gene is directly upstream of two transcription factors which drive PGC specification Prdm14 and Prdm1 (Blimp1) (Aramaki *et al.*, 2013; Günesdogan, Magnúsdóttir and Surani, 2014), it was hypothesised that 'ETS-embryos' might specify a PGC-like population in the T/Bra- positive region of the ESC compartment. To test this, 'ETS-embryos' were allowed to develop for up to 120h and then fixed and stained to detect PGC markers.

After 120 hours in culture, a small population of cells could be detected which were double-positive for Oct4 and the PGC marker AP2-γ (Fig. 5.7., A). These cells lay in the T/Bra-postive domain, in a cluster close to the embryonic extra-embryonic boundary (Fig. 5.7. A, B). This is comparable to the site of PGC specification *in vivo* (Lawson and Hage, 1994; Lawson *et al.*, 1999; Günesdogan, Magnúsdóttir and Surani, 2014). To confirm this result, 'ETS-embryos' were generated using stella:GFP reporter ESCs (Payer *et al.*, 2006) and therefore any PGC-like cells in 'ETS-embryos' would express GFP in culture. In agreement with the previous observation, a small population of stella:GFP-positive cells could be detected in 'ETS-embryos' after 120h of culture (Fig. 5.7., C). Again, this cell population lay close to the ESC-TSC boundary and was restricted to one side of the midline (long-axis of the structure) as confirmed by plotting the GFP-positive cells upon a projection of all cells in 2D (Fig. 5.7. D). For both markers (stella:GFP and AP2-γ) an average of 5 positive cells per 'ETS-embryo' were detected (n= 10). In addition, when compared to 'ETS-embryos', a significantly lower proportion of ESC cysts generated using the stella:GFP reporter line expressed GFP, and did so in a disorganised manner that did not reflected the clustering of PGCs observed in the mouse embryo (Fig. 5.8. A, B).

The gene expression patterns of this population of PGC-like cells in 'ETS-embryos' was then investigated by performing qRT-PCR analysis, as in section 5.2.2. 'ETS-embryos' were first generated using T:GFP reporter ESCs, and then dissected to isolated positive and negative cell populations. The presumptive PGC-like cells located at the ESC-TSC boundary but within the T:GFP positive region, were compared to T:GFP negative cells at the boundary on the opposite side of the ESC compartment. In support of the results at the protein level, the T:GFP positive cells were found to express elevated levels of PGC-marker genes *Ap2-γ, Stella, Prdm14, Nanos3,* and *Dnmt3b*, and even markers of late PGC

specification, such as *Ddx4* (Tanaka *et al.*, 2000) ($P<0.05$) suggesting that these cells were indeed competent to form PGC-like cells in 'ETS-embryos' (Fig. 5.8. C).

5.4.2 PGC-like cell specification in 'ETS-embryos' is dependent on BMP signalling

To investigate the mechanism of PGC-like cell specification in 'ETS embryos', the signalling pathways known to govern these processes in the mouse were monitored. Both *in vivo* and *in vitro*, PGC specification is dependent on an active BMP signalling cascade, which in the embryo is initiated by a BMP4 signal secreted from the ExE tissue (Lawson *et al.*, 1999; Hayashi and Saitou, 2013). It was therefore hypothesised that BMP signalling may play a similar role during PGC-like cell specification in 'ETS-embryos''. This hypothesis was supported by the observation that the BMP signalling pathway was active in all cells of 'ETS-embryos', both in ESC and TSC compartments. This was revealed by immunofluorescence staining for Phospho-smad 1/5 (P-SMAD1) which showed a similar pattern to that in the post-implantation mouse embryo (Fig. 5.9. A).

To determine whether BMP signalling was required for PGC-like cell specification in this system, 'ETS-embryos' were cultured either in control conditions, or in the presence of the BMP4 antagonist Noggin (Zimmerman, De Jesús-Escobar and Harland, 1996), from 48 hours after initial plating in ECM. 'ETS-embryos' were fixed after 96 hours in control or experimental conditions. Downregulation of the BMP-signalling pathway was first verified by immunofluorescence staining of P-SMAD1, which was not detected in noggin-treated conditions (Fig. 5.9. B, left panels). When BMP was inhibited, the majority of 'ETS-embryos' failed to specify PGC-like cells (with only 7% of Noggin treated 'ETS-embryos' having detectable stella:GFP expression in comparison to 60% of control 'ETS-embryos' n= 15 per group, $P<0.05$) (Fig. 5.9. B, C). These results indicated that BMP signalling was required for PGC-like cell specification in 'ETS-embryos', just as it is required for PGC specification *in vivo*.

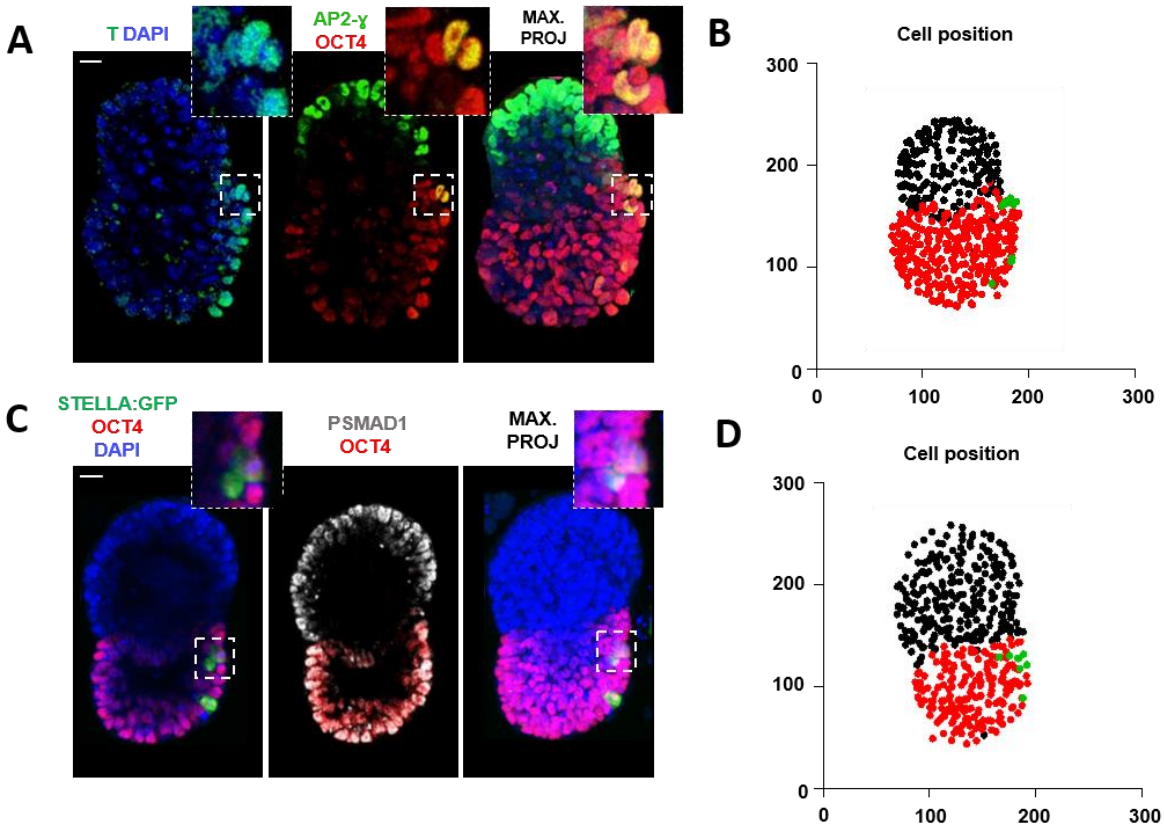

Fig. 5.7. **(A)** ETS-embryo at 120 hours showing asymmetric expression of mesoderm and PGC markers. Staining marks: Oct4, red; T/Brachyury, green; AP2γ, green; and DNA, blue. Insets highlight the Oct4- AP2γ double-positive cells which occupy the boundary in the T/Brachyury-positive region. Scale Bar= 20µm. n=13, 2 separate experiments. Maximum projection shows merge of AP2γ -Oct4-DAPI. **(B)** Projected cell coordinates for the same ETS-embryo as in (a): black points, Oct4 and AP2γ negative cells; Red points; Oct4 positive, AP2γ negative cells; green points, Oct4 and AP2γ double positive cells. **(C)** ETS-embryo at 120 hours stained to reveal: Stella:GFP, green; p-SMAD1, grey; Oct4, red; DNA, blue. Scale Bar=20µm. n=15, 3 separate experiments. Insets highlight Stella:GFP-positive cells in ESC compartment. Maximum projection shows merge of Stella:GFP-Oct4-DAPI. **(D)** Projected cell coordinates for same ETS-embryo as in (b). Black points, Stella:GFP and Oct4 negative cells; red points, Oct4-positive and Stella:GFP negative cells; green points, Oct4- and Stella:GFP positive cells.

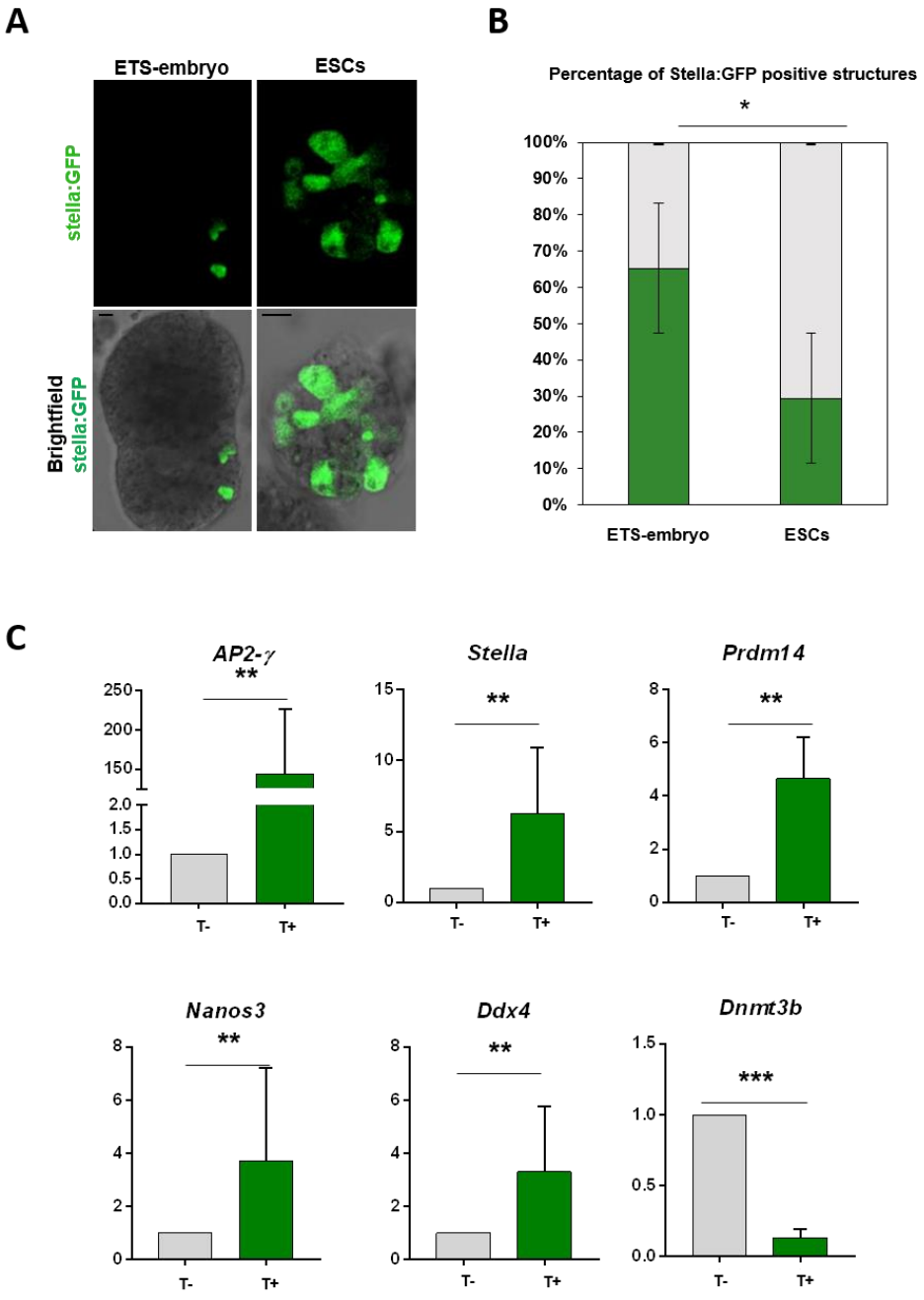

Fig. 5.8. **(A)** Stella:GFP-expressing ESCs (green) growing alone (right) or as part of a ETS-embryo (left) in Matrigel. Scale Bar=20µm. n=40 "ETS-embryos", 2 experiments; n=20 ESC-alone structures, 2 experiments. **(B)** Quantification showing the proportion of ETS-embryos expressing Stella:GFP at 120 hours is significantly higher in comparison to ESCs-alone structures. Fisher's exact test, P<0.001, n=80: 40 ETS-embryos and 40 ESC-alone structures counted in 2 experiments. Error bars=SEM. **(C)** RT-qPCR analysis of the expression of PGC markers in ETS-embryo. AP2γ, *Stella, Prdm14, Nanos3, Ddx4* and *Dnmt3b* in T:GFP positive and T:GFP negative cells from the same ETS-embryos collected after 120 hours in culture. Expression of PGC markers is significantly increased in T:GFP positive cells, Student's t-test, P<0.05. n=5 biological replicates. Error bars= SEM.

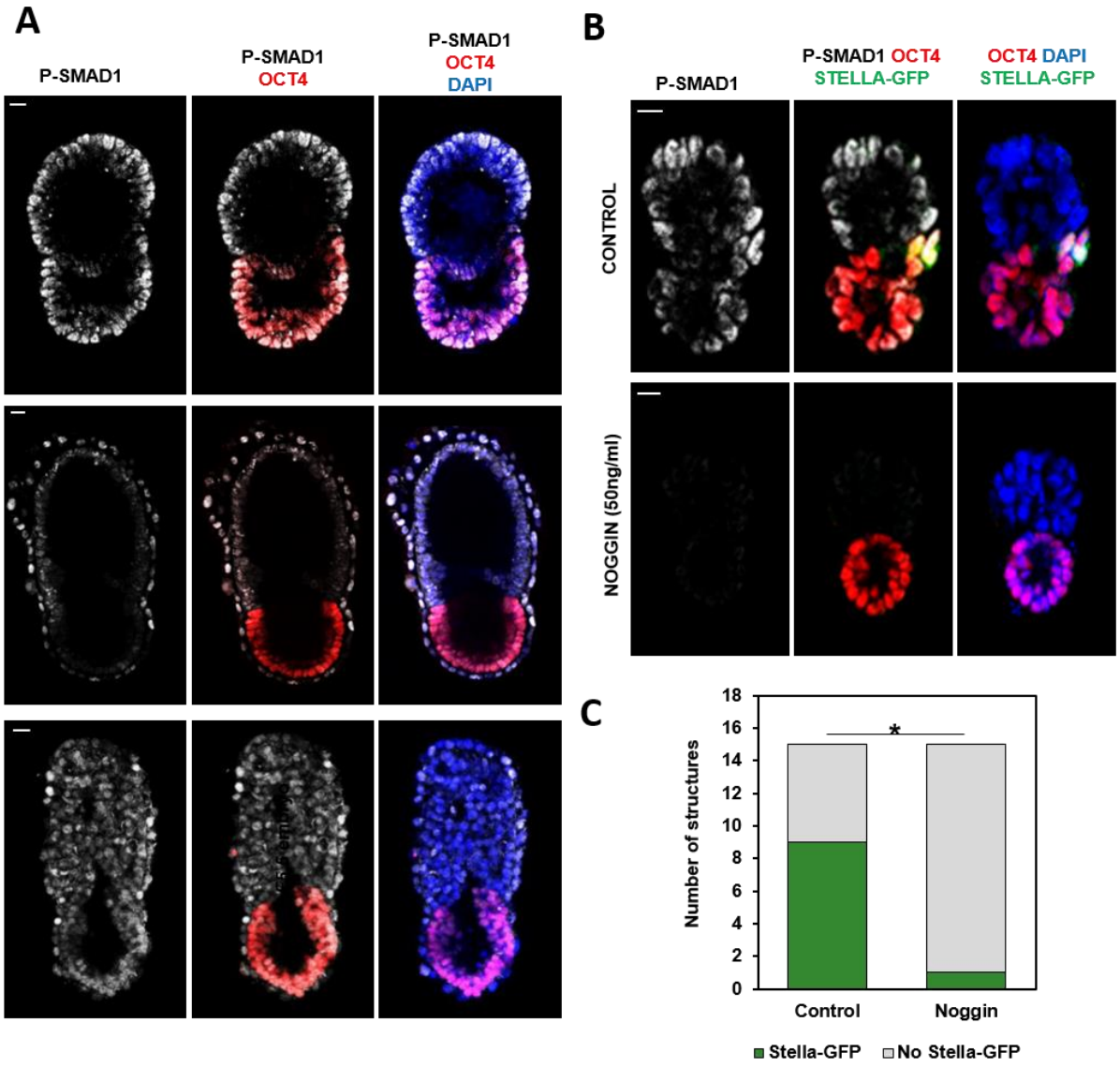

Fig. 5.9. (A) Comparison of P-SMAD1 expression in ETS-embryo*;* an *in vitro* cultured embryo and an embryo recovered from the mother at E5.5, stained to reveal: P-SMAD1, grey; Oct4, red; DNA blue. Scale Bar= 20µm. **(B)** ETS-embryos at 96 hours cultured in control conditions or with BMP antagonist Noggin (50ng/ml). Oct4, red; DNA, blue; P-SMAD1, grey; Stella-GFP, green. Scale Bar=20µm. n=15, 2 separate experiments. **(C)** Quantification of the number of ETS-embryos with Stella:GFP expression at the boundary between ESC and TSC compartments after 120 hours in culture in control conditions and in the presence of Noggin. Count data are presented as a bar chart, and a contingency table was used to perform the statistical test. n=15 per group, 3 separate experiments. Fisher's exact test, $P<0.05$.

5.5 Posterior-identity including PGC-like cell specification is dependent on Wnt signalling

In combination with BMP, Wnt signalling is also required in the embryo to confer competence on posterior EPI cells to become PGCs (Aramaki *et al.*, 2013; Günesdogan, Magnúsdóttir and Surani, 2014). To determine whether Wnt signalling was also required for the induction of posterior character (both mesoderm and PGC-like populations) in 'ETS-embryos', cells were collected from structures developing in either control conditions or in the presence of DKK1 (as described in section 5.2.2). In both conditions, 'ETS-embryos' were grown using T:GFP reporter ESCs, and after 96 hours, asymmetric T:GFP expression could be detected in the ESC compartment of control 'ETS-embryos'. Two populations of cells, T:GFP- positive and T:GFP negative cells, could therefore be isolated from the ESC-TSC boundary of control structures and analysed. However, in DKK1-treated conditions, the T:GFP signal indicative of mesoderm specification was abrogated. Therefore, all cells in the ESC compartment at the boundary with the TSCs were isolated and collected for analysis as a single group (Fig. 5.10. A). qRT-PCR analysis of Wnt-pathway readout genes *Axin1* and *Wnt3* were down-regulated in DKK1-treated cells compared with T:GFP-positive control cells, confirming that Wnt pathway activity was reduced in DKK1 treated conditions (Fig. 5.10., B, top row). In addition, these genes were also down-regulated in the T:GFP-negative 'control' cells, suggesting that the Wnt-pathway is more active in the 'posterior' region of 'ETS-embryos' in comparison to the 'anterior'. This was in agreement with results using the H2B-GFP::Tcf/LEF reporter ESC line.

Down-regulation of Wnt signalling in Dkk1-treated conditions also reduced the expression of T/Bra in comparison to control T:GFP-positive cells. In fact the levels of *T/Bra* in Dkk1-treated cells were similar to those in the T:GFP-negative control cells, suggesting that the whole ESC compartment had become more 'anteriorised' in these conditions (Fig. 5.10., B, top row).

Similarly, the levels of PGC marker genes *Blimp1*, *Stella*, and *Prdm14* were also significantly reduced compared to T:GFP-positive control cells, and were again comparable with levels in T:GFP-negative control cells from the region opposite the mesoderm (Fig. 5.10. B, bottom row).

Together, these results show that both mesoderm and PGC specification, characteristic features of the posterior of the mouse embryo, are dependent on Wnt signalling activity for their induction in 'ETS-embryos'. This supports the conclusion that Wnt is important for axial-patterning events in 'ETS-embryos', and that similar signalling pathways are involved in the specification of these cell types in both 'ETS-embryos' and in the post-implantation egg cylinder.

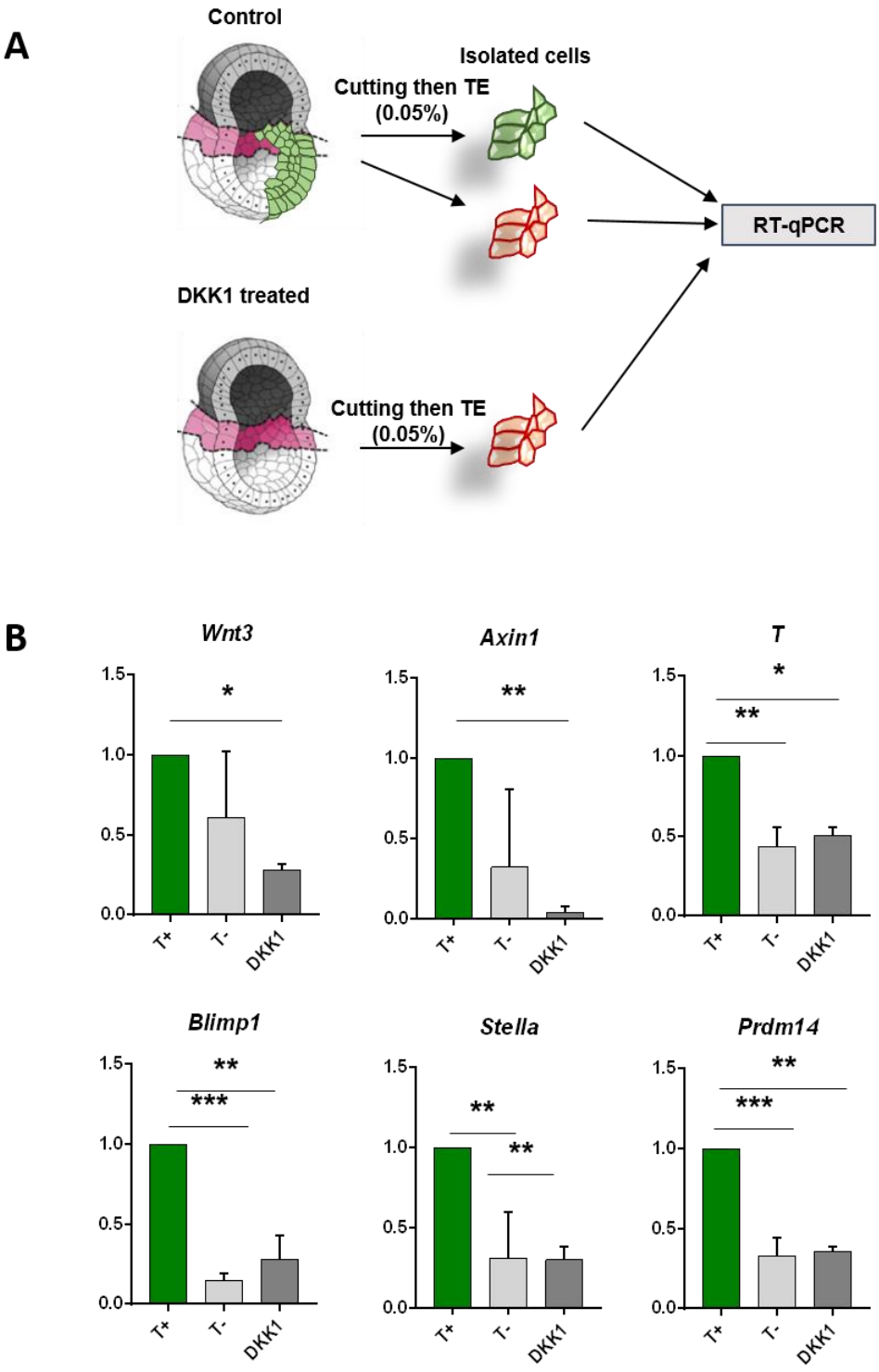

Fig. 5.10. **(A)** Schematic representation of the procedure used to isolate T:GFP positive and negative cells from control and DKK1-treated ETS-embryos for qRT-PCR analysis. **(B)** RT-qPCR analysis of the expression of PGC markers in 'border cells' collected from ETS-embryos in the presence of DKK1 (200ng/ml) versus T:GFP positive / negative cells collected from ETS-embryos in control conditions (collected after 120 hours in culture). Expression of PGC markers (*Blimp1*, *Stella,* and *Prdm14*) is significantly increased in T:GFP positive cells in control conditions, but this effect is abrogated when DKK1 is introduced into culture conditions . ANOVA followed by Tukey test. $P<0.05$. n=4 biological replicates. Error bars= SEM. Wnt pathway inhibition by DKK1 treatment was confirmed by analysis of the expression of *Axin1*, *Wnt3* and *T* in all samples.

5.6 Discussion

The results presented in this chapter demonstrate that early tissue specification events that are associated with post-implantation embryogenesis can be mimicked *in vitro* using 'ETS-embryos'. Reporter ESCs, qRT-PCR data and immunofluorescence have shown that mesodermal lineages become specified in 'ETS-embryos' after 96h of culture, and in a subset of structures, this region is confined to one side of the ESC-compartment at the embryonic-extra-embryonic boundary. Using a custom-designed quantitative analysis pipeline (Materials and Methods), expression of the mesodermal-marker T/Bra was judged to be 'asymmetric' when it formed this pattern in the structure. A remarkably similar pattern of T/Bra expression can be observed in the post-implantation mouse embryo after 6 days of gestation. It is at this time that the formation of the primitive streak initiates (Rivera-Pérez and Magnuson, 2005; Tam and Loebel, 2007). This specialised structure is characterised by a thickening of the EPI at the posterior, which gives way to a region of EMT as EPI cells ingress through the streak to form the germ layers (Bellairs, 1986; Williams *et al.*, 2013; Stower and Bertocchini, 2017).

The asymmetric localisation of mesoderm in 'ETS-embryos' is intriguing because this occurs in the apparent absence of any 'anterior' organising centre to inhibit posterior character being acquired throughout the whole ESC compartment. In the embryo, the AVE at the anterior of the embryo secretes Nodal antagonists Cer-l and Lefty1 (Belo *et al.*, 1997; Meno *et al.*, 1999; Yamamoto *et al.*, 2004). These antagonists act on cells within the epiblast in a graded manner, restricting Nodal activity to the proximo-posterior EPI. It is this gradient in Nodal activity which permits the formation of the primitive streak in one particular location only, and specifies the A-P axis of the embryo (Brennan *et al.*, 2001; Perea-Gomez *et al.*, 2002). Hence, the current model for axis establishment in the mouse heavily implicates the AVE as an anterior organiser (Arnold and Robertson, 2009). Despite the fact that Cer-l and Lefty expression has been detected in the pre-implantation blastocyst (Torres-Padilla, Richardson, *et al.*, 2007; Takaoka, Yamamoto and Hamada, 2011), suggesting A-P axis establishment may begin to occur prior to implantation, what lies upstream of DVE migration in this patterning still remains unknown.

In the previous chapter, Fig. 4.10. A shows that Nodal signalling is active in all cells of 'ETS-embryos', as demonstrated by P-SMAD 2/3 staining. This result suggests that there is no detectable gradient in Nodal signalling activity in 'ETS-embryos' and therefore the 'symmetry breaking' event observed in this system, when mesoderm becomes asymmetrically localised, cannot occur as a result of Nodal inhibition in the side opposite mesoderm specification. This is unsurprising, given that there is no evidence for the development of VE-like tissue in 'ETS embryos' (Chapter 3) nor an AVE-like signalling

centre. This is seemingly a deviation of the 'ETS-embryo' system from the mechanism which is known to underpin patterning in the mouse embryo. In the embryo, several studies have shown that A-P axis specification fails in the absence of the AVE (Thomas and Beddington, 1996; Kimura *et al.*, 2000; Stuckey *et al.*, 2011), and when both Cer-l and Lefty1 are knocked out, multiple primitive streaks appear in the EPI (Perea-Gomez *et al.*, 2002).

However, 30% of these double-mutants do position the primitive streak correctly, and gastrulation is not affected, suggesting that there is some functional redundancy in the system and that signalling pathways other than Nodal could also contribute to A-P axis specification (Stower and Srinivas, 2014). Indeed, other studies have implicated the Wnt signalling pathway in this patterning event. Wnt3 is expressed in the posterior EPI, and also in the posterior VE at timepoints that precede mesoderm specification (Rivera-Pérez and Magnuson, 2005; Yoon *et al.*, 2015), and a canonical inhibitor of the Wnt pathway, DKK1, is known to be secreted by the AVE. Interestingly, it has been shown that DKK1 can guide the migration of the DVE to the future anterior of the embryo (Kimura-Yoshida *et al.*, 2005), suggesting it plays a role in specifying the anterior side. However, DKK1 mutants are still able to correctly position the primitive streak, and mesoderm specification is normal, whilst the development of anterior structures such as the forebrain are defective. Interestingly, this suggests that anterior and posterior tissue specification can be decoupled (Mukhopadhyay *et al.*, 2001).

In the 'ETS-embryo' system, active canonical Wnt signalling was detected on one side of the ESC compartment, and this was followed by the expression of T/Bra. This was to be expected, given that Wnt signalling is directly upstream of mesoderm specification (Liu *et al.*, 1999; Lindsley *et al.*, 2006). Yet, what localises Wnt to one side of the ESC compartment remains to be identified. In some embryoid body systems, a similar asymmetric localisation of Wnt signalling activity is observed (ten Berge *et al.*, 2008; Fuchs *et al.*, 2012; van den Brink *et al.*, 2014), which leads to regionalisation of mesoderm in these structures. This occurs spontaneously, either as a response to endogenous signalling activity of the differentiating cells, or as a result of uniform induction of the Wnt pathway using recombinant Wnt ligand in the medium, or GSK3β-inhibitor. In these systems, patterning is thought to arise from initial heterogeneity within the starting population of ESCs, which becomes amplified over time and interacts with morphogen signalling, leading to the development of tissue boundaries (Etoc *et al.*, 2016; Turner, Baillie-Johnson and Martinez Arias, 2016).

Whilst it is possible that a similar mechanism may operate in 'ETS-embryos', the situation may be more complex due to the extra-embryonic TSC-compartment, which is not present in embryoid bodies. If the mechanism of Wnt induction is similar to that in the mouse embryo, then we would expect a signal, namely BMP4, provided by the extra-embryonic compartment to function in mesoderm

specification in the 'ETS-embryo' system. The fact that ESCs cultured alone in identical conditions to 'ETS-embryos' were less prone to T:GFP expression than compound structures consisting of both embryonic and extra-embryonic compartments, suggests that the extra-embryonic TSCs do indeed promote mesoderm specification in the *in vitro* model. This is consistent with studies in the mouse embryo which show that mesoderm specification and posterior epiblast identity is abrogated if the ExE is removed (Rodriguez *et al.*, 2005). Indeed, inhibition of BMP4 in 'ETS-embryos' leads to abrogation of the posterior cell types, suggesting that this signal, which comes from the TSC compartment of the structure, induces Wnt and leads to mesodermal and PGC-like cell specification in a manner which mimics their specification *in vivo*. In the next chapter, mRNA sequencing is used to confirm whether the source of BMP4 signalling in 'ETS-embryos' is indeed the TSC compartment, and to further characterise the posterior-like region which emerges in 'ETS-embryos' at a molecular level.

Despite the similarity in the molecular identity of the mesodermal cells observed in 'ETS-embryos' to those of the mouse embryo, expression of markers alone does not equate to the undertaking of gastrulation. This process not only requires the specification of germ layers, but it also requires that these nascent layers of tissue form in specified regions within the embryo, resulting in a trilaminar structure (Tam and Loebel, 2007). At the primitive streak, cells lose their epithelial integrity, ingress through the epiblast and undergo FGF-mediated migration away from the site of ingression to form the mesoderm as a separate tissue layer (Ciruna and Rossant, 2001). In 'ETS-embryos' T/Bra-positive mesodermal cells do not reproducibly undergo ingression and do not form a new tissue layer within the structure. However, genes associated with EMT at the primitive streak, such as *Snai1* (Cano *et al.*, 2000; Carver *et al.*, 2001) and *Vimentin* (Thiery *et al.*, 2009) are upregulated when compared with cells elsewhere in the ESC compartment. This suggests that T:GFP-positive cells in 'ETS-embryos' initiate a transcriptional program associated with EMT, but changes in cell shape and behaviour do not follow suit.

This could be explained by the fact that in the embryo, the basement membrane becomes broken at the site of the primitive streak, allowing cells to ingress through (Williams *et al.*, 2013). In 'ETS-embryos', the Matrigel mimicking the basement membrane is very thick and surrounds all of the tissue. It is possible that this thick, exogenous layer of ECM cannot be broken down by cells producing physiological levels of matrix-metalloproteinases, enzymes which breakdown the basal lamina during EMT (Thiery *et al.*, 2009). If this barrier is not broken, cells cannot escape the EPI layer and do not undergo ingression. Furthermore, without the VE monolayer surrounding the rest of the structure, if the cells of nascent mesoderm were to ingress, they would have nothing to restrict their migration. This means they may not necessarily form a tissue layer as in the embryo, where the mesoderm is

sandwiched between the ectoderm and the VE. It may be that mesodermal cells in the 'ETS-embryo' might be permitted to undergo EMT and migrate if the Matrigel were to be chemically or physically degraded in the local area. This would demonstrate whether basement membrane breakdown is permissive for EMT in this context, yet this remains to be explored.

Despite the fact that cells do not ingress in the 'ETS-embryo' system, the model is more similar to the mouse embryo than other *in vitro* models in which posterior cell types, particularly PGC-like cells are specified from embryoid bodies.

In the context of PGCs, similarity to embryo may also be derived from the fact that 'ETS-embryos' do not require the delivery of exogenous signals contained within the medium. Existing protocols to specify PGC-like cells *in vitro* first rely on 'priming' ESCs by converting them to EPI-like stem cells via treatment with recombinant FGF and Activin A (Hayashi and Saitou, 2013), before they can become responsive to PGC induction by BMP signalling. In the 'ETS-embryo' system, the cells are not pre-treated with these factors and instead spontaneously exit the 'naïve', 'ground-state' of pluripotency when embedded in ECM. The fact that the cells in the ESC compartment become competent to induce PGC-like cells suggests that they acquire a state similar to the primed epiblast of the early post-implantation embryo. Given that this state was not achieved through by dosing the cells with large quantities of growth factor far in excess of the levels that they would be exposed to *in vivo*, the process of posterior cell fate specification in this *in vitro* system might be more comparable to the process in the real embryo, as both systems rely on self-organised, endogenous signals between tissue compartments.

In summary, these results show that 'ETS-embryos' are capable of spatially restricted cell fate specification associated with A-P axis establishment during mouse embryogenesis. Whilst the mechanism of symmetry breaking in these structures remains unclear, the fact that the signals which specify posterior cell types are the same as those that do so in the mouse egg cylinder indicate that 'ETS-embryos' might be informative about this process *in vivo*. In the next chapter, the asymmetric acquisition of cell fate across the ESC compartment of 'ETS-embryos' is explored in more detail using transcriptomics, as is the overall similarity of the *in vitro* model to the post-implantation embryo.

6. Results IV: Transcriptional profiling of 'ETS-embryos' compared with post-implantation mouse embryos

6.1 Introduction:

Although (as introduced above) attempts have been made in the past to model the embryo *in vitro*, using embryoid bodies or micropatterned hESCs, the patterning processes that these systems exhibit can be uninformative about body axis patterning. This is because, owing to the fact that most are amorphous spheroids or radially symmetrical, we cannot relate differences in cell fate to any absolute position in space. In the main, embryoid body/ gastruloid models have relied on *in situ* hybridisation techniques or the use of transgenic ESC reporter lines to readout transcriptional differences between groups of cells in different positions (ten Berge *et al.*, 2008; van den Brink *et al.*, 2014). These studies then compare polarised domains of gene expression in embryoid bodies to different domains across the EPI which result in A-P patterning during embryogenesis (Tam and Loebel, 2007; Arnold and Robertson, 2009). Although such an approach is useful to dissect signalling pathways which lead to tissue specification events (Warmflash *et al.*, 2014; Etoc *et al.*, 2016), transcriptional similarity to the embryo is often assumed without overwhelming evidence, and the similarity of such *in vitro* models to the real *in vivo* situation remains uncharacterised by a transcriptomics approach where thousands of genes can be compared.

In contrast, the development of RNA-sequencing ('RNA-seq') techniques on single and small groups of cells has allowed the us to characterise the transcriptome of the mouse embryo in more depth than ever before. Cellular heterogeneity, pattern formation and symmetry breaking have been elucidated at the transcriptional level by recent studies which use bulk and single-cell mRNA sequencing to identify differentially expressed genes and relate them to position within the whole embryo and their subsequent fate. Such studies have been performed focussing on both pre-implantation development (Hamatani *et al.*, 2004; Guo *et al.*, 2010; Goolam *et al.*, 2016), and post-implantation development (Peng *et al.*, 2016; Scialdone *et al.*, 2016). In addition, several studies have used similar techniques to understand transcriptional differences between developmental stages of the mouse embryo. Some studies also include datasets gathered from ESCs and EPISCs to determine how similar these cultured cell lines are to the embryonic epiblast, and which developmental stage they represent (Boroviak *et al.*, 2014; Kojima *et al.*, 2014; Peng *et al.*, 2016). Such studies have greatly enhanced our understanding of the transcriptional regulation of development, and have shed light on how transcriptional nuances can bias tissue specification and impact on embryogenesis.

In this chapter, similar RNA-seq techniques were used to compare 'ETS-embryos' and post-implantation mouse embryos at a global transcriptional level. These experiments aimed to determine the similarity between the *in vitro* model and the real embryo and also to further investigate the axis-like patterning observed in 'ETS-embryos' which emerged after 4 days of culture. 'ETS-embryos' were found to be most similar to the early post-implantation mouse embryo at E6.5-7.5, and were more similar to the embryo when compared with the published transcriptomes of EPISCs maintained in conventional 2D culture. Overall, these results suggest that 'ETS-embryos' represent a more embryo-like state in terms of transcriptional output compared to pluripotent stem cells, and support the idea that 'ETS-embryos' can be used to model early post-implantation development.

6.2 Sample collection, mRNA sequencing and data quality assessment

6.2.1 Isolation of cells for sequencing

Two groups of samples from 'ETS-embryos' were taken for mRNA sequencing. One group was used to investigate the similarity of the ESC and TSC compartments of 'ETS-embryos' to embryonic and extra-embryonic tissues of the mouse embryo, and a second group to compare mesodermal cells and non-mesodermal cells in the ESC compartment of 'ETS-embryos' to the anterior and posterior EPI of the gastrula. Three independent biological replicates of each sample were taken and used for downstream analysis.

To prepare samples belonging to the first group, 'ETS-embryos' were generated using CAG-GFP reporter ESCs (Rhee *et al.*, 2006) to demarcate the fluorescent ESC compartment from the TSC compartment. 'ETS-embryos' were manually picked from the ECM substrate and then dissected into separate ESC and TSC compartments before snap-freezing in lysis buffer (see Materials & Methods) (Fig. 6.1. A). Three 'ETS-embryos' were dissected and sent for sequencing as a pair of samples, called 'ES1' and 'TS1', 'ES2 and 'TS2' plus 'ES3' and 'TS3'.

To prepare samples belonging to the second group, 'ETS-embryos' were generated using T:GFP reporter ESCs (Fehling, *et al*. 2003), and those expressing T:GFP in a regionalised domain after 100h were dissected to isolate the ESC compartment. The ESC compartment was further dissected into a GFP-positive and a GFP-negative region opposite, then these halves were dissociated by gentle trypsinisation. Cells were then checked for GFP signal under a confocal microscope, then collected into GFP-positive and GFP-negative groups (consisting of cells directly opposite the GFP-positive region) before being placed in lysis buffer (Fig. 6.1. B). Owing to the technical difficulty of manually isolating pure populations of T:GFP positive and T:GFP negative samples by manually dissection whilst preserving RNA quality, five pairs of samples were isolated from 'ETS-embryos'. A pair of samples

constituted the T:GFP-positive cells from an 'ETS-embryo' after 120h in culture, which were labelled as 'P' and the T:GFP negative cells lying directly opposite the asymmetric region of mesoderm, which were labelled as 'A'. These pairs of samples were labelled with a number from 1-5. As such, the full set of samples in the second group which were sequenced were as follows (See Table 4.1 for a detailed list of samples):

- A1 (TGFP-negative cells from ETS embryo 1) and P1 (TGFP-positive cells from ETS embryo 1)
- A2 (TGFP-negative cells from ETS embryo 2) and P2 (TGFP-positive cells from ETS embryo 2)
- A3 (TGFP-negative cells from ETS embryo 3) and P3 (TGFP-positive cells from ETS embryo 3)
- A4 (TGFP-negative cells from ETS embryo 4) and P4 (TGFP-positive cells from ETS embryo 4)
- A5 (TGFP-negative cells from ETS embryo 5) and P5 (TGFP-positive cells from ETS embryo 5)

6.2.2 mRNA sequencing and quality assessment

cDNA libraries were prepared using the 'SmartSeq2' protocol (Picelli *et al.*, 2014) and libraries were sequenced using a HiSeq2500 machine running in rapid mode. Reads were mapped to the *Mus musculus* genome (assembly mm10, ENSEMBL) using the Tophat2 v2.0.4 program (Trapnell, Pachter and Salzberg, 2009). Reads for all samples were subjected to quality assessment using the FASTQC tool (Andrews, 2010) (Fig. 6.2. A, Materials & Methods). All intact ESC and TSC samples from the first group passed the quality control analysis, and had a high number of mapped reads and good mapping ratio of >70%, suggesting good quality RNA had been preserved during sample collection. In contrast, two pairs of samples from the second group (A1, P1, A2 and P2) had a low number of reads and low mapping ratios (Table 4.1, rows in red and highlighted in grey). These data indicated that good quality RNA had not been preserved during the isolation of these samples, and thus they were excluded from downstream analysis. However, the rest of the paired T:GFP positive and T:GFP negative samples (A3, P3, A4, P4, A5 and P5) did yield a high number of mapped reads and a good mapping ratio, so the data from these three remaining biological replicates were retained for further analysis.

For samples which passed the quality assessment, the number of genes detected was quantified, and gene expression density distribution was plotted to check for outliers (Fig. 6.2. B-D). Reads from samples which passed all these checks were then subjected to downstream analysis. The 'Fragment per kilobase million' (FPKM) was calculated using the Cufflinks v2.0.2 program with default parameters (Kim *et al.*, 2013) and used as a measure of gene expression level. Genes with an FPKM > 1.0 in at least one sample across all samples were used in subsequent analysis, and the expression level data were log-transformed (using $\log_2(\text{FPKM}+1)$).

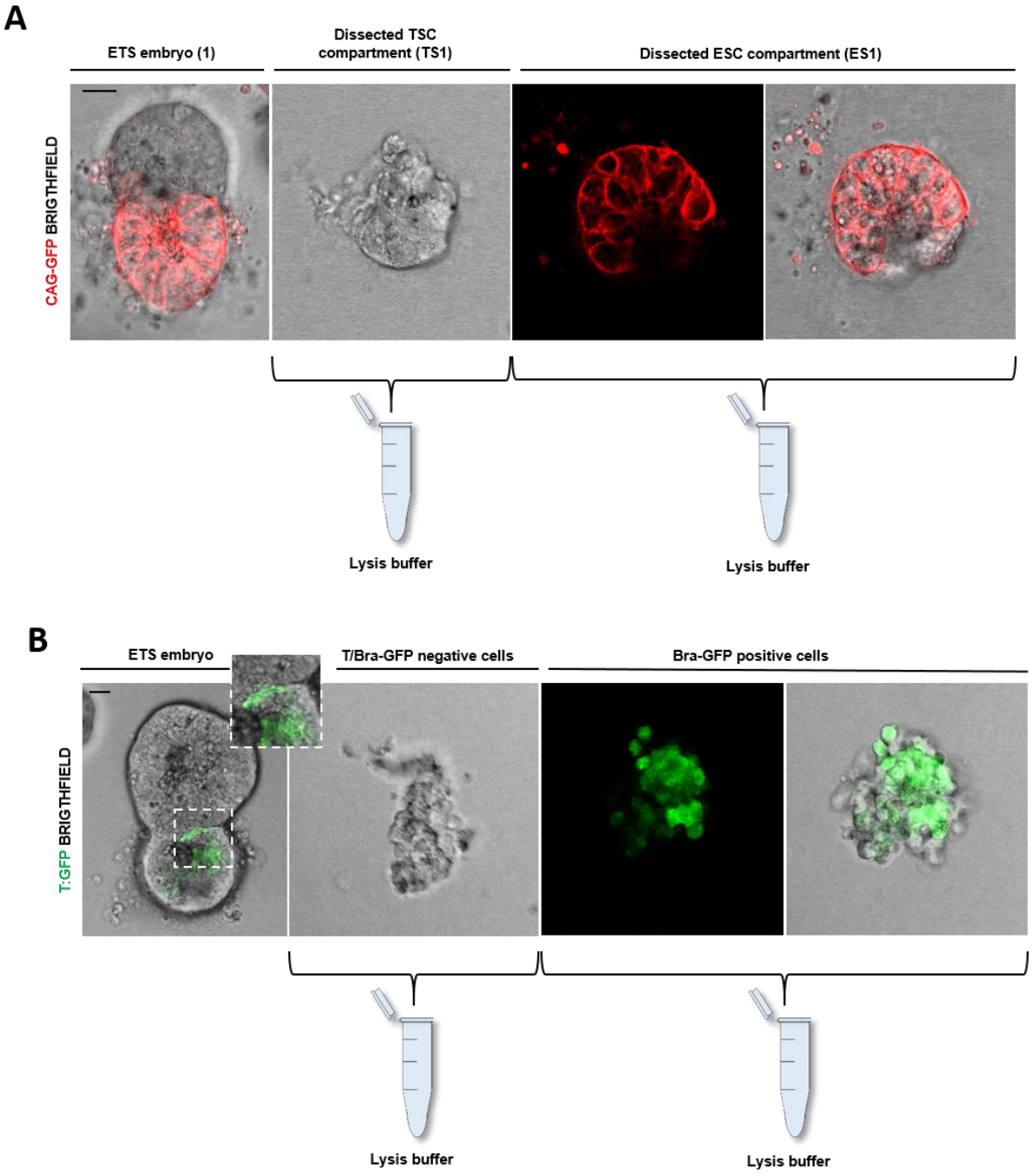

Fig. 6.1. **(A)** Confocal snapshots of an intact (left panel) and dissected ETS-embryo isolated for mRNA sequencing of whole ESC and TSC compartments. The cells of the ESC compartment carry a CAG:GFP reporter which is false-coloured in red. ESC and TSC compartments were dissected and collected separately in lysis buffer as shown. Scale Bar= 20 µm. **(B)** Confocal snapshots of an intact (left panel) and dissected ETS-embryo isolated for mRNA sequencing of mesodermal cells and the non-mesodermal cells opposite. The cells of the ESC compartment carry a T/Bra:GFP reporter, and so mesodermal (GFP-positive) cells were collected and non-mesodermal (GFP-negative) cells lying opposite were dissected and collected separately in lysis buffer as shown. Scale Bar= 20 µm. Inset highlights the asymmetric GFP-positive region from which mesodermal cells were collected.

Table 4.1: List of tissue samples taken from 'ETS-embryos' for mRNA sequencing

Samples	Sample description	Estimated Cell number	Reads	Aligned	Ratio
ES1	ESC compartment isolated from ETS embryo	150	8,838,584	7,091,946	80.24%
ES2	ESC compartment isolated from ETS embryo	150	7,351,484	5,316,333	72.32%
ES3	ESC compartment isolated from ETS embryo	150	7,405,442	5,403,035	72.96%
TS1	TSC compartment isolated from ETS embryo	150	8,523,992	6,201,394	72.75%
TS2	TSC compartment isolated from ETS embryo	150	7,398,888	6,090,181	82.31%
TS3	TSC compartment isolated from ETS embryo	150	3,689,714	2,755,404	74.68%
A1	T/Bra:GFP negative cells isolated from ETS embryo	10	1,77,214	571,336	48.53%
P1	T/Bra:GFP positive cells isolated from ETS embryo	10	2,022,990	1,045,569	51.68%
A2	T/Bra:GFP negative cells isolated from ETS embryo	10	6,771,906	5,734,342	84.68%
P2	T/Bra:GFP positive cells isolated from ETS embryo	10	5,069,392	1,858,344	36.66%
A3	T/Bra:GFP negative cells isolated from ETS embryo	10	5,344,218	3,973,903	74.36%
P3	T/Bra:GFP positive cells isolated from ETS embryo	10	2,768,668	2,352,931	84.98%
A4	T/Bra:GFP negative cells isolated from ETS embryo	10	8,158,596	5,951,789	72.95%
P4	T/Bra:GFP positive cells isolated from ETS embryo	10	6,711,810	5,639,235	84.02%
A5	T/Bra:GFP negative cells isolated from ETS embryo	10	8,139,128	6,121,725	75.21%
P5	T/Bra:GFP positive cells isolated from ETS embryo	10	6,245,282	5,471,767	87.61%

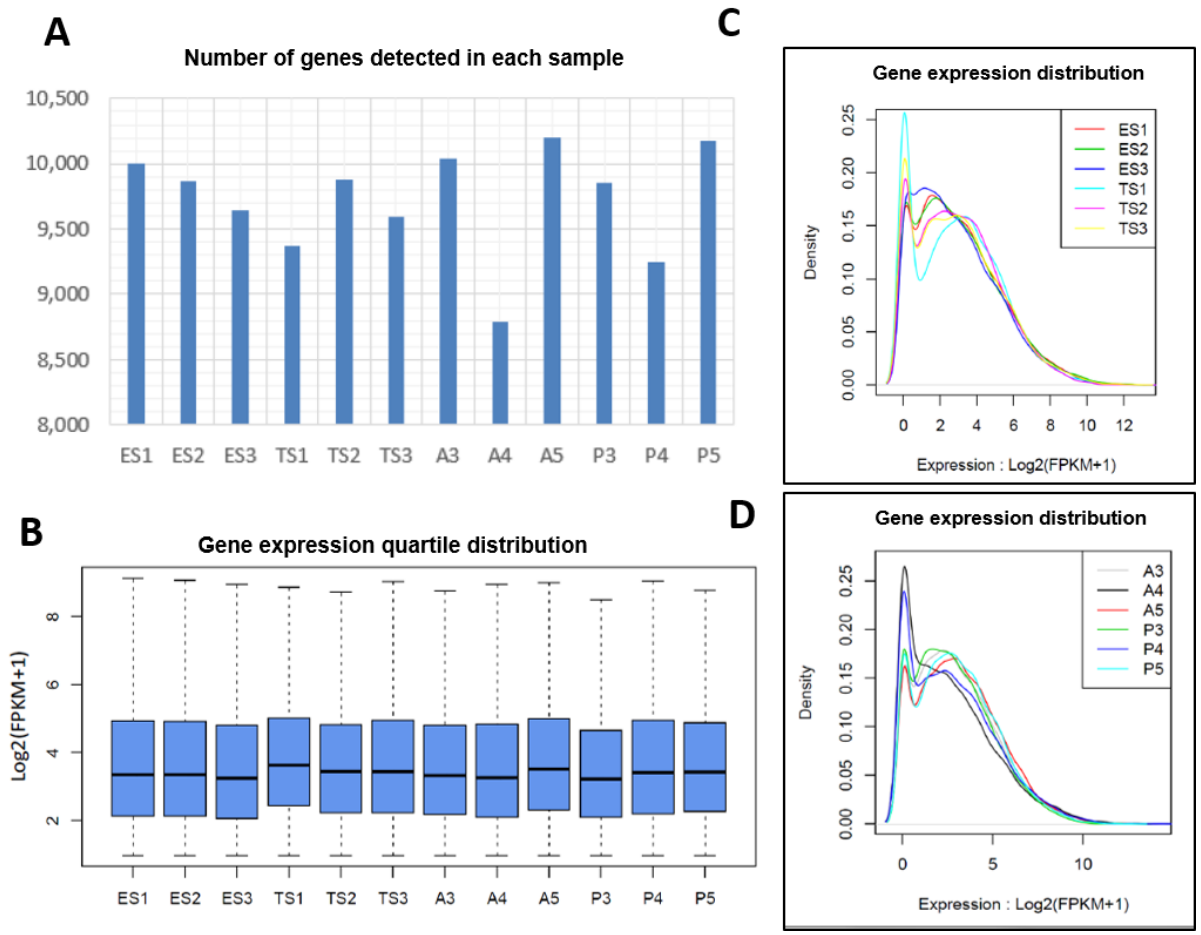

Fig. 6.2. **(A)** Bar graph showing the number of expressed genes detected in each sample collected from ETS-embryos and sent for mRNA sequencing. No outliers were identified. (**B)** Box-and-whisker plot showing the variation in gene expression levels across all samples. All samples show a similar spread in variation and thus can be compared to one another. No outliers were identified. **(C)** The distribution in gene expression level plotted for samples ES1, ES2, ES3, TS1, TS2, TS3. Distributions were similar for all samples and no outliers were identified. **(D)** The distribution in gene expression level plotted for samples A3, A4, A5, P3, P4, P5. Distributions were similar for all samples and no outliers were identified.

6.3 Transcriptional comparison of 'ETS-embryos' to embryonic and extra-embryonic tissues of the mouse embryo

6.3.1 Clustering analysis of samples

The identity of ESC and TSC samples were first confirmed as embryonic and extra-embryonic respectively by analysis of the expression of a suite of embryonic and extra-embryonic markers in both ESC and TSC samples. In ESC samples (ES1, ES2, ES3) markers of embryonic epiblast *Oct4, Nanog, Otx2* and *Fgf5* were highly expressed whilst in TSC samples (TS1, TS2, TS3) these genes were expressed at low levels or not detected. In contrast, *Elf5, Cdx2* and *AP2γ (Tfap2C)* were expressed at high levels in TSC samples but were low in ESC samples (Fig. 6.3. A, B). Importantly, the TGF-β ligand BMP4 was also highly expressed in TSC compartments, while there was little or no expression detected in ESC compartments (Fig. Fig. 6.3. B, bottom-righthand panel) confirming the hypothesis that the TSC compartment acts as a source of BMP4 required for mesoderm and PGC specification in 'ETS-embryos'. Furthermore, these data are in agreement with q-RT PCR data presented in Chapter 1, and confirm that ESC and TSC compartments in 'ETS-embryos' represent different embryonic and extra-embryonic tissue types.

Next, the transcriptome data was subject to unsupervised hierarchical clustering analysis (as described by (Peng *et al.*, 2016)), which grouped samples in a lineage tree by similarity to each other. The samples formed two clearly defined groups by cell type, with ES1, ES2, and ES3 forming a separate cluster on the left-hand side of the tree from TS1, TS2 and TS3 which grouped together on the right (Fig 6.3. C). Log-transformed read-count data from each sample was then subject to a Principal Component Analysis (PCA). The two highest 'principal components' accounting for the most variation in the data were plotted as X and Y dimensions respectively, and samples were plotted in space along these axes. In the analysis in Fig. 6.3. D, PC1 can account for 48.96% of the total variation in the data, whilst PC2 accounts for 17.86%. For the PC1 dimension, ESC samples (ES1, ES2, and ES3) clustered closely together whilst TSC samples (TS1, TS2, TS3) clustered separately, suggesting that PC1 accounts for variation in gene expression which can be attributed to cell/tissue type. This demonstrated that ESC and TSC compartments are distinct and have different transcriptional profiles.

6.3.2 ESC compartments express genes associated with embryonic development

Next, the differentially expressed genes (DEGs) between the ESC 'cluster' of samples and TSC 'cluster' of samples were analysed. 677 genes were identified as expressed more highly (with a false discovery rate p-value of <0.05 and a fold-change of >2) in ESC samples than in TSC samples (Fig. 6.4. A). A gene-ontology (GO analysis, see Materials & Methods) performed on this gene list identified several

biological processes associated with embryonic development as enriched terms (Fig. 6.4. A). From the most highly expressed genes, a clear difference emerged between pairs of ESC and TSC samples. Genes were identified in this list which are associated with the early post-implantation mouse epiblast, and are known to be involved in both pluripotency, such as *Oct4/Pou5f1* (Pesce and Scholer, 2001) and also with differentiation such as *Tdgf1/Cripto* (Kimura *et al.*, 2001)(Fig. 6.4. B, C).

6.3.3 TSC compartments express genes associated with placenta development

In contrast, the same analysis also identified 766 DEGs which were more highly expressed in the TSC compartment of 'ETS-embryos' (with a false discovery rate p-value of < 0.05 and a fold change >2) compared with the ESC compartment. A GO analysis revealed that these genes were associated with biological processes such as angiogenesis and placental development, consistent with the hypothesis that TSC compartments represented a more ExE-like tissue in 'ETS-embryos' (Fig. 6.5. A). This was corroborated by the presence of known ExE markers in this list including *Elf5* (Latos *et al.*, 2015), which were not detected in ESC samples (Fig. 6.5. B, C). These results confirm that the ESC compartments of 'ETS-embryos' express genes similar to the mouse embryonic epiblast, whilst TSC compartments express genes associated with the ExE, and confirm that the ESC compartment represents a distinct tissue compartment to the TSC compartment in 'ETS-embryos'.

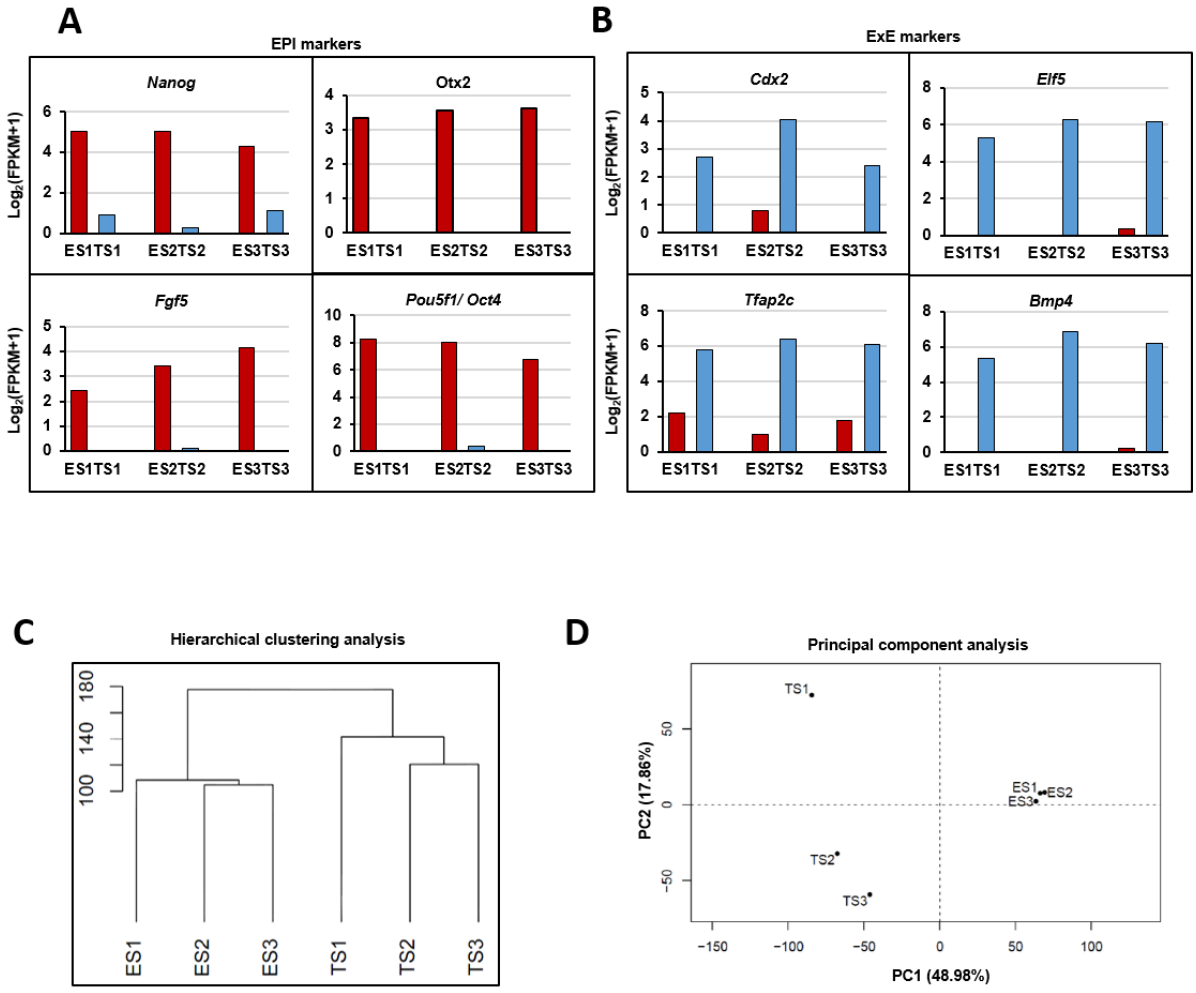

Fig. 6.3. (A) Expression levels of known EPI markers Nanog, Otx2, Fgf5 and Pou5f1/Oct4 plotted for ESC samples ES1, ES2, ES3 (red bars), and TSC samples TS1, TS2, and TS3 (blue bars) isolated from ETS embryos. **(B)** Expression levels of known ExE markers Cdx2, Elf5, AP2γ (Tfap2C) and Bmp4 plotted for ESC samples ES1, ES2, ES3 (red bars), and TSC samples TS1, TS2, and TS3 (blue bars) isolated from 'ETS-embryos'. **(C)** Unsupervised hierarchical clustering analysis of ESC and TSC samples showing the samples form two clusters which group by tissue type. ES1, ES2, and ES3 form one cluster whilst TS1, TS2, and TS3 form a separate cluster. **(D)** A PCA plot of the data from ESC and TSC samples isolated from 'ETS-embryos'. PC1 (x-axis) explains 48.98% of the variation in the data whilst PC2 (y-axis) explains 17.86% of the variation in the data. Samples group along the x-axis according to tissue type.

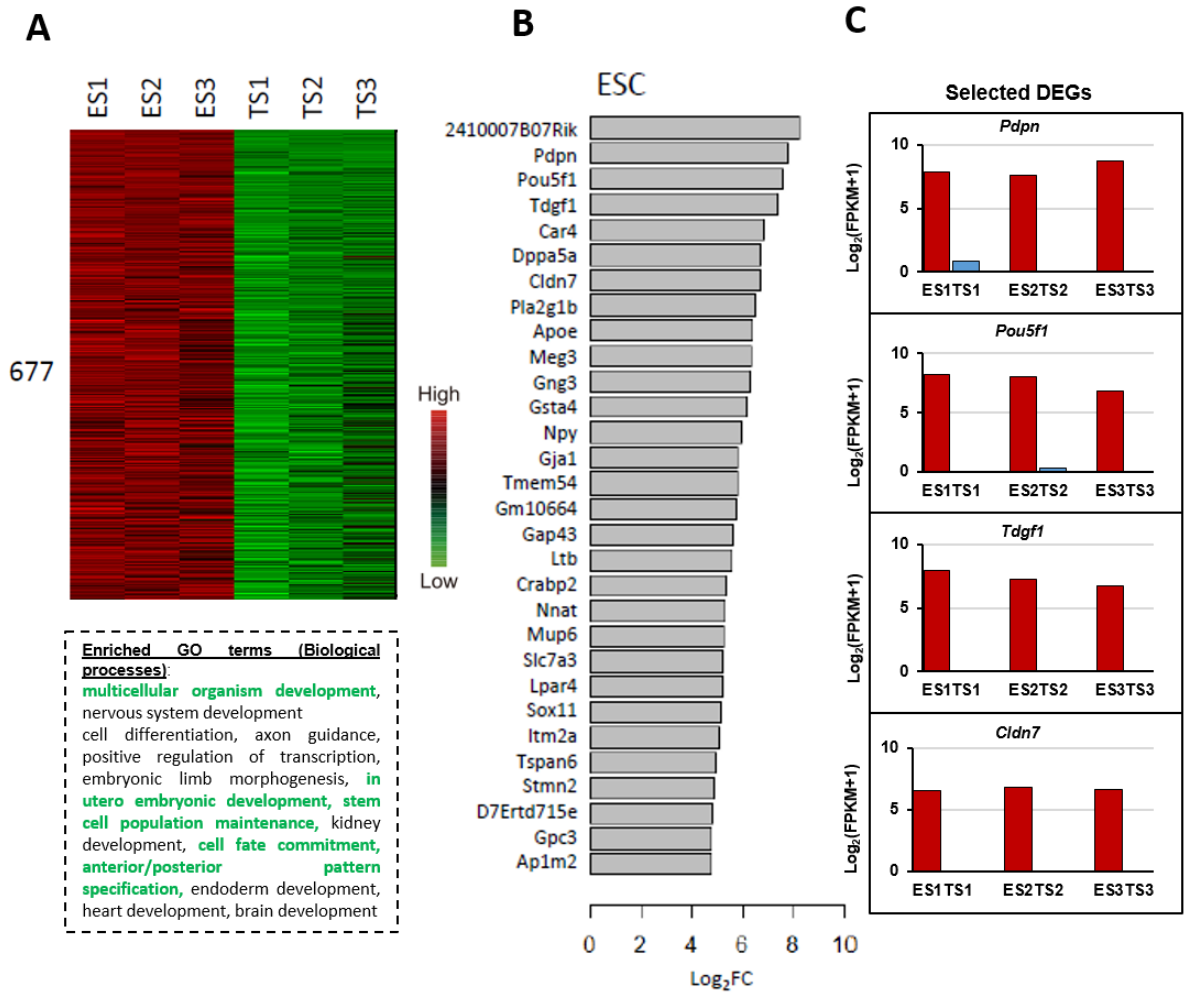

Fig. 6.4. **(A)** A heat map showing the 677 genes which are more highly expressed in ESC compartments across samples compared to TSC compartments. Red indicates high expression, green indicates low expression. Lower text-box shows the enriched GO analysis terms obtained when this gene list was analysed using DAVID software (see Materials & Methods). Terms which are particularly relevant to post-implantation mouse epiblast development are highlighted in green. **(B)** A list of the top 30 differentially expressed genes with expression levels higher in ESC compartments than in TSC compartments across samples. Grey bars show the mean expression level of each gene as $\log_2$(FPKM+1) in ESC samples. **(C)** Expression levels of randomly selected DEGs with higher expression in ESC compartment samples (red bars) compared with TSC compartments (blue bars) across all three samples.

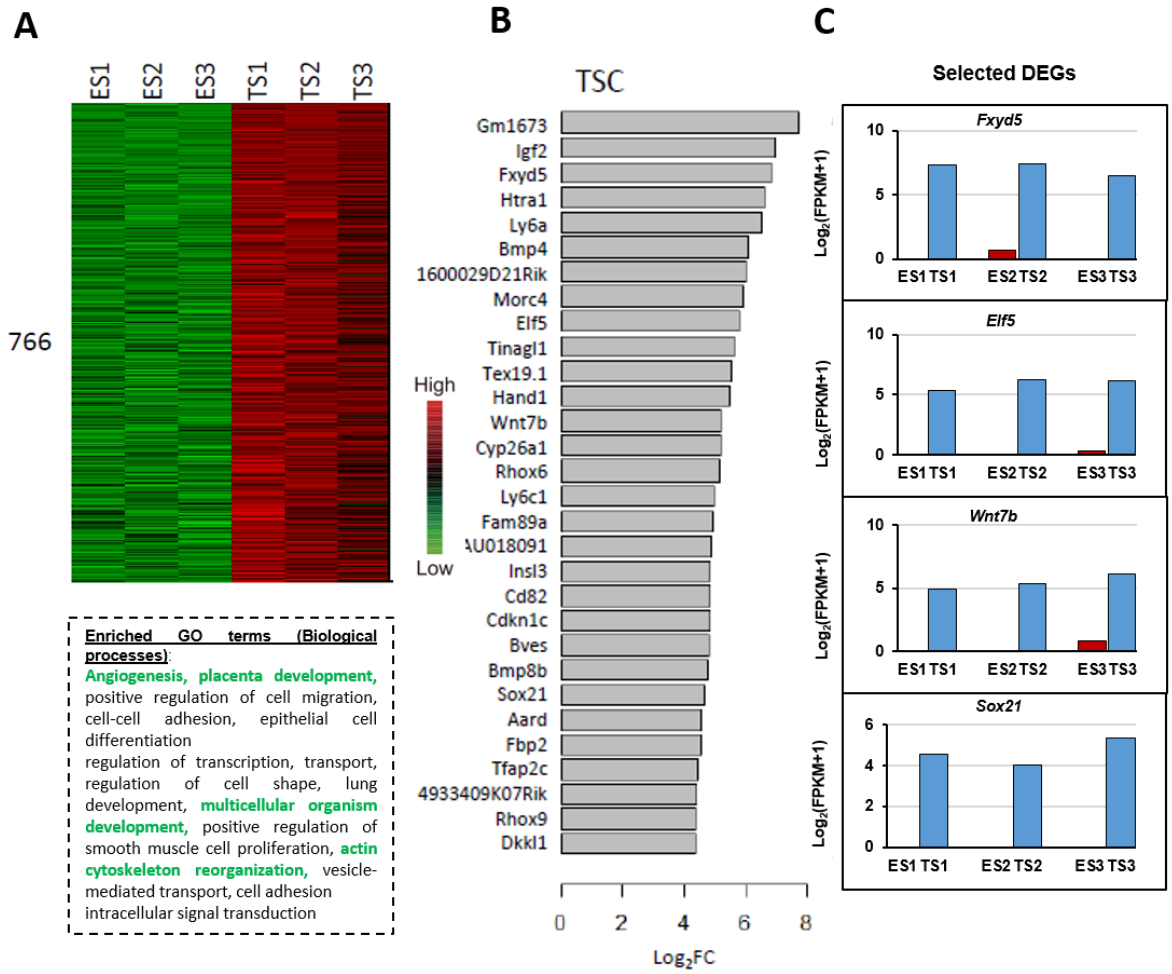

Fig. 6.5. **(A)** A heat map showing the 766 genes which are more highly expressed in TSC compartments across samples compared to ESC compartments. Red indicates high expression, green indicates low expression. Lower text-box shows the enriched GO analysis terms obtained when this gene list was analysed using DAVID software (see Materials & Methods). Terms which are particularly relevant to post-implantation mouse ExE development are highlighted in green. **(B)** A list of the top 30 differentially expressed genes with expression levels higher in TSC compartments than in ESC compartments across samples. Grey bars show the mean expression level of each gene as log_2(FPKM+1) in ESC samples. **(C)** Expression levels of randomly selected DEGs with higher expression in TSC compartment samples (blue bars) compared with ESC compartments (red bars) across all three samples.

6.3.4 Clustering analysis with post-implantation embryos

In order to compare global gene expression patterns in ESC and TSC compartments with those of the ExE and EPI of the real embryo, datasets from Peng et al (2016) were used in an unsupervised hierarchical clustering analysis with data produced in this study. Data from E6.5 ExE, E7.0 ExE, E7.5 ExE, E6.5 EPI, E7.0 EPI, E7.5 EPI were used. TSC samples were clustered within a larger group comprised of ExE samples from the real embryo, between the datasets from younger (E6.5) and older (E7.5) embryos. Similarly, ESC samples were clustered between the datasets from the E6.5 and E7.5 EPI tissue (Fig. 6.6. A). A PCA analysis performed on these data showed that across PC1, which accounts for 32.25% of the variation in the data, embryonic and extra-embryonic tissue samples emerge in two distinct groupings, with ESC and TSC samples from 'ETS-embryos' forming two tight subclusters (Fig. 6.6. B). TSC samples grouped with ExE samples, and ESC samples grouped with embryonic samples, again suggesting that PC1 accounts for variation in gene expression due to tissue type. Taken together, these results show that ESC and TSC compartments represent two distinct tissues in 'ETS-embryos' and that the tissues of 'ETS-embryos' are transcriptionally similar to those of post-implantation embryos at gastrulation stages. This provides further evidence that 'ETS-embryos' are a faithful model of embryonic development at these stages, with comparable transcriptomes.

6.4 Comparison of 'ETS-embryos' to stem cell lines in 2D culture

6.4.1 'ETS-embryos' have a more similar transcriptome to the mouse egg cylinder than EPISCs

Next these same 'ETS-embryo' samples, plus the EPI and EXE samples were compared to published transcriptomes of EPISCs using another PCA. Given that EPISCs in 2D culture are used as an *in vitro* model of the embryonic epiblast (Tesar *et al.*, 2007; Chenoweth, McKay and Tesar, 2010), this analysis was performed in order to find out whether 'ETS-embryos' might be a closer model of embryogenesis than cells in this established culture at the transcriptome level. To ensure that a spectrum of cell lines were represented, published data from 6 lines of EPISCs, derived from embryos at different developmental stages were used for the comparison (Kojima *et al.*, 2014). Strikingly, these six EPISC lines clustered separately from the other data-points, and the ESC and TSC samples from 'ETS-embryos' clustered more closely with the samples taken from the embryo at E6.5, suggesting that they were more similar to the real embryonic tissue. The names of the EPISC lines in Fig. 6.6. C refer to the stage of embryo from which they were derived (CAV: Pro-amniotic cavity stage, PS: Pre-streak stage, LMS: Late mid stage, LS: Late streak stage, EB: Early bud stage, LB: Late bud stage) (Kojima *et al.*, 2014). In agreement with what has been published, these data also suggested that the EPISCs had very similar transcriptomes, regardless of the developmental stage at which they were derived (Kojima

et al., 2014) forming separate sub-clusters in between the bone-fide embryonic and extra-embryonic tissue from the mouse egg cylinder (Fig 6.6. C).

Overall, these data show that 'ETS-embryos' have a more comparable transcriptome to real embryos than conventional *in vitro* cultured cell lines and hence more faithfully recapitulate the transcriptional signature of the embryonic and extra-embryonic tissues *in vivo*.

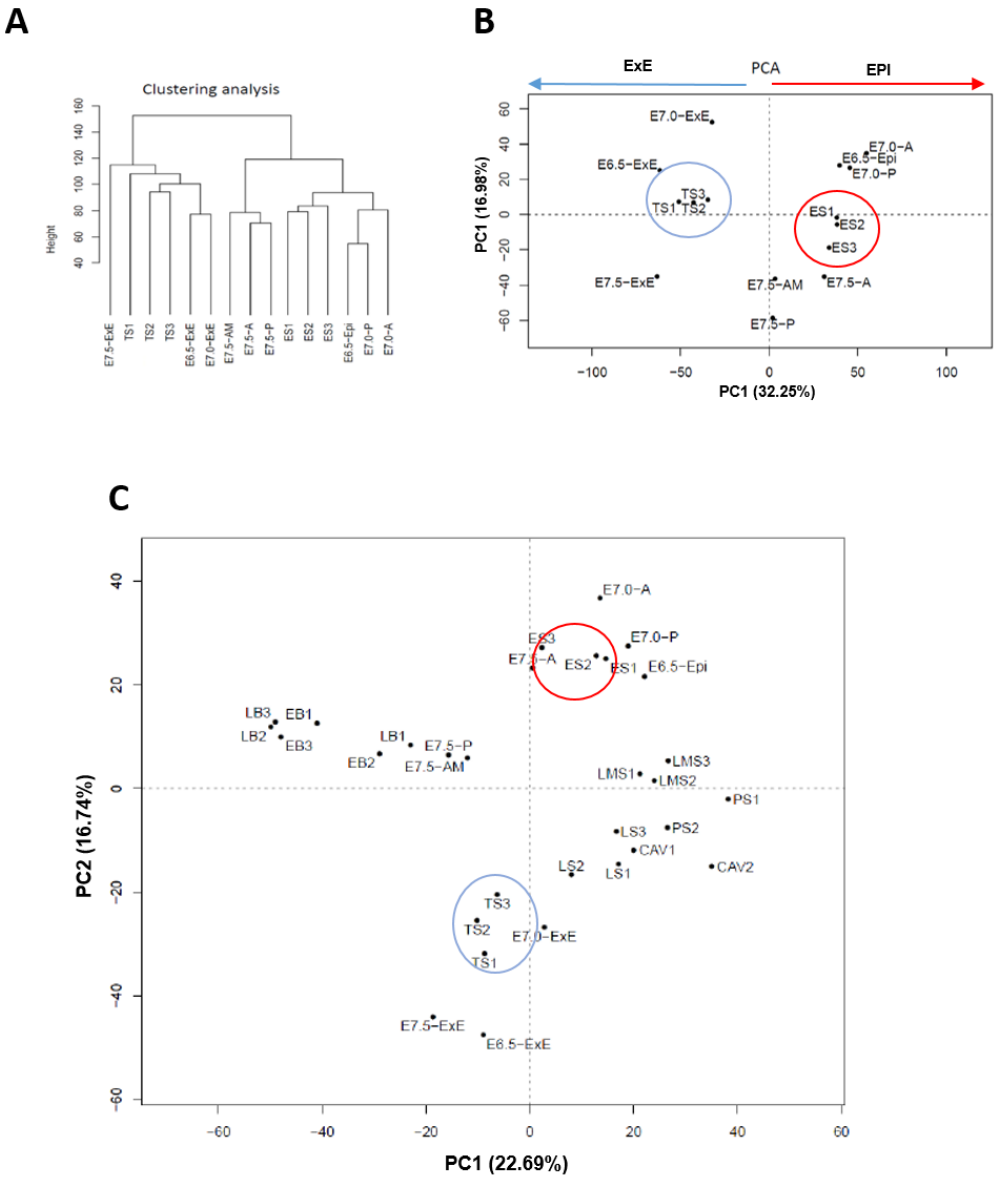

Fig. 6.6. **(A)** Unsupervised hierarchical clustering analysis of ESC and TSC samples, plus existing data from EPI and ExE compartments of post-implantation mouse embryos at the stages indicated. ES1, ES2, and ES3 form one cluster with the E6.5 EPI, E7.0 regionalised EPI (E7.0-A (anterior), E7.0-P (posterior)) and E7.5 regionalised EPI (E7.5-A (anterior), E7.5-P (posterior), E7.5-AM (anterior mesoderm)). TS1, TS2, and TS3 form a separate cluster with the E6.5 ExE, E7.0 ExE and E7.5 ExE. **(B)** A PCA plot of the data from ESC and TSC samples isolated from 'ETS-embryos' together with existing data from EPI and ExE compartments of post-implantation mouse embryos at the stages indicated. ES1, ES2, and ES3 (red circle) form one cluster with the E6.5 EPI, E7.0 regionalised EPI and E7.5 regionalised EPI. TS1, TS2, and TS3 (blue circle) form a separate cluster with the E6.5 ExE, E7.0 ExE and E7.5 ExE. Samples group along the x-axis according to tissue type. ESC samples are highlighted in red, TSC samples are highlighted in blue. **(C)** A PCA plot of the data from ESC (red) and TSC samples (blue) isolated from 'ETS-embryos' together with existing data from EPI and ExE compartments of natural mouse embryos at the post-implantation stages indicated, plus existing datasets from 6 EPISC lines derived from different stages of the mouse embryo (CAV: Pro-amniotic cavity stage, PS: Pre-streak stage, LMS: Late mid stage, LS: Late streak stage, EB: Early bud stage, LB: Late bud stage). Samples from 'ETS-embryos' cluster tightly in 2D space with samples from the embryo, whilst samples from cultured from EPISCs cluster separately.

6.5 Transcriptome analysis of axial patterning in 'ETS-embryos'

6.5.1 Differential gene expression in T:GFP positive and T:GFP negative cells isolated from 'ETS-embryos'

In addition to tissue characterisation, RNA-seq was also used to investigate body-axis-like patterning events observed in the ESC compartment in 'ETS-embryos'.

First, the mesodermal identity of the T:GFP positive samples was confirmed by analysis of the expression of mesodermal genes between GFP positive and GFP-negative samples. Canonical mesodermal markers *Mesp1*, *T/Bra*, *Wnt3* and *Mixl1* were more highly expressed in T:GFP-positive samples than in T:GFP negative samples, as were posterior markers more recently identified in the mouse embryo, *Sall3* and *Sp5* (Peng *et al.*, 2016) (Fig. 6.7.). In contrast, T:GFP negative samples expressed increased relative levels of markers associated with the anterior epiblast of the mouse embryo (ectoderm) including *Sox2* and *Pou3f1* (Zhu *et al.*, 2014) as well as more-recently identified anterior markers *Utf1, Sall2, Cbx7,* and *Zfp462* (Peng *et al.*, 2016) (Fig. 6.8.). However, there was some variation between samples, suggesting that these 'anterior-like' fates were less robust in 'ETS-embryos' than in the post-implantation egg cylinder.

62 DEGs were identified which were consistently more highly expressed in T:GFP-negative samples (A3, A4, A5) (with a p-value < 0.05 and a fold change >2) than in T:GFP positive samples (P3, P4, P5) (Fig. 6.9. A, B). A GO analysis on this gene list identified biological processes such as protein transport and neuron development as enriched terms (Fig. 6.9. A). These results are consistent with the T:GFP-negative samples of 'ETS-embryos' having a similar identity to the anterior EPI of the mouse embryo, which is the site of neural tissue development.

In contrast, 55 DEGS (with a p-value < 0.05 and a fold change >2) were identified which were consistently more highly expressed in T:GFP positive samples than in T:GFP negative samples. A similar GO analysis was performed on this list of genes and enriched terms were identified as being associated with biological processes such as protein localisation and protein secretion (Fig. 6.9. D, E).

Taken together, these results demonstrate that T:GFP positive and T:GFP negative cells in 'ETS-embryos' represent distinctly different populations of cells with different cell fate programs. They support results presented in the previous chapter that there is a gradient of cells fates present in the ESC compartment and that mesoderm specification can be regionalised in 'ETS-embryos' in a similar manner to how cells with different fates become regionalised during patterning of the embryonic EPI during early post-implantation mouse development.

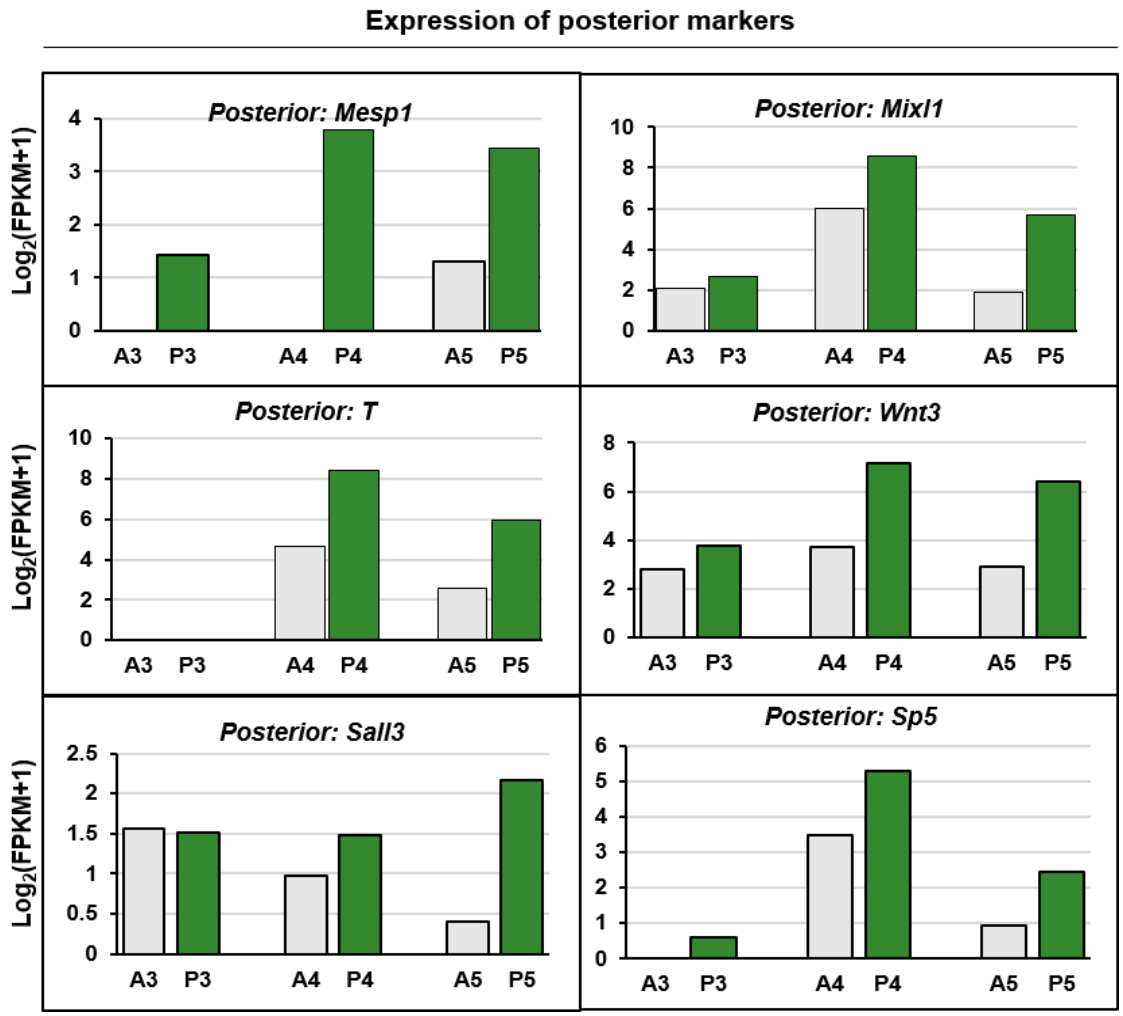

Fig. 6.7. Expression levels of known posterior/mesodermal markers of the patterned mouse epiblast T/Bra, Mesp1, Sall3, Mixl1, Sp5 and Wnt3 in paired (GFP-positive and GFP-negative) samples isolated from 'ETS-embryos'. These posterior markers are consistently more highly expressed in GFP-positive samples (P3, P4 and P5 (green bars)) than in the GFP-negative samples (A3, A4, A5 (grey bars)).

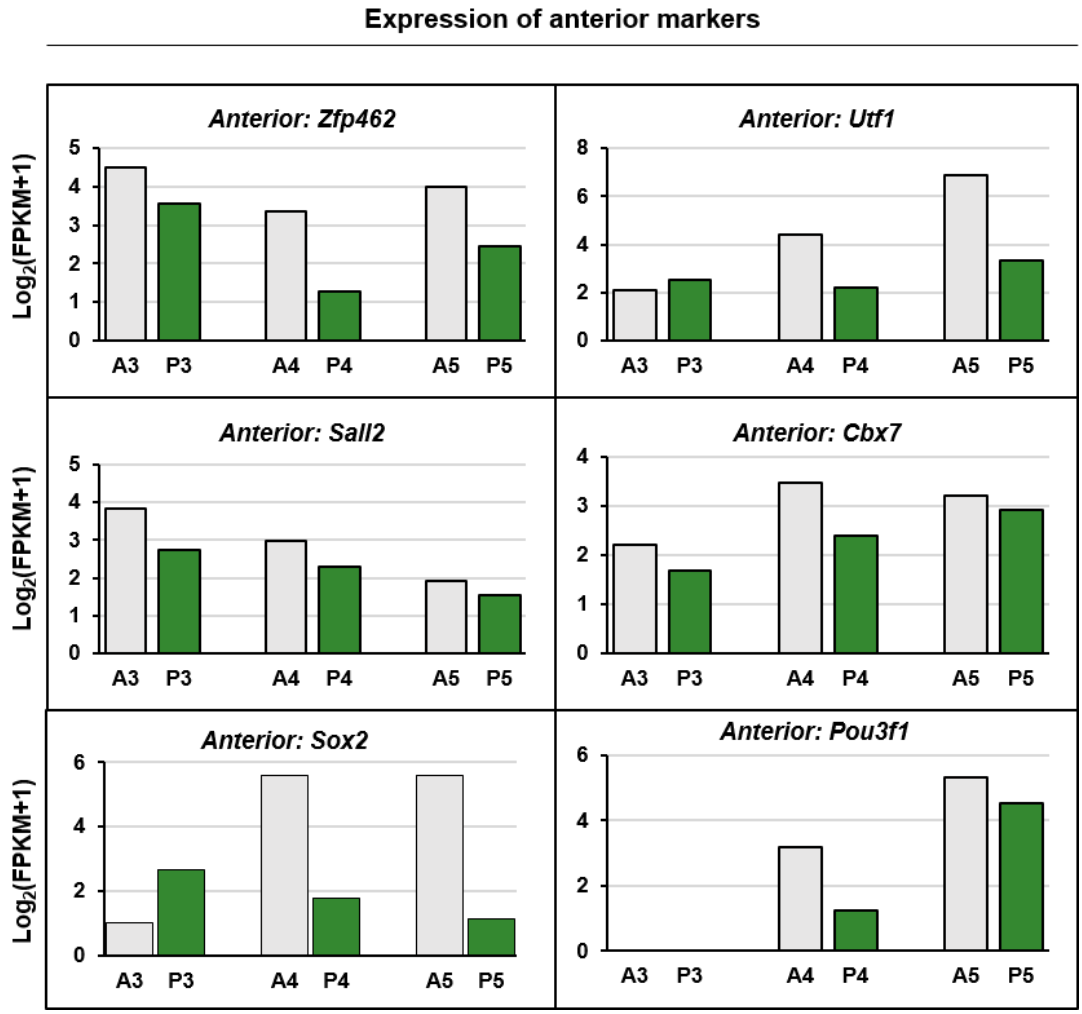

Fig. 6.8. Expression levels of known 'anterior' markers expressed opposite the proximo-posterior region of the patterned mouse epiblast Sox2, Zfp462, Sall2, Cbx7, Utf1 and Pou3f1 in paired (GFP-positive and GFP-negative) samples isolated from 'ETS-embryos'. These anterior markers are consistently more highly expressed in GFP-negative samples (A3, A4, A5 (grey bars)) than in the GFP-positive samples (P3, P4 and P5 (green bars)).

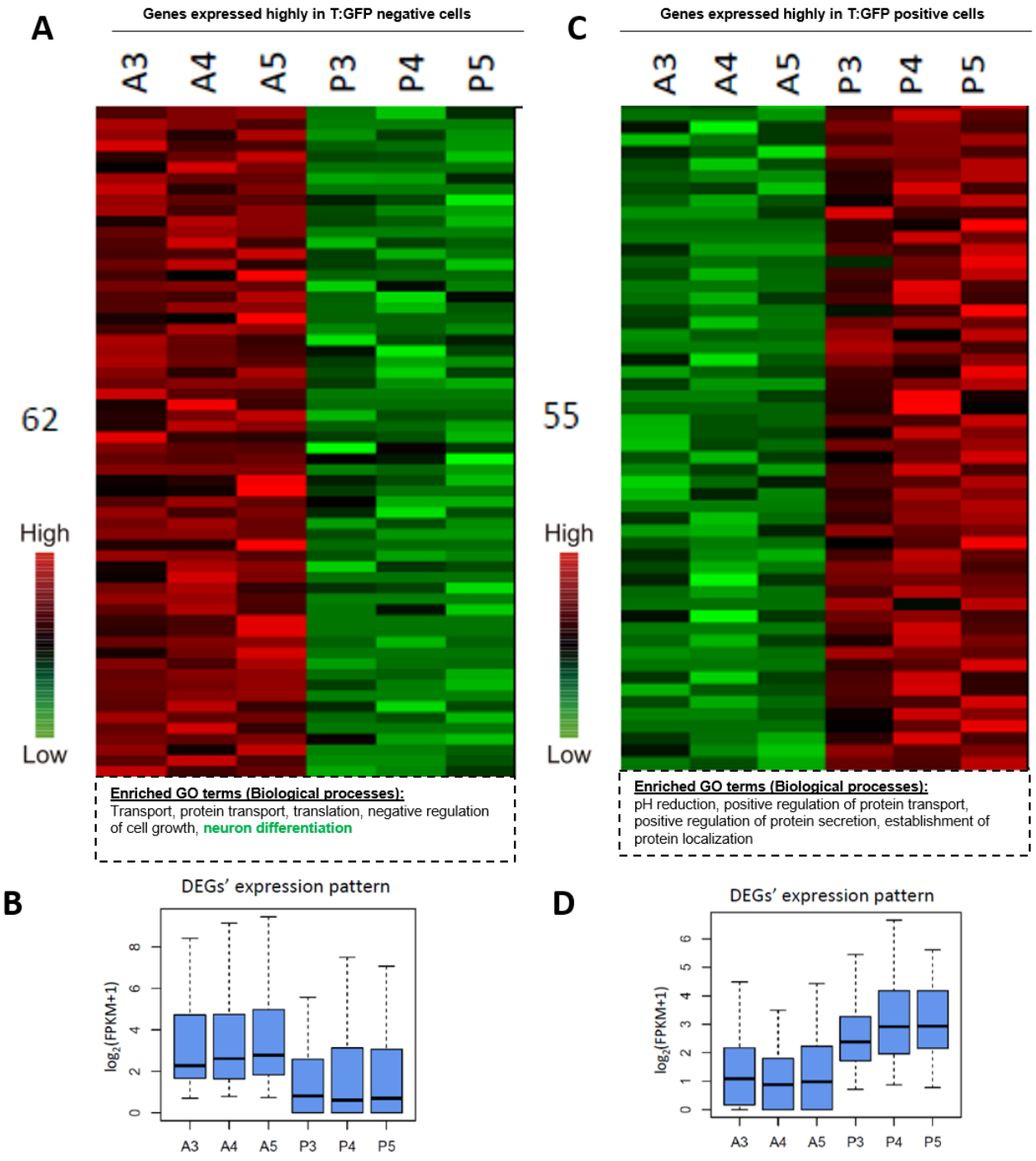

Fig. 6.9. **(A)** A heat map showing the 62 genes which are more highly expressed in GFP-negative samples (A3, A4, A5) compared to GFP-positive samples (P3, P4, P5). Red indicates high expression, green indicates low expression. Lower text-box shows the enriched GO analysis terms obtained when this gene list was analysed using DAVID software (see Materials & Methods). Terms which are particularly relevant to anterior epiblast development are highlighted in green. **(B)** Box-and-whisker plot showing the difference in expression levels of these 62 genes across GFP-negative and GFP-positive samples. Expression levels of these genes was consistently lower in GFP-positive samples as shown. **(C)** A heat map showing the 55 genes which are more highly expressed in GFP-positive samples (P3, P4, P5) compared to GFP-negative samples (A3, A4, A5). Red indicates high expression, green indicates low expression. Lower text-box shows the enriched GO analysis terms obtained when this gene list was analysed using DAVID software (see Materials & Methods). **(D)** Box-and-whisker plot showing the difference in expression levels of these 55 genes across GFP-negative and GFP-positive samples. Expression levels of these genes was consistently higher in GFP-positive samples as shown.

6.6 Comparison of T:GFP positive and T:GFP negative cells with the post-implantation EPI

6.6.1 Mapping T:GFP positive and T:GFP negative samples onto the mouse embryo using corn-plot analyses

Next, T:GFP positive and T:GFP negative cells in 'ETS-embryos' were compared to different spatial domains of the post-implantation EPI, to determine which domains of the epiblast T:GFP positive and T:GFP negative cells isolated from 'ETS-embryos' might be most similar to, in terms of gene expression. This was performed by first calculating the correlation between gene expression levels from a T:GFP positive a sample and a particular reference region of the epiblast of a reference embryo, and then these data were visualised using a 'corn plot' analysis , as developed by Naihe Jing and colleagues (Peng *et al.*, 2016)). In brief, the transcriptome data from T:GFP positive samples were compared in turn to each of several sub-domains of the EPI (identified in (Peng *et al.*, 2016)) and given a correlation score (the Pearson's correlation coefficient, PCC) to represent the similarity in gene expression between them. A score of 0 would therefore mean the transcriptome data from a region of the EPI and the 'ETS-embryo' were completely uncorrelated, whilst a score of 1 would indicate a perfect positive correlation between the two datasets. This correlation score was then mapped onto a graphical representation of the epiblast split into subdomains (with each subdomain representing one reference sample from the embryo). The subdomains were coloured according to the correlation score each had (Fig. 6.10.). This analysis was performed using datasets from EPIs of embryos at three different stages (E6.5, E7.0, and E7.5) as a reference.

Each sample (P3, P4 and P5) was compared separately, using the pipeline described in Fig. 6.10. A, revealing the variation in the data between samples. Each showed a striking positive correlation in gene expression pattern with that of the posterior subdomains of the EPI of embryos used for reference. However, this posterior pattern was least evident when samples were compared to the youngest embryos, at E6.5. P4 was the only sample to show a convincing similarity to the posterior domain at E6.5 (Fig.6.10. B, middle panel), whilst P3 and P5 were shown to be somewhat similar to both anterior and posterior regions from these embryos (Fig.6.10. B, upper and lower panels). In fact, P4 and P5 samples correlated most strongly with the posterior domain of E7.0 embryos, suggesting that these samples most closely resembled tissue from this developmental stage. This correlation held when the samples were compared to the posterior domain of E7.5 embryos, confirming that the similarity to posterior embryonic lineages was robust. In contrast, the P3 sample did not correlate highly with the posterior of the E7.0 embryo, and instead, the P3 transcriptome was most similar to the posterior domain at the later stage of E7.5, suggesting that this sample most closely resembled tissue from a later stage embryo.

The variation described here suggests that the different samples isolated from the different 'ETS-embryos' may represent slightly different stages in development. However, overall, each sample showed a striking positive correlation with the posterior EPI, and thus these data supported the conclusion that T:GFP positive cells induced by 'ETS-embryos' represent a regionalised domain of mesoderm comparable to that induced in the posterior EPI of the embryo at gastrulation.

A similar analysis was subsequently performed using the data from T:GFP negative samples isolated from 'ETS-embryos'. Although there was some correlation between the gene expression pattern of the anterior subdomains of the embryos and the T:GFP negative samples, this was less obvious than the correlation between the T:GFP positive samples and the posterior subdomains of the embryos, suggesting that this more 'anterior' cell fate specification was less robust than in the real embryo (Fig. 6.10. C). In addition, this analysis again revealed that there was variation between T:GFP negative samples.

Like the T:GFP positive samples, when compared to E6.5 embryos, there was no difference between the level of similarity in anterior and posterior subdomains. In fact, the pattern revealed from the corn-plot for the A3 sample compared to embryos at every developmental stage was very similar to the pattern produced using the P3 sample, suggesting the transcriptomes from each of these samples were very similar, and that complete symmetry breaking had not occurred for this 'ETS-embryo' (Fig. 6.10. B, C, top panels). However, the patterns generated were distinctly different between T:GFP positive and T:GFP negative samples for the other two sample-pairs. The T:GFP negative samples did not correlate with that of the posterior subdomains of the EPI at any developmental stage, supporting the conclusion that the cells, residing opposite the site of mesodermal specification, had acquired a different fate to those in the T:GFP positive, putative 'posterior' region. In fact, when compared to E7.0 embryos, A4 and A5 samples were most similar to the anterior subdomains of the EPI, indicating that these samples contained cells similar to anterior tissue in embryos at this developmental stage. Interestingly, this similarity to the anterior EPI did not hold when samples were compared to E7.5 embryos. At this later stage, samples A4 and A5 showed little correlation to the anterior-most subdomains of the EPI, and instead correlated better with more internal subdomains representing left and right regions (Fig. 6.10. C, middle and bottom panels).

Overall these results supported the conclusion that in a subset of 'ETS-embryos,' cells in the ESC compartment acquire different fates in line with A-P axis specification, but that posterior specification is more robust than anterior specification in this system.

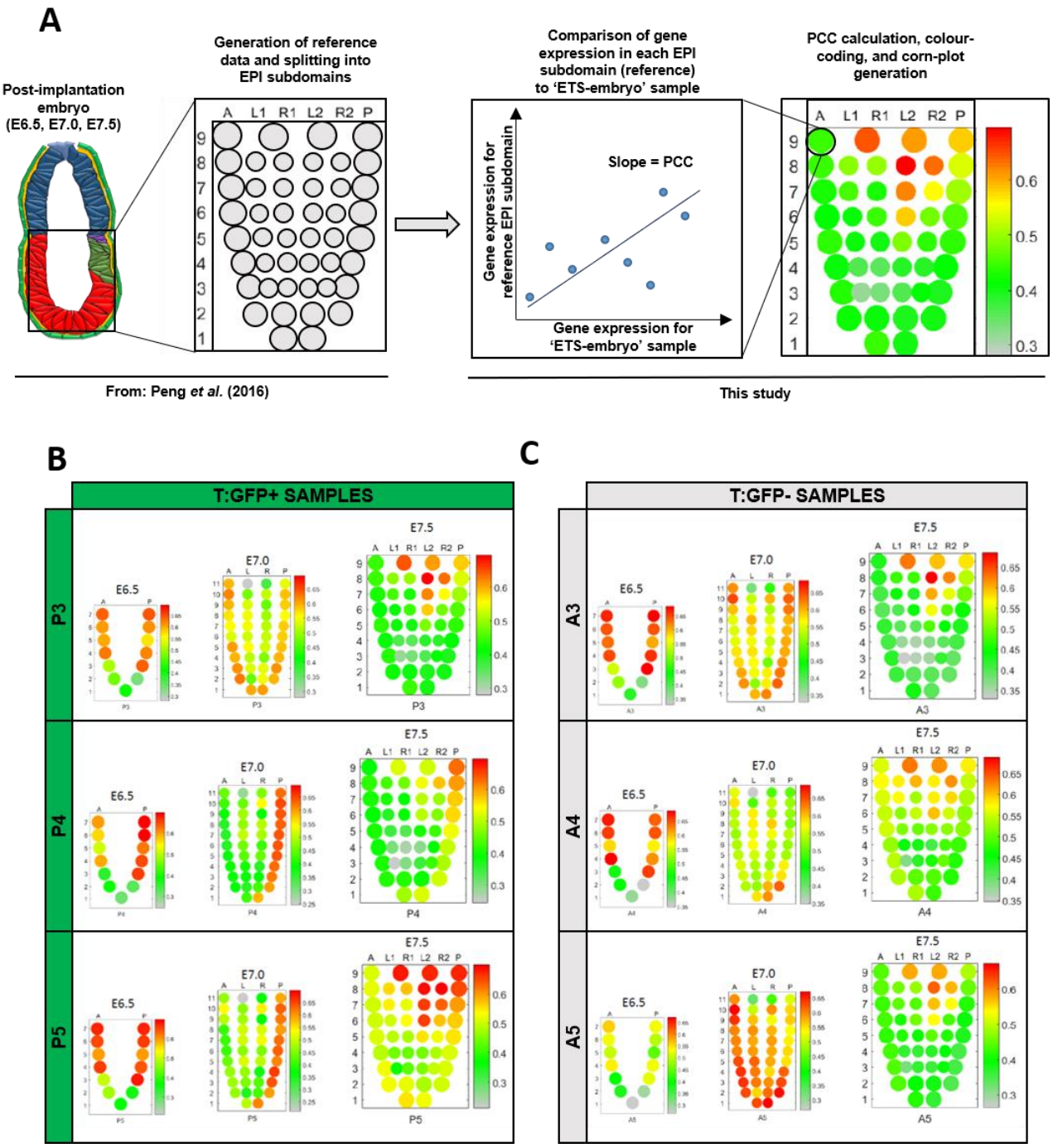

Fig. 6.10. **(A)** The analysis pipeline used to compare T:GFP positive and T:GFP negative samples from 'ETS-embryos' to subdomains of the epiblast. First, spatial transcriptome data from the EPI of three different embryos at E6.5, E7.0, and E7.5, were divided into subdomains and sequenced to generate reference gene expression data (Peng *et al*., 2016). Then, gene expression data from each reference subdomain in turn was compared to the data from an 'ETS-embryo' sample. The correlation was quantified as the 'Pearson's correlation coefficient' (PCC). A schematic of the embryonic EPI at each stage was then constructed with each circle representing a different subdomain/reference sample (13 circles make up the EPI at E6.5, 42 circles make up the EPI at E7.0, and 46 circles make up the EPI at E7.5). These were colour-coded according to the PCC value (red= high correlation, green= low correlation), to generate a corn plot. This analysis was repeated separately for all six 'ETS embryo samples' and all three reference embryos. 'A'= anterior pole, 'P' = posterior pole. '9' = proximal pole, '1' =distal pole. 'L' and 'R' indicate the left-right axis of reference EPIs. **(B)** A corn-plot analysis showing the transcriptional similarity between different regions of the mouse EPI at successive stages in egg cylinder development and each T:GFP-positive sample isolated from 'ETS-embryos' (P3, top; P4, middle; P5, bottom). **(C)** A corn-plot analysis showing the transcriptional similarity between different regions of the mouse EPI at successive stages in egg cylinder development and each T:GFP-negative sample isolated from 'ETS-embryos' (A3, top; A4, middle; A5, bottom).

6.6.2 Clustering analysis of T:GFP positive and T:GFP negative cells with post-implantation embryos

Finally, T:GFP positive and T:GFP negative samples and samples from egg cylinder stage embryos at E6.5, E7.0 and E7.5 were subject to hierarchical clustering analysis and PCA analysis. As expected, all T:GFP positive and T:GFP negative samples, apart from A5 grouped with EPI samples as opposed to those from the ExE, as they represented embryonic tissue. Within the 'embryonic' group, two subgroups could be identified which separated the tissues of E7.5 EPI in one group and E6.5 EPI plus E7.0 EPI in a second group. The T:GFP positive and T;GFP negative samples from 'ETS-embryos' were present in both subgroups, suggesting that different samples represented slightly different developmental stages (Fig. 6.11. A). A PCA analysis also reflected that the majority of samples from 'ETS-embryos' clustered with embryonic tissue across PC1, which accounted for 25.12% of variation in the data, and likely represents variation in gene expression that can be explained by tissue type (embryonic versus extra-embryonic), as ExE samples clustered separately along this axis. In the 2D space however, these samples did not cluster tightly with any particular epiblast tissue from the embryo, reflecting the variation between samples. Whilst samples A4 and P4 clustered closer to the E7.5 EPI, samples A3, P3, and P5 clustered closer to earlier embryonic tissue, supporting the idea that each sample pair might represent developmental stages (Fig. 6.11. B).

Overall, these results support the conclusion that 'ETS-embryos' which induce regionalised mesoderm have subdomains of cells with different fates across the ESC compartment, and the strong posterior signature of T:GFP positive samples suggests that these cells are equivalent to the primitive streak cells in the EPI at early stages of gastrulation. The variation between samples, especially in those that are T:GFP negative, suggests that they resemble different EPI stages most closely, and also indicates that patterning in 'ETS-embryos,' although undeniably present, may be less robust than in the real embryo, as the AVE organising centre is lacking.

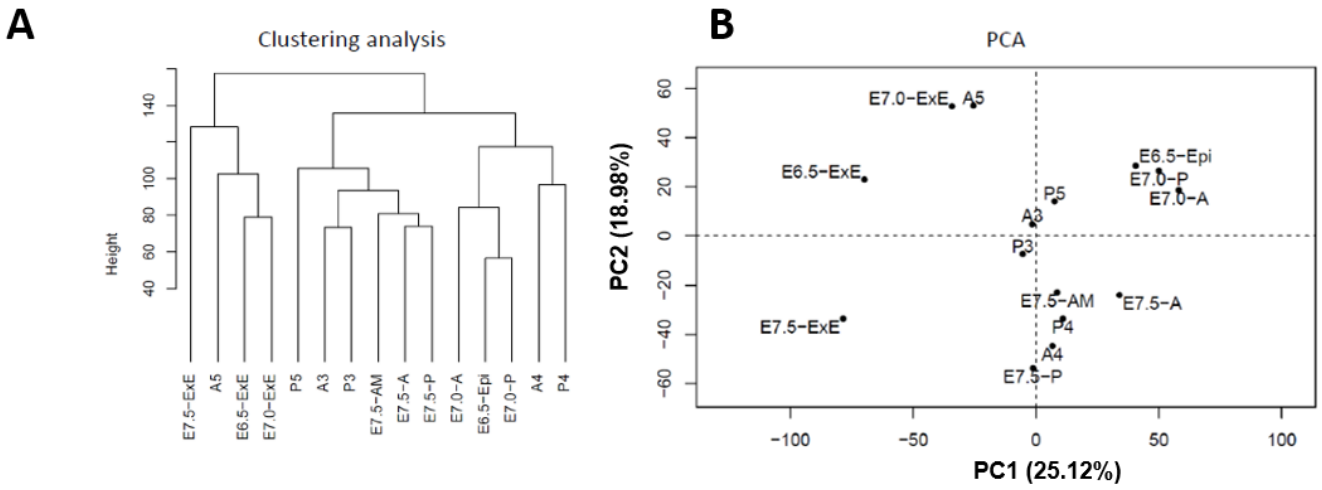

Fig. 6.11. **(A)** GFP-positive and GFP-negative samples isolated from 'ETS-embryos' together with existing data from regionalised EPI and ExE compartments of natural mouse embryos at the post-implantation stages indicated. **(B)** A PCA plot of the data from GFP-positive and GFP-negative samples isolated from 'ETS-embryos' together with existing data from regionalised EPI and ExE compartments of natural mouse embryos at the post-implantation stages indicated. PC1 (x-axis) explains 25.12% of the variation in the data whilst PC2 (y-axis) explains 18.98% of the variation in the data.

6.7 Discussion

In previous chapters, the similarity of 'ETS-embryos' to the post-implantation mouse embryo has been inferred at the protein level using a small number of markers which demonstrate broadly comparable patterns of expression to what has been observed *in vivo*. In this chapter, the comparison is taken further by assessing the similarity of 'ETS-embryos' to the real mouse embryo at the level of thousands of genes simultaneously, by employing RNA sequencing techniques.

Whole ESC and TSC compartments were first compared to the transcriptomes of the post-implantation egg cylinder at various developmental timepoints, to establish which stage in embryogenesis 'ETS-embryos' most closely resemble. It was found that ESC and TSC compartments clearly faithfully model EPI and ExE of the post-implantation embryo, and most closely resemble egg cylinder stages E6.5-E7.5 *in vivo*. Surprisingly, this analysis shows that 'ETS-embryos' are closer to the embryo in terms of overall gene expression than EPISCs, said to represent the 'primed state' of the post-implantation mouse epiblast (Nichols and Smith, 2009). This is particularly important, given that the embryonic compartment of 'ETS-embryos' is initially made up of once-naïve ESCs derived from the pre-implantation ICM, which exit naïve pluripotency and differentiate whilst in the culture system. The fact that these cells end up more like the post-implantation EPI than cells which were actually derived from egg cylinder stage embryos, highlights how culture conditions can impact on the transcriptome, and indicates that 2D culture and propagation of cell lines *in vitro* can lead to a drift in gene expression patterns away from the tissue from which they were originally taken. The culture conditions can therefore very powerfully impact on the transcriptional output of the cells and the state which they are in. Simple addition of a third dimension, ECM containing laminin and collagen (EPISCs in culture are normally grown on fibronectin) and the presence of the TSCs has changed the transcriptome such that it more closely resembles that of the EPI *in vivo*. It has been shown in a variety of contexts that ECM substrate composition can alter the morphological characteristics of a cell (Takito and Al-Awqati, 2004) as can the mechanical properties of a substrate, so it follows that gene expression is also altered by changes in these conditions (Benham-pyle, Pruitt and Nelson, 2015).

According to this analysis, and the analysis of Kojima *et al*, EPISCs most closely represent a subset of the EPI cells *in vivo*, namely those found in the anterior primitive streak, regardless of the stage of embryo from which they have been derived (Kojima *et al.*, 2014). EPISCs are conventionally cultured with recombinant Activin A and FGF2 present in the medium at doses far in excess of the physiological concentration cells are exposed to *in vivo* (Brons *et al.*, 2007). Given that both FGF and Nodal/Activin are signals which pattern the EPI in a dose-dependent manner and are known to be active in the primitive streak (Brennan *et al.*, 2001; Ciruna and Rossant, 2001; Tam and Loebel, 2007), it is not

surprising that these factors may bias cell fate specification towards a particular subset of EPI cells associated with gastrulation. Given that 'ETS-embryos' are not dosed with exogeneous Activin and FGF2 (although FGF4 is provided in the medium) their ESC compartments perhaps represent a more 'unbiased' population of cells, representing the cross-section of cell fates and tissue precursors known to be present in the post-implantation EPI (Arnold and Robertson, 2009).

These results provide further support for the idea that 'ETS-embryos' can be used as a faithful model of the mouse embryo, and although the focus here was on more detailed characterisation of 'ETS-embryos', the dataset generated in this work has much potential for future studies.

For example, the ESC and TSC datasets generated here could inform about how interactions between embryonic and extra-embryonic tissues can affect gene expression. This analysis showed that the ESC compartments collected from 'ETS-embryos' were clearly different to EPISCs. Whist the culture conditions and genetic background of the different cell lines will undoubtedly introduce some transcriptional variation, the fact that 'ETS-embryos' clustered so closely with post-implantation mouse egg cylinders may indicate that another effect is acting. It might be that the presence of the TSCs and signalling interactions between tissues can remodel the transcriptome to give it a unique signature that is closer to that of the real embryo than can ever be achieved in monoculture, as this analysis suggests.

Further work might use datasets generated here to identify differences between 'ETS-embryos' and the real mouse embryo. One important difference between this *in vitro* model and the real embryo is that 'ETS-embryos' do not possess a VE-like compartment (the consequences of which have been discussed throughout this thesis). The transcriptome dataset generated here may provide a unique opportunity to understand how the VE contributes to embryogenesis, by comparing structures with a similar transcriptome but no VE (i.e 'ETS-embryos') to real embryos which possess this tissue. Specifically, it would be interesting determine how the VE can affect gene expression in embryonic tissues and in the ExE, as several studies have shown that reciprocal signalling interactions between the VE and the other two tissue compartments are important for subsequent development (Rodriguez *et al.*, 2005; Richardson, Torres-Padilla and Zernicka-Goetz, 2006; Kumar *et al.*, 2015) even before the AVE has been specified.

The sequencing and analysis presented here also provides greater insight as to the identity of cells across the ESC compartment in 'ETS embryos' and the extent to which EPI patterning is recapitulated in 'ETS-embryos' which specified regionalised mesoderm. These results are broadly in support of those

presented in Chapter 5, suggesting that patterning between 'ETS-embryos' and the egg cylinder is comparable, but that specification of a true anterior requires a signalling centre such as the AVE.

The posterior signature from T:GFP positive cells, located on one side of the ESC compartment in these 'ETS-embryos' cells is very robust, and is in agreement with published data from *in vivo* studies that signalling from the ExE (or in the case of 'ETS-embryos', the TSC compartment) induces the posterior (Winnier *et al.*, 1995; Lawson and Schoenwolf, 2003; Richardson, Torres-Padilla and Zernicka-Goetz, 2006).

In contrast, the transcriptional signature from the T:GFP negative cells, although clearly and consistently different to that of the T:GFP positive cells, was more difficult to define, and varied between samples. Although these samples did express some markers associated with the anterior epiblast (Peng *et al.*, 2016; Scialdone *et al.*, 2016) comparing these samples to the anterior domains of the embryo did not reveal a particularly strong correlation, especially at later stages of development. These data therefore suggest that T:GFP negative cells opposite the regionalised mesoderm of 'ETS-embryos' are certainly not posterior in identity, but nor are they robustly anteriorised. This makes sense in light of the absence of the anterior organiser, the AVE. The transcriptional similarity between T:GFP negative samples from 'ETS-embryos' and anterior regions of the EPI is evident at E7.0 but tails off by E7.5. At E7.5 the neural plate is formed and the head-fold appears, so by this time in development, anterior structures are becoming more advanced. Without the AVE, true head region cannot form (Stower and Srinivas, 2014). These results are in broad agreement with studies on AVE mutants (such as the DKK1 mutant discussed in the previous chapter) (Mukhopadhyay *et al.*, 2001; Perea-Gomez *et al.*, 2002), and provide strong support for the idea that at early stages, anterior and posterior fate acquisition can be decoupled.

However, the question still remains: what breaks the symmetry then, if the AVE is not present? The results presented here confirm that The TSC compartment expresses BMP4 ligand in 'ETS-embryos', and thus is the likely source of the 'posteriorizing' signal that leads to mesoderm specification, as occurs in mouse embryos. It is possible that, due to heterogeneity in the ESCs used for 'ETS-embryo' culture, that some cells are more competent to respond to the BMP4 signal and therefore induce Wnt activity and mesoderm first. Then, this heterogeneity could become amplified over time, similar to the mechanism that is proposed to operate in embryoid bodies (Turner, Baillie-Johnson and Martinez Arias, 2016). Alternatively, a recent study of pattern formation in hESCs exposed to a directional BMP signal has shown that cells can acquire different fates due to differential orientation of their receptors in different locations within the tissue (Etoc *et al.*, 2016). Given that ESCs appear to reorient during cavity fusion in 'ETS-embryos' (as presented in Chapter 4) it may be that receptors for TGF-β ligands

on the surface of cells also become re-positioned as cavities merge. If cells and receptors in the ESC compartment were to re-orient asymmetrically, then some cells may sense the BMP4 signal before others are able to, and this would break the symmetry in the ESC compartment. Whether it be due to heterogeneity or asymmetry in receptor localisation, cells less competent to respond to the signal from the TSC compartment may simply acquire a 'default' fate, in the absence of the BMP4 signal, and maintain high levels of Oct4 expression, but are unable to acquire a fully-committed neural fate because they lack anteriorising signals from the AVE. Without further study, these ideas are speculative, but 'ETS-embryos' present a unique opportunity to investigate reproducible pattern formation in the absence of a directional source of inhibitors, within a structure that recapitulates the egg cylinder.

In summary, the RNA sequencing used in this chapter has shown that 'ETS-embryos' closely resemble the early post-implantation mouse embryo at a global transcriptional level. In line with results presented in earlier chapters, the ESC and TSC compartments represent the EPI and ExE tissues of the mouse embryo respectively, and the specification of a 'posteriorised' population of cells in the ESC compartment can occur in the absence of an AVE organiser. Taken together, this strongly supports the use of 'ETS-embryos' as a tool to investigate processes underpinning early mammalian embryogenesis, and the datasets generated here can be used in future studies to further define the instructive role of each tissue in patterning the embryo during development.

7. Concluding remarks

The study of mouse embryos through the early stages of development has elucidated much about how the embryonic lineage segregates from the extra-embryonic lineages of the conceptus, and how signals emanating from each of these tissues guides the morphogenesis of the embryo and the establishment of the body plan. However, several aspects surrounding the mechanisms underpinning these events during embryogenesis remain mysterious, and are often inaccessible in a system which comprises so many inter-dependent parts.

In recent years, there has been great interest utilising pluripotent stem cells to model tissue specification and organogenesis events which occur during mammalian development. These models can complement studies in the embryo, and these organoids, which recapitulate both the structure and function of the system they model, provide researchers with access to processes that are difficult to study *in vivo*. The system developed in the present investigation represents a new tool for the study of mammalian embryogenesis and demonstrates the intrinsic ability of the constituent cells of the early embryo to self-assemble into an organised structure (Fig. 7.0). Whilst the 'ETS-embryo' model of mouse embryogenesis undoubtedly carries some limitations, it may also provide a unique insight into how cells interact within the early embryo and how patterns can form in this system.

In Results I, a co-culture system was developed to support the simultaneous growth of embryonic and extra-embryonic stem cells derived from the mouse embryo, embedded in three-dimensional ECM. This system permits the interaction between the two cell types, and leads to the self-assembly of embryo-like structures, termed 'ETS-embryos' within four days of culture. Even though the system is heterogeneous, with only ~22% of all the structures present in the Matrigel being 'ETS-embryos', a great number of structures can be generated in a single experiment. Because of the unlimited supply of ESCs and TSCs that can be generated in culture and placed in the system, it is very easy to produce many structures at once, simply by seeding a lot of ESCs and TSCs in Matrigel. This allows the generation of many biological replicates without sacrificing mice. For example, one litter from a naturally mated mouse may provide 12 natural embryos, whilst a single experiment using ESCs and TSCs could easily generate 50-100 'ETS-embryos' if not more, depending on how many plates are seeded with cells.

Importantly, 'ETS-embryos' are the first model of mammalian embryogenesis that recapitulates the embryonic-extra-embryonic boundary between EPI and ExE, and therefore might be a good system to study how embryonic and extra-embryonic tissues coordinate their development. Although 'ETS-embryos' lack a VE-like layer, which is thought to be critical for mouse embryogenesis, this may in fact

be advantageous if using the 'ETS-embryo' to model the specific interactions between one extra-embryonic lineage (the ExE/ TSCs) and the epiblast (ESCs). How one tissue affects the development of the other may be easier to elucidate in this *in vitro* system than it would be in the real embryo, because the VE is not present, which could otherwise confound results by producing its own signals which affect embryogenesis.

In Results II, cavity morphogenesis in 'ETS-embryos' was characterised, and was found to recapitulate the sequence of events known to occur during pro-amniotic cavity formation in the mouse. Since relatively little is known about the formation or function of this cavity in the embryo, 'ETS-embryos' present an opportunity to investigate how the pro-amniotic cavity forms, and potentially what its function might be.

In this study, a novel function for the Nodal/Activin signalling pathway has been proposed in initiating cavitation in the extra-embryonic compartment, and the full extent of the phenotype uncovered here should now be explored in both the *in vitro* and *in vivo* systems. Given that ESCs and TSCs are amenable to genetic manipulation, using ESCs or TSCS to generate 'ETS-embryos' which are knockout for a particular gene-of-interest is an efficient way to reveal novel functions of genes in early embryogenesis, and to perform molecular studies, without generating knockout animals. This approach may help to screen for 'hidden' developmental phenotypes, which may be overlooked when using the mouse model, where maternally produced protein can compensate when the zygotic genome is compromised, as appears to be the case for Nodal/Activin.

In Results III, 'ETS-embryos' were shown to be capable of mesoderm and PGC specification in a polarised manner, which is dependent on signals originating from the extra-embryonic compartment, as in the mouse embryo. *In vivo*, proximity to the EPI-ExE interface is important to for the specification of EPI cells in the posterior of the embryo, both in the context of PGCs, and when cells ingress through different regions of the primitive streak. For example, it has been shown that cells transplanted from elsewhere in the EPI become competent to form PGCs if they are moved to the proximo-posterior region (Tam and Zhou, 1996). Cells 1-2 cell diameters away from the boundary are the ones which form PGCs, so cell position in relation to this interface is undoubtedly important for their specification. In 'ETS-embryos' the embryonic-extra-embryonic boundary may prove to be just as critical to posterior cell fate specification as it is in natural embryogenesis, especially given that the formation of these cell types is much less efficient when the extra-embryonic tissue is not present in culture.

The question of when and how the A-P axis first arises in the mouse embryo has been long debated, and this study cannot provide any clear answer. However, the system developed here does offer a

unique opportunity to address this question in an *in vitro* system which lacks an anterior organising centre, the AVE. Whilst embryoid bodies, comprising of ESCs only, have been shown to form germ layers *in vitro*, the 'ETS-embryo' represents the first model of embryogenesis which includes the extra-embryonic tissue important for specification of the posterior domain *in vivo*.

Additionally, because 'ETS-embryos' are formed from clonal cell lines, all 'ETS-embryos' generated in the same experiment are genetically identical. Therefore, the cellular and tissue-level mechanisms which govern axial patterning in this system can be elucidated, knowing that there is no underlying genetic difference between 'ETS-embryos' generated in a single experiment which break symmetry and those that do not. This of course, is not possible with mouse embryos, which possess genetic differences between littermates.

The use of state-of-the art mRNA sequencing techniques in Results IV allowed the comparison of 'ETS-embryos' to the real post-implantation mouse embryo at a global molecular level, and showed that indeed, the two are very similar. It also provided greater insight into how axial patterning can occur in the absence of the AVE. Analysis of the different cell types within the patterned ESC compartment suggested that whilst posterior specification in 'ETS-embryos' was similar to the mouse embryo, specification of anterior cell types was less robust in this system. The dataset generated in this study could complement the ever-increasing number of transcriptional datasets which describe mouse embryogenesis and be used in future investigations to determine the precise effect the VE-tissue has on the transcriptional output of the other two tissue compartments in the mouse egg cylinder.

Finally, it is important to note that 'ETS-embryos' are essentially a model system that recapitulates the mouse embryo, which, in itself, is a model for human development. The results in this study, combined with recent progress in generating human embryonic stem cells in different states of pluripotency (Morgani, Nichols and Hadjantonakis, 2017), begs the question whether a similar technique could be used to model human embryogenesis *in vitro*. A recent study which uses human pluripotent cells to model human post-implantation amniotic sac development suggests that this may indeed be possible, but the extent to which such structures resemble the human embryo in terms of transcription and signalling events has yet to be investigated (Shao *et al.*, 2017).

Returning to the model system of the mouse presented here, whilst there is much scope to improve this co-culture system, it is undoubtedly an informative tool to study mammalian embryogenesis. Like embryoid body models, it has great potential to elucidate how cells generate reproducible patterns, and uniquely, it can also provide insight into how tissues coordinate their growth and signalling functions, in order to generate a foetus capable of development to term.

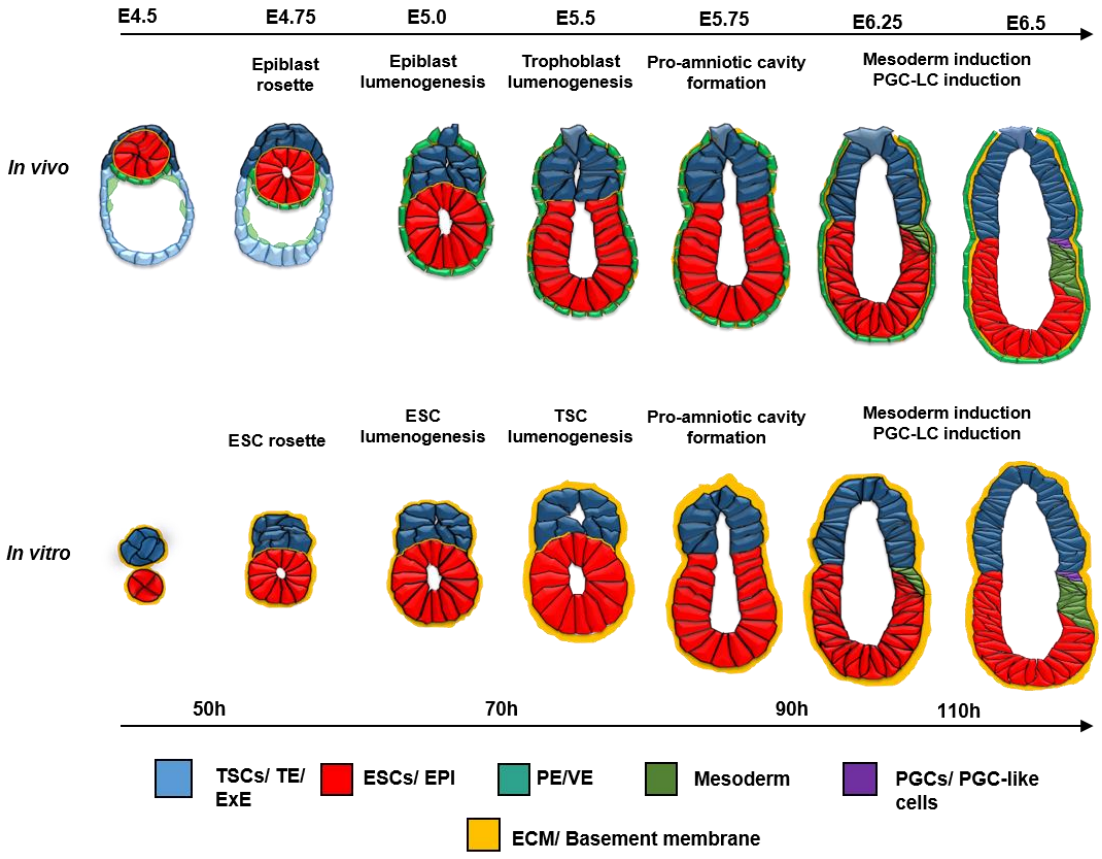

Fig. 7.0.. ETS-embryos are a simplified model of embryo development from the blastocyst stage to mesoderm specification in the egg cylinder. Comparison of development of natural and "ETS-embryos" mouse embryos. Red cells, ESC/epiblast; dark blue cells, TSC/trophectoderm/ extra-embryonic ectoderm cells; light green cells, mesoderm cells; Purple cells, Primordial Germ Cells; yellow line, basement membrane/ECM. In the embryo, dark green cells are primitive endoderm/visceral endoderm cells. The ETS-embryo is surrounded by ECM in similar manner to basement membrane of visceral endoderm in natural embryo. Mesoderm-expression domain is similarly positioned and occupies similar area of the embryonic compartment in both ETS-embryos and natural embryos.

References

Aiken, C. E. M., Swoboda, P. P. L., Skepper, J. N. and Johnson, M. H. (2004) 'The direct measurement of embryogenic volume and nucleo-cytoplasmic ratio during mouse pre-implantation development.', *Reproduction (Cambridge, England)*. England, 128(5), pp. 527–535. doi: 10.1530/rep.1.00281.

Amack, J. D. and Manning, M. L. (2012) 'Knowing the boundaries: extending the differential adhesion hypothesis in embryonic cell sorting.', *Science (New York, N.Y.)*, 338(6104), pp. 212–5. doi: 10.1126/science.1223953.

Anani, S., Bhat, S., Honma-Yamanaka, N., Krawchuk, D. and Yamanaka, Y. (2014) 'Initiation of Hippo signaling is linked to polarity rather than to cell position in the pre-implantation mouse embryo', *Development*, 141(14), p. 2813 LP-2824. Available at: http://dev.biologists.org/content/141/14/2813.abstract.

Anders, S., Pyl, P. T. and Huber, W. (2015) 'HTSeq—a Python framework to work with high-throughput sequencing data', *Bioinformatics*. Oxford University Press, 31(2), pp. 166–169. doi: 10.1093/bioinformatics/btu638.

Andrew, D. J. and Ewald, A. J. (2011) 'Morphogenesis of epithelial tubes: Insights into tube formation, elongation and elaboration', *Cell*, 341(1), pp. 34–55. doi: 10.1016/j.ydbio.2009.09.024.Morphogenesis.

Andrews, S. (2010) 'FastQC: A Quality Control tool for High Throughput Sequence Data'. Available at: https://www.bioinformatics.babraham.ac.uk/projects/fastqc/.

Aramaki, S., Hayashi, K., Kurimoto, K., Ohta, H., Yabuta, Y., Iwanari, H., Mochizuki, Y., Hamakubo, T., Kato, Y., Shirahige, K. and Saitou, M. (2013) 'A mesodermal factor, T, specifies mouse germ cell fate by directly activating germline determinants', *Developmental Cell*. Elsevier Inc., 27(5), pp. 516–529. doi: 10.1016/j.devcel.2013.11.001.

Arman, E., Haffner-Krausz, R., Chen, Y., Heath, J. K. and Lonai, P. (1998) 'Targeted disruption of fibroblast growth factor (FGF) receptor 2 suggests a role for FGF signaling in pregastrulation mammalian development.', *Proceedings of the National Academy of Sciences of the United States of America*, pp. 5082–7. doi: 10.1073/pnas.95.9.5082.

Arnold, S. J. and Robertson, E. J. (2009) 'Making a commitment: cell lineage allocation and axis patterning in the early mouse embryo.', *Nature reviews. Molecular cell biology*, 10(2), pp. 91–103. doi: 10.1038/nrm2618.

Artus, J., Douvaras, P., Piliszek, A., Isern, J., Baron, M. H. and Hadjantonakis, A. K. (2012) 'BMP4 signaling directs primitive endoderm-derived XEN cells to an extraembryonic visceral endoderm identity', *Developmental Biology*. Elsevier Inc., 361(2), pp. 245–262. doi: 10.1016/j.ydbio.2011.10.015.

Avilion, A. A., Nicolis, S. K., Pevny, L. H., Perez, L., Vivian, N. and Lovell-Badge, R. (2003) 'Multipotent cell lineages in early mouse development depend on SOX2 function.', *Genes & development*. United States, 17(1), pp. 126–140. doi: 10.1101/gad.224503.

Bachvarova, R. (1985) 'Gene expression during oogenesis and oocyte development in mammals.', *Developmental biology (New York, N.Y. : 1985)*. United States, 1, pp. 453–524.

Bany, B. M. and Cross, J. C. (2006) 'Post-implantation mouse conceptuses produce paracrine signals that regulate the uterine endometrium undergoing decidualization', *Developmental Biology*, 294(2), pp. 445–456. doi: http://dx.doi.org/10.1016/j.ydbio.2006.03.006.

Barcroft, L. C., Offenberg, H., Thomsen, P. and Watson, A. J. (2003) 'Aquaporin proteins in murine trophectoderm mediate transepithelial water movements during cavitation.', *Developmental biology*. United States, 256(2), pp. 342–354.

Barkauskas, C. E., Cronce, M. J., Rackley, C. R., Bowie, E. J., Keene, D. R., Stripp, B. R., Randell, S. H., Noble, P. W. and Hogan, B. L. M. (2013) 'Type 2 alveolar cells are stem cells in adult lung', *The Journal of Clinical Investigation*. American Society for Clinical Investigation, 123(7), pp. 3025–3036. doi: 10.1172/JCI68782.

Basak, S., Dhar, R. and Das, C. (2002) 'Steroids modulate the expression of alpha4 integrin in mouse blastocysts and uterus during implantation.', *Biology of reproduction*. United States, 66(6), pp. 1784–1789.

Beck, S., Le Good, J. A., Guzman, M., Ben Haim, N., Roy, K., Beermann, F. and Constam, D. B. (2002) 'Extraembryonic proteases regulate Nodal signalling during gastrulation.', *Nature cell biology*. England, 4(12), pp. 981–985. doi: 10.1038/ncb890.

Bedzhov, I., Graham, S. J. L., Leung, C. Y. and Zernicka-goetz, M. (2014) 'Developmental plasticity , cell fate specification and morphogenesis in the early mouse embryo', *Philosophical Transactions of the Royal Society B: Biological Sciences*, 639(1657).

Bedzhov, I., Leung, C. Y., Bialecka, M. and Zernicka-Goetz, M. (2014) 'In vitro culture of mouse blastocysts beyond the implantation stages', *Nature Protocols*. Nature Publishing Group, 9(12), pp. 2732–2739. doi: 10.1038/nprot.2014.186.

Bedzhov, I. and Zernicka-Goetz, M. (2014) 'Self-Organizing Properties of Mouse Pluripotent Cells Initiate Morphogenesis upon Implantation.', *Cell*. Elsevier Inc., 156(5), pp. 1032–44. doi: 10.1016/j.cell.2014.01.023.

Bellairs, R. (1986) 'The Primitive Streak', *Anatomy and embryology*, 174(1), pp. 1–14. Available at: http://link.springer.com/article/10.1007/BF00318331 (Accessed: 29 March 2014).

Belo, J. A., Bouwmeester, T., Leyns, L., Kertesz, N., Gallo, M., Follettie, M. and De Robertis, E. M. (1997) 'Cerberus-like is a secreted factor with neutralizing activity expressed in the anterior primitive endoderm of the mouse gastrula.', *Mechanisms of development*, 68(1–2), pp. 45–57.

Ben-Haim, N., Lu, C., Guzman-Ayala, M., Pescatore, L., Mesnard, D., Bischofberger, M., Naef, F., Robertson, E. J. and Constam, D. B. (2006) 'The nodal precursor acting via activin receptors induces mesoderm by maintaining a source of its convertases and BMP4.', *Developmental cell*, 11(3), pp. 313–23. doi: 10.1016/j.devcel.2006.07.005.

Benham-pyle, B. W., Pruitt, B. L. and Nelson, W. J. (2015) 'Mechanical strain induces E-cadherin – dependent Yap1 and β -catenin activation to drive cell cycle entry', *Science*, 348(6238), pp. 1024–1028.

ten Berge, D., Koole, W., Fuerer, C., Fish, M., Eroglu, E. and Nusse, R. (2008) 'Wnt signaling mediates self-organization and axis formation in embryoid bodies.', *Cell stem cell*, 3(5), pp. 508–18. doi: 10.1016/j.stem.2008.09.013.

ten Berge, D., Kurek, D., Blauwkamp, T., Koole, W., Maas, A., Eroglu, E., Siu, R. K. and Nusse, R. (2011) 'Embryonic stem cells require Wnt proteins to prevent differentiation to epiblast stem cells', *Nat Cell Biol*. Nature Publishing Group, a division of Macmillan Publishers Limited. All Rights Reserved., 13(9), pp. 1070–1075. Available at: http://dx.doi.org/10.1038/ncb2314.

Bertocchini, F. and Stern, C. (2002) 'The hypoblast of the chick embryo positions the primitive streak by antagonizing nodal signaling', *Developmental cell*, 3(5), pp. 735–744. Available at:

http://www.sciencedirect.com/science/article/pii/S1534580702003180 (Accessed: 31 March 2014).

Birey, F. *et al.* (2017) 'Assembly of functionally integrated human forebrain spheroids', *Nature*. Macmillan Publishers Limited, part of Springer Nature. All rights reserved., 545(7652), pp. 54–59. doi: 10.1038/nature22330.

Bischoff, M., Parfitt, D.-E. and Zernicka-Goetz, M. (2008) 'Formation of the embryonic-abembryonic axis of the mouse blastocyst: relationships between orientation of early cleavage divisions and pattern of symmetric/asymmetric divisions.', *Development (Cambridge, England)*, 135(5), pp. 953–62. doi: 10.1242/dev.014316.

Blancas, A. A., Chen, C.-S., Stolberg, S. and McCloskey, K. E. (2011) 'Adhesive forces in embryonic stem cell cultures', *Cell adhesion & migration*, 5(6), pp. 472–479. doi: 10.4161/cam.5.6.18270.

Boroviak, T., Loos, R., Bertone, P., Smith, A. and Nichols, J. (2014) 'The ability of inner-cell-mass cells to self-renew as embryonic stem cells is acquired following epiblast specification.', *Nature cell biology*, 16(6), pp. 516–28. doi: 10.1038/ncb2965.

Brennan, J., Lu, C. C., Norris, D. P., Rodriguez, T. a, Beddington, R. S. and Robertson, E. J. (2001) 'Nodal signalling in the epiblast patterns the early mouse embryo.', *Nature*, 411(6840), pp. 965–9. doi: 10.1038/35082103.

van den Brink, S. C., Baillie-Johnson, P., Balayo, T., Hadjantonakis, A., Nowotschin, S., Turner, D. A. and Martinez Arias, A. (2014) 'Symmetry breaking, germ layer specification and axial organisation in aggregates of mouse embryonic stem cells.', *Development (Cambridge, England)*, 141(22), pp. 4231–42. doi: 10.1242/dev.113001.

Brons, I. G. M., Smithers, L. E., Trotter, M. W. B., Rugg-Gunn, P., Sun, B., Chuva de Sousa Lopes, S. M., Howlett, S. K., Clarkson, A., Ahrlund-Richter, L., Pedersen, R. a and Vallier, L. (2007) 'Derivation of pluripotent epiblast stem cells from mammalian embryos.', *Nature*, 448(7150), pp. 191–5. doi: 10.1038/nature05950.

Brown, K., Doss, M. X., Legros, S., Artus, J., Hadjantonakis, A. K. and Foley, A. C. (2010) 'Extraembryonic endoderm (XEN) stem cells producefactors that activate heart formation', *PLoS ONE*, 5(10). doi: 10.1371/journal.pone.0013446.

Calarco, P. G. and Brown, E. H. (1969) 'An ultrastructural and cytological study of preimplantation development of the mouse.', *The Journal of experimental zoology*. United States, 171(3), pp. 253–283. doi: 10.1002/jez.1401710303.

Cambuli, F., Murray, A., Dean, W., Dudzinska, D., Krueger, F., Andrews, S., Senner, C. E., Cook, S. J. and Hemberger, M. (2014) 'Epigenetic memory of the first cell fate decision prevents complete ES cell reprogramming into trophoblast.', *Nature communications*. Nature Publishing Group, 5(5538). doi: 10.1038/ncomms6538.

Camus, A., Perea-Gomez, A., Moreau, A. and Collignon, J. (2006) 'Absence of Nodal signaling promotes precocious neural differentiation in the mouse embryo', *Developmental Biology*, 295(2), pp. 743–755. doi: 10.1016/j.ydbio.2006.03.047.

Cano, A., Pérez-Moreno, M. a, Rodrigo, I., Locascio, A., Blanco, M. J., del Barrio, M. G., Portillo, F. and Nieto, M. a (2000) 'The transcription factor snail controls epithelial-mesenchymal transitions by repressing E-cadherin expression.', *Nature cell biology*, 2(2), pp. 76–83. doi: 10.1038/35000025.

Carver, E. A., Jiang, R., Lan, Y., Oram, K. F. and Gridley, T. (2001) 'The Mouse Snail Gene Encodes a Key Regulator of the Epithelial-Mesenchymal Transition', *Molecular and Cellular Biology*. American Society for Microbiology, 21(23), pp. 8184–8188. doi: 10.1128/MCB.21.23.8184-8188.2001.

Casser, E., Israel, S., Witten, A., Schulte, K., Schlatt, S., Nordhoff, V. and Boiani, & M. (2017) 'Totipotency segregates between the sister blastomeres of two-cell stage mouse embryos', *Scientific Reports*. Springer US, 7(8299), pp. 1–15. doi: 10.1038/s41598-017-08266-6.

Chambers, I., Colby, D., Robertson, M., Nichols, J., Lee, S., Tweedie, S. and Smith, A. (2003) 'Functional expression cloning of Nanog, a pluripotency sustaining factor in embryonic stem cells.', *Cell*. United States, 113(5), pp. 643–655.

Chazaud, C., Yamanaka, Y., Pawson, T. and Rossant, J. (2006) 'Early lineage segregation between epiblast and primitive endoderm in mouse blastocysts through the Grb2-MAPK pathway.', *Developmental cell*, 10(5), pp. 615–24. doi: 10.1016/j.devcel.2006.02.020.

Chen, G. *et al.* (2016) 'Single-cell analyses of X Chromosome inactivation dynamics and pluripotency during differentiation', *Genome Research*. Cold Spring Harbor Laboratory Press, 26(10), pp. 1342–1354. doi: 10.1101/gr.201954.115.

Chen, U. and Kosco, M. (1993) 'Differentiation of mouse embryonic stem cells in vitro: III. Morphological evaluation of tissues developed after implantation of differentiated mouse embryoid bodies.', *Developmental dynamics : an official publication of the American Association of Anatomists*, 197(3), pp. 217–226. doi: 10.1002/aja.1001970306.

Chenoweth, J. G., McKay, R. D. G. and Tesar, P. J. (2010) 'Epiblast stem cells contribute new insight into pluripotency and gastrulation.', *Development, growth & differentiation*, 52(3), pp. 293–301. doi: 10.1111/j.1440-169X.2010.01171.x.

Choi, J. *et al.* (2017) 'Prolonged Mek1/2 suppression impairs the developmental potential of embryonic stem cells', *Nature*. Macmillan Publishers Limited, part of Springer Nature. All rights reserved., 548(7666), pp. 219–223. Available at: http://dx.doi.org/10.1038/nature23274.

Christodoulou, N., Kyprianou, C. and Zernicka-Goetz, M. (2017) 'Epithelial rosettes drive tissue remodeling and cavity fusion in the implanting mouse embryo', *Submitted*.

Ciruna, B. G., Schwartz, L., Harpal, K., Yamaguchi, T. P. and Rossant, J. (1997) 'Chimeric analysis of fibroblast growth factor receptor-1 (Fgfr1) function: a role for FGFR1 in morphogenetic movement through the primitive streak.', *Development (Cambridge, England)*. England, 124(14), pp. 2829–2841.

Ciruna, B. and Rossant, J. (2001) 'FGF Signaling Regulates Mesoderm Cell Fate Specification and Morphogenetic Movement at the Primitive Streak', *Developmental Cell*, 1(1), pp. 37–49. doi: 10.1016/S1534-5807(01)00017-X.

Cockburn, K. and Rossant, J. (2010) 'Making the blastocyst: Lessons from the mouse', *Journal of Clinical Investigation*, 120(4), pp. 995–1003. doi: 10.1172/JCI41229.

Coucouvanis, E. and Martin, G. R. (1999) 'BMP signaling plays a role in visceral endoderm differentiation and cavitation in the early mouse embryo.', *Development (Cambridge, England)*, 126(3), pp. 535–46. Available at: http://www.ncbi.nlm.nih.gov/pubmed/9876182.

Deglincerti, A., Croft, G. F., Pietila, L. N., Zernicka-Goetz, M., Siggia, E. D. and Brivanlou, A. H. (2016) 'Self-organization of the in vitro attached human embryo', *Nature*. Nature Publishing Group, 533, pp. 1–13. doi: 10.1038/nature17948.

Delhaise, F., Bralion, V., Schuurbiers, N. and Dessy, F. (1996) 'Establishment of an embryonic stem cell line from 8-cell stage mouse embryos.', *European journal of morphology*. England, 34(4), pp. 237–243.

Denker, H.-W. (2016) 'Self-Organization of Stem Cell Colonies and of Early Mammalian Embryos:

Recent Experiments Shed New Light on the Role of Autonomy vs. External Instructions in Basic Body Plan Development', *Cells*, 5(4), p. 39. doi: 10.3390/cells5040039.

Desbaillets, I., Ziegler, U., Groscurth, P. and Gassmann, M. (2000) 'Embryoid bodies: an in vitro model of mouse embryogenesis.', *Experimental physiology*, 85(6), pp. 645–651.

Ding, J., Yang, L., Yan, Y.-T., Chen, A., Desai, N., Wynshaw-Boris, A. and Shen, M. M. (1998) 'Cripto is required for correct orientation of the anterior-posterior axis in the mouse embryo', *Nature*, 395(6703), pp. 702–707. Available at: http://dx.doi.org/10.1038/27215.

Donnison, M., Beaton, A., Davey, H. W., Broadhurst, R., L'Huillier, P. and Pfeffer, P. L. (2005) 'Loss of the extraembryonic ectoderm in Elf5 mutants leads to defects in embryonic patterning.', *Development*, 132(10), pp. 2299–308. doi: 10.1242/dev.01819.

Ducibella, T., Albertini, D. F., Anderson, E. and Biggers, J. D. (1975) 'The preimplantation mammalian embryo: characterization of intercellular junctions and their appearance during development.', *Developmental biology*. United States, 45(2), pp. 231–250.

Ducibella, T. and Anderson, E. (1975) 'Cell shape and membrane changes in the eight-cell mouse embryo: prerequisites for morphogenesis of the blastocyst.', *Developmental biology*. United States, 47(1), pp. 45–58.

Durdu, S., Iskar, M., Revenu, C., Schieber, N., Kunze, A., Bork, P., Schwab, Y. and Gilmour, D. (2014) 'Luminal signalling links cell communication to tissue architecture during organogenesis', *Nature*. Nature Publishing Group, 515(7525), pp. 120–124. doi: 10.1038/nature13852.

Eiraku, M., Takata, N., Ishibashi, H., Kawada, M., Sakakura, E., Okuda, S., Sekiguchi, K., Adachi, T. and Sasai, Y. (2011) 'Self-organizing optic-cup morphogenesis in three-dimensional culture.', *Nature*. Nature Publishing Group, 472(7341), pp. 51–6. doi: 10.1038/nature09941.

Eldred, M. K., Charlton-Perkins, M., Muresan, L. and Harris, W. A. (2017) 'Self-organising aggregates of zebrafish retinal cells for investigating mechanisms of neural lamination', *Development*, 144(6), pp. 1097–1106. doi: 10.1242/dev.142760.

Erlebacher, A., Price, K. A. and Glimcher, L. H. (2004) 'Maintenance of mouse trophoblast stem cell proliferation by TGF-B/Activin', *Developmental Biology*, 275(1), pp. 158–169. doi: 10.1016/j.ydbio.2004.07.032.

Etoc, F., Metzger, J., Ruzo, A., Kirst, C., Yoney, A., Ozair, M. Z., Brivanlou, A. H. and Siggia, E. D. (2016) 'A Balance between Secreted Inhibitors and Edge Sensing Controls Gastruloid Self-Organization', *Developmental Cell*. Elsevier Inc., 39(3), pp. 302–315. doi: 10.1016/j.devcel.2016.09.016.

Evans, M. and Kaufman, M. (1981) 'Establishment in culture of pluripotential cells from mouse embryos', *Nature*, 292, pp. 154–156. Available at: http://download.bioon.com.cn/upload/month_0911/20091124_1dd267377e5b7eaca806j5u1icjkiTpk.attach.pdf (Accessed: 10 April 2014).

Eyal-Giladi, H., Debby, A. and Harel, N. (1992) 'The posterior section of the chick's area pellucida and its involvement in hypoblast and primitive streak formation', *Development*, 830, pp. 819–830. Available at: http://dev.biologists.org/content/116/3/819.short (Accessed: 31 March 2014).

Faul, F., Erdfelder, E., Lang, A.-G. and Buchner, A. (2007) 'G*Power: A flexible statistical power analysis program for the social, behavioral, and biomedical sciences.', *Behavior Research Methods*, 39(2), pp. 175–191. doi: 10.3758/BF03193146.

Faure, E. *et al.* (2016) 'A workflow to process 3D+time microscopy images of developing organisms

and reconstruct their cell lineage', *Nature Communications*, 7(in press), p. 8674. doi: 10.1038/ncomms9674.

Fehling, H. J., Lacaud, G., Kubo, A., Kennedy, M., Robertson, S., Keller, G. and Kuskoff, V. (2003) 'Tracking mesoderm induction and its specification to the hemangioblast during embryonic stem cell differentiation', *Development*, 130(17), pp. 4217–4227. doi: 10.1242/dev.00589.

Feldman, B., Poueymirou, W., Papaioannou, V. E., DeChiara, T. M. and Goldfarb, M. (1995) 'Requirement of FGF-4 for postimplantation mouse development.', *Science (New York, N.Y.)*. United States, 267(5195), pp. 246–249.

Ferrer-Vaquer, A., Piliszek, A., Tian, G., Aho, R. J., Dufort, D. and Hadjantonakis, A.-K. (2010) 'A sensitive and bright single-cell resolution live imaging reporter of Wnt/ß-catenin signaling in the mouse.', *BMC developmental biology*, 10, p. 121. doi: 10.1186/1471-213X-10-121.

Foty, R. a, Pfleger, C. M., Forgacs, G. and Steinberg, M. S. (1996) 'Surface tensions of embryonic tissues predict their mutual envelopment behavior', *Development (Cambridge, England)*, 122(5), pp. 1611–20. doi: 10.1007/bf00047737.

Frankenberg, S., Gerbe, F., Bessonnard, S., Belville, C., Pouchin, P., Bardot, O. and Chazaud, C. (2011) 'Primitive Endoderm Differentiates via a Three-Step Mechanism Involving Nanog and RTK Signaling', *Developmental Cell*. Elsevier, 21(6), pp. 1005–1013. doi: 10.1016/j.devcel.2011.10.019.

Fuchs, C., Scheinast, M., Pasteiner, W., Lagger, S., Hofner, M., Hoellrigl, A., Schultheis, M. and Weitzer, G. (2012) 'Self-organization phenomena in embryonic stem cell-derived embryoid bodies: axis formation and breaking of symmetry during cardiomyogenesis.', *Cells, tissues, organs*, 195(5), pp. 377–91. doi: 10.1159/000328712.

Fujimori, T., Miyatani, S. and Takeichi, M. (1990) 'Ectopic expression of N-cadherin perturbs histogenesis in Xenopus embryos', *Development*, 110(1), p. 97 LP-104. Available at: http://dev.biologists.org/content/110/1/97.abstract.

Gafni, O. *et al.* (2013) 'Derivation of novel human ground state naive pluripotent stem cells.', *Nature*. England, 504(7479), pp. 282–286. doi: 10.1038/nature12745.

Gerhart, J., Danilchik, M., Doniach, T., Roberts, S., Rowning, B. and Stewart, R. (1989) 'Cortical rotation of the Xenopus egg: consequences for the anteroposterior pattern of embryonic dorsal development.', *Development (Cambridge, England)*. England, 107 Suppl, pp. 37–51.

Gilbert, S. F. (2010) *Developmental Biology*. 9th edn. Sinauer Associates.

Goolam, M., Scialdone, A., Graham, S. J. L., MacAulay, I. C., Jedrusik, A., Hupalowska, A., Voet, T., Marioni, J. C. and Zernicka-Goetz, M. (2016) 'Heterogeneity in Oct4 and Sox2 Targets Biases Cell Fate in 4-Cell Mouse Embryos', *Cell*. The Authors, 165(1), pp. 61–74. doi: 10.1016/j.cell.2016.01.047.

Grabarek, J. B., Zyzynska, K., Saiz, N., Piliszek, A., Frankenberg, S., Nichols, J., Hadjantonakis, A.-K. and Plusa, B. (2012) 'Differential plasticity of epiblast and primitive endoderm precursors within the ICM of the early mouse embryo.', *Development (Cambridge, England)*. England, 139(1), pp. 129–139. doi: 10.1242/dev.067702.

Granier, C. *et al.* (2011) 'Nodal cis-regulatory elements reveal epiblast and primitive endoderm heterogeneity in the peri-implantation mouse embryo.', *Developmental biology*. United States, 349(2), pp. 350–362. doi: 10.1016/j.ydbio.2010.10.036.

Greggio, C., De Franceschi, F., Figueiredo-Larsen, M., Gobaa, S., Ranga, A., Semb, H., Lutolf, M. and Grapin-Botton, A. (2013) 'Artificial three-dimensional niches deconstruct pancreas development in

vitro.', *Development*, 140, pp. 4452–4462. doi: 10.1242/dev.096628.

Günesdogan, U., Magnúsdóttir, E. and Surani, M. A. (2014) 'Primoridal germ cell specification : a context-dependent cellular differentiation event', *Philosophical Transactions of the Royal Society B: Biological Sciences*, 369(1657), pp. 2–11.

Guo, G., Huss, M., Tong, G. Q., Wang, C., Li Sun, L., Clarke, N. D. and Robson, P. (2010) 'Resolution of Cell Fate Decisions Revealed by Single-Cell Gene Expression Analysis from Zygote to Blastocyst', *Developmental Cell*. Elsevier Ltd, 18(4), pp. 675–685. doi: 10.1016/j.devcel.2010.02.012.

Guzman-Ayala, M., Ben-Haim, N., Beck, S. and Constam, D. B. (2004) 'Nodal protein processing and fibroblast growth factor 4 synergize to maintain a trophoblast stem cell microenvironment.', *Proceedings of the National Academy of Sciences of the United States of America*, 101(44), pp. 15656–15660. doi: 10.1073/pnas.0405429101.

Hagios, C., Lochter, A. and Bissell, M. J. (1998) 'Tissue architecture: the ultimate regulator of epithelial function?', *Philosophical transactions of the Royal Society of London. Series B, Biological sciences*. England, 353(1370), pp. 857–870. doi: 10.1098/rstb.1998.0250.

Hajkova, P., Erhardt, S., Lane, N., Haaf, T., El-Maarri, O., Reik, W., Walter, J. and Surani, M. A. (2002) 'Epigenetic reprogramming in mouse primordial germ cells.', *Mechanisms of development*. Ireland, 117(1–2), pp. 15–23.

Hamatani, T., Carter, M. G., Sharov, A. A. and Ko, M. S. (2004) 'Dynamics of global gene expression changes during mouse preimplantation development', *Dev Cell*, 6(1), pp. 117–131. doi: 10.1016/S1534-5807(03)00373-3.

Hamazaki, T., Oka, M., Yamanaka, S. and Terada, N. (2004) 'Aggregation of embryonic stem cells induces Nanog repression and primitive endoderm differentiation.', *Journal of cell science*, 117(Pt 23), pp. 5681–5686. doi: 10.1242/jcs.01489.

Harrison, S. E., Sozen, B., Christodoulou, N., Kyprianou, C. and Zernicka-goetz, M. (2017) 'Assembly of embryonic and extra-embryonic stem cells to mimic embryogenesis in vitro', *Science*. doi: 10.1126/science.aal1810.

Hayashi, K. and Saitou, M. (2013) 'Generation of eggs from mouse embryonic stem cells and induced pluripotent stem cells', *Nature Protocols*. Nature Publishing Group, 8(8), pp. 1513–1524. doi: 10.1038/nprot.2013.090.

Heard, E. (2004) 'Recent advances in X-chromosome inactivation.', *Current opinion in cell biology*. England, 16(3), pp. 247–255. doi: 10.1016/j.ceb.2004.03.005.

Hermitte, S. and Chazaud, C. (2014) 'Primitive endoderm differentiation: from specification to epithelium formation', *Philosophical Transactions of the Royal Society of London. Series B.*, 369(1657), p. 20130537. doi: 10.1098/rstb.2013.0537.

Herrmann, B. G. (1991) 'Expression pattern of the Brachyury gene in whole-mount TWis/TWis mutant embryos.', *Development (Cambridge, England)*, 113(3), pp. 913–917.

Hillman, N., Sherman, M. I. and Graham, C. (1972) 'The effect of spatial arrangement on cell determination during mouse development.', *Journal of embryology and experimental morphology*. England, 28(2), pp. 263–278.

Himeno, E., Tanaka, S. and Kunath, T. (2008) 'Isolation and Manipulation of Mouse Trophoblast Stem Cells', *Current Protocols in Stem Cell Biology*.

Hirate, Y. *et al.* (2013) 'Polarity-dependent distribution of angiomotin localizes Hippo signaling in

preimplantation embryos.', *Current biology : CB*. England, 23(13), pp. 1181–1194. doi: 10.1016/j.cub.2013.05.014.

Hogan, B. L. M., Cooper, A. R. and Kurkinen, M. (1980) 'Incorporation into Reichert's membrane of laminin-like extracellular proteins synthesized by parietal endoderm cells of the mouse embryo', *Developmental Biology*, 80(2), pp. 289–300. doi: 10.1016/0012-1606(80)90405-4.

Hooper, M., Hardy, K., Handyside, A., Hunter, S. and Monk, M. (1987) 'HPRT-deficient (Lesch–Nyhan) mouse embryos derived from germline colonization by cultured cells', *Nature*, 326(6110), pp. 292–295. doi: 10.1038/326292a0.

Hough, S. R., Thornton, M., Mason, E., Mar, J. C., Wells, C. A. and Pera, M. F. (2017) 'Single-Cell Gene Expression Profiles Define Self-Renewing, Pluripotent, and Lineage Primed States of Human Pluripotent Stem Cells', *Stem Cell Reports*. Elsevier, 2(6), pp. 881–895. doi: 10.1016/j.stemcr.2014.04.014.

Huang, Y., Osorno, R., Tsakiridis, A. and Wilson, V. (2012) 'In Vivo differentiation potential of epiblast stem cells revealed by chimeric embryo formation.', *Cell reports*. United States, 2(6), pp. 1571–1578. doi: 10.1016/j.celrep.2012.10.022.

Huch, M. *et al.* (2013) 'In vitro expansion of single Lgr5+ liver stem cells induced by Wnt-driven regeneration.', *Nature*. Nature Publishing Group, 494(7436), pp. 247–50. doi: 10.1038/nature11826.

Huelsken, J., Vogel, R., Brinkmann, V., Erdmann, B., Birchmeier, C. and Birchmeier, W. (2000) 'Requirement for beta-catenin in anterior-posterior axis formation in mice.', *The Journal of cell biology*. United States, 148(3), pp. 567–578.

Hughes, M., Dobric, N., Scott, I. C., Su, L., Starovic, M., St-Pierre, B., Egan, S. E., Kingdom, J. C. P. and Cross, J. C. (2004) 'The Hand1, Stra13 and Gcm1 transcription factors override FGF signaling to promote terminal differentiation of trophoblast stem cells.', *Developmental biology*. United States, 271(1), pp. 26–37. doi: 10.1016/j.ydbio.2004.03.029.

Humphreys, R. C., Krajewska, M., Krnacik, S., Jaeger, R., Weiher, H., Krajewski, S., Reed, J. C. and Rosen, J. M. (1996) 'Apoptosis in the terminal endbud of the murine mammary gland: a mechanism of ductal morphogenesis.', *Development (Cambridge, England)*. England, 122(12), pp. 4013–4022.

Hyafil, F., Morello, D., Babinet, C. and Jacob, F. (1980) 'A cell surface glycoprotein involved in the compaction of embryonal carcinoma cells and cleavage stage embryos', *Cell*, 21(3), pp. 927–934. doi: 10.1016/0092-8674(80)90456-0.

Inman, G. J., Nicolás, F. J., Callahan, J. F., Harling, J. D., Gaster, L. M., Reith, A. D., Laping, N. J. and Hill, C. S. (2002) 'SB-431542 is a potent and specific inhibitor of transforming growth factor-beta superfamily type I activin receptor-like kinase (ALK) receptors ALK4, ALK5, and ALK7.', *Molecular pharmacology*, 62(1), pp. 65–74. doi: 10.1124/mol.62.1.65.

Irion, S., Nostro, M. C., Kattman, S. J. and Keller, G. M. (2008) 'Directed differentiation of pluripotent stem cells: from developmental biology to therapeutic applications.', *Cold Spring Harbor symposia on quantitative biology*. United States, 73, pp. 101–110. doi: 10.1101/sqb.2008.73.065.

Ishiuchi, T. and Torres-Padilla, M. E. (2013) 'Towards an understanding of the regulatory mechanisms of totipotency', *Current Opinion in Genetics and Development*. Elsevier Ltd, 23(5), pp. 512–518. doi: 10.1016/j.gde.2013.06.006.

Itskovitz-Eldor, J., Schuldiner, M., Karsenti, D., Eden, a, Yanuka, O., Amit, M., Soreq, H. and Benvenisty, N. (2000) 'Differentiation of human embryonic stem cells into embryoid bodies compromising the three embryonic germ layers.', *Molecular medicine (Cambridge, Mass.)*, 6(2), pp.

88–95. doi: 10859025.

Jedrusik, A., Parfitt, D.-E., Guo, G., Skamagki, M., Grabarek, J. B., Johnson, M. H., Robson, P. and Zernicka-Goetz, M. (2008) 'Role of Cdx2 and cell polarity in cell allocation and specification of trophectoderm and inner cell mass in the mouse embryo.', *Genes & development*, 22(19), pp. 2692–706. doi: 10.1101/gad.486108.

Johnson, M. H. and McConnell, J. M. L. (2004) 'Lineage allocation and cell polarity during mouse embryogenesis.', *Seminars in cell & developmental biology*. England, 15(5), pp. 583–597. doi: 10.1016/j.semcdb.2004.04.002.

Johnson, M. H. and Ziomek, C. A. (1981) 'The foundation of two distinct cell lineages within the mouse morula.', *Cell*. United States, 24(1), pp. 71–80.

Jones, R. L., Findlay, J. K., Farnworth, P. G., Robertson, D. M., Wallace, E. and Salamonsen, L. A. (2006) 'Activin A and inhibin A differentially regulate human uterine matrix metalloproteinases: potential interactions during decidualization and trophoblast invasion.', *Endocrinology*. United States, 147(2), pp. 724–732. doi: 10.1210/en.2005-1183.

Kim, D., Pertea, G., Trapnell, C., Pimentel, H., Kelley, R. and Salzberg, S. L. (2013) 'TopHat2: accurate alignment of transcriptomes in the presence of insertions, deletions and gene fusions', *Genome Biology*, 14(4), p. R36. doi: 10.1186/gb-2013-14-4-r36.

Kimura-Yoshida, C., Nakano, H., Okamura, D., Nakao, K., Yonemura, S., Belo, J. a, Aizawa, S., Matsui, Y. and Matsuo, I. (2005) 'Canonical Wnt signaling and its antagonist regulate anterior-posterior axis polarization by guiding cell migration in mouse visceral endoderm.', *Developmental cell*, 9(5), pp. 639–50. doi: 10.1016/j.devcel.2005.09.011.

Kimura, C., Shen, M. M., Takeda, N., Aizawa, S. and Matsuo, I. (2001) 'Complementary Functions of Otx2 and Cripto in Initial Patterning of Mouse Epiblast', *Developmental Biology*, 235(1), pp. 12–32. doi: 10.1006/dbio.2001.0289.

Kimura, C., Yoshinaga, K., Tian, E., Suzuki, M., Aizawa, S. and Matsuo, I. (2000) 'Visceral endoderm mediates forebrain development by suppressing posteriorizing signals.', *Developmental biology*, 225(2), pp. 304–21. doi: 10.1006/dbio.2000.9835.

Kojima, Y. *et al.* (2014) 'The transcriptional and functional properties of mouse epiblast stem cells resemble the anterior primitive streak', *Cell Stem Cell*. Elsevier Inc., 14(1), pp. 107–120. doi: 10.1016/j.stem.2013.09.014.

Korotkevich, E., Niwayama, R., Courtois, A., Friese, S., Berger, N., Buchholz, F. and Hiiragi, T. (2017) 'The Apical Domain Is Required and Sufficient for the First Lineage Segregation in the Mouse Embryo', *Developmental cell*. Developmental Biology Unit, European Molecular Biology Laboratory (EMBL), 69117 Heidelberg, Germany., 40(3), p. 235–247.e7. doi: 10.1016/j.devcel.2017.01.006.

Koutsourakis, M., Langeveld, A., Patient, R., Beddington, R. and Grosveld, F. (1999) 'The transcription factor GATA6 is essential for early extraembryonic development.', *Development (Cambridge, England)*. England, 126(9), pp. 723–732.

Krieg, M., Arboleda-Estudillo, Y., Puech, P.-H., Käfer, J., Graner, F., Müller, D. J. and Heisenberg, C.-P. C.-P. (2008) 'Tensile forces govern germ-layer organization in zebrafish.', *Nature cell biology*, 10(4), pp. 429–36. doi: 10.1038/ncb1705.

Krupa, M., Mazur, E., Szczepańska, K., Filimonow, K., Maleszewski, M. and Suwińska, A. (2014) 'Allocation of inner cells to epiblast vs primitive endoderm in the mouse embryo is biased but not determined by the round of asymmetric divisions (8→16- and 16→32-cells).', *Developmental*

biology, 385(1), pp. 136–48. doi: 10.1016/j.ydbio.2013.09.008.

Kubaczka, C., Senner, C., Arauzo-Bravo, M. J., Sharma, N., Kuckenberg, P., Becker, A., Zimmer, A., Brustle, O., Peitz, M., Hemberger, M. and Schorle, H. (2014) 'Derivation and maintenance of murine trophoblast stem cells under defined conditions', *Stem Cell Reports*, 2(2), pp. 232–242. doi: 10.1016/j.stemcr.2013.12.013.

Kumar, A., Lualdi, M., Lyozin, G. T., Sharma, P., Loncarek, J., Fu, X.-Y. and Kuehn, M. R. (2015) 'Nodal signaling from the visceral endoderm is required to maintain Nodal gene expression in the epiblast and drive DVE/AVE migration', *Developmental Biology*. Elsevier, 400(1), pp. 1–9. doi: 10.1016/j.ydbio.2014.12.016.

Kunath, T., Arnaud, D., Uy, G. D., Okamoto, I., Chureau, C., Yamanaka, Y., Heard, E., Gardner, R. L., Avner, P. and Rossant, J. (2005) 'Imprinted X-inactivation in extra-embryonic endoderm cell lines from mouse blastocysts.', *Development (Cambridge, England)*, 132(7), pp. 1649–1661. doi: 10.1242/dev.01715.

Kwon, G. S., Viotti, M. and Hadjantonakis, A.-K. (2008) 'The endoderm of the mouse embryo arises by dynamic widespread intercalation of embryonic and extraembryonic lineages.', *Developmental cell*. United States, 15(4), pp. 509–520. doi: 10.1016/j.devcel.2008.07.017.

Lancaster, M. A. and Knoblich, J. A. (2014) 'Organogenesis in a dish: Modeling development and disease using organoid technologies', *Science*, 345(6194), pp. 1247125–1247125. doi: 10.1126/science.1247125.

Lancaster, M. A., Renner, M., Martin, C.-A., Wenzel, D., Bicknell, L. S., Hurles, M. E., Homfray, T., Penninger, J. M., Jackson, A. P. and Knoblich, J. A. (2013) 'Cerebral organoids model human brain development and microcephaly.', *Nature*. England, 501(7467), pp. 373–379. doi: 10.1038/nature12517.

Larabell, C. A., Torres, M., Rowning, B. A., Yost, C., Miller, J. R., Wu, M., Kimelman, D. and Moon, R. T. (1997) 'Establishment of the dorso-ventral axis in Xenopus embryos is presaged by early asymmetries in beta-catenin that are modulated by the Wnt signaling pathway.', *The Journal of cell biology*. United States, 136(5), pp. 1123–1136.

Latos, P. A., Sienerth, A. R., Murray, A., Senner, C. E., Muto, M., Ikawa, M., Oxley, D., Burge, S., Cox, B. J. and Hemberger, M. (2015) 'Elf5-centered transcription factor hub controls trophoblast stem cell self-renewal and differentiation through stoichiometry-sensitive shifts in target gene networks.', *Genes & development*, 29(23), pp. 2435–48. doi: 10.1101/gad.268821.115.

Lawson, A. and Schoenwolf, G. C. (2003) 'Epiblast and primitive-streak origins of the endoderm in the gastrulating chick embryo', *Development*, 130(15), pp. 3491–3501. doi: 10.1242/dev.00579.

Lawson, K. A., Dunn, N. R., Roelen, B. A. J., Lawson, K. A., Dunn, N. R., Roelen, B. A. J., Zeinstra, L. M., Davis, A. M., Wright, C. V. E., Korving, J. P. W. F. M. and Hogan, B. L. M. (1999) 'Bmp4 is required for the generation of primordial germ cells in the mouse embryo', *Genes & Development Development*, 13, pp. 424–436.

Lawson, K. A. and Hage, W. J. (1994) 'Clonal analysis of the origin of primordial germ cells in the mouse.', *Ciba Foundation symposium*. Netherlands, 182, pp. 68–91.

Layer, P. G. and Willbold, E. (1993) 'Histogenesis of the Avian Retina in Reaggregation Culture: From Dissociated Cells to Laminar Neuronal Networks', *International Review of Cytology*, 146, pp. 1–47. doi: http://dx.doi.org/10.1016/S0074-7696(08)60378-2.

Lee, G. Y., Kenny, P. a, Lee, E. H. and Bissell, M. J. (2007) 'Three-dimensional culture models of

normal and malignant breast epithelial cells.', *Nature Protocols*, 4(4), pp. 359–65. doi: 10.1038/nmeth1015.

Leung, B., Hermann, G. J. and Priess, J. R. (1999) 'Organogenesis of the Caenorhabditis elegans intestine.', *Developmental biology*. United States, 216(1), pp. 114–134. doi: 10.1006/dbio.1999.9471.

Leung, C. Y. and Zernicka-Goetz, M. (2013) 'Angiomotin prevents pluripotent lineage differentiation in mouse embryos via Hippo pathway-dependent and -independent mechanisms.', *Nature communications*. Nature Publishing Group, 4, p. 2251. doi: 10.1038/ncomms3251.

Li, M. L., Aggeler, J., Farson, D. A., Hatier, C., Hassell, J. and Bissell, M. J. (1987) 'Influence of a reconstituted basement membrane and its components on casein gene expression and secretion in mouse mammary epithelial cells.', *Proceedings of the National Academy of Sciences of the United States of America*, 84(1), pp. 136–40. doi: 10.1073/pnas.84.1.136.

Li, S., Edgar, D., Fässler, R., Wadsworth, W. and Yurchenco, P. D. (2003) 'The Role of Laminin in Embryonic Cell Polarization and Tissue Organization', *Developmental Cell*. Elsevier, 4(5), pp. 613–624. doi: 10.1016/S1534-5807(03)00128-X.

Li, S., Harrison, D., Carbonetto, S., Fässler, R., Smyth, N., Edgar, D. and Yurchenco, P. D. (2002) 'Matrix assembly, regulation, and survival functions of laminin and its receptors in embryonic stem cell differentiation', *Journal of Cell Biology*, 157(7), pp. 1279–1290. doi: 10.1083/jcb.200203073.

Li, X., Chen, Y., Scheele, S., Arman, E., Haffner-Krausz, R., Ekblom, P. and Lonai, P. (2001) 'Fibroblast growth factor signaling and basement membrane assembly are connected during epithelial morphogenesis of the embryoid body', *Journal of Cell Biology*, 153(4), pp. 811–822. doi: 10.1083/jcb.153.4.811.

Li, Z. *et al.* (2012) 'BMP4 Signaling Acts via dual-specificity phosphatase 9 to control ERK activity in mouse embryonic stem cells.', *Cell stem cell*. United States, 10(2), pp. 171–182. doi: 10.1016/j.stem.2011.12.016.

Lian, X., Bao, X., Al-ahmad, A., Liu, J., Wu, Y., Dong, W., Dunn, K. K., Shusta, E. V and Palecek, S. P. (2016) 'Naive Pluripotent Stem Cells Derived Directly from Isolated Cells of the Human Inner Cell Mass', *Stem Cell Reports*. The Authors, 3, pp. 323–336. doi: 10.1016/j.stemcr.2015.07.005.

Liguori, G. L., Cristina, A., Andrea, D. D., Liguoro, A., Gonçalves, L., Marisa, A., Persico, M. G. and Antonio, J. (2008) 'Cripto-independent Nodal signaling promotes positioning of the A – P axis in the early mouse embryo', 315, pp. 280–289. doi: 10.1016/j.ydbio.2007.12.027.

Lin, J., Khan, M., Zapiec, B. and Mombaerts, P. (2016) 'Efficient derivation of extraembryonic endoderm stem cell lines from mouse postimplantation embryos', *Scientific Reports*. Nature Publishing Group, 6(May), p. 39457. doi: 10.1038/srep39457.

Lindsley, R. C., Gill, J. G., Kyba, M., Murphy, T. L. and Murphy, K. M. (2006) 'Canonical Wnt signaling is required for development of embryonic stem cell-derived mesoderm.', *Development (Cambridge, England)*. England, 133(19), pp. 3787–3796. doi: 10.1242/dev.02551.

Liu, P., Wakamiya, M., Shea, M. J., Albrecht, U., Behringer, R. R. and Bradley, A. (1999) 'Requirement for Wnt3 in vertebrate axis formation.', *Nature genetics*. United States, 22(4), pp. 361–365. doi: 10.1038/11932.

Liu, W., Brown, K., Legros, S. and Foley, a. C. (2012) 'Nodal mutant eXtraembryonic ENdoderm (XEN) stem cells upregulate markers for the anterior visceral endoderm and impact the timing of cardiac differentiation in mouse embryoid bodies', *Biology Open*, 1(3), pp. 208–219. doi:

10.1242/bio.2012038.

Livet, J., Weissman, T. A., Kang, H., Draft, R. W., Lu, J., Bennis, R. A., Sanes, J. R. and Lichtman, J. W. (2007) 'Transgenic strategies for combinatorial expression of fluorescent proteins in the nervous system', *Nature*, 450(7166), pp. 56–62. doi: 10.1038/nature06293.

Lu, C.-W., Yabuuchi, A., Chen, L., Viswanathan, S., Kim, K. and Daley, G. Q. (2008) 'Ras-MAPK signaling promotes trophectoderm formation from embryonic stem cells and mouse embryos.', *Nature genetics*. United States, 40(7), pp. 921–926. doi: 10.1038/ng.173.

Lu, C. C. and Robertson, E. J. (2004) 'Multiple roles for Nodal in the epiblast of the mouse embryo in the establishment of anterior-posterior patterning', *Developmental Biology*, 273(1), pp. 149–159. doi: 10.1016/j.ydbio.2004.06.004.

Lu, R. Z., Matsuyama, S., Nishihara, M. and Takahashi, M. (1993) 'Developmental expression of activin/inhibin beta A, beta B, and alpha subunits, and activin receptor-IIB genes in preimplantation mouse embryos.', *Biology of reproduction*. United States, 49(6), pp. 1163–1169.

Ma, W., Song, H., Das, S. K., Paria, B. C. and Dey, S. K. (2003) 'Estrogen is a critical determinant that specifies the duration of the window of uterine receptivity for implantation.', *Proceedings of the National Academy of Sciences of the United States of America*. United States, 100(5), pp. 2963–2968. doi: 10.1073/pnas.0530162100.

Magnusdottir, E., Dietmann, S., Murakami, K., Gunesdogan, U., Tang, F., Bao, S., Diamanti, E., Lao, K., Gottgens, B. and Azim Surani, M. (2013) 'A tripartite transcription factor network regulates primordial germ cell specification in mice.', *Nature cell biology*. England, 15(8), pp. 905–915. doi: 10.1038/ncb2798.

Maitre, J.-L., Niwayama, R., Turlier, H., Nedelec, F. and Hiiragi, T. (2015) 'Pulsatile cell-autonomous contractility drives compaction in the mouse embryo.', *Nature cell biology*. England, 17(7), pp. 849–855. doi: 10.1038/ncb3185.

Martín-Belmonte, F., Yu, W., Rodríguez-Fraticelli, A. E., Ewald, A., Werb, Z., Alonso, M. A. and Mostov, K. (2008) 'Cell-Polarity Dynamics Controls the Mechanism of Lumen Formation in Epithelial Morphogenesis', *Current Biology*, 18(7), pp. 507–513. doi: 10.1016/j.cub.2008.02.076.

Martin, G. (1981) 'Isolation of a pluripotent cell line from early mouse embryos cultured in medium conditioned by teratocarcinoma stem cells', *Proceedings of the National Academy of Sciences*, 78(12), pp. 7634–7638. Available at: http://www.pnas.org/content/78/12/7634.short (Accessed: 10 April 2014).

McDole, K., Xiong, Y., Iglesias, P. A. and Zheng, Y. (2011) 'Lineage mapping the pre-implantation mouse embryo by two-photon microscopy, new insights into the segregation of cell fates.', *Developmental biology*. United States, 355(2), pp. 239–249. doi: 10.1016/j.ydbio.2011.04.024.

Meder, D., Shevchenko, A., Simons, K. and Füllekrug, J. (2005) 'Gp135/podocalyxin and NHERF-2 participate in the formation of a preapical domain during polarization of MDCK cells', *Journal of Cell Biology*, 168(2), pp. 303–313. doi: 10.1083/jcb.200407072.

Meilhac, S. M., Adams, R. J., Morris, S. a, Danckaert, A., Le Garrec, J.-F. and Zernicka-Goetz, M. (2009) 'Active cell movements coupled to positional induction are involved in lineage segregation in the mouse blastocyst.', *Developmental biology*. Elsevier Inc., 331(2), pp. 210–21. doi: 10.1016/j.ydbio.2009.04.036.

Meinhardt, A., Eberle, D., Tazaki, A., Ranga, A., Niesche, M., Wilsch-Bräuninger, M., Stec, A., Schackert, G., Lutolf, M. and Tanaka, E. M. (2014) '3D Reconstitution of the Patterned Neural Tube

from Embryonic Stem Cells', *Stem Cell Reports*, 3(6), pp. 1–13. doi: 10.1016/j.stemcr.2014.09.020.

Meissner, A. *et al.* (2008) 'Genome-scale DNA methylation maps of pluripotent and differentiated cells.', *Nature*. England, 454(7205), pp. 766–770. doi: 10.1038/nature07107.

Meno, C. *et al.* (1999) 'Mouse lefty2 and zebrafish antivin are feedback inhibitors of nodal signaling during vertebrate gastrulation', *Molecular Cell*, 4(3), pp. 287–298. doi: 10.1016/S1097-2765(00)80331-7.

Mesnard, D. (2006) 'Nodal specifies embryonic visceral endoderm and sustains pluripotent cells in the epiblast before overt axial patterning', *Development*, 133(13), pp. 2497–2505. doi: 10.1242/dev.02413.

Mesnard, D., Guzman-Ayala, M. and Constam, D. B. (2006) 'Nodal specifies embryonic visceral endoderm and sustains pluripotent cells in the epiblast before overt axial patterning', *Development*, 133.

Miller, J. R., Rowning, B. A., Larabell, C. A., Yang-Snyder, J. A., Bates, R. L. and Moon, R. T. (1999) 'Establishment of the dorsal-ventral axis in Xenopus embryos coincides with the dorsal enrichment of dishevelled that is dependent on cortical rotation.', *The Journal of cell biology*. United States, 146(2), pp. 427–437.

Miner, J. H., Li, C., Mudd, J. L., Go, G. and Sutherland, A. E. (2004) 'Compositional and structural requirements for laminin and basement membranes during mouse embryo implantation and gastrulation.', *Development (Cambridge, England)*, 131(10), pp. 2247–2256. doi: 10.1242/dev.01112.

Mitalipov, S., Kuo, H. C., Byrne, J., Clepper, L., Meisner, L., Johnson, J., Zeier, R. and Wolf, D. (2006) 'Isolation and characterization of novel rhesus monkey embryonic stem cell lines', *Stem Cells*, 24(10), pp. 2177–2186. doi: 2006-0125 [pii]\r10.1634/stemcells.2006-0125.

Mitsui, K., Tokuzawa, Y., Itoh, H., Segawa, K., Murakami, M., Takahashi, K., Maruyama, M., Maeda, M. and Yamanaka, S. (2003) 'The homeoprotein Nanog is required for maintenance of pluripotency in mouse epiblast and ES cells.', *Cell*. United States, 113(5), pp. 631–642.

Molkentin, J. D., Lin, Q., Duncan, S. A. and Olson, E. N. (1997) 'Requirement of the transcription factor GATA4 for heart tube formation and ventral morphogenesis.', *Genes & development*. United States, 11(8), pp. 1061–1072.

Montesano, R., Schaller, G. and Orci, L. (1991) 'Induction of epithelial tubular morphogenesis in vitro by fibroblast-derived soluble factors.', *Cell*, 66(4), pp. 697–711. doi: 10.1016/0962-8924(92)90128-A.

Moore, K. L., Persaud, T. V. N. and Torchia, M. G. (2013) *The Developing Human: Clinically Oriented Embryology*. Elsevier/Saunders (ClinicalKey 2012). Available at: https://books.google.co.uk/books?id=qmX9LgEACAAJ.

Moore, R., Tao, W., Meng, Y., Smith, E. R. and Xu, X.-X. (2014) 'Cell adhesion and sorting in embryoid bodies derived from N- or E-cadherin deficient murine embryonic stem cells.', *Biology open*, 3(2), pp. 121–8. doi: 10.1242/bio.20146254.

Morgani, S. M., Canham, M. A., Nichols, J., Sharov, A. A., Migueles, R. P., Ko, M. S. H. and Brickman, J. M. (2013) 'Totipotent embryonic stem cells arise in ground-state culture conditions.', *Cell reports*. United States, 3(6), pp. 1945–1957. doi: 10.1016/j.celrep.2013.04.034.

Morgani, S., Nichols, J. and Hadjantonakis, A.-K. (2017) 'The many faces of Pluripotency: in vitro adaptations of a continuum of in vivo states.', *BMC developmental biology*. BMC Developmental Biology, 17(1), p. 7. doi: 10.1186/s12861-017-0150-4.

Morikawa, M., Koinuma, D., Mizutani, A., Kawasaki, N., Holmborn, K., Sundqvist, A., Tsutsumi, S., Watabe, T., Aburatani, H., Heldin, C.-H. and Miyazono, K. (2016) 'BMP Sustains Embryonic Stem Cell Self-Renewal through Distinct Functions of Different Kruppel-like Factors.', *Stem cell reports*. United States, 6(1), pp. 64–73. doi: 10.1016/j.stemcr.2015.12.004.

Morris, S. A., Graham, S. J. L., Jedrusik, A. and Zernicka-Goetz, M. (2013) 'The differential response to Fgf signalling in cells internalized at different times influences lineage segregation in preimplantation mouse embryos.', *Open biology*, 3(11), p. 130104. doi: 10.1098/rsob.130104.

Morris, S. A., Grewal, S., Barrios, F., Patankar, S. N., Strauss, B., Buttery, L., Alexander, M., Shakesheff, K. M. and Zernicka-Goetz, M. (2012) 'Dynamics of anterior-posterior axis formation in the developing mouse embryo.', *Nature communications*. Nature Publishing Group, 3, p. 673. doi: 10.1038/ncomms1671.

Morris, S. A., Guo, Y. and Zernicka-Goetz, M. (2012) 'Developmental plasticity is bound by pluripotency and the Fgf and Wnt signaling pathways.', *Cell reports*. The Authors, 2(4), pp. 756–65. doi: 10.1016/j.celrep.2012.08.029.

Morris, S. A., Teo, R. T. Y., Li, H., Robson, P., Glover, D. M. and Zernicka-Goetz, M. (2010) 'Origin and formation of the first two distinct cell types of the inner cell mass in the mouse embryo.', *Proceedings of the National Academy of Sciences of the United States of America*, 107(14), pp. 6364–9. doi: 10.1073/pnas.0915063107.

Morrisey, E. E., Tang, Z., Sigrist, K., Lu, M. M., Jiang, F., Ip, H. S. and Parmacek, M. S. (1998) 'GATA6 regulates HNF4 and is required for differentiation of visceral endoderm in the mouse embryo', *Genes and Development*, 12(22), pp. 3579–3590. doi: 10.1101/gad.12.22.3579.

Moscona, A. and Moscona, H. (1952) 'The dissociation and aggregation of cells from organ rudiments of the early chick embryo', *Journal of anatomy*, 86(Pt 3), pp. 287–301.

Mukhopadhyay, M. *et al.* (2001) 'Dickkopf1 is required for embryonic head induction and limb morphogenesis in the mouse.', *Developmental cell*. United States, 1(3), pp. 423–434.

Murakami, K., Günesdogan, U., Zylicz, J. J., Tang, W. W. C., Sengupta, R., Kobayashi, T., Kim, S., Butler, R., Dietmann, S. and Azim Surani, M. (2016) 'NANOG alone induces germ cells in primed epiblast in vitro by activation of enhancers', *Nature*, 529(7586), pp. 1–22. doi: 10.1038/nature16480.

Murry, C. E. and Keller, G. (2008) 'Differentiation of Embryonic Stem Cells to Clinically Relevant Populations: Lessons from Embryonic Development', *Cell*, pp. 661–680. doi: 10.1016/j.cell.2008.02.008.

Natale, D. R. C., Hemberger, M., Hughes, M. and Cross, J. C. (2009) 'Activin promotes differentiation of cultured mouse trophoblast stem cells towards a labyrinth cell fate', *Developmental Biology*. Elsevier Inc., 335(1), pp. 120–131. doi: 10.1016/j.ydbio.2009.08.022.

Niakan, K. K. *et al.* (2010) 'Sox17 promotes differentiation in mouse embryonic stem cells by directly regulating extraembryonic gene expression and indirectly antagonizing self-renewal.', *Genes & development*. United States, 24(3), pp. 312–326. doi: 10.1101/gad.1833510.

Niakan, K. K., Schrode, N., Cho, L. T. Y. and Hadjantonakis, A.-K. (2013) 'Derivation of extraembryonic endoderm stem (XEN) cells from mouse embryos and embryonic stem cells.', *Nature protocols*, 8(6), pp. 1028–41. doi: 10.1038/nprot.2013.049.

Nichols, J. and Smith, A. (2009) 'Naive and Primed Pluripotent States', *Cell Stem Cell*. Elsevier Inc., 4(6), pp. 487–492. doi: 10.1016/j.stem.2009.05.015.

Nichols, J., Zevnik, B., Anastassiadis, K., Niwa, H., Klewe-Nebenius, D., Chambers, I., Scholer, H. and Smith, A. (1998) 'Formation of pluripotent stem cells in the mammalian embryo depends on the POU transcription factor Oct4.', *Cell*. United States, 95(3), pp. 379–391.

Niida, A., Hiroko, T., Kasai, M., Furukawa, Y., Nakamura, Y., Suzuki, Y., Sugano, S. and Akiyama, T. (2004) 'DKK1, a negative regulator of Wnt signaling, is a target of the beta-catenin/TCF pathway.', *Oncogene*, 23(52), pp. 8520–8526. doi: 10.1038/sj.onc.1207892.

Nishioka, N. *et al.* (2009) 'The Hippo signaling pathway components Lats and Yap pattern Tead4 activity to distinguish mouse trophectoderm from inner cell mass.', *Developmental cell*. United States, 16(3), pp. 398–410. doi: 10.1016/j.devcel.2009.02.003.

Nishioka, N., Yamamoto, S., Kiyonari, H., Sato, H., Sawada, A., Ota, M., Nakao, K. and Sasaki, H. (2008) 'Tead4 is required for specification of trophectoderm in pre-implantation mouse embryos.', *Mechanisms of development*. Ireland, 125(3–4), pp. 270–283. doi: 10.1016/j.mod.2007.11.002.

Niwa, H., Toyooka, Y., Shimosato, D., Strumpf, D., Takahashi, K., Yagi, R. and Rossant, J. (2005) 'Interaction between Oct3/4 and Cdx2 determines trophectoderm differentiation.', *Cell*. United States, 123(5), pp. 917–929. doi: 10.1016/j.cell.2005.08.040.

Oda, M., Shiota, K. and Tanaka, S. (2006) 'Trophoblast stem cells.', *Methods in enzymology*, 419(6), pp. 387–400. doi: 10.1016/S0076-6879(06)19015-1.

Ohinata, Y. *et al.* (2005) 'Blimp1 is a critical determinant of the germ cell lineage in mice.', *Nature*, 436(7048), pp. 207–213. doi: 10.1038/nature03813.

Ohinata, Y., Ohta, H., Shigeta, M., Yamanaka, K., Wakayama, T. and Saitou, M. (2009) 'A signaling principle for the specification of the germ cell lineage in mice.', *Cell*. United States, 137(3), pp. 571–584. doi: 10.1016/j.cell.2009.03.014.

Ohinata, Y. and Tsukiyama, T. (2014) 'Establishment of trophoblast stem cells under defined culture conditions in mice', *PLoS ONE*, 9(9). doi: 10.1371/journal.pone.0107308.

Ohnishi, Y., Huber, W., Tsumura, A., Kang, M., Xenopoulos, P., Kurimoto, K., Oleś, A. K., Araúzo-Bravo, M. J., Saitou, M., Hadjantonakis, A.-K. and Hiiragi, T. (2014) 'Cell-to-cell expression variability followed by signal reinforcement progressively segregates early mouse lineages', *Nature cell biology*, 16(1), pp. 27–37. doi: 10.1038/ncb2881.

Oppenheimer, J. M. (1936) 'Transplantation experiments on developing teleosts (Fundulus and Perca)', *Journal of Experimental Zoology*. Wiley Subscription Services, Inc., A Wiley Company, 72(3), pp. 409–437. doi: 10.1002/jez.1400720304.

Orimo, T., Taga, M., Matsui, H. and Minaguchi, H. (1996) 'The effect of activin-a on the development of mouse preimplantation embryos in vitro', *Journal of Assisted Reproduction and Genetics*, 13(8), pp. 669–674. doi: 10.1007/BF02069647.

Orlando, R. a, Takeda, T., Zak, B., Schmieder, S., Benoit, V. M., McQuistan, T., Furthmayr, H. and Farquhar, M. G. (2001) 'The glomerular epithelial cell anti-adhesin podocalyxin associates with the actin cytoskeleton through interactions with ezrin.', *Journal of the American Society of Nephrology : JASN*, 12(8), pp. 1589–1598.

Paca, A., Séguin, C. A., Clements, M., Ryczko, M., Rossant, J., Rodriguez, T. A. and Kunath, T. (2012) 'BMP signaling induces visceral endoderm differentiation of XEN cells and parietal endoderm', *Developmental Biology*. Elsevier Inc., 361(1), pp. 90–102. doi: 10.1016/j.ydbio.2011.10.013.

Papanayotou, C. and Collignon, J. (2014) 'Activin / Nodal signalling before implantation : setting the

stage for embryo patterning', *Philosophical transactions of the Royal Society of London. Series B, Biological sciences*, 3, pp. 1–8. doi: 10.1098/rstb.2013.0539.

Park, C. B. and Dufort, D. (2011) 'Nodal expression in the uterus of the mouse is regulated by the embryo and correlates with implantation.', *Biology of reproduction*, 84(6), pp. 1103–10. doi: 10.1095/biolreprod.110.087239.

Parr, E. L., Tung, H. N. and Parr, M. B. (1987) 'Apoptosis as the mode of uterine epithelial cell death during embryo implantation in mice and rats.', *Biology of reproduction*. United States, 36(1), pp. 211–225.

Payer, B., Chuva de Sousa Lopes, S. M., Barton, S. C., Lee, C., Saitou, M. and Surani, M. A. (2006) 'Generation of stella-GFP transgenic mice: a novel tool to study germ cell development.', *Genesis (New York, N.Y. : 2000)*, 44(2), pp. 75–83. doi: 10.1002/gene.20187.

Peng, G. *et al.* (2016) 'Spatial Transcriptome for the Molecular Annotation of Lineage Fates and Cell Identity in Mid-gastrula Mouse Embryo', *Developmental Cell*. Elsevier Inc., 36(6), pp. 681–697. doi: 10.1016/j.devcel.2016.02.020.

Perea-Gomez, A. *et al.* (2002) 'Nodal antagonists in the anterior visceral endoderm prevent the formation of multiple primitive streaks', *Developmental Cell*, 3(5), pp. 745–756. doi: 10.1016/S1534-5807(02)00321-0.

Perea-Gomez, A., Camus, A., Moreau, A., Grieve, K., Moneron, G., Dubois, A., Cibert, C. and Collignon, J. (2004) 'Initiation of gastrulation in the mouse embryo is preceded by an apparent shift in the orientation of the anterior-posterior axis.', *Current biology : CB*, 14(3), pp. 197–207. doi: 10.1016/j.cub.2004.01.030.

Perea-Gomez, A., Meilhac, S. M., Piotrowska-Nitsche, K., Gray, D., Collignon, J. and Zernicka-Goetz, M. (2007) 'Regionalisation of the mouse visceral endoderm as the blastocyst transforms into the egg cylinder', *BMC Developmental Biology*, 7(1), p. 96. doi: 10.1186/1471-213X-7-96.

Perea-Gomez, A., Shawlot, W., Sasaki, H., Behringer, R. R. and Ang, S. (1999) 'HNF3beta and Lim1 interact in the visceral endoderm to regulate primitive streak formation and anterior-posterior polarity in the mouse embryo.', *Development (Cambridge, England)*. England, 126(20), pp. 4499–4511.

Pesce, M. and Scholer, H. R. (2001) 'Oct-4: gatekeeper in the beginnings of mammalian development.', *Stem cells (Dayton, Ohio)*. United States, 19(4), pp. 271–278. doi: 10.1634/stemcells.19-4-271.

Pfister, S., Steiner, K. A. and Tam, P. P. L. (2007) 'Gene expression pattern and progression of embryogenesis in the immediate post-implantation period of mouse development.', *Gene expression patterns : GEP*. Netherlands, 7(5), pp. 558–573. doi: 10.1016/j.modgep.2007.01.005.

Picelli, S., Bjorklund, A. K., Faridani, O. R., Sagasser, S., Winberg, G. and Sandberg, R. (2013) 'Smart-seq2 for sensitive full-length transcriptome profiling in single cells', *Nat Meth*. Nature Publishing Group, a division of Macmillan Publishers Limited. All Rights Reserved., 10(11), pp. 1096–1098. Available at: http://dx.doi.org/10.1038/nmeth.2639.

Picelli, S., Faridani, O. R., Björklund, A. K., Winberg, G., Sagasser, S. and Sandberg, R. (2014) 'Full-length RNA-seq from single cells using Smart-seq2.', *Nature protocols*, 9(1), pp. 171–81. doi: 10.1038/nprot.2014.006.

Pineda, E., Nerem, R. and Ahsan, T. (2013) 'Differentiation patterns of embryonic stem cells in two- versus three-dimensional culture', *Cells Tissues Organs*, 197(5), pp. 399–410. doi:

10.1159/000346166.DIFFERENTIATION.

Piotrowska-Nitsche, K., Perea-Gomez, A., Haraguchi, S. and Zernicka-Goetz, M. (2005) 'Four-cell stage mouse blastomeres have different developmental properties.', *Development (Cambridge, England)*. England, 132(3), pp. 479–490. doi: 10.1242/dev.01602.

Piotrowska-Nitsche, K. and Zernicka-Goetz, M. (2005) 'Spatial arrangement of individual 4-cell stage blastomeres and the order in which they are generated correlate with blastocyst pattern in the mouse embryo', *Mechanisms of Development*, 122(4), pp. 487–500. doi: 10.1016/j.mod.2004.11.014.

Piotrowska, K., Wianny, F., Pedersen, R. A. and Zernicka-Goetz, M. (2001) 'Blastomeres arising from the first cleavage division have distinguishable fates in normal mouse development.', *Development (Cambridge, England)*. England, 128(19), pp. 3739–3748.

Plusa, B., Piliszek, A., Frankenberg, S., Artus, J. and Hadjantonakis, A.-K. (2008) 'Distinct sequential cell behaviours direct primitive endoderm formation in the mouse blastocyst.', *Development (Cambridge, England)*, 135(18), pp. 3081–91. doi: 10.1242/dev.021519.

Ralston, A., Cox, B. J., Nishioka, N., Sasaki, H., Chea, E., Rugg-Gunn, P., Guo, G., Robson, P., Draper, J. S. and Rossant, J. (2010) 'Gata3 regulates trophoblast development downstream of Tead4 and in parallel to Cdx2', *Development*, 137(3), p. 395 LP-403. Available at: http://dev.biologists.org/content/137/3/395.abstract.

Rastan, S. (1982) 'Timing of X-chromosome inactivation in postimplantation mouse embryos.', *Journal of embryology and experimental morphology*. England, 71, pp. 11–24.

Rhee, J. M., Pirity, M. K., Lackan, C. S., Long, J. Z., Kondoh, G., Takeda, J. and Hadjantonakis, A. K. (2006) 'In vivo imaging and differential localization of lipid-modified GFP-variant fusions in embryonic stem cells and mice', *Genesis*, 44(4), pp. 202–218. doi: 10.1002/dvg.20203.

Richardson, L., Torres-Padilla, M.-E. and Zernicka-Goetz, M. (2006) 'Regionalised signalling within the extraembryonic ectoderm regulates anterior visceral endoderm positioning in the mouse embryo.', *Mechanisms of development*, 123(4), pp. 288–96. doi: 10.1016/j.mod.2006.01.004.

Rivera-Pérez, J. A. and Hadjantonakis, A. K. (2015) 'The Dynamics of Morphogenesis in the Early Mouse Embryo'.

Rivera-Pérez, J. A., Mager, J. and Magnuson, T. (2003) 'Dynamic morphogenetic events characterize the mouse visceral endoderm', *Developmental Biology*, 261(2), pp. 470–487. doi: 10.1016/S0012-1606(03)00302-6.

Rivera-Pérez, J. A. and Magnuson, T. (2005) 'Primitive streak formation in mice is preceded by localized activation of Brachyury and Wnt3', *Developmental Biology*, 288(2), pp. 363–371. doi: 10.1016/j.ydbio.2005.09.012.

Roberts, R. M. and Fisher, S. J. (2011) 'Trophoblast stem cells.', *Biology of reproduction*, 84(3), pp. 412–21. doi: 10.1095/biolreprod.110.088724.

Rodriguez, T. a, Srinivas, S., Clements, M. P., Smith, J. C. and Beddington, R. S. P. (2005) 'Induction and migration of the anterior visceral endoderm is regulated by the extra-embryonic ectoderm.', *Development (Cambridge, England)*, 132(11), pp. 2513–2520. doi: 10.1242/dev.01847.

Rossant, J. (2015) 'Mouse and human blastocyst-derived stem cells: vive les differences', *Development*, 142(1), pp. 9–12. doi: 10.1242/dev.115451.

Rossant, J. and Tam, P. P. L. (2009) 'Blastocyst lineage formation, early embryonic asymmetries and

axis patterning in the mouse.', *Development (Cambridge, England)*, 136(5), pp. 701–13. doi: 10.1242/dev.017178.

Sato, T., Vries, R. G., Snippert, H. J., van de Wetering, M., Barker, N., Stange, D. E., van Es, J. H., Abo, A., Kujala, P., Peters, P. J. and Clevers, H. (2009) 'Single Lgr5 stem cells build crypt-villus structures in vitro without a mesenchymal niche.', *Nature*. Nature Publishing Group, 459(7244), pp. 262–5. doi: 10.1038/nature07935.

Schneider, S., Steinbeisser, H., Warga, R. M. and Hausen, P. (1996) 'Beta-catenin translocation into nuclei demarcates the dorsalizing centers in frog and fish embryos.', *Mechanisms of development*. Ireland, 57(2), pp. 191–198.

Scholer, H. R., Dressler, G. R., Rohdewohid, H. and Gruss, P. (1990) 'Oct-4: a germline-specific transcription factor mapping to the mouse t-complex', *EMBO Journal*, 9(7), pp. 2185–2195.

Scialdone, A., Tanaka, Y., Jawaid, W., Moignard, V., Wilson, N. K., Macaulay, I. C., Marioni, J. C. and Göttgens, B. (2016) 'Resolving early mesoderm diversification through single-cell expression profiling', *Nature*. Nature Publishing Group, 535(7611), pp. 289–293. doi: 10.1038/nature18633.

Seki, Y., Hayashi, K., Itoh, K., Mizugaki, M., Saitou, M. and Matsui, Y. (2005) 'Extensive and orderly reprogramming of genome-wide chromatin modifications associated with specification and early development of germ cells in mice.', *Developmental biology*. United States, 278(2), pp. 440–458. doi: 10.1016/j.ydbio.2004.11.025.

Shahbazi, M. N. *et al.* (2016) 'Self-organization of the human embryo in the absence of maternal tissues', *Nature Cell Biology*, (February). doi: 10.1038/ncb3347.

Shao, Y., Taniguchi, K., Townshend, R. F., Miki, T., Gumucio, D. L. and Fu, J. (2017) 'A pluripotent stem cell-based model for post-implantation human amniotic sac development', *Nature Communications*. Springer US, 8(1), p. 208. doi: 10.1038/s41467-017-00236-w.

Simmons, D. G., Fortier, A. L. and Cross, J. C. (2007) 'Diverse subtypes and developmental origins of trophoblast giant cells in the mouse placenta.', *Developmental biology*. United States, 304(2), pp. 567–578. doi: 10.1016/j.ydbio.2007.01.009.

Skamagki, M., Wicher, K. B., Jedrusik, A., Ganguly, S. and Zernicka-Goetz, M. (2013) 'Asymmetric localization of Cdx2 mRNA during the first cell-fate decision in early mouse development.', *Cell reports*. United States, 3(2), pp. 442–457. doi: 10.1016/j.celrep.2013.01.006.

Smyth, N., Vatansever, H. S., Murray, P., Meyer, M., Frie, C., Paulsson, M. and Edgar, D. (1999) 'Absence of basement membranes after targeting the LAMC1 gene results in embryonic lethality due to failure of endoderm differentiation.', *The Journal of cell biology*. United States, 144(1), pp. 151–160.

Snippert, H. J., van der Flier, L. G., Sato, T., van Es, J. H., van den Born, M., Kroon-Veenboer, C., Barker, N., Klein, A. M., van Rheenen, J., Simons, B. D. and Clevers, H. (2010) 'Intestinal Crypt Homeostasis Results from Neutral Competition between Symmetrically Dividing Lgr5 Stem Cells', *Cell*. Elsevier, 143(1), pp. 134–144. doi: 10.1016/j.cell.2010.09.016.

Snow, M. H. L. (1977) 'Gastrulation in the mouse: growth and regionalization of the epiblast', *Journal of Embryology and Experimental Morphology*, Vol. 42(2), pp. 293–303. Available at: http://www.scopus.com/inward/record.url?eid=2-s2.0-0017739051&partnerID=tZOtx3y1.

Snow, M. L. H. (1976) 'Embryo growth during the immediate post-implantation period', *Embryogenesis in mammals*, 40, pp. 53–70.

Soares, M. L., Haraguchi, S., Torres-Padilla, M.-E., Kalmar, T., Carpenter, L., Bell, G., Morrison, A., Ring, C. J. a, Clarke, N. J., Glover, D. M. and Zernicka-Goetz, M. (2005) 'Functional studies of signaling pathways in peri-implantation development of the mouse embryo by RNAi.', *BMC developmental biology*, 5, p. 28. doi: 10.1186/1471-213X-5-28.

Soriano, P. (1999) 'Generalized lacZ expression with the ROSA26 Cre reporter strain.', *Nature genetics*, 21(1), pp. 70–71. doi: 10.1038/5007.

Soudais, C., Bielinska, M., Heikinheimo, M., MacArthur, C. A., Narita, N., Saffitz, J. E., Simon, M. C., Leiden, J. M. and Wilson, D. B. (1995) 'Targeted mutagenesis of the transcription factor GATA-4 gene in mouse embryonic stem cells disrupts visceral endoderm differentiation in vitro.', *Development (Cambridge, England)*, 121(11), pp. 3877–3888. Available at: http://eutils.ncbi.nlm.nih.gov/entrez/eutils/elink.fcgi?dbfrom=pubmed&id=8582296&retmode=ref&cmd=prlinks%5Cnpapers3://publication/uuid/4A48406E-16A9-4D64-A469-D303C7944AE1.

Southon, E. and Tessarollo, L. (2009) 'Manipulating mouse embryonic stem cells.', *Methods in molecular biology (Clifton, N.J.)*. United States, 530, pp. 165–185. doi: 10.1007/978-1-59745-471-1_9.

Spemann, H. and Mangold, H. (1924) 'Induction of embryonic primordia by implantation of organizers from a different species.', *Foundations of Experimental Embryology*, pp. 144–184.

Spence, J. R. *et al.* (2011) 'Directed differentiation of human pluripotent stem cells into intestinal tissue in vitro.', *Nature*. Nature Publishing Group, 470(7332), pp. 105–9. doi: 10.1038/nature09691.

Srinivas, S., Rodriguez, T., Clements, M., Smith, J. C. and Beddington, R. S. (2004) 'Active cell migration drives the unilateral movements of the anterior visceral endoderm', *Development*, 131. doi: 10.1242/dev.01005.

Steinberg, M. S. (1963) 'Reconstruction of Tissues by Dissociated Cells', *Science*, 141(3579), p. 401 LP-408. Available at: http://science.sciencemag.org/content/141/3579/401.abstract.

Stemmler, M. P. (2008) 'Cadherins in development and cancer.', *Molecular bioSystems*, 4(8), pp. 835–50. doi: 10.1039/b719215k.

Stephens, L. E., Sutherland, A. E., Klimanskaya, I. V, Andrieux, A., Meneses, J., Pedersen, R. A. and Damsky, C. H. (1995) 'Deletion of beta 1 integrins in mice results in inner cell mass failure and peri-implantation lethality.', *Genes & development*. United States, 9(15), pp. 1883–1895.

Stern, C. D. (2004) *Gastrulation: From Cells to Embryo*. Cold Spring Harbor Laboratory Press.

Stower, M. J. and Bertocchini, F. (2017) 'The evolution of amniote gastrulation: the blastopore-primitive streak transition.', *Wiley interdisciplinary reviews. Developmental biology*. United States, 6(2). doi: 10.1002/wdev.262.

Stower, M. J. and Srinivas, S. (2014) 'Heading forwards: anterior visceral endoderm migration in patterning the mouse embryo', *Philosophical Transactions of the Royal Society B: Biological Sciences*. The Royal Society, 369(1657), p. 20130546. doi: 10.1098/rstb.2013.0546.

Strumpf, D., Mao, C.-A., Yamanaka, Y., Ralston, A., Chawengsaksophak, K., Beck, F. and Rossant, J. (2005) 'Cdx2 is required for correct cell fate specification and differentiation of trophectoderm in the mouse blastocyst', *Development*, 132(9), p. 2093 LP-2102. Available at: http://dev.biologists.org/content/132/9/2093.abstract.

Stuckey, D. W., Di Gregorio, A., Clements, M. and Rodriguez, T. A. (2011) 'Correct patterning of the primitive streak requires the anterior visceral endoderm', *PLoS ONE*, 6(3), pp. 1–9. doi:

10.1371/journal.pone.0017620.

Surani, M. A. (2001) 'Reprogramming of genome function through epigenetic inheritance.', *Nature*, 414(6859), pp. 122–128. doi: 10.1038/35102186.

Takagi, N., Sugawara, O. and Sasaki, M. (1982) 'Regional and temporal changes in the pattern of X-chromosome replication during the early post-implantation development of the female mouse.', *Chromosoma*. Austria, 85(2), pp. 275–286.

Takahashi, K. and Yamanaka, S. (2006) 'Induction of pluripotent stem cells from mouse embryonic and adult fibroblast cultures by defined factors.', *Cell*. United States, 126(4), pp. 663–676. doi: 10.1016/j.cell.2006.07.024.

Takaoka, K., Yamamoto, M. and Hamada, H. (2011) 'Origin and role of distal visceral endoderm, a group of cells that determines anterior-posterior polarity of the mouse embryo.', *Nature cell biology*. England, 13(7), pp. 743–752. doi: 10.1038/ncb2251.

Takaoka, K., Yamamoto, M., Shiratori, H., Meno, C., Rossant, J., Saijoh, Y. and Hamada, H. (2006) 'The mouse embryo autonomously acquires anterior-posterior polarity at implantation.', *Developmental cell*. United States, 10(4), pp. 451–459. doi: 10.1016/j.devcel.2006.02.017.

Takasato, M., Er, P. X., Becroft, M., Vanslambrouck, J. M., Stanley, E. G., Elefanty, A. G. and Little, M. H. (2014) 'Directing human embryonic stem cell differentiation towards a renal lineage generates a self-organizing kidney.', *Nature cell biology*. Nature Publishing Group, 16(1), pp. 118–26. doi: 10.1038/ncb2894.

Takasato, M., Er, P. X., Chiu, H. S. and Little, M. H. (2016) 'Generation of kidney organoids from human pluripotent stem cells', *Nature Protocols*. Nature Publishing Group, a division of Macmillan Publishers Limited. All Rights Reserved., 11(9), pp. 1681–1692. doi: 10.1038/nprot.2016.098.

Takebe, T., Zhang, R.-R., Koike, H., Kimura, M., Yoshizawa, E., Enomura, M., Koike, N., Sekine, K. and Taniguchi, H. (2014) 'Generation of a vascularized and functional human liver from an iPSC-derived organ bud transplant.', *Nature protocols*. Nature Publishing Group, 9(2), pp. 396–409. doi: 10.1038/nprot.2014.020.

Takito, J. and Al-Awqati, Q. (2004) 'Conversion of ES cells to columnar epithelia by hensin and to squamous epithelia by laminin', *Journal of Cell Biology*, 166(7), pp. 1093–1102. doi: 10.1083/jcb.200405159.

Tam, P. P. and Beddington, R. S. (1987) 'The formation of mesodermal tissues in the mouse embryo during gastrulation and early organogenesis.', *Development (Cambridge, England)*. England, 99(1), pp. 109–126.

Tam, P. P. L., Kanai-Azuma, M. and Kanai, Y. (2003) 'Early endoderm development in vertebrates: lineage differentiation and morphogenetic function.', *Current opinion in genetics & development*. England, 13(4), pp. 393–400.

Tam, P. P. L. and Loebel, D. a F. (2007) 'Gene function in mouse embryogenesis: get set for gastrulation.', *Nature reviews. Genetics*, 8(5), pp. 368–81. doi: 10.1038/nrg2084.

Tam, P. P. and Zhou, S. X. (1996) 'The allocation of epiblast cells to ectodermal and germ-line lineages is influenced by the position of the cells in the gastrulating mouse embryo.', *Developmental biology*. United States, 178(1), pp. 124–132. doi: 10.1006/dbio.1996.0203.

Tan, T., Tang, X., Zhang, J., Niu, Y., Chen, H., Li, B., Wei, Q. and Ji, W. (2011) 'Generation of trophoblast stem cells from rabbit embryonic stem cells with BMP4', *PLoS ONE*, 6(2). doi:

10.1371/journal.pone.0017124.

Tanaka, S., Kunath, T., Hadjantonakis, A., Nagy, A. and Rossant, J. (1998) 'Promotion of Trophoblast Stem Cell Proliferation by FGF4', *Science*, 282(5396), pp. 2072–2075. doi: 10.1126/science.282.5396.2072.

Tanaka, S. S., Toyooka, Y., Akasu, R., Katoh-fukui, Y., Nakahara, Y., Suzuki, R., Yokoyama, M. and Noce, T. (2000) 'The mouse homolog of Drosophila Vasa is required for the development of male germ cells', *Genes and Development*, pp. 841–853. doi: 10.1101/gad.14.7.841.

Tarkowski, A. (1959) 'Experiments on the development of isolated blastomeres of mouse eggs', *Nature*, 184, pp. 1286–7. Available at: http://adsabs.harvard.edu/abs/1959Natur.184.1286T (Accessed: 8 April 2014).

Tesar, P. J. (2005) 'Derivation of germ-line-competent embryonic stem cell lines from preblastocyst mouse embryos.', *Proceedings of the National Academy of Sciences of the United States of America*. United States, 102(23), pp. 8239–8244. doi: 10.1073/pnas.0503231102.

Tesar, P. J., Chenoweth, J. G., Brook, F. a, Davies, T. J., Evans, E. P., Mack, D. L., Gardner, R. L. and McKay, R. D. (2007) 'New cell lines from mouse epiblast share defining features with human embryonic stem cells', *Nature*, 448(7150), pp. 196–199. doi: 10.1038/nature05972.

Teshima, T. H. N., Wells, K. L., Lourenco, S. V and Tucker, A. S. (2016) 'Apoptosis in Early Salivary Gland Duct Morphogenesis and Lumen Formation.', *Journal of dental research*. United States, 95(3), pp. 277–283. doi: 10.1177/0022034515619581.

Theunissen, T. W. *et al.* (2014) 'Systematic identification of culture conditions for induction and maintenance of naive human pluripotency.', *Cell stem cell*. United States, 15(4), pp. 471–487. doi: 10.1016/j.stem.2014.07.002.

Thiery, J. P., Acloque, H., Huang, R. Y. J. and Nieto, M. A. (2009) 'Epithelial-Mesenchymal Transitions in Development and Disease', *Cell*, 139(5), pp. 871–890. doi: 10.1016/j.cell.2009.11.007.

Thomas, P. and Beddington, R. (1996) 'Anterior primitive endoderm may be responsible for patterning the anterior neural plate in the mouse embryo.', *Current biology : CB*, 6(11), pp. 1487–1496. doi: 10.1016/S0960-9822(96)00753-1.

Thomson, J. A., Itskovitz-Eldor, J., Shapiro, S. S., Waknitz, M. A., Swiergiel, J. J., Marshall, V. S. and Jones, J. M. (1998) 'Embryonic stem cell lines derived from human blastocysts.', *Science (New York, N.Y.)*. United States, 282(5391), pp. 1145–1147.

Thomson, J. A., Kalishman, J., Golos, T. G., Durning, M., Harris, C. P. and Hearn, J. P. (1996) 'Pluripotent cell lines derived from common marmoset (Callithrix jacchus) blastocysts.', *Biology of reproduction*, 55(2), pp. 254–259. doi: 10.1172/JCI200521137.102.

Torres-Padilla, M.-E., Parfitt, D.-E., Kouzarides, T. and Zernicka-Goetz, M. (2007) 'Histone arginine methylation regulates pluripotency in the early mouse embryo.', *Nature*, 445(7124), pp. 214–218. doi: 10.1038/nature05458.

Torres-Padilla, M.-E., Richardson, L., Kolasinska, P., Meilhac, S. M., Luetke-Eversloh, M. V. and Zernicka-Goetz, M. (2007) 'The anterior visceral endoderm of the mouse embryo is established from both preimplantation precursor cells and by de novo gene expression after implantation', *Developmental biology*, 309(1), pp. 97–112. doi: 10.1016/j.ydbio.2007.06.020.

Tortelote, G. G., Hernández-Hernández, J. M., Quaresma, A. J. C., Nickerson, J. A., Imbalzano, A. N. and Rivera-Pérez, J. A. (2013) 'Wnt3 function in the epiblast is required for the maintenance but not

the initiation of gastrulation in mice', *Developmental Biology*, 374(1), pp. 164–173. doi: 10.1016/j.ydbio.2012.10.013.

Trapnell, C., Pachter, L. and Salzberg, S. L. (2009) 'TopHat: Discovering splice junctions with RNA-Seq', *Bioinformatics*, 25(9), pp. 1105–1111. doi: 10.1093/bioinformatics/btp120.

Trichas, G. *et al.* (2012) 'Multi-cellular rosettes in the mouse visceral endoderm facilitate the ordered migration of anterior visceral endoderm cells.', *PLoS biology*, 10(2), p. e1001256. doi: 10.1371/journal.pbio.1001256.

Tsakiridis, A., Huang, Y., Blin, G., Skylaki, S., Wymeersch, F., Osorno, R., Economou, C., Karagianni, E., Zhao, S., Lowell, S. and Wilson, V. (2014) 'Distinct Wnt-driven primitive streak-like populations reflect in vivo lineage precursors', *Development*, 141(6), pp. 1209–1221. doi: 10.1242/dev.101014.

Tsunoda, Y. and McLaren, A. (1983) 'Effect of various procedures on the viability of mouse embryos containing half the normal number of blastomeres.', *Journal of reproduction and fertility*. England, 69(1), pp. 315–322.

Turner, D. A., Baillie-Johnson, P. and Martinez Arias, A. (2016) 'Organoids and the genetically encoded self-assembly of embryonic stem cells', *BioEssays*, 38(2), pp. 181–191. doi: 10.1002/bies.201500111.

Turner, D. A., Glodowski, C. R., Hayward, P. C., Collignon, J., Serup, P. and A, M. A. (2016) 'Interactions between Nodal and Wnt signalling Drive Robust Symmetry-Breaking and Axial Organisation in Gastruloids (Embryonic Organoids)'. doi: 10.1101/051722.

Vandevoort, C. a, Thirkill, T. L. and Douglas, G. C. (2007) 'Blastocyst-derived trophoblast stem cells from the rhesus monkey.', *Stem cells and development*, 16(5), pp. 779–788. doi: 10.1089/scd.2007.0020.

Vincent, J. P. and Gerhart, J. C. (1987) 'Subcortical rotation in Xenopus eggs: an early step in embryonic axis specification.', *Developmental biology*. United States, 123(2), pp. 526–539.

Waldrip, W. R., Bikoff, E. K., Hoodless, P. A., Wrana, J. L. and Robertson, E. J. (1998) 'Smad2 signaling in extraembryonic tissues determines anterior-posterior polarity of the early mouse embryo.', *Cell*. United States, 92(6), pp. 797–808.

Wang, Q. T., Piotrowska, K., Ciemerych, M. A., Milenkovic, L., Scott, M. P., Davis, R. W. and Zernicka-Goetz, M. (2004) 'A genome-wide study of gene activity reveals developmental signaling pathways in the preimplantation mouse embryo', *Dev Cell*, 6(1), pp. 133–144. doi: 10.1016/S1534-5807(03)00404-0.

Wang, S., Tang, X., Niu, Y., Chen, H., Li, B., Li, T., Zhang, X., Hu, Z., Zhou, Q. and Ji, W. (2007) 'Generation and characterization of rabbit embryonic stem cells.', *Stem Cells*, 25(2), pp. 481–9. doi: 10.1634/stemcells.2006-0226.

Wang, X. and Yang, P. (2008) 'In vitro differentiation of mouse embryonic stem (mES) cells using the hanging drop method.', *Journal of visualized experiments : JoVE*, (17), pp. 2–3. doi: 10.3791/825.

Warga, R. M. and Kimmel, C. B. (1990) 'Cell movements during epiboly and gastrulation in zebrafish.', *Development (Cambridge, England)*. England, 108(4), pp. 569–580.

Warmflash, A., Sorre, B., Etoc, F., Siggia, E. D. and Brivanlou, A. H. (2014) 'A method to recapitulate early embryonic spatial patterning in human embryonic stem cells.', *Nature methods*, 11(8). doi: 10.1038/nmeth.3016.

Watabe, T. and Miyazono, K. (2009) 'Roles of TGF-beta family signaling in stem cell renewal and

differentiation.', *Cell research*, 19(1), pp. 103–115. doi: 10.1038/cr.2008.323.

Weber, R. J., Pedersen, R. A., Wianny, F., Evans, M. J. and Zernicka-Goetz, M. (1999) 'Polarity of the mouse embryo is anticipated before implantation.', *Development (Cambridge, England)*. England, 126(24), pp. 5591–5598.

Weber, S., Eckert, D., Nettersheim, D., Gillis, A. J. M., Schafer, S., Kuckenberg, P., Ehlermann, J., Werling, U., Biermann, K., Looijenga, L. H. J. and Schorle, H. (2009) 'Critical Function of AP-2gamma/TCFAP2C in Mouse Embryonic Germ Cell Maintenance', *Biology of Reproduction*, 82(1), pp. 214–223. doi: 10.1095/biolreprod.109.078717.

Weiss, P. and Taylor, A. C. (1960) 'Reconstitution of complete organs from single-cell suspensions of Chick embryos Advanced stages of Differentiation', *Proceedings of the National Academy of Sciences of the United States of America*, 46(9), pp. 1177–1185. Available at: http://www.ncbi.nlm.nih.gov/pmc/articles/PMC223021/.

Weitzer, G. (2006) 'Embryonic Stem Cell-Derived Embryoid Bodies: An In Vitro Model of Eutherian Pregastrulation Development and Early Gastrulation BT - Stem Cells', in Wobus, A. M. and Boheler, K. R. (eds). Berlin, Heidelberg: Springer Berlin Heidelberg, pp. 21–51. doi: 10.1007/3-540-31265-X_2.

White, M. D., Angiolini, J. F., Alvarez, Y. D., Kaur, G., Zhao, Z. W., Mocskos, E., Bruno, L., Bissiere, S., Levi, V. and Plachta, N. (2016) 'Long-Lived Binding of Sox2 to DNA Predicts Cell Fate in the Four-Cell Mouse Embryo', *Cell*. Elsevier Inc., 165(1), pp. 75–87. doi: 10.1016/j.cell.2016.02.032.

White, M. D., Bissiere, S., Alvarez, Y. D. and Plachta, N. (2016) *Mouse Embryo Compaction*. 1st edn, *Current Topics in Developmental Biology*. 1st edn. Elsevier Inc. doi: 10.1016/bs.ctdb.2016.04.005.

Wilkinson, D. G., Bhat, S. and Herrmann, B. (1990) 'Expression of the mouse T gene and its role in mesoderm formation', *Letters To Nature*, 346, pp. 183–187. doi: 10.1038/346183a0.

Williams, L. H., Kalantry, S., Starmer, J. and Magnuson, T. (2011) 'Transcription precedes loss of Xist coating and depletion of H3K27me3 during X-chromosome reprogramming in the mouse inner cell mass.', *Development (Cambridge, England)*. England, 138(10), pp. 2049–2057. doi: 10.1242/dev.061176.

Williams, M., Burdsal, C., Periasamy, A., Lewandowski, M. and Sutherland, A. (2013) 'The mouse primitive streak forms in situ by initiation of epithelial to mesenchymal transition without migration of a cell population', *Developmental dynamics : an official publication of the American Association of Anatomists*, 241(2), pp. 270–283. doi: 10.1002/dvdy.23711.The.

Williams, R. L., Hilton, D. J., Pease, S., Willson, T. A., Stewart, C. L., Gearing, D. P., Wagner, E. F., Metcalf, D., Nicola, N. A. and Gough, N. M. (1988) 'Myeloid leukaemia inhibitory factor maintains the developmental potential of embryonic stem cells.', *Nature*. England, 336(6200), pp. 684–687. doi: 10.1038/336684a0.

Wilson, H. V (1907) 'A New Method by which Sponges may be Artificially Reared', *Science*, 25(649), p. 912 LP-915. Available at: http://science.sciencemag.org/content/25/649/912.abstract.

Wilson, V., Manson, L., Skarnes, W. C. and Beddington, R. S. (1995) 'The T gene is necessary for normal mesodermal morphogenetic cell movements during gastrulation.', *Development (Cambridge, England)*. England, 121(3), pp. 877–886.

Winnier, G., Blessing, M., Labosky, P. A. and Hogan, B. L. M. (1995) 'Bone morphogenetic protein-4 is required for mesoderm formation and patterning in the mouse', *Genes and Development*, 9(17), pp. 2105–2116. doi: 10.1101/gad.9.17.2105.

Wray, J., Kalkan, T., Gomez-Lopez, S., Eckardt, D., Cook, A., Kemler, R. and Smith, A. (2011) 'Inhibition of glycogen synthase kinase-3 alleviates Tcf3 repression of the pluripotency network and increases embryonic stem cell resistance to differentiation.', *Nature cell biology*. England, 13(7), pp. 838–845. doi: 10.1038/ncb2267.

Wu, G., Lei, L. and Schöler, H. R. (2017) 'Totipotency in the mouse', *Journal of Molecular Medicine*. Journal of Molecular Medicine, 95(7), pp. 687–694. doi: 10.1007/s00109-017-1509-5.

Wu, J. *et al.* (2015) 'An alternative pluripotent state confers interspecies chimaeric competency', *Nature*, 521. doi: 10.1038/nature14413.

Wu, Q., Kanata, K., Saba, R., Deng, C.-X., Hamada, H. and Saga, Y. (2013) 'Nodal/activin signaling promotes male germ cell fate and suppresses female programming in somatic cells.', *Development (Cambridge, England)*, 140(2), pp. 291–300. doi: 10.1242/dev.087882.

Xia, Y., Sancho-Martinez, I., Nivet, E., Rodriguez Esteban, C., Campistol, J. M. and Izpisua Belmonte, J. C. (2014) 'The generation of kidney organoids by differentiation of human pluripotent cells to ureteric bud progenitor-like cells.', *Nature protocols*. Nature Publishing Group, 9(11), pp. 2693–704. doi: 10.1038/nprot.2014.182.

Xiao, L.-J., Chang, H., Ding, N.-Z., Ni, H., Kadomatsu, K. and Yang, Z.-M. (2002) 'Basigin expression and hormonal regulation in mouse uterus during the peri-implantation period.', *Molecular reproduction and development*. United States, 63(1), pp. 47–54. doi: 10.1002/mrd.10128.

Yagi, M., Kishigami, S., Tanaka, A., Semi, K., Mizutani, E., Wakayama, S., Wakayama, T., Yamamoto, T. and Yamada, Y. (2017) 'Derivation of ground-state female ES cells maintaining gamete-derived DNA methylation', *Nature*. Macmillan Publishers Limited, part of Springer Nature. All rights reserved., 548(7666), pp. 224–227. Available at: http://dx.doi.org/10.1038/nature23286.

Yagi, R., Kohn, M. J., Karavanova, I., Kaneko, K. J., Vullhorst, D., DePamphilis, M. L. and Buonanno, A. (2007) 'Transcription factor TEAD4 specifies the trophectoderm lineage at the beginning of mammalian development', *Development*, 134(21), p. 3827 LP-3836. Available at: http://dev.biologists.org/content/134/21/3827.abstract.

Yamaji, M., Seki, Y., Kurimoto, K., Yabuta, Y., Yuasa, M., Shigeta, M., Yamanaka, K., Ohinata, Y. and Saitou, M. (2008) 'Critical function of Prdm14 for the establishment of the germ cell lineage in mice.', *Nature genetics*, 40(8), pp. 1016–1022. doi: 10.1038/ng.186.

Yamamoto, M., Beppu, H., Takaoka, K., Meno, C., Li, E., Miyazono, K. and Hamada, H. (2009) 'Antagonism between Smad1 and Smad2 signaling determines the site of distal visceral endoderm formation in the mouse embryo.', *The Journal of cell biology*. United States, 184(2), pp. 323–334. doi: 10.1083/jcb.200808044.

Yamamoto, M., Saijoh, Y., Perea-Gomez, A., Shawlot, W., Behringer, R. R., Ang, S.-L., Hamada, H. and Meno, C. (2004) 'Nodal antagonists regulate formation of the anteroposterior axis of the mouse embryo.', *Nature*, 428(6981), pp. 387–392. doi: 10.1038/nature02418.

Yamanaka, Y., Ralston, A., Stephenson, R. O. and Rossant, J. (2006) 'Cell and molecular regulation of the mouse blastocyst.', *Developmental dynamics : an official publication of the American Association of Anatomists*. United States, 235(9), pp. 2301–2314. doi: 10.1002/dvdy.20844.

Yan, J., Tanaka, S., Oda, M., Makino, T., Ohgane, J. and Shiota, K. (2001) 'Retinoic acid promotes differentiation of trophoblast stem cells to a giant cell fate.', *Developmental biology*. United States, 235(2), pp. 422–432. doi: 10.1006/dbio.2001.0300.

Yan, Y., Liu, J., Luo, Y., Chaosu, E., Robert, S., Abate-shen, C., Shen, M. M. and Haltiwanger, R. S.

(2002) ‘Dual Roles of Cripto as a Ligand and Coreceptor in the Nodal Signaling Pathway Dual Roles of Cripto as a Ligand and Coreceptor in the Nodal Signaling Pathway’, 22(13), pp. 4439–4449. doi: 10.1128/MCB.22.13.4439.

Yeo, C. Y. and Whitman, M. (2001) ‘Nodal signals to Smads through Cripto-dependent and Cripto-independent mechanisms’, *Molecular Cell*, 7(5), pp. 949–957. doi: 10.1016/S1097-2765(01)00249-0.

Ying, Q.-L. and Smith, A. G. (2003) ‘Defined Conditions for Neural Commitment and Differentiation’, *Methods in Enzymology*, 365, pp. 327–341. doi: http://dx.doi.org/10.1016/S0076-6879(03)65023-8.

Ying, Q.-L., Stavridis, M., Griffiths, D., Li, M. and Smith, A. (2003) ‘Conversion of embryonic stem cells into neuroectodermal precursors in adherent monoculture.’, *Nature biotechnology*, 21(2), pp. 183–6. doi: 10.1038/nbt780.

Ying, Q. L., Nichols, J., Chambers, I. and Smith, A. (2003) ‘BMP induction of Id proteins suppresses differentiation and sustains embryonic stem cell self-renewal in collaboration with STAT3.’, *Cell*. United States, 115(3), pp. 281–292.

Ying, Q., Wray, J., Nichols, J., Batlle-Morera, L., Doble, B., Woodgett, J., Cohen, P. and Smith, A. (2008) ‘The ground state of embryonic stem cell self-renewal’, *Nature*, 453(7194), pp. 519–24. doi: 10.1038/nature06968.

Ying, Y., Qi, X. and Zhao, G. Q. (2001) ‘Induction of primordial germ cells from murine epiblasts by synergistic action of BMP4 and BMP8B signaling pathways.’, *Proceedings of the National Academy of Sciences of the United States of America*. United States, 98(14), pp. 7858–7862. doi: 10.1073/pnas.151242798.

Yoon, Y., Huang, T., Tortelote, G. G., Wakamiya, M., Hadjantonakis, A.-K., Behringer, R. R. and Rivera-Pérez, J. a. (2015) ‘Extra-embryonic Wnt3 regulates the establishment of the primitive streak in mice’, *Developmental Biology*. Elsevier, 403(1), pp. 80–88. doi: 10.1016/j.ydbio.2015.04.008.

Yoshioka, K., Suzuki, C. and Iwamura, S. (1998) ‘Activin A and follistatin regulate developmental competence of In vitro-produced bovine embryos.’, *Biology of reproduction*. United States, 59(5), pp. 1017–1022.

Yu, J. *et al.* (2007) ‘Induced pluripotent stem cell lines derived from human somatic cells.’, *Science (New York, N.Y.)*. United States, 318(5858), pp. 1917–1920. doi: 10.1126/science.1151526.

Zernicka-Goetz, M. (1998) ‘Fertile offspring derived from mammalian eggs lacking either animal or vegetal poles.’, *Development (Cambridge, England)*. England, 125(23), pp. 4803–4808.

Zhu, Q. *et al.* (2014) ‘The transcription factor Pou3f1 promotes neural fate commitment via activation of neural lineage genes and inhibition of external signaling pathways’, *eLife*, 3, pp. 1–21. doi: 10.7554/eLife.02224.

Zimmerman, L. B., De Jesús-Escobar, J. M. and Harland, R. M. (1996) ‘The Spemann Organizer Signal noggin Binds and Inactivates Bone Morphogenetic Protein 4’, *Cell*. Elsevier, 86(4), pp. 599–606. doi: 10.1016/S0092-8674(00)80133-6.

Ziomek, C. and Johnson, M. (1981) ‘Properties of polar and apolar cells from the 16-cell mouse morula’, *Wilhelm Roux’s archives of developmental …*, pp. 287–296. Available at: http://link.springer.com/article/10.1007/BF00848757 (Accessed: 11 April 2014).

Appendix I: Original publications and manuscripts in preparation

Harrison, S.E; Sozen, B; Christodoulou, N; Kyprianou, C & Zernicka-Goetz, M. 'Assembly of embryonic and extra-embryonic stem cells to mimic embryogenesis *in vitro'* (2017) *Science* 356(6334).

Harrison, S.E; Sozen, B; & Zernicka-Goetz, M. '*In vitro* generation of embryo-like structures from embryonic and trophoblast stem cells' *Nature Protocols* (2018, *In Press*).